EVALUATION OF THE POTENTIAL FOR REPAIR OF DEGENERATE HYALINE CARTILAGE IN THE OSTEOARTHRITIC KNEE BY CARTILAGE STEM CELLS

A thesis submitted to Cardiff University for the degree of
Doctor of Philosophy

Larissa Nelson BSc (Hons)

Cardiff School of Biosciences
Cardiff University

August 2012

Abstract

Osteoarthritis (OA) is a highly prevalent, debilitating disease affecting many joints including the knee. Despite the involvement of several tissues, it is believed that the articular cartilage is the primary site of pathogenesis in humans.

Within this study, a new scoring system of OA was devised, incorporating the articular cartilage and underlying bone, aimed at providing a more comprehensive means of grading the severity of tissue damage. We examined changes progressively from mild to severe and were able to deduce from the scoring system that bone changes may precede those of the overlying cartilage.

Immunohistochemistry was used to assess stem cell marker expression, proliferation and progressive changes within the extracellular matrix of sectioned osteochondral plugs, however no distinct pattern of change could be extrapolated, highlighting the variable nature of this taxing disease.

Previous studies have demonstrated the presence of a sub-population of chondroprogenitor cells present in normal hyaline cartilage. We demonstrated in this study that a similar group of cells reside in osteoarthritic articular cartilage. We were able to isolate and expand clonally derived primary cell lines to beyond 50 population doublings whilst maintaining a chondrogenic phenotype, and demonstrated the tri-lineage potential of these cells. That said, a significant amount of variation was observed and it was, therefore, postulated that there may be a smaller cohort of viable cells within this sub-population isolated from osteoarthritic cartilage.

A preliminary study was also carried out comparing chondroprogenitors from normal articular cartilage to those isolated from OA tissue. Heterogeneity was again encountered, suggesting that there was a group of OA chondroprogenitors with similar characteristics to the normal cells, which differed from the other less metabolically active cells. This finding was agreeable with the aforementioned postulation. Data from our preliminary integration study was promising as we demonstrated the potential for using these chondroprogenitor cells in combination with other cells whilst achieving successful integration. However, further work is necessary to distinguish between the cell lines with the potential for integration from those that lacked this ability, thereby eliminating the heterogeneity.

The presence of viable chondroprogenitor cells in OA tissue challenges the dogma that the tissue is irrecoverable, and opens the scope for regenerative medicine using resident progenitor cells. This is an exciting prospect that could significantly contribute to articular cartilage repair.

Acknowledgements

I would like to thank Professor Charlie Archer and Professor John Fairclough for their supervision and support throughout the course of my PhD. Many thanks are also due to my friends and colleagues in BIOSI, in particular Dr Kirsty Richardson, Dr Helen McCarthy, Dr Rebecca Williams and Dr Ilyas Khan for their encouragement and guidance over the years. Much appreciation must also be given to Chris Fellows for his help with statistical analysis.

I would also like to thank Simon and all my friends outside of Cardiff University who helped, motivated and encouraged me throughout the course of my PhD.

In addition I would like to thank my family for all of their support throughout the years. Special thanks to Annelise and Nik, who unknowingly motivated me to finish writing up before they completed their round the world sailing trip.

Contents

List of figures

Chapter 3

Chapter 4

Chapter 5

Chapter 6

List of tables

Abbreviations

AC	Articular cartilage
ACT	Atologous chondrocyte transplantation
ADAMTS	A disintegrin and metalloproteinase domain with thrombospondin motifs
BMP	Bone morphogenetic protein
BMSCs	Bone marrow-derived stromal cells
BrdU	Bromodeoxyuridine
BSA	Bovine serum albumin
CD	Cluster of differentiation
CFE	Colony forming efficiency
CILP	Cartilage intermediate-layer protein
CM	Cartilage morphology
CMFDA	5-Chloromethylfluorescein diacetate
CMP	Cartilage matrix protein
CMTPX	CellTracker Red
COMP	Cartilage oligomeric matrix protein
CS	Chondroitin sulphate
CT	Cartilage thickness
DAB	3,3'Diaminobenzidine
DAPI	4',6-Diamidino-2-phenylindole
DMEM	Dulbecco's Modified Eagle Medium
DMEM/F12	Dulbecco's Modified Eagle Medium containing Hams F12
DMMB	Dimethylmethylene blue
DMSO	Dimethyl sulfoxide
dNTP	Deoxyribonucleotide triphosphate
DS	Dermatan sulphate
DTT	DL-Dithiothreitol

DZ	Deep zone
ECM	Extracellular matrix
EDTA	Ethylenediaminetetraacetic acid
FACIT	Fibril-associated collagen with an interrupted triple helix
FACS	Fluorescence-activated cell sorting
FCS	Foetal calf serum
FGF	Fibroblast growth factor
GAGs	Glycosaminoglycans
GDF	Growth and differentiation factor
HA	Hyaluronan
HHGS	Histological-Histochemical Grading System
HIF-2α	Hypoxia inducible factor-2α
HS	Heparan sulfate
IBMX	3-Isobutyl-1-methyl xanthine
ICRS	International Cartilage Repair Society
IL-1	Interleukin-1
ISCT	International Society for Cellular Therapy
ITS	Insulin transferring selenium
KS	Keratan sulphate
LPL	Lipoprotein lipase
MMPs	Matrix metalloproteinaseS
MRI	Magnetic resonance imaging
MSCs	Mesenchymal stem cells
MZ	Mid‑zone
NBFS	Neutral buffered formalin solution
NF-kB	Nuclear factor kB
OA	Osteoarthritis

OARSI	Osteoarthritis Research Society International
OCP	Osteochondral plug
PBS	Phosphate buffered saline
PBS-T	Phosphate buffered saline containing tween 20
PCNA	Proliferation cell nuclear antigen
PCR	Polymerase chain reaction
PD	population doubling
RA	Rheumatoid arthritis
ROS	Reactive oxygen species
RT-PCR	Real time polymerase chain reaction
SA-β-Gal	Senescence associated β-Galactosidase
SCB	Subchondral bone
SD	Standard deviation
SEM	Standard error of the mean
SI	Surface integrity
SLRPs	small leucine-rich proteoglycan family
SZ	Superficial zone
SZP	Surface zone protein
TBE	Tris Borate EDTA
TGF-β	Transforming growth factor-β ()
TI	Tidemark integrity
TIMP	Tissue inhibitors of metalloproteinases
TKR	Total knee replacement
TM	Tidemark
TNF-α	Tumor necrosis factor –alpha
TP	Tibial plateau
X-Gal	5-Bromo-4-chloro-3-indolyl β-D-galactopyranoside

Chapter 1:

General Introduction

1.1. Joints

A joint refers to the structural arrangement at the union between two or more parts of the skeleton. There are several different bases of classification of joints including structural classification and functional classification (figure 1.1) (Tortora and Anagnostakos, 1990). Synovial joints (otherwise known as diarthroses) are the most evolved and consequently the most mobile type of joint in the vertebrate. They comprise a joint cavity enclosed by a fibrous capsule linking skeletal elements including bone, ligament, meniscus and synovium. Within the capsule, a synovial membrane lines the surface and secretes a vital, lubricating fluid known as the synovial fluid. A thin layer of hyaline cartilage covers the surface of the articulating bones and this is commonly referred to as the articular cartilage. The structure of normal synovial joints enables high tensile strengths to be absorbed whilst providing a surface with low levels of friction permitting smooth, pain free movement. Synovial joints can withstand loads of up to ten times the body weight with a very low friction coefficient (Ratcliffe and Mow, 1996).
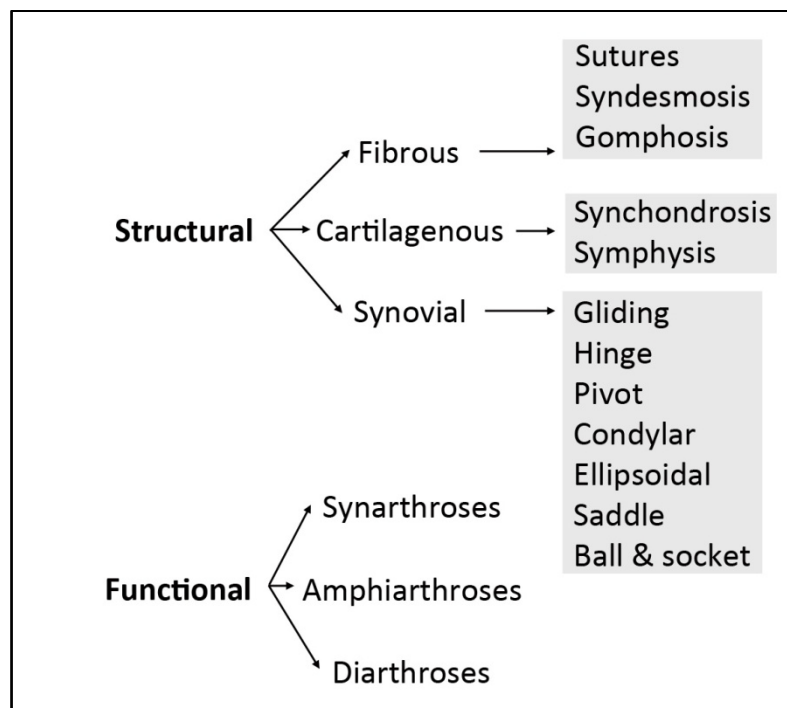
Figure 1.1. Diagrammatic presentation of joint classifications.

Synovial joints fall under the structural classification of joints.
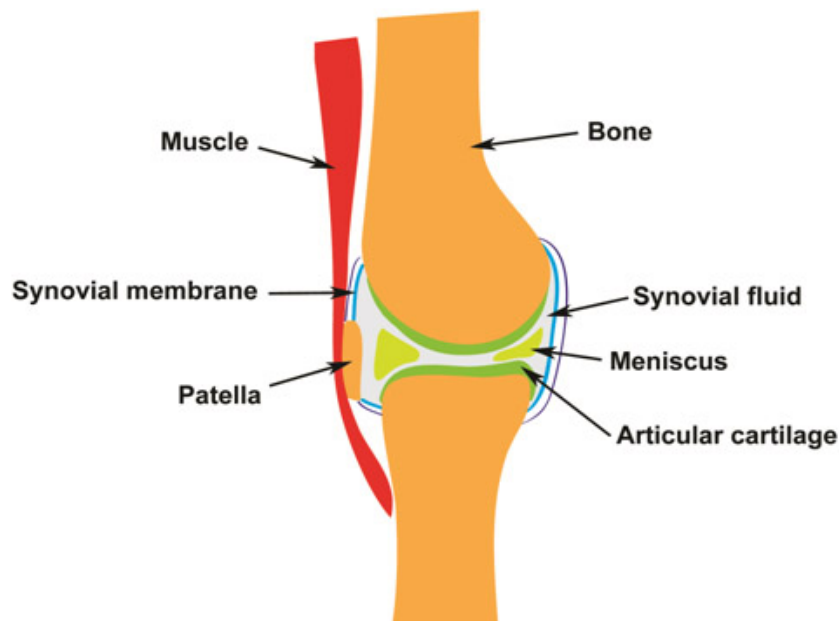
Figure 1.2. Diagram of a synovial joint.

Articular cartilage covers the opposing surfaces of the skeletal elements. *(Figure kindly donated by Dr. Kirsty Richardson).*

1.2. Development of cartilage

The development of the skeleton is a crucial process beginning early in embryogenesis, initiated by the formation of cartilage. Undifferentiated mesenchymal cells from the paraxial mesoderm give rise to somites; short segments of bead-like elevations that appear along the dorsolateral surface of the embryo and later differentiate into the axial and appendicular skeleton (Moore and Persaud, 2003). Cartilage develops from cells within the limb bud condensing to form a cartilaginous model of bone through a sequence of synchronised steps. This involves commitment and proliferation of cells into chondrogenesis, followed by the acquisition of a chondrogenic phenotype; events which are not only controlled by the chondrocytes themselves, but also by the local environment. An important transcription factor involved during chondrogenic condensation is Sox9, which is known to precede the expression of early cartilage marker collagen type IIa (Akiyama et al., 2002).

The process by which the cartilage anlagen develops into skeletally mature bone is called endochondral ossification. This process involves chondrocyte proliferation, chondrocyte hypertrophy and matrix production, followed by the invasion of blood vessels. Apoptosis or transdifferentiation of hypertrophic chondrocytes into osteoprogenitor cells occurs which leads to the establishment of primary ossification centres in the diaphyses. At these sites mineralisation occurs, through which the cartilaginous anlagen is replaced by bone. In humans at birth, secondary ossification centres are established at either ends of diaphyseal shafts. Between the secondary centres and the developing diaphyseal bone is an area known as the epiphyseal growth plate (Stevens et al., 1992). Many similarities exist between chondrocytes of the growth plate, articular cartilage and permanent cartilage including metabolism and markers such as collagens, however there also many biochemical and physiological differences due to local surroundings. Understanding the different mechanisms involved in chondrocyte fate remains to be fully elucidated.

1.3. Development of synovial joints

Synovial joints arise from mesenchymal condensations at specified sites through a process mediated by cell adhesion molecules and matrix receptors. Following the early stages of development in which the condensations chondrify, there is a secondary phase of remodelling. During this phase a region of cells at the presumptive joint flatten and become non-chondrogenic; at which point the region is known as the interzone (Archer et al., 2003, Craig et al., 1987). It is believed that the joint tissues are derived and develop from the cells of the interzone (Mitrovic, 1977), which in humans is seen as a thin layer of two to three flattened cells (Edwards et al., 1994).

There is a plethora of data to suggest a defined pattern is involved in specification of developing joints. Positioning and patterning of limbs involve cellular interactions between the mesenchymal cells that form the core of the limb bud and surrounding ectoderm (Khan et al., 2007). This process is controlled by three main signalling centres, which drive patterned limb growth along each of the three axes of the limb; namely proximal-distal, anterior-posterior and dorsal-ventral (Niswander, 2002). During the initial phases of joint specification, Noggin and Chordin, secreted bone morphogenetic protein (BMP) antagonists are expressed throughout the mesenchymal condensation and

presumptive joint space, and are crucial during joint development (Brunet et al., 1998). Growth and differentiation factor (GDF) -5, a member of transforming growth factor-β (TGF-β) superfamily is known to be heavily involved in the formation of the joint interzone, despite being from a chondrogenesis-promoting family (Archer et al., 2003, Storm et al., 1994). It is believed that GDF-5 was the first recognised gene marker in the developing joint and, therefore, much work has been focused on analysing its role during joint specification (Archer et al., 2003). Mutations to the GDF-5 gene disrupts normal skeletal development and results in abnormal joint development (Francis-West et al., 1999, Storm and Kingsley, 1999).

Despite its involvement in joint development, it has been found that GDF-5 is not directly involved in specifying joint type and it is believed that synovial joints are specified and controlled by an upstream activator of GDF-5 from the Wnt family of genes (Hartmann and Tabin, 2001). Wnt14 specifically has been identified as a key factor in the development of synovial joints, and localised production of Wnt14 induces the expression of GDF-5 (Khan et al., 2007). Convincing data by Hartmann and Tabin (2001) demonstrate how Wnt14 is sufficient to direct joint development in the chick, based on its ability to induce and/or maintain relevant gene markers for joint development including chordin, CD44 and GDF-5.

Several studies have also focussed on Hox genes, homeodomain-containing transcription factors which have been shown to be critical for the specification and patterning of vertebrate embryo (Nowicki and Burke, 2000). Having stated that, the extent to which these genes are in fact critical for joint patterning and determination is unknown as little work has been followed up to confirm and/or extend from the initial proposals (Pacifici et al., 2005).

The next phase of development is joint cavitation at which point there is a significant reduction of chondrogenic marker expression, namely sox9 and collagen type II. As described by Khan et al., 2007, 'the process of cavitation involves the generation of a cavity between two cartilaginous elements that are growing against each other through forces largely generated by hypertrophy and matrix secretion'. This process is achieved through upregulation of mechanically induced hyaluronan (HA) synthesis by cells of the

interzone, articular surface and synovium. There are several other factors which have been postulated to be involved in the formation of the synovial cavity including cell death, enzymatic degradation, differential matrix synthesis and mechanical stimulation.

1.4. Articular cartilage

Articular cartilage is a thin layer of hyaline cartilage that covers the surface of bones at large articulating diarthrodial joints. It is renowned for being avascular and aneural, and for being a tissue with a poor reparative capacity. The function of articular cartilage is to provide a wear-resistant surface with low frictional properties, whilst having the ability to bear high tensile strengths; withstanding compression and shear (Benjamin, 1999).

The characteristic properties of articular cartilage are achieved through its highly structured organisation. Its uniquely dense extracellular matrix (ECM) is produced and maintained by a single specialised cell; the chondrocyte, whose relative numbers are low and make up less than 5% of the tissues total volume (Bora and Miller, 1987) . The ECM is abundant in collagens (10-30% of wet weight) that provide a network in which proteoglycans (5-10% of wet weight) and other molecules can embed. The negatively charged proteoglycans are responsible for a high osmotic swelling pressure, resulting in a large proportion of water within the tissue (65-80% of wet weight) (Buckwalter and Mankin, 1998). It is through the interactions between collagens, proteoglycans and water, that hyaline cartilage becomes a resilient tissue capable of lasting a lifetime.

The gross appearance of articular cartilage is smooth and iridescently white; however the thickness, cell density, matrix composition and mechanical properties are variable even within a joint. Due to the avascular nature of the tissue, the chondrocytes are sustained by the diffusion of nutrients and gases. Compared to other tissues like muscles and bone, articular cartilage has a low level of metabolic activity. Despite its low metabolic activity and 'unimpressive appearance', articular cartilage is an elaborate, and highly ordered structure in which complex interactions between chondrocytes and surrounding matrix actively maintain the tissue (Buckwalter and Hunziker, 1999).
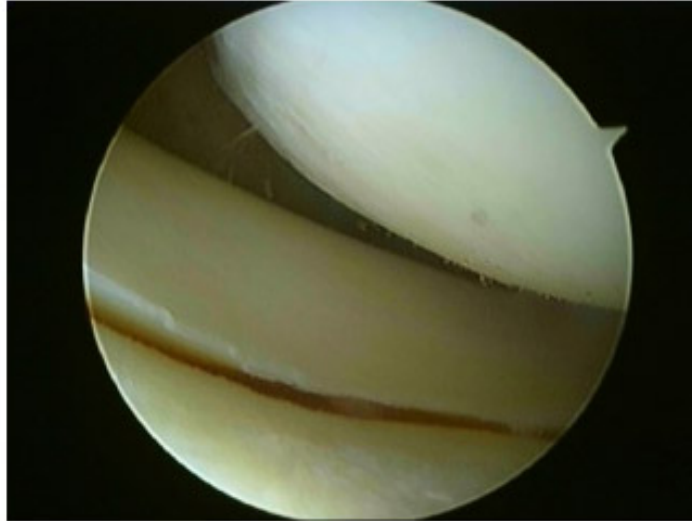
Figure 1.3. Normal human hyaline cartilage on tibia and femur.

Normal fibrocartilagenous meniscus between the articulating surfaces can also be seen. Photograph taken by Professor John Fairclough during arthroscopic surgery.

1.4.1. Development of articular cartilage

The pathways involved in the development of articular cartilage have been an area of interest within many groups for decades, as a result of the inherent lack of understanding. The questions that are commonly raised are a) how do articular chondrocytes develop at the extremities of developing long bones early in embryogenesis and become distinguished from surrounding tissues and structures, and b) how do the articular cells avoid entering the endochondral ossification route through which the majority of the chondrocytes form skeletal elements (Pacifici, 1995).

Extensive work by Pacifici (1995) has provided strong evidence to suggest that tenascin-C (an ECM macromolecule) and syndecan-3 (a cell surface receptor) have roles in not only developing synovial joints, but also articular cartilage specifically. Chiquet and Fambrough (1984) initially identified tenascin-C as a factor involved in joint development as it had been found to be rich at boundaries between different adjacent tissues and structures. In the case of the synovial joint, the formation of this boundary; the interzone, is what leads to the creation of distinct skeletal elements. Tenascin-C was also found to maintain cells in a round configuration which is characteristic of chondrocytes that give

rise to articular cartilage and unlike growth plate chondrocytes which are flat and irregularly shaped (Chiquet-Ehrismann et al., 1988, Howlett, 1979, Lutfi, 1974). It was also found that tenascin-C has the ability to interact with a variety of cell surface receptors, including syndecan-3; a component that had previously been shown to be expressed by limb prechondrogenic condensations (Gould et al., 1992, Salmivirta et al., 1991). Based on these findings, several authors pursued this work with the aim to develop a greater understanding of the roles and involvement of these macromolecules in joint development (Koyama et al., 1995, Pacifici, 1995, Pacifici et al., 1993). Experiments in chick embryo unveiled that at day 6-6.5 of embryogenesis, syndecan-3 gene expression was strongly expressed by perichondral cells around the border of the diaphysis. Tenascin-C gene expression was weaker than that of syndecan-3, and particularly evident in the inner layer of the diaphyseal perichondrium (Pacifici et al., 1999). Throughout development as separation of the skeletal elements occurs, there is a gradual increase of tenascin-C at the epiphyses with levels reducing at the diaphyses. At later stages, when articular and growth plate chondrocytes emerge at the epiphyses (day 18 in chick embryogenesis) tenascin-C becomes extremely abundant but confined to articular chondrocytes, precisely delineating boundaries between structures. At this same stage, syndecan-3 is absent from articular chondrocytes, yet evident in the region of proliferating chondrocytes in the top zone of the growth plate (Pacifici, 1995, Pacifici et al., 1993, Savarese et al., 1996). As previously mentioned tenascin-C maintains chondrocytes in their stable round configuration allowing for the preservation of a normal phenotype throughout postnatal life (Pacifici et al., 1999).

There is no doubt a pattern of organisation throughout the growth and development of articular cartilage; the uncertainty lies in what triggers these mechanisms. In the late embryo, articular chondrocytes are rounded, randomly dispersed throughout the tissue, display low mitotic activity and are separated by a relatively low amount of extracellular matrix (ECM) (Howlett, 1979, Lutfi, 1974). Mature articular cartilage on the other hand has a distinct, structured organisation and a relatively high matrix-to-cell ratio. It is also well documented that when cartilage matures, tissue thickness and overall cell density also decrease (Stockwell, 1979). The spatial and temporal patterns of matrix components have also been studied. As such there is a distinct shift from an immature isotropic structure to a highly anisotropic mature articular cartilage (Archer et al., 1996, Morrison et al., 1996).

Collagen expression is not overly dynamic throughout the development of articular cartilage. Type I collagen is initially detected throughout the presumptive articular cartilage, however it is not detected in later stages following maturation of the tissue. Type II collagen is ubiquitous throughout the cartilage matrix. Type V collagen is seen pericellularly together with type III collagen during cavitation, and then within the articular cartilage following cavitation resulting in the suggestion that the chondrogenous cells of the interzone give rise to the articular cartilage (Archer et al., 2003). The gross collagenous structure of collagens within the tissue also changes as it develops, going from an arrangement that runs generally parallel to the articular surface, to the arrangement of the Benninghof 'arcade' pattern in which the fibre orientation develops perpendicularly from the basal region and arches over to run parallel to the articular surface (Benninghof, 1925). The presence of proteoglycans during the development of articular cartilage is highly varied depending on age, joint or species.

Despite the wealth of information above, the underlying question of how does the structure of articular cartilage develop, remains to be answered. Work by Mankin (1962) demonstrated how articular cartilage grew by a combination of appositional and interstitial growth following experiments on immature rabbit knees. Tritiated thymidine was incorporated as a marker for chondrocyte proliferation, showing the two bands of proliferative activity. The first lies just inferior to the articular surface and the second superior to the resident hypertrophic chondrocytes. Studies by Archer et al., (1994) confirmed that in the marsupial *Monodelphis domestica*, once a secondary centre of ossification begins to develop, growth of the presumptive articular cartilage does indeed become increasingly appositional. The tissue, with the exception of the articular surface, is renewed at or near the articular surface and is resorbed at the base through endochondral ossification during the establishment of the subchondral bone. This process is similar to the process that occurs at the epiphyseal growth plate; however it suggests the existence of an articular cartilage progenitor, or 'stem' cell residing within the articular surface (Archer and Francis-West, 1999).

Studies by Hayes et al., (2001) confirmed this notion of appositional growth in the development of articular cartilage. *Monodelphis domestica* knee joints were injected with bromodeoxyuridine (BrDU) which blocks chondrocyte proliferation after incorporation

into the DNA at S-phase. It was found that the transitional layer of cells usually present following normal development was absent, and that the cartilage comprised superficial and basal layers only. In addition to this, the expression of many growth factors and receptors present at the articular surface suggests the possibility that it represents an important signalling centre (Archer, 1994, Hayes et al., 2001). Members of the Notch receptor family; a group of cell surface signalling receptors which have the ability to regulate cell fate decisions, have been found to reside in the surface of bovine articular cartilage (Dowthwaite et al., 2004). This family of receptors is involved in a complex signalling pathway that regulates the elongation of the growth plate and ossification. Dowthwaite et al., (2004) demonstrated that there is a subpopulation of chondrocytes in the articular surface that expresses Notch-1, and that these cells may contain a progenitor population. Their work goes on to suggest that Notch-1 signalling functions to control proliferation in cartilage, based on work which shows that blocking Notch-1 signalling inhibits the formation of colonies by cartilage progenitor cells. The precise mechanisms involved in the Notch signalling pathway are yet to be fully established, and further work in this area would be fruitful in further understanding the development of articular cartilage.
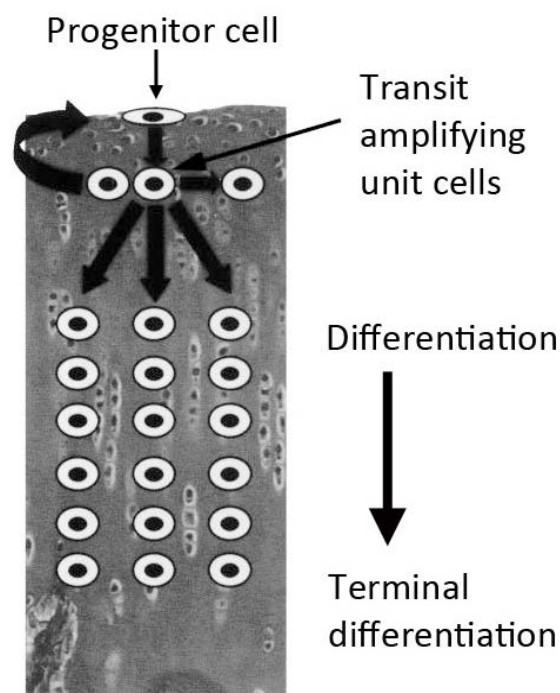
Figure 1.4. Diagram summarising hypothetical cell lineage of articular cartilage.

Progenitor cells in the articular surface divide to give two daughter cells, one being another progenitor cell and the second being a transit-amplifying unit cell within the transitional zone. The transit-amplifying cell can then undergo further cell divisions along the chondrocyte differentiation pathway. *[Image and figure legend adapted from Hayes et al., (2001)].*

1.4.2. Articular cartilage morphology

The structure of articular cartilage varies with the depth from the surface in terms of matrix composition, organisation and mechanical properties, as well as cell morphology and function (Buckwalter et al., 1990). This organised structure however can be affected and altered by age and pathology.

Articular cartilage has four distinct zones, the size and appearance of which varies between species, and in different joints within the same species (Hendren and Beeson, 2009). These zones are the superficial tangential zone (approximately 10 – 20% of the cartilage thickness), the middle zone (60% of the cartilage thickness), the deep zone (30% of the cartilage thickness) and the calcified cartilage zone. The shape and orientation of chondrocytes differ within these four regions, as does the content and organisation of collagen and other macromolecules. In the superficial zone, the chondrocytes are flattened and the collagen content is relatively high; tightly organised in a tangential manner so that they are parallel to the joint surface. In the middle and deep zones, the chondrocytes have a more spherical appearance, and the collagen content decreases with increasing tissue depth. There are no distinct boundaries between the upper three zones with the morphological changes occurring gradually and through development.
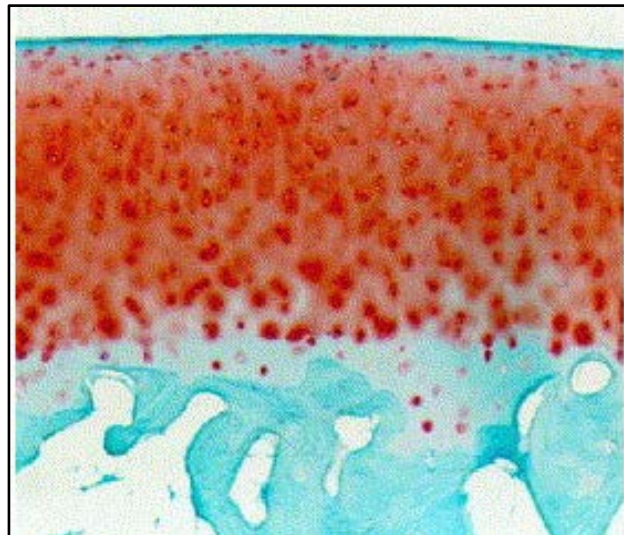
Figure 1.5. Normal human articular knee cartilage stained with safranin O/fast green.

Note the smooth surface, small and flat cells in the tangential zone; intermediate and radial zone cells are arranged in columns. The tidemark is intact. *[Image and figure legend adapted from Lorenz and Richter et al., (2006)].*

11

Superficial zone

The superficial zone is possibly the most important region in articular cartilage and it has sparked the most interest within researchers. Studies have shown that the superficial zone is centrally involved in the regulation of tissue development and growth and that this region plays a major role in the morphogenesis of the synovial joint as a whole (Ward et al., 1999). Expression of many growth factors and their receptors in this region suggests that the articular surface represents an important signalling centre (Archer et al., 1994, Hayes et al., 2001).

Despite the superficial zone being the thinnest zone, the structure and composition gives this region specialised mechanical and biological properties. It consists of two layers; an acellular layer and a deeper cellular layer of flattened, discoid shaped chondrocytes in a collagenous matrix. The chondrocytes arrange themselves so that their major axes are parallel to the articular surface. The matrix synthesised by these chondrocytes has a high collagen concentration and a low proteoglycan concentration when compared to other cartilage matrix zones. There is also an increased fibronectin content in this zone, which together with surface zone protein (SZP) and hyaluronic acid (HA), may have a role in joint lubrication and protection (Nishida et al., 1995).

The parallel arrangement of collagen fibrils in the superficial zone helps to determine the tissues mechanical properties as it provides the region with greater tensile stiffness and strength, and provides resistance to shear forces generated through movement and loading. The dense collagen network also functions to regulate the movement of molecules in and out of the cartilage. Removal of the superficial zone increases tissue permeability and increases loading of the deeper zones of the structural framework during compression (Setton et al., 1993). As such, it is thought that disruptions and/or alterations in this zone may contribute to the development of osteoarthritis (OA) by altering the mechanical behaviour of the tissue (Guilak et al., 1994).

Middle zone

The middle zone of articular cartilage is sometimes known as the transitional zone as the morphology and matrix composition of this region is intermediate between the superficial and deep zones. As previously mentioned it comprises approximately 60% of the cartilage thickness. The chondrocytes residing in this zone are spheroidal in shape and contain a higher concentration of synthetic organelles, endoplasmic reticulum and Golgi complex membranes when compared to the superficial zone chondrocytes. There is a higher proteoglycan content in this region but lower concentrations of water and collagen when compared to the superficial zone matrix. The collagen fibrils in the middle zone have a larger diameter relative to the fibrils of the superficial zone (Buckwalter and Hunziker, 1999).

Deep zone

The deep zone of articular cartilage is a progression from the middle zone, whereby the collagen fibril diameter is larger, the proteoglycan content in the ECM is higher and the water concentration is at its lowest. The cells remain spheroidal in shape, however they tend to arrange themselves into columns perpendicular to the joint surface (figure 1.6). The collagen bundles of this zone pass through the tidemark and provide and anchoring system between the non-calcified and calcified cartilage regions (Buckwalter and Hunziker, 1999).

The tidemark is a thin basophilic line that corresponds with the boundary between non calcified and calcified cartilage. It behaves as a mineralisation watermark demonstrating the advancement of the calcified layer to the articular surface (Havelka and Horn, 1999). The nature of this interface remains uncertain however it is of interest as it can be duplicated during osteoarthritis, suggesting the involvement of this region in the pathology of the disease.

Calcified cartilage zone

The calcified cartilage zone is a thin region that separates the non-calcified cartilage from the subchondral bone. Within this region the chondrocytes are smaller and rounded, and contain lesser amounts of endoplasmic reticulum and Golgi complex membranes, indicating a low metabolic state (Morris et al., 2002). The calcified cartilage/subchondral bone interface is known as the osteochondral junction.
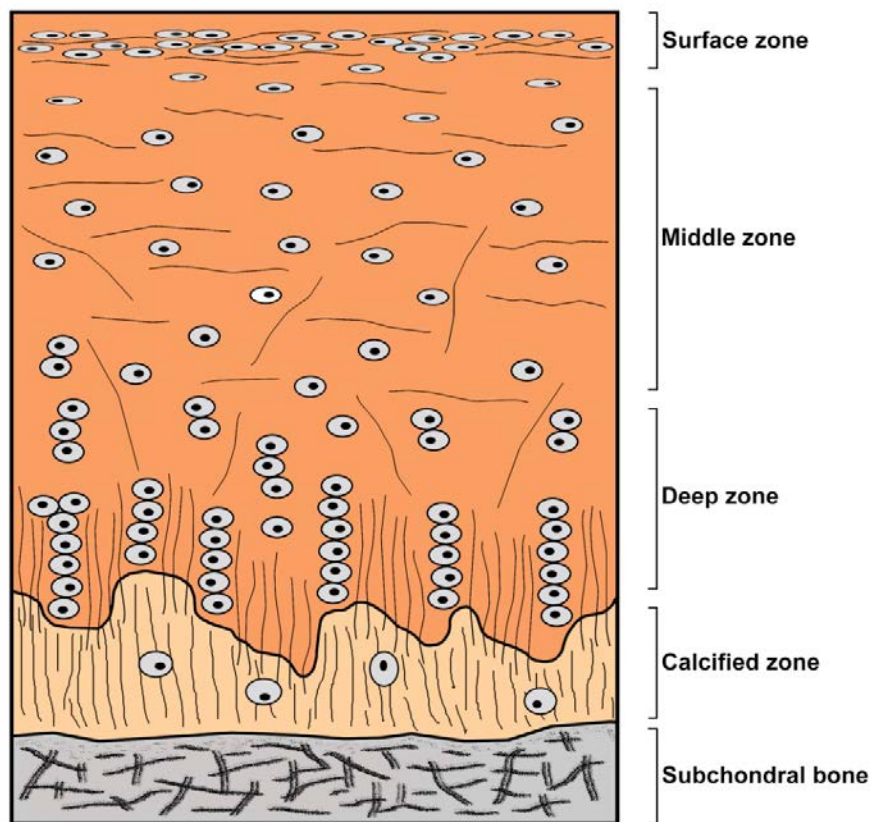
Figure 1.6. Diagram showing zonal variation in articular cartilage.

Articular cartilage is composed of four distinct zones: surface (superficial), middle, deep and calcified zones. *(Image kindly donated by Dr. Kirsty Richardson).*

1.4.3. Matrix regions

There are three major compartments through which the ECM can be organised. These are the pericellular, the territorial and the interterritorial matrix regions which were first described by Meachim and Roy (1967) and Meachim and Stockwell (1973). Together, the pericellular and territorial matrices provide protection to the chondrocytes from damage during loading and deformation of the tissue by binding the cell membranes to the matrix macromolecules. They also have a role in transmitting mechanical signals to the chondrocytes following loading. The function of the interterritorial matrix is to provide mechanical properties to the tissue (Buckwalter and Hunziker, 1999).

Pericellular matrix

The pericellular compartment is the region of variable width surrounding each chondrocyte. It is an area that is rich in proteoglycans synthesised by the chondrocytes themselves. The pericellular matrix is free of fibrillar collagens but contains non-collagenous matrix proteins and non-fibrillar collagens including collagens type VI and IX that form a fine meshwork of fibres (Hagiwara et al., 1993, Poole et al., 1992, Wotton et al., 1991). The cells membrane is attached to a thin rim of pericellular matrix, and cytoplasmic extensions from the cells project into and through this matrix to the territorial matrix (Buckwalter and Hunziker, 1999). A word that is commonly used is the 'chondron' which refers to the chondrocyte with its pericellular matrix, bounded by a capsule of fine fibrous material. The chondron forms a functional unit with the ability to absorb loads and provide protection for the chondrocyte (Poole et al., 1987). The pericellular matrix is adjacent to the territorial domain.

Territorial matrix

The territorial matrix contains a basket like arrangement of collagen fibrils that envelopes individual, pairs or even clusters of chondrocytes and their pericellular matrices, making them distinct morphologic entities. Thin collagen fibrils of the territorial matrix that are adjacent to cells adhere to the pericellular matrix, giving this basket like arrangement. The function of this matrix is similar to the pericellular matrix in that it serves as further

protection to the chondrocytes. The territorial matrix gives way to the interterritorial compartment. A distinct increase in collagen fibril diameter and a transition from the basket-like like orientation of collagen fibrils to a more parallel arrangement marks the conversion between the territorial and interterritorial matrices (Buckwalter and Hunziker, 1999).

Interterritorial matrix

This region constitutes the bulk of the extracellular space and can be characterised by a marked increase in fibril diameter. In this region, the collagen fibrils are not organised to surround the chondrocyte; instead the interterritorial matrix contains two populations, namely fibrils and fibril bundles, which are either arranged parallel to the surface forming arcade-like structures, or randomly oriented fibres (Buckwalter and Hunziker, 1999). The general orientation also varies depending on the location within the articular cartilage. In the superficial zone, fibril diameters are smaller and the fibrils generally lie parallel to the articular surface. In the transition from the middle to the deep zones, the fibrils convert from an oblique orientation (relative to the articular surface) to lying in bundles perpendicular to the articular surface. This arrangement of collagen fibres is known as the 'Benninghoff arcades' and was originally described by Benninghoff (1925).
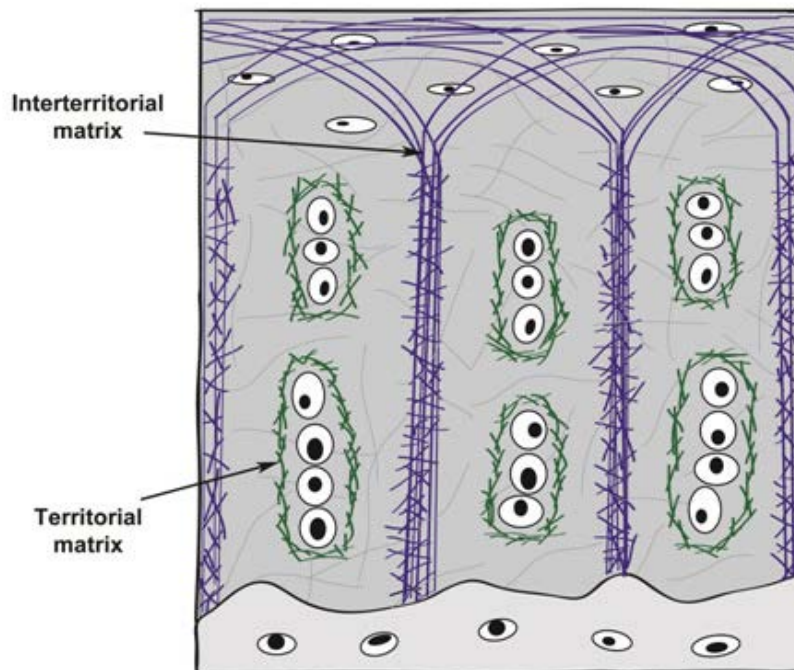
Figure 1.7. Diagram showing organisation of the fibrillar components within articular cartilage.

The territorial matrix contains a basketlike arrangement of collagen fibrils and organises chondrons into distinct morphological entities. The interterritorial matrix forms the bulk of the tissue. *(Buckwalter and Hunziker, 1999).*

1.4.4. Articular cartilage components

The chondrocyte

Chondrocytes are the sole constituent cell residing within normal articular cartilage. As such, they are responsible for synthesising major structural components including type II collagen, large aggregating proteoglycans and other less abundant proteins. They are also accountable for the highly organised ECM in which they are surrounded. Intracellularly, chondrocytes demonstrate typical features of a metabolically active cell, and comprise organelles such as endoplasmic reticulum and Golgi complexes. Chondrocytes may also possess short processes or microvilli; extending from the cell into the matrix, and playing a role in sensing mechanical changes in the ECM (Buckwalter and Hunziker, 1999).

Chondrocytes differ morphologically based on their orientation within the tissue. Cells reside singly at the articular surface, and appear flattened or discoid (Archer and Francis-West, 2003) when compared to cells in the middle zone which appear more spherical. In the deep region near the subchondral bone, chondrocytes are generally organised into columns which run perpendicular to the articular surface. As articular cartilage is not vascularised, chondrocytes rely on diffusion for nutrient and metabolic exchange. As such, this system leaves the chondrocytes with a low oxygen concentration (ranging from 10% at the surface to less than 1% in the deep layers) relative to other tissues and, therefore, the chondrocytes primarily rely on anaerobic metabolism (Archer and Francis-West, 2003). Consequently, chondrocytes usually have relatively low numbers of mitochondria and most of the cells energy requirements come from glycolysis (Buckwalter and Hunziker, 1999).

Despite the low metabolic activity of the chondrocyte, the cells must remain active as maintaining the articular surface requires turnover of matrix macromolecules. Joint use and biomechanical loading also influence the alteration in the matrix macromolecular framework.

Chondrocyte activity and function varies as articular cartilage matures. In immature articular cartilage, chondrocytes proliferate rapidly and there is a high cell density as the cells produce new tissue to expand and remodel the articular surface. With skeletal maturation, the cartilage thickness largely remains unchanged and instead, the chondrocytes work to maintain and/or replace degraded matrix macromolecules including the collagens, proteoglycans and non-collagenous proteins (Buckwalter, 1995a).

Cell distribution within mature articular cartilage is not uniform, and zoned differences are detectable and will be summarised later. One interesting hypothesis which was proposed by Stockwell (1975) was that there is a large proportion of chondrocytes at the articular surface and within the superficial zone, due to the proximity of the synovial fluid and its nutrients.

Extra-cellular matrix

The ECM of articular cartilage comprises two main components namely a framework of structural macromolecules and mobile, interstitial fluid. Together, these give rise to the tissue stability which account for the mechanical properties of the tissue as a whole (Buckwalter and Mow, 1992).

Interstitial tissue fluid

The fluid phase of the ECM consists of water and inorganic salts, and makes up between 70 and 80 % of the tissue wet weight. High concentrations of cations within the fluid interact with matrix macromolecules and balance out the negatively charged proteoglycans. This interaction is essential in maintaining mechanical properties of stiffness and resilience within articular cartilage (Buckwalter and Mow, 1992). There is a certain degree of mobility of fluid within the tissue which supplies nutrients to the chondrocytes and also aids joint lubrication (Buckwalter et al., 1990).

1.4.5. Structural macromolecules

Within articular cartilage the three classes of macromolecules; namely collagens, proteoglycans and non-collagenous proteins, together contribute to 20 to 40% of the overall tissue wet weight (Buckwalter et al., 1990). These are synthesised by chondrocytes from amino acids and sugar. The collagens provide a fibrillar frame in which the proteoglycans and non-collagenous proteins bind; and the interstitial fluid fills the molecular framework. The concentration of the macromolecules differs throughout the cartilage, as does their contribution to the tissue properties.

1.4.5.1. Collagens

The collagen network gives cartilage its form and tensile strength (Buckwalter and Mow, 1992), and accounts for approximately two-thirds of the dry weight of mature articular cartilage. Specifically, the collagens found in articular cartilage include types I, II, III, V, VI, IX, X, XI, XII and XIV, however the ratios of these macromolecules shift as the

cartilage develops. In mature cartilage, type II is the most abundant and accounts for 90% of the total collagen (Eyre et al., 1987).

Type I collagen

Type I collagen, a heterotrimer comprising two α1(I) chains and an α2(I) chain (Benya et al., 1978), is a fibrillar collagen that is present at the onset of chondrogenesis early in development (von der Mark et al., 1976). It is also present at the articular surface during development and in repair tissues. At the growth plate during endochondral ossification, type II collagen is replaced by type I collagen, which is secreted within the lacunae of hypertrophic chondrocytes (Leboy et al., 1988). In bone, type I collagen is reinforced with calcium hydroxyapatite providing tensile strength (Ayad et al., 1998).

Type II collagen

As mentioned, type II collagen is the principal articular cartilage collagen. It is a fibril forming collagen synthesised as a homotrimer; consisting of 3 identical polypeptide α1(II) chains that exists in two variants, IIA and IIB due to differential splicing (Ryan and Sandell, 1990). The two variants show differential distributions during development; with type IIA mRNA being expressed by perichondral cells and prechondrocytes, and type IIB mRNA expression in overt chondrocytes (Sandell et al., 1991). The type II collagen α chains are synthesised as procollagens, with non collagenous N- and C- propeptides. Through extracellular processing, proteinases cleave these terminal extensions and produce mature triple helices. Striated fibrils are assembled as a result of quarter staggering of individual molecules (Eyre, 1991). Type II collagen supports chondrocyte adhesion by binding through its helical domain with specific cell surface integrins (Holmvall et al., 1995). Integrins mediate the attachment of chondrocytes to the surrounding ECM macromolecules increasing the tissue integrity (Ruoslahti, 1991).

Type III collagen

Type III collagen, another fibrillar collagen is a minor collagenous component of articular cartilage. It is primarily associated with type I collagen, and the interaction between these

two collagens are thought to regulate fibril formation and fibril growth (Duance et al., 1999). Cross linking studies have also revealed that type III collagen co-localises with type II collagen as a minor, but regular component. The exact function of type III collagen in cartilage remains unknown; however there is speculation that it is synthesised by chondrocytes in response to matrix damage, perhaps as part of a remodelling process (Eyre et al., 2006).

Type V collagen

The importance of type V collagen in articular cartilage has not been extensively studied, however it is thought to be synthesised in small amounts. There is a high homology between type V and type XI collagen and, as such, there is evidence to suggest that there hybrid molecules exist (Duance et al., 1999). In several tissues, type V collagen appears to co-polymerise with type I collagen, where it may act to control fibril diameter (Birk et al., 1988). As type V collagen is also found in the meniscus, joint capsule and subchondral bone, it has been suggested that this collagen may have significant involvement on the normal functioning of the joint (Duance et al., 1999).

Type VI collagen

Type VI collagen is a microfibrillar collagen synthesised as a heterotrimer of three distinct chains (Timpl and Engel, 1987). Type VI collagen is preferentially located to the pericellular chondron of chondrocytes, where the microfibrils are stabilised by interaction with hyaluronan (Kielty et al., 1992). This collagen has also been shown to bind to the surface of many cells including chondrocytes (Marcelino and McDevitt, 1995). In osteoarthritis, increased type VI collagen expression has led to suggestions that it may have an involvement in tissue repair (Arican et al., 1996, Chang and Poole, 1996).

Type IX collagen

Type IX collagen is a cartilage specific fibril-associated collagen with an interrupted triple helix (FACIT). It is a heterotrimeric molecule comprised three different chains [α1(IX) α2(IX) α3(IX)], each consisting of three collagenous triple-helical domains (COL1-3)

separated by four non-collagenous domains (NC1-4) (figure 1.8). Unlike the fibrillar collagens, type IX collagen undergoes no processing before depositing into the ECM. In some cases, the α2(IX) chain contains an attachment site for chondroitin-sulphate at the non-collagenous region NC3 domain. As a result, type IX collagen is often described as both a collagen and a proteoglycan (Eyre et al., 1987, van der Rest and Mayne, 1988). Type IX collagen is always found in co-existence with type II collagen through covalent links, and it has been shown to modulate fibril formation by preventing close parallel alignment of the collagen type II fibrils (Wotton et al., 1988). The type IX collagen chains contain intermolecular cross-linking sites between type IX and type II collagen, or simply between type IX molecules (Eyre et al., 2004). The linkages formed contribute to the overall stability of the fibril network and help to resist the swelling pressure of the proteoglycans. In mammalian articular cartilage, amounts of type IX collagen decrease in relation to type II collagen with increasing cartilage maturity. It makes up approximately 10% of the collagenous content of foetal mammalian articular cartilage, and 1% in adults (Eyre, 1991). This has lead to postulations that type IX collagen contributes to the growth and fibre diameter of type II collagen.

Type X collagen

Type X collagen is a short-chain non-fibrillar homotrimer consisting of three α1(X) chains, with a short non-helical amino terminus, a single triple-helical domain and a globular C-terminal domain (Eyre, 1991). It is a cartilage specific collagen that is involved in localised regulation; the protein is highly restricted to ECM in the hypertrophic zone following synthesis by terminally differentiating chondrocytes (Schmid and Linsenmayer, 1985). It is thought that the function of type X collagen is to facilitate the process of calcification possibly through changes in the matrix organisation (Kwan et al., 1991).Due to the localised production of type X collagen in the matrix of hypertrophic chondrocytes at the growth plate, it is believed that it is of major importance in endochondral ossification. In mature hypertrophic chondrocytes, type X collagen constitutes 45% of the total collagen and is therefore often used as a marker for this type of cell (reviewed by Shen, 2005).

Type XI collagen

This collagen type, together with collagen type II and IX, forms a heteropolymer by covalent interactions that result in a fibrillar matrix that gives rise to mechanical stability (Mendler et al., 1989). Collagen type XI itself is synthesised as a heterotrimeric procollagen comprising three distinct proα1-3(XI) chains. It contains two collagenous domains (COL1-2) and three non-collagenous domains (NC1-3). Glycosylation of the triple helix creates a bulkier molecule that alters intermolecular spacing in the fibril. Alternative splicing of the N-terminal domains may influence interactions between other matrix molecules, resulting in fibrils to be stabilised at certain diameters (Duance et al., 1999). Type XI collagen also interacts with proteoglycans and the chondrocytes themselves, suggesting a direct involvement in cell-matrix interactions (Vaughan-Thomas et al., 2001).

Type XII and type XIV collagens

These collagens are members of the FACIT family, and are minor collagenous components of articular cartilage. Their functions are unknown, however both molecules form close associations with type I collagen. Despite being unable to form fibrils and do not affect fibril diameter, it has been suggested that they may "bridge adjacent fibrils or be involved in mediating matrix deformability through interaction of their NC3 domains with other tissue components (Duance et al., 1999).

A

TYPE XI   TYPE IX   TYPE II

B

NC4

COL3   COL2   COL1

NC2   NC1

α1(IX)
α3(IX)
α2(IX)

NC3

DISULPHIDE BONDS

CHONDROITIN
SULPHATE CHAIN

C

NC3

COL 2

pro α1(XI)
pro α2(XI)
pro α1(II)/α3(XI)

NC2   COL 1   NC1
(disulphide linked)
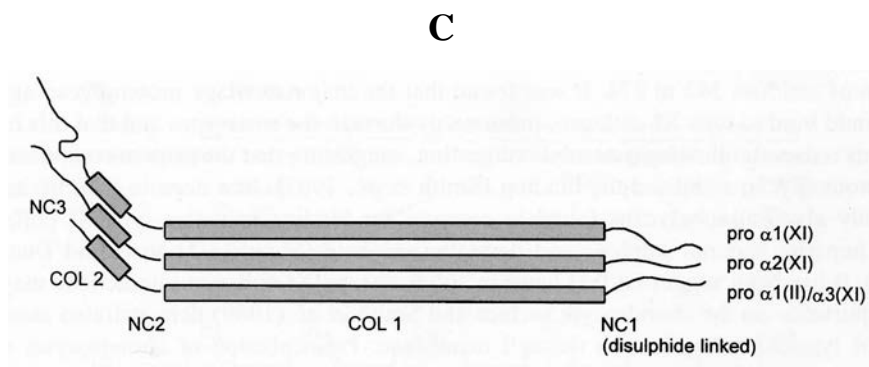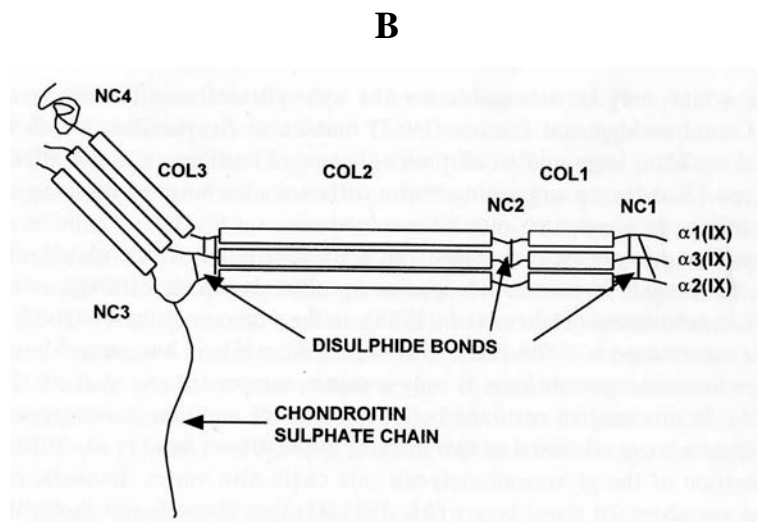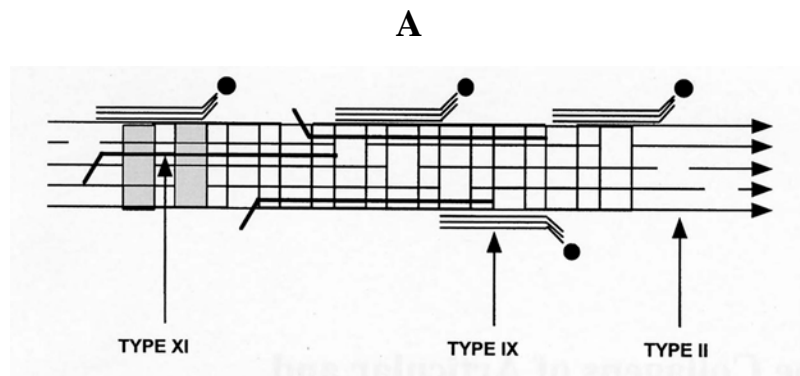
Figure 1.8. Schematic representation of the major collagen types present in articular cartilage.

A). Heterotypic fibril consisting of types: II, IX and XI collagen. B). Type IX collagen. C). Type XI collagen. *(Image taken from Duance et al., (1999)].*

1.4.5.2. Proteoglycans

Proteoglycans are ubiquitous components of the ECM, and are integral, key components underlying many interactions within the cartilage matrix. They are a diverse family of molecules comprising a core protein component to which one or more glycosaminoglycans (GAGs) covalently attach, giving them an extremely high negative charge. The anionic proteoglycans form domains with high osmotic pressure which have the ability to take in large amounts of water creating a high swelling pressure. Tension is created by collagen fibres resisting this swelling, and application of any load to the tissue simply leads to temporary minor deformations (Heinegard and Oldberg, 2002). GAGs are unbranched polysaccharide chains, with repeating disaccharide units containing a hexuronic acid and a hexosamine that is usually sulphated. It is through the negative charge on the carboxyl and sulphate groups that the GAGs gain their poly-anionic properties (Heinegard and Oldberg, 2002). The GAGs found within articular cartilage are hyaluronon (HA), chondroitin sulphate (CS), keratan sulphate (KS), dermatan sulphate (DS) and heparan sulphate (HS).

There are two major classes of proteoglycans within articular cartilage; namely large aggregating proteoglycans such as aggrecan and versican, and small, non-aggregating proteoglycans such as decorin and biglycan. The large aggregating proteoglycans have a high affinity for other matrix components leading to the formation of stable structures. The small proteoglycans can exist independently within the ECM.

Hyaluronic acid (HA)

Hyaluronic acid is a nonsulphated GAG that is composed of repeating disaccharide units of D-glucuronic acid linked to N-acetly-D-glucosamine which form large, negatively charged molecules (Rapport et al., 1951). It is an integral component of articular cartilage ECM and forms very large molecular aggregates due to its interactions with aggrecan and link protein. Cellular interactions between chondrocytes and HA also play an important role in organising the tissue and retaining the matrix PG-aggregants within the articular cartilage (Ishida et al., 1997). Early in development, HA plays a role in joint cavitation at diarthrodial joints, at the site of initial separation whilst also maintaining a regulatory role of movement (Pitsillides, 1999).

CD44 is a family of surface molecules expressed on many cell types including chondrocytes and it is the principal receptor for HA, implicated in many cellular functions such as mediating cell migration. Synthesis of HA is in part regulated by the TGF-β family of polypeptide growth factors and mis-regulation of CD44 can contribute to a number of disease pathologies (Isacke, 1994, Ishida et al., 1997).

Large aggregating proteoglycans

<u>Aggrecan</u>

Aggrecan is one of the major structural proteins of articular cartilage. It has a protein core of approximately 250kD and has between 100-150 CS chains and 60 KS chains (Kreis and Vale, 1999). The molecule is important due to its interaction with HA and link protein, which allow the formation of large, charged aggregates required for normal cartilage function (Holmes et al., 1988). It is believed that chondrocytes actively metabolise aggrecan throughout the lifetime of the tissue (Hascall et al., 1999).
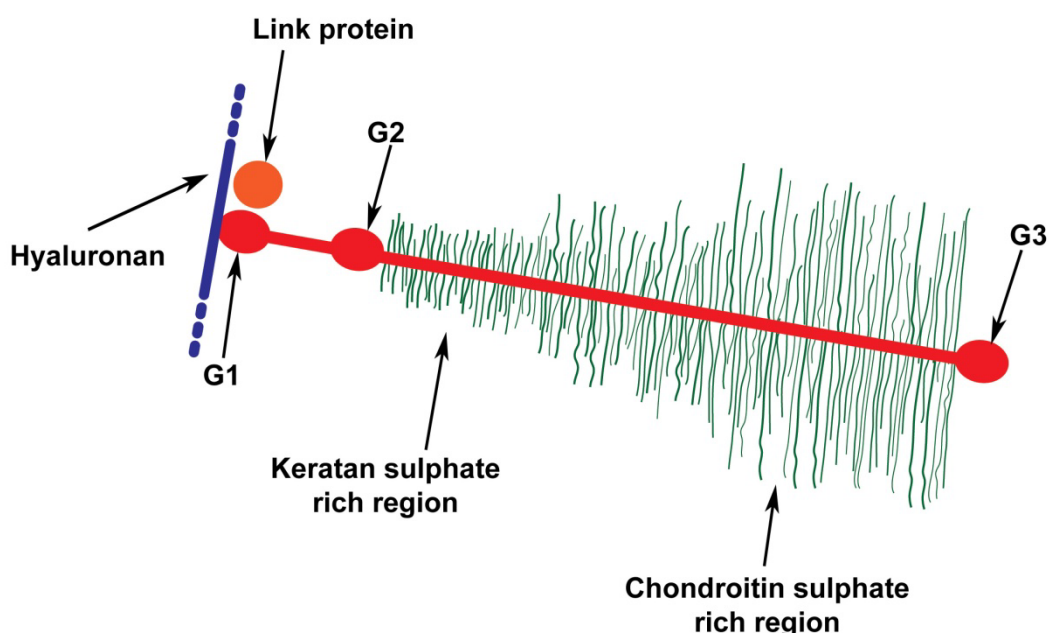
Figure 1.9. Schematic representation of aggrecan aggregate.

Diagram of proteoglycan aggregate comprising aggrecan, HA and link protein. *(Image kindly donated by Dr. Kirsty Richardson).*

Versican

Versican is another member of the large aggregating proteoglycans which is found transitorily within prechondrogenic condensations. As the cartilage develops, versican is removed and substituted with aggrecan (Hall and Miyake, 1995).

Small proteoglycans

Biglycan and decorin

Biglycan and decorin are members of the small leucine-rich proteoglycan family (SLRPs) consisting of a small 38kD leucine-rich protein core containing CS or DS chains. They account for only a small percentage of the ECM of articular cartilage. Biglycan contains two extended CS or DS chains whereas decorin has only a single CS or DS chain (Kreis and Vale, 1999). The functioning of the molecules is dependent on both the core protein and the GAG chains. The core proteins allow the molecules to interact with fibrillar collagens and in doing so, help to regulate fibril formation and ECM interactions. It is also evident that these SLRPs limit the access of collagenases to their cleavage sites on collagen molecules, protecting the fibrils from proteolytic damage. Biglycan and decorin have also been reported to interact with other macromolecules in modulating chondrocyte metabolism and regulation (Roughley, 2006).

Surface zone protein

Surface zone protein (SZP) is a proteoglycan that has been identified more recently to have an involvement in articular cartilage (Schumacher et al., 1994). It has been shown that SZP is widely distributed during development, however in the adult it is only synthesised by chondrocytes residing in the surface zone of articular cartilage (Flannery et al., 1999a). SZP has been classified as a unique proteoglycan based on its distinctive biochemical properties. It is thought that SZP is not retained in the ECM as it is also present in the synovial fluid. This has led to suggestions that it may be secreted by the superficial zone chondrocytes into the synovial fluid rather than being retained in the ECM like other proteoglycans. Another interesting factor is that its molecular weight is not altered

substantially following the removal of its GAG chains, indicating that it may only have few GAG chains on its core protein (Jay et al., 2001). Although the precise function of SZP is unknown, the structural composition of the protein allows for cell proliferation, cytoprotection and self-aggregation; attributes that are crucial for maintaining the articular surface during joint articulation (Flannery et al., 1999a). Furthermore, SZP is known to share sequence homology with lubricin, a proteoglycan involved in protecting the articular surface and aid in lubrication of the joint further suggesting its role in maintaining articular cartilage integrity during movement (Rhee et al., 2005).

Non-collagenous proteins and glycoproteins

In addition to collagens and proteoglycans, articular cartilage also contains a range of non-collagenous matrix proteins, some of which are specific for the tissue and some with a more ubiquitous distribution among connective tissues (Heinegard and Oldberg, 1989). As a whole, they consist primarily of protein, and have a few monosaccharides and oligosaccharides attached (Heinegard et al., 1995). Specific functions of these matrix macromolecules have been poorly studied, however it is believed that they are involved in matrix organisation, maintenance and cell-matrix interactions (Neame et al., 1999).

Fibronectin

Fibronectin is a glycoprotein of the ECM that binds to integrins and other matrix components. The protein has a major role in cell adhesion and is also involved in cell attachment, migration during embryonic development and wound healing, and the regulation of cell growth, differentiation and homeostasis (Pierschbacher and Ruoslahti, 1984). Fibronectin is also involved in cell signalling pathways via α5β1 integrin-mediated pathways (Burton-Wurster et al., 1997, Homandberg et al., 2002). In articular cartilage, fibronectin is synthesised by chondrocytes as a very minor constituent of the ECM (Heinegard and Oldberg, 1989), however it is also present in the synovial fluid at low concentrations. During disease, production of fibronectin is elevated by both chondrocytes and synoviocytes (Burton-Wurster et al., 1997).

Tenascin

Tenascin comprises a family of large ECM glycoproteins including tenascin-C, -X and –R. Tenascin-C contains a series of structural domains homologous to those of other proteins including fibronectin, however unlike fibronectin, tenascin-C possesses anti-adhesion and anti-spreading properties as well as the pro-adhesive effects (Chiquet-Ehrismann et al., 1988, Spring et al., 1989). Tenascin-C is involved in embryonic development where it is present in mesenchymal condensations, cartilage and bone (Erickson and Bourdon, 1989). Studies by Mackie et al., (1987) found that as mesenchymal cells differentiate, tenascin-C becomes detectable only in the perichondrium and undifferentiated chondrocytes. They also found that tenascin-C stimulated chondrogenic cell differentiation, probably via its ability to inhibit cell attachment and favouring a round cell shape. Further studies by other authors have revealed that tenascin-C resides within the pericellular matrix of cartilage where it functions by interacting with integrins and cell surface receptors such as syndecans (Salmivirta et al., 1991). In adult articular cartilage, tenascin-C expression is low and is confined to the surface zone and perichondrium (Chevalier et al., 1994, Salter, 1993). This is interesting as tenascin-C is not present in non-articular hyaline cartilage, leading to speculation that this glycoprotein may be involved in the load bearing properties of articular cartilage (Archer et al., 1990). Similar to fibronectin, expression of tenascin-C is elevated in diseased or damaged joints, yet the mechanisms of it involvement in disease remain to be fully elucidated (Salter, 1993).

Cartilage oligomeric matrix protein (COMP)

COMP is a cartilage specific acidic protein that is concentrated primarily within the chondrocyte territorial matrix. Although its functions are not fully understood, it is thought to be involved in cell adhesion via chondrocyte-matrix attachments (Hedbom et al., 1992). There has also been a suggestion that COMP may have a value as a marker of cartilage turnover and of the progression of cartilage degeneration in patients with osteoarthritis (Lohmander et al., 1994, Saxne and Heinegard, 1992, Sharif et al., 1995b).

1.4.6. Cartilage matrix turnover

Chondrocytes are ultimately the sole cell type responsible for the tissue homeostasis of normal articular cartilage. In the words of Hascall et al., (1999) "a chondrocyte in a normal matrix operates to maintain its matrix". This includes synthetic and catabolic events of matrix components as well as the incorporation and organisation of these components into the matrix.

1.4.6.1. Proteoglycans

Aggrecan, as previously outlined, is the major proteoglycan in the cartilage matrix that is metabolised throughout the lifetime of the tissue (Hascall et al., 1999). Its synthesis involves transcription and translation of mRNA, resulting in a protein core to which GAG chains are substituted post translationally. These molecules are released into the ECM where they form aggregates with HA (stabilised by the link protein). The HA is synthesised separately at the plasma membrane. Through a phenomenon known as delayed aggregation, secreted proteoglycans are able to first move away from the chondrocyte before forming aggregates. This occurs due to the G1 domain of the proteoglycan not being fully functional on secretion, and allows for the highly organised structure to be ordered appropriately (Bayliss and Roughley, 1985).

The catabolic mechanisms of aggrecan differ from that of the smaller proteoglycans; reflecting the distinctly different organisations of the two classes of proteoglycans. Having stated that, the key family of enzymes involved in the breakdown of proteoglycans are proteinases that are synthesised by the chondrocytes themselves. Matrix metalloproteinases (MMPs) are considered to be the main enzymes responsible for degradation of aggrecan (and collagens) in cartilage. The mechanisms of proteoglycan degradation are finely orchestrated in order to retain a precise balance between synthesis and degradation, as elevated levels of MMPs and increased degradation are factors which are thought to be instrumental in the development of pathology, including osteoarthritis (OA) and rheumatoid arthritis (RA) (Tetlow et al., 2001).

Ratcliffe et al., (1988) demonstrated that the major proteolytic cleavage site on aggrecan is between the G1 and G2 domains at the Glu^{373}-Ala^{374} bond, by aggrecanases. Since the discovery, aggrecanase-1 and -2 have been designated as ADAMTS-4 and -5 respectively as they fall into the family of zinc metalloproteinases whose structure is homologous to the ADAMTS (a disintegrin and metalloproteinase domain with thrombospondin motifs) gene family (Tang, 2001). It has been shown that ADAMTS-1 also exhibits aggrecanase activity in cartilage (Flannery et al., 1999b).

In order to regulate the fine balance of matrix degradation, tissue inhibitors of metalloproteinases (TIMP) are also produced locally by the chondrocytes to inhibit MMP activity. Specifically, TIMP-3 is a potent inhibitor of ADAMTS-4 and ADAMTS-5 and is therefore beneficial for protecting cartilage from degradation (Hashimoto et al., 2001, Kashiwagi et al., 2001).

1.4.6.2. Collagen

The family of collagens to date is comprised of 28 distinct molecular types produced by one or more genes. They are synthesised by transcription of specific mRNA's and then translated into α chains containing signal peptides, collagenous and non-collagenous domains. There are modifications of the procollagen polypeptide in the endoplasmic reticulum, including hydroxylation, glycosylation and disulphide bond formation. Interchain disulphide bonds between the carboxyl terminal propeptides align the chains and initiate the formation of the triple helix. The procollagen molecules then pass into the Golgi complex and are then secreted into the ECM in their proforms where they are processed by enzymes outside of the cell. The collagen molecules then aggregate into collagen fibrils through the formation of covalent cross links. The precise sequence ensures the incorporation of the collagens in the ECM in quarter staggered arrays. The aggregation of collagen fibrils through intrafibrillar crosslinks is known as fibrillogenesis (Alberts et al., 2002).
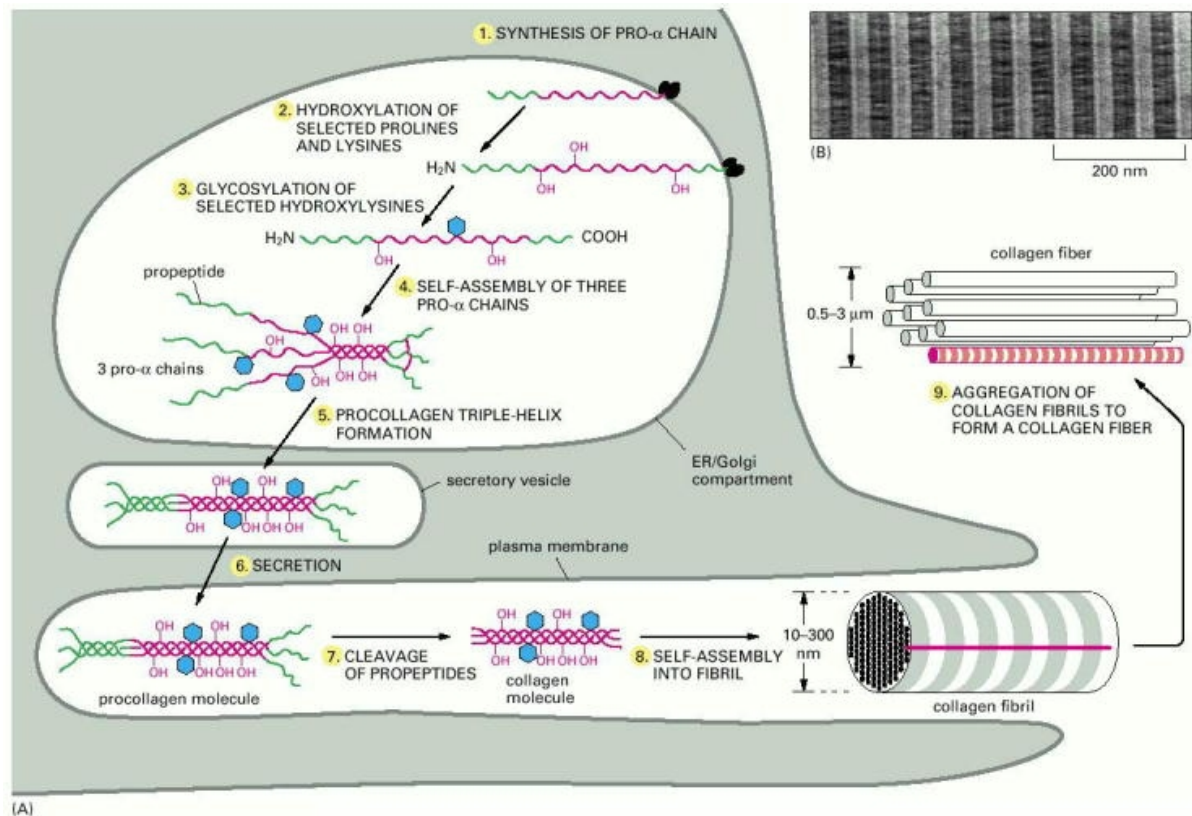
Figure 1.10. Schematic presentation of intra- and extracellular events in the formation of a collagen fibril.

(A) Collagen fibrils are shown assembling in the extracellular space contained within a large infolding in the plasma membrane. Here they are shown further assembling into large collagen fibres in the extracellular space. Covalent cross-links that stabilize the extracellular assemblies are not shown. (B) Electron micrograph of a negatively stained collagen fibril reveals its typical striated appearance. *[Image and figure legend taken from Alberts et al., (2002)].*

In adult tissue the turnover of collagen is controlled at a very slow rate (a process that can be dramatically accelerated following injury). Observations based on the synthetic rate of hydroxyproline have led to an estimated turnover time of 400 years for human femoral head cartilage (Maroudas, 1979), however, it has also been suggested that there is a possibility that a subfraction of the collagenous matrix is remodelled more rapidly in response to mechanical and molecular signals (Eyre, 2002).

In terms of degradation, collagens have a higher resistance when compared to the proteoglycans due to their tightly arranged fibrils and their interactions with glycoproteins.

According to Eyre et al, (2002) "the classical concept of collagen fibril degradation is through an initial cleavage of the collagen (type I, II or III) by collagenase into three-quarter and one-quarter length fragments". Collagenase -3 (MMP13), expressed by the chondrocytes, is the most active in cleaving type II collagen (Dahlberg et al., 2000). Having stated that an essential role for collagenases in all forms of collagen breakdown and turnover has become less certain following experiments using genetically engineered mice lacking a functional cleavage sequence, in which no abnormal phenotype was evident at birth and only mild skin and uterine abnormalities developed after birth (Krane et al., 1996).

1.4.7. Chondrocyte-matrix interactions

The reciprocal relationship and interdependence of chondrocytes and the ECM ensures that the articular cartilage is maintained throughout life. The chondrocytes synthesise the matrix which in return provides protection to the chondrocytes from mechanical damage during joint use. "Nutrients, substrates for synthesis of matrix molecules, newly synthesised molecules, degraded matrix molecules, metabolic waste products and molecules that help regulate cell function, like cytokines and growth factors, all pass through the matrix, and in some instances may be stored in the matrix" (Buckwalter and Mankin, 1998).

The cells are able to bind to the matrix macromolecules through specialised cell surface receptors including integrins, providing a means of transmitting signals between the two (Loeser, 2000). The exact mechanisms involved in controlling the activities between the chondrocytes and the ECM have not been fully elucidated, however it is thought that cytokines play important roles (Lotz et al., 1995). A few examples include i) interleukin-1 (IL-1) as it induces the expression of MMPs resulting in degradation of matrix molecules, ii) transforming growth factor-β (tgf-β) that opposes these catabolic activities by stimulating matrix synthesis and iii) basic fibroblast growth factor (bFGF) which acts as a powerful mitogen. It is thought that the anabolic activities are responses to certain structural needs of the matrix, whereas the catabolic activities are the result of "complex cascades that includes the activation or inhibition of IL-1, stromelysin, aggrecanase, plasmin and collagenase" by several macromolecules (Buckwalter and Mankin, 1998).

The ECM also acts as a mechanical signal transducer for the chondrocytes acting through a positive feedback mechanism. The matrix can transmit signals that result from mechanical loading to the chondrocytes, which as a result, respond to these signals by altering the matrix. Studies have demonstrated cyclic loading of the articular surface induces matrix synthesis whilst static loading causes matrix degradation (Quinn et al., 1998). Similarly, persistent abnormal decreases in joint loading decreases the proteoglycan content in articular cartilage consequently altering the mechanical properties of the cartilage (Buckwalter, 1995a). Following on from these studies it was found that resumption of normal joint use restored the composition and mechanical properties of the matrix, leading to the conclusion that "articular cartilage requires a minimum level of loading and motion of the joint"(Buckwalter, 1995b).

Upon mechanical loading, the resultant deformation of the matrix triggers physiochemical, mechanical and electrical signals that subsequently have roles in stimulating chondrocytic responses, whilst also altering or accelerating the flow of nutrients and metabolites throughout the ECM. As summarised by Buckwalter and Mankin (1998), "loading may also cause persistent changes in the molecular organisation of the matrix, altering the response of the chondrocytes to subsequent loading. Thus, the matrix may not only transduce and transmit signals, it may record the loading history of the tissue and alter the response of the cells on the basis of the loading history."

1.4.8. Integrins and receptors in cartilage matrix

Integrins are heterodimeric transmembrane glycoproteins that consist of α and β subunits, that act as cell surface receptors when attached to specific ECM components. Integrins have unique specificities that arise due to varying combinations of α and β subunits. There are over 20 known specific receptor combinations although the potential for further combinations are great. Integrins are widely distributed throughout the ECM, and are essential for many functions including cell adhesion, migration, signal transduction, mechanotransduction and matrix assembly. Through these cellular actions, integrins are involved in many biological responses including cell differentiation and proliferation, tissue organisation and immune response (Hynes, 1992). They recognise and bind their ligands by specialised cell attachment sites. Although many integrins have been reported

in articular cartilage (including α1β1, α3β1, α5β1, α10β1, αvβ3, and αvβ5) (Ostergaard et al., 1998, Salter et al., 1992), the expression of the α5β1 integrin has been found to be relatively high in relation to the others (Durr et al., 1993, Salter et al., 1995). This integrin functions largely as a fibronectin receptor involved in the adhesion and spreading of chondrocytes, as well as a major mechanoreceptor in the articular chondrocytes (Enomoto-Iwamoto et al., 1997, Ramage et al., 2009).

Annexin V, from the annexin family of matrix binding proteins has also been identified on the surface of chondrocytes (Mollenhauer et al., 1999). In cartilage it is believed to bind chondrocytes to type II and type X collagen by binding phospholipids in a calcium dependent manner (von der Mark and Mollenhauer, 1997). More recently, it has also been suggested that annexin V may also have a role in regulating chondrocyte metabolism (Reid et al., 2000).

CD44 is a transmembrane protein expressed by chondrocytes that serves as a hyaluronan receptor in articular cartilage. Binding of CD44 to hyaluronan regulates matrix assembly and retains proteoglycan aggregates in the chondrocyte pericellular matrix (Knudson, 1993). CD44 exists in a number of molecular weight isoforms; the extracellular domain and can be glycosylated or have CS or HS chains attached (Naot et al., 1997), whilst the cytoplasmic domain is involved in the regulation of ligand binding affinity (Isacke, 1994).

1.5. Degradation of articular cartilage

In healthy articular cartilage, despite the relatively low metabolic rate as a result of low cell density, there is a tightly regulated balance between synthesis and degradation. If disturbed however, the tissue lacks the ability to actively respond to damage, and is therefore hindered by its limited repair response (Bora and Miller, 1987). In 1743, Hunter stated that "an ulcerated cartilage is universally allowed to be a very troublesome disease and when destroyed, it is never recovered" (Hunter, 1743). Since then, despite numerous studies and strategies developed to combat the problem, this paradigm has not yet been disproved.

Damaged articular cartilage results either from trauma or injury, or from degeneration due to osteoarthritis; a degenerative disease of the joint which affects the cartilage, bone and surrounding tissues. These, however, are not isolated cases as cartilage damaged by trauma will quite often display early onset of osteoarthritis (OA).

Lesions as a result of injury can occur in people of all ages and can be classified into focal or large lesions; depending on size, or depth of the defects. However, ultimately, regardless of the size of the defect there is evidence clinically to suggest that when left untreated, lesions may develop into symptomatic joint degeneration (Buckwalter and Lohmander, 1994). Partial thickness defects are incapable of healing spontaneously and it has been suggested this is because they do not penetrate to the subchondral bone and, therefore, do not have access to progenitor cells within the bone marrow space (Redman et al., 2005). In full-thickness defects, the lesion passes through the tidemark to the calcified cartilage and penetrates the subchondral bone, allowing access to the bone marrow constituents. Compared with the partial-thickness defects, there is a more extensive repair response triggered by this type of defect, commonly resulting in the formation of a fibrocartilagenous tissue that does not integrate well with the native tissue, and that forms a poor substitute for the original hyaline cartilage (Shapiro et al., 1993). Despite the poor reparative response, the knowledge that there appears to be some repair mechanism has resulted in the development of many operative procedures based on this idea (Redman et al., 2005).

1.6. Osteoarthritis

Osteoarthritis is a multifactoral joint disease through which progressive remodelling and degeneration occurs in articular cartilage and surrounding tissues (Wieland et al., 2005). It is the most common form of arthritis in the elderly and a major cause of pain, disability and dependence due to joint contractures, muscle atrophy and limb deformity (Buckwalter and Mankin, 1997). It was believed for many years the changes seen early in OA were age related, however it is now accepted that age is not the sole contributor to the development of the disease. Onset of OA may occur as a result of trauma or injury to the joint, subsequent to infection, as a result of aging or genetic disposition (Mobasheri et al., 2009).

According to Martel-Pelletier (2010), the joints most commonly affected by OA are in the thumb and fingers, hips, and knees; although the neck and the lower back are also affected.

OA is commonly characterised by the loss of articular cartilage, accompanied by attempted repair of articular cartilage, remodelling and sclerosis of the subchondral bone, and osteophyte formation (Buckwalter and Martin, 2006), however the disease is more widespread and also affects the meniscus and synovial membrane. It results from a breakdown in homeostasis due to "mechanical, biological, biochemical, molecular and enzymatic feedback loops" (Martel-Pelletier and Pelletier, 2010). The exact etiology of the disease is yet to be fully understood due to the nature of the disease, and as such, the progressive course of joint degeneration remains to be understood. In order to achieve a greater understanding, studies have been carried out on patients with OA however these studies are inherently hindered from the start for several reasons; a) once a patient seeks medical attention, the disease has passed the early stages and therefore doctors are often faced with late stage OA and early changes cannot be assessed, b) patients have different pain thresholds and so present to the doctor at different stages of the disease, and c) the course of the disease is not consistent between patients. As a result, many animal models have been developed in order to elucidate the course of OA, especially in the early stages. However, as with many animal models the findings are not always directly transferrable to the course of OA in humans (reviewed by Lorenz and Richter, 2006) .

1.6.1. Morphological and clinical signs of OA

Morphologically, articular cartilage displays discolouration and softening as it transforms from a firm, shiny white healthy cartilage to a dull, irregular off-white colour in OA (Matyas et al., 1999). The extent of damage is highly variable between patients, joints and even within a joint, due to different loading conditions within distinct regions.

Clinical signs of OA include joint space narrowing, the formation of osteophytes, changes to the subchondral bone including sclerosis and fibrillation of the cartilage. These are detected through x-rays, magnetic resonance imaging (MRI) and arthroscopically.

1.6.2. Pathophysiology of OA

As chondrocytes are the sole cellular component of articular cartilage, research often focuses on the role of the chondrocyte and changes in the cartilaginous compartment of the joint when looking into the pathogenesis of OA. As a result, much more is known about the changes that occur in the cartilage compared to the changes in the surrounding tissues.

1.6.3. Cartilage changes in OA

Progressive loss of the structure and function of articular cartilage is one of the typical features of OA. The progression of the disease can be divided into three overlapping stages. At the beginning, an imbalance between anabolic and catabolic processes leads to the overexpression of matrix degrading enzymes, consequentially resulting in a loss of collagen and proteoglycans from the matrix. This stage is also coupled with an increase in water content due to an increase in permeability, resulting in a reduction to the stiffness of the ECM (Martin and Buckwalter, 2002). In the second stage, chondrocytes proliferate and synthesise augmented levels of matrix molecules in an attempt to compensate for the damage, however enzymes and cytokines capable of degrading matrix macromolecules are also produced; further increasing the overall degradation. Cell clusters are formed as a result of chondrocyte proliferation, and a repair tissue of newly formed matrix is sometimes apparent. In the third stage, the reparative attempts are outweighed by degradation and the tissue lacks the ability to restore itself. There is a decline in chondrocytic anabolic and proliferative responses, concurrent with a progressive loss of articular cartilage (Lorenz and Richter, 2006). The end stage of the disease is reached when there is a complete loss of articular cartilage, and the joint consists of articulating surfaces of thickened subchondral bone.

1.6.4. Histological changes in OA

A recent review by Lorenz and Richter (2006) has outlined the histological changes in OA as summarised below.

In the early stages of OA changes to the cartilage surface are usually seen, as it changes from a smooth surface to an irregular one as a result of mild fibrillations in the superficial zone (McDevitt et al., 1977). As the disease progresses, cellular structure is altered and a loss of proteoglycans is evident (Fernandes et al., 1998). The discoid cells of the superficial zone become round and hypertrophic, before disappearing from the tissue and chondrocyte clusters with large nuclei become evident in the tangential zone.

In more advanced stages of OA, the cartilage surface is broken by large fissures which sometimes extend into the calcified zone (Pfander et al., 1999). Chondrocyte clusters are especially apparent around fissures and the organisation of the cartilage becomes completely disordered. The hyaline cartilage is replaced by a repair tissue resembling fibrocartilage, with fibroblast like cells (Miosge et al., 2004); and in some cases pannus overlays the cartilage (Shibakawa et al., 2003). Proteoglycan loss extends into the deep zone if not lost completely and the tissue shows signs of complete breakdown, where the bone becomes totally denuded of cartilage.

1.6.5. Molecular changes in OA

Changes can be assessed by various methods including immunohistochemical analysis, biochemical analysis as well as gene expression analysis; all of which help in gaining a greater understanding of the progressive changes seen in OA. Having said that the patterns seen through the different methods are similar and agreeable to one another.

1.6.6. Collagen changes in OA

During OA when cartilage metabolism is increased, type II collagen expression is increased in the deep zone and decreased in the upper cartilage regions (Pfander et al., 1999, Young et al., 2005). As OA progresses, type II collagen staining becomes apparent in the region of chondrocyte clusters, fibrillations and clefts (Miosge et al., 2004, Pfander et al., 1999). Collagen type I expression is known to be upregulated in OA, especially in the superficial zone where collagen type II is reduced (Pfander et al., 1999). Osteophytes, a common feature of OA also mainly consist of collagen type I, with an outer layer of collagen type III (Nerlich et al., 1993). Immunohistological labelling for collagen type VI

revealed an increase in the middle, mildly damaged cartilage regions, whilst the upper, more affected regions showed a loss of collagen type VI staining, concurrent with the reduced proteoglycan labelling (Hambach et al., 1998). Collagen type X expression is also altered in OA, as irregular distributions indicate a shift towards a hypertrophic phenotype. Type X collagen is seen predominantly around chondrocyte clusters, and in the deep regions of osteoarthritic cartilage (Boos et al., 1999, von der Mark et al., 1992). Disruptions to the minor collagens IX and XI that function to stabilise the collagen-fibril meshwork also lead to the weaker matrix seen in OA cartilage (Muir, 1986). Interestingly, the overall content of collagen remains unchanged (Appleyard et al., 2003), however, the ratios of collagens changes highlighting the altered balance between synthesis and degradation. A table summarising these changes through immunohistochemistry can be seen in table 1.1, adapted from Lorenz and Richter (2006).

Table 1.1. Immunohistological analysis of arthritic cartilage in relation to normal cartilage. *[Adapted from Lorenz and Richter, (2006)].*

	Early or mild OA		Advanced OA	
Collagen type I	↑	(Miosge et al., 2004; Pfander et al., 1999; Teshima et al., 2004; Young et al., 2005)	↑↑	(Miosge et al., 2004)
Collagen type II	↓	(Pfander et al., 1999; Young et al., 2005)	→	(Nerlich et al., 1993; Pfander et al., 1999)
	↑	(Pfander et al., 1999)	↓	(Nerlich et al., 1993; Pfander et al., 1999)
Collagen type III	↑	(Aigner et al., 1993)		
Collagen type VI	↑	(Hambach et al., 1998)	↑↓	(Hambach et al., 1998)
Collagen type X	↑	(von der Mark et al., 1992)		

↑ upregulated versus control, ↑↑ upregulated versus early OA, (↑) upregulated versus control only at distinct locations, → unchanged versus control, ↓ downregulated versus control, ↑↓ upregulated or downregulated versus control dependent on cartilage zone.

1.6.7. Matrix metalloproteinases and aggrecanases in OA

As a result of the increased cartilage metabolism, there is an enhanced production of degradative proteinase genes which is associated with the gradual loss of proteoglycans and type II collagen degradation. These include MMP -1, MMP-2, MMP-3, MMP-8, MMP-9, MMP-13 and MMP-14, together with the aggrecanases ADAMTS-4, ADAMTS-5 and ADAMTS-9 (Mohtai et al., 1993, Murphy and Nagase, 2008). In unison, these are responsible for the degradation of the cartilage matrix macromolecules. Despite the collagenases (MMP-1, -8 and -13) collectively acting upon collagen fibrils, they are specific to certain collagens and as such, they also have specific topographical locations, indicating that perhaps there is a selective process during OA. There is speculation that MMP-9 could be responsible for progressive cartilage changes in OA, as it is selectively expressed in the fibrillated cartilage (Aigner et al., 2003).

1.6.8. Other proteins & OA

There is also increased expression in regulatory proteins such as IL-1 and TNF-a; IL-Iβ is a major inflammatory cytokine that is capable of inducing chondrocytes to synthesise MMPs in OA joints (Pelletier et al., 2001). Expression of stress and apoptotic markers (including caspases 3 and 9), and transcription factors (including Sox9 and Runx2) are also elevated during the course of OA (Goldring and Marcu, 2009, Goldring et al., 2008).

COMP, one of the structural proteins in the ECM undergoes degradation during normal cartilage turnover, and fragments are released into the synovial fluid. An increase in these fragments in the synovial fluid has been linked to the early stages of OA (Lohmander et al., 1994). Similarly, other structural proteins including; cartilage matrix protein (CMP) and cartilage intermediate-layer protein (CILP) expression is increased in osteoarthritic cartilage (Okimura et al., 1997, Lorenzo et al., 2004). Fibronectin is also greatly increased in osteoarthritic cartilage (Brown and Jones, 1990). Through the words of Roughley (2001) "is it interesting that fibronectin fragments, resulting from proteolytic degradation, are able to propagate degradation of aggrecan at the same sites as expected for the action of aggrecanase (Homandberg et al., 1997). It has been suggested that the fibronectin

fragments that accumulate in the joint may stimulate the local production of inflammatory cytokines, such as IL-1, that upregulate aggrecanase expression."

1.6.9. TGF-β & OA

TGF-β has both pro- and anti-inflammatory properties, and although it is crucial in regulating vital cellular activities, active TGF-β is also markedly increased in the osteoarthritic joint. It is pivotal in the formation of osteophytes, and has the ability to stimulate MMP expression contributing to the degradation seen in diseased cartilage (Bertrand et al., 2010, Scharstuhl et al., 2002). In terms of pathways, the protective role of TGF-β acts via the ALK5 receptor and downstream signalling pathway SMAD2/3 resulting in increased TIMP, counteraction of IL-1 and overall prevention of hypertrophy. The destructive role of TGF-β occurs when it interacts with the ALK-1 receptor which signals to SMAD1,5,8 inducing MMP-13 and other degradative enzymes. As such, Davidson et al., (2009) recently demonstrated that in OA, there is a shift in receptor usage from ALK5 to ALK-1 emphasising the pathogenic role of TGF-β.

1.6.10. Syndecan-4 & OA

More recently, the transmembrane heparan sulphate proteoglycan syndecan-4 has been shown to be of pivotal importance for chondrocyte mediated cartilage breakdown in OA (Echtermeyer et al., 2009). Through the GAG chains, syndecan-4 interacts with ECM molecules including collagens, fibronectin and tenascin amongst others. It also acts as a receptor for integrins and for a number of growth factor receptors (Molteni et al., 1999, Tkachenko et al., 2005). Whilst other syndecans have also been detected in chondrocytes and in OA, syndecan-4 is of particular interest as it regulates mesenchymal cell function during tissue repair (Echtermeyer et al., 2001, Lim et al., 2003). A review by Bertrand et al., (2010) raises the question of whether syndecan-4 is functionally involved in the cartilage remodelling process during OA, as studies by the author have revealed that it is expressed in hypertrophic chondrocytes in OA, and that its inhibition by specific antibodies results in decreased activation of ADAMTS-5 (Echtermeyer et al., 2009). In summary, "syndecan-4 is a key player in cartilage degradation during OA, by regulating on the one hand, the expression of matrix degrading enzymes (MMP-3) by mediating IL-1

signalling and on the other hand, by directly binding ADAMTS-5 and thereby participating directly in cartilage degradation" (Bertrand et al., 2010).

1.6.11. Hypoxia inducible factor-2α (HIF-2α) & OA

New targets for therapeutic strategies are constantly being sought, and recent studies have identified transcription factor HIF-2α as a central mediator of OA development; induced by IL-1β and other pro-inflammatory cytokines. *In vivo* experiments have shown that ectopic expression of HIF-2α in mouse knee joints resulted in severe cartilage destruction, conversely mice in which HIF-2α was knocked down were found to resist degradation usually found in OA induction models (Yang et al., 2010). In OA patients, it was found that HIF-2α levels were elevated in damaged regions compared with undamaged regions. Parallel to this finding Saito et al., (2010) identified HIF-2α whilst screening for factors that induce collagen type X expression. Proinflammatory cytokines as well as nuclear factor kB (NF-kB) are upstream regulators of HIF-2α, and it is thought that mechanical stress might trigger OA by inducing the NF-kB signalling and therefore HIF-2α expression in joint cartilage (Flemming, 2010).

1.6.12. Mechanisms

Despite the breadth of knowledge regarding OA, mechanisms and pathways involved in the disease process have yet to be fully understood. It is often suggested that many of the changes occurring in the osteoarthritic process recapitulate changes which are seen early in development; including cell proliferation and differentiation. As such, many of the signalling pathways involved in cartilage development are now linked to OA process, including those induced by FGF, Wnt, BMP, TGF-β and hedgehog signalling (Chia et al., 2009, Dell'Accio et al., 2006, Lin et al., 2009, Lories and Luyten, 2005, van den Berg, 1995).

1.7. OA: a disease involving other tissues

1.7.1. Subchondral bone

There has been a recent surge in the number of articles relating to subchondral bone changes associated with osteoarthritis, challenging the previous concept that degeneration and erosion of articular cartilage is the primary pathological mechanism of OA. The subchondral bone is an active element during OA as it provides catabolic factors to the neighbouring cartilage; promoting abnormal cartilage metabolism. A study by Petersson et al., in 1998 demonstrated through biochemical investigation that the serum levels of factors released from cartilage and bone during the early stages of OA in humans suggested that the pathological processes in cartilage and bone did coincide. Evidence from other human and animal models have also shown not only that the subchondral bone and cartilage should be seen as an interdependent unit, but also that in certain cases, changes to the subchondral bone may precede the cartilage degeneration (Buckland-Wright, 2004, Johnson, 1962, Radin and Rose, 1986).

In support of an altered metabolism early in the OA process in the subchondral bone is that osteocalcin (a common marker of bone formation) and osteopontin (a bone specific matrix protein) levels in synovial fluid and serum respectively were significantly higher in patients with knee OA (Sharif et al., 1995a). As levels of serum osteopontin rise quickly following trauma, this implies that alterations in bone cell activity may occur quite early in the disease (Lajeunesse et al., 2003).

The alterations in the subchondral bone which are evident in OA include subchondral sclerosis (thickening), changes in the architecture of the trabecular bone, the formation of new bone at joint margins, known as osteophytes and the development of subchondral cysts. Histologically, there is also evidence of tidemark advancements and duplications associated with vascular invasions of the calcified cartilage from the subchondral bone (Martel-Pelletier and Pelletier, 2010, Petersson et al., 1998).

With regards to subchondral bone sclerosis, it is interesting to note that it is not accompanied by an increase in mineral density. The scleroses result from increased

stiffness and an increase in material density, but not bone mineral density. As such, subchondral bone demonstrates an increased osteoid collagen matrix and abnormal mineralisation patterns during OA resulting in overall hypomineralisation (Grynpas et al., 1991). There is speculation that abnormal collagen type I content, as a result of elevated TGF-β levels, is a major contributing factor leading to abnormal mineralisation (Couchourel et al., 2009). Type I collagen, a heterotrimer of α1 and α2 chains, is elevated in OA. The average ratio of alpha chains in normal bone is 2.4:1; however studies have shown that in OA this ratio varied between 4:1 and 17:1 (Bailey et al., 2002). As summarised by Lajeunesse et al., (2003) "a reduction in α2 chains may lead to a tighter packing of collagen fibrils and, coupled with the reduction in cross-links observed in bone tissue (Mansell and Bailey, 1998) and the overhydroxylation of lysine in collagen fibrils (Bailey et al., 2002), may explain the reduction in bone mineralisation."

1.7.2. Synovial membrane

Through enzymatic feedback loops, the synovial membrane and surrounding tissues maintain an equilibrium to ensure normal homeostasis is achieved. In OA, this equilibrium is disrupted and pro-inflammatory cytokines are activated in an attempt to counteract the destructive changes in the neighbouring cartilage. This in turn results in an increased response by the synovial membrane and as such, a vicious circle is created.

IL-1β and TNF-α production by the synovial membrane are key perpetrators in the development of OA (Smith et al., 1997). IL-1β stimulates proteolytic and catabolic pathways of ECM degradation whilst also suppressing the anabolic pathways. As such, IL-1β can either decrease the synthesis of essential matrix macromolecules including collagen type II, or increase collagens which are not usually associated with normal articular cartilage; contributing to the loss of strength seen in diseased cartilage (Goldring et al., 1988). Other pro-inflammatory cytokines such as IL-6 as well as some chemokines such as IL-8 are also considered to be potential contributing factors in the pathogenesis of OA; however the precise roles in the process have yet to be established (Martel-Pelletier and Pelletier, 2010).

Histologically changes can also be seen in the synovial membrane from patients with all grades of OA. These include thickening of the lining layer, increased vascularity coupled with inflammatory cell infiltration (Smith et al., 1997).

1.7.3. Meniscus

An integral part of the biomechanical system of the knee joint is the meniscus. It is not only essential for the distribution of axial forces but also for the absorption of shock. Meniscal extrusion and menisectomy both modify the pattern of load distribution, leading to compartmental instability (Thompson et al., 1991). Meniscal extrusion is frequently associated with established knee OA (Berthiaume et al., 2005) and consequently, the femoral and tibial bone surfaces are faced with increased susceptibility of OA during dynamic movements of the knee.

1.8. Repair

Achieving successful repair of articular cartilage is an ongoing battle that has faced scientists and surgeons for decades. As the tissue is avascular, aneural and alymphatic it lacks the ability to actively respond to damage, and is therefore hindered by its limited repair response (Bora and Miller, 1987). Hunter, in 1743 claimed that articular cartilage 'once destroyed, is not repaired', and this observation directed many of the early treatments aimed to alleviate pain and discomfort, and allow greater movement as opposed to repairing the cartilage itself. More recent treatments involve surgical interventions aimed at inducing repair (Hunziker, 2001).

1.8.1. Surgical interventions

Strategies have developed from basic surgical techniques into technical methods which combine current knowledge of chondrogenesis and pathogenesis together with advances in tissue engineering.

1.8.2. Conservative strategies

Arthroscopic repair procedures represent more conservative and less invasive treatments for damaged cartilage; at the expense of effectiveness. Lavage and debridement are common methods used to alleviate pain, however are not known to biologically repair damaged tissue (Jackson and Dieterichs, 2003). Lavage involves irrigation of the joint (Livesley et al., 1991) and it is suggested that this irrigation process washes away active pain-signalling or pain mediating molecules, as well as removing proteoglycans from the superficial cartilage matrix (Hunziker and Kapfinger, 1998). There is still little evidence to show that this method does in fact initiate a repair response in damaged cartilage, and there is no evidence to suggest that lavage has symptom improving benefit. Debridement and shaving are also arthroscopic techniques, popularised by Magnuson in 1946 which aim to remove diseased or damaged tissue, allowing for a smoother surface and the consequent reduced friction at the joint interface (Chang et al., 1993). Apart from being a temporary method of pain relief, it is similar to lavage in that biologically it does not aid cartilage repair.

Other arthroscopic procedures involve bone marrow stimulation techniques, which require penetration of the subchondral bone (Gilbert, 1998). These techniques, namely abrasion arthroplasty, Pridie drilling and microfracture mimic full-thickness defects; potentially allowing for repair responses to be triggered within the damaged areas. It is believed that the underlying bone provides access to pools of various stem cells and growth factors which aid the reparative process (Shapiro et al., 1993, Rodan, 1992). Having stated that, these methods were used mainly for patients with painful conditions with the aim of bringing symptomatic relief and as such, the procedures are palliative, not curative, and the outcome is variable (Hunziker, 2001, Beris et al., 2005, Steadman et al., 2003).

1.8.3. More invasive strategies

Osteotomies are surgical procedures whereby the bone is cut in order to shorten, lengthen or change the alignment. This intervention is most frequently adopted to relieve pain, and to reduce or prevent the progression of osteoarthritis. Improving the joint alignment alters the biomechanics, inducing a change in contact areas. The aim is to alter the forces so that

weight is transferred through an area of healthy cartilage, resulting in less pain following joint movement (Arnoldi et al., 1971). Another important aspect of osteotomies are that they induce focal bleeding, which is followed by a localised healing response and a change in the pattern of vascular supply to the joint. It is also common for surgeons to combine osteotomies with other surgical procedures such as debridement, or Pridie drilling in an attempt to trigger a more extensive repair mechanism. In fact, there have been reports that osteotomies lead to the formation of a new articular surface however results are variable among patients (Buckwalter, 1999).

1.8.4. Surgical interventions: introducing materials

1.8.4.1. Autologous tissue grafts

Perichondrial and periosteal grafts involve transplantation techniques where tissue is grafted into full-thickness articular cartilage defects. This procedure began in the 1970's as a method of inducing repair of damaged articular cartilage. The underlying principle behind this technique was based on the knowledge that the cambial layer of periosteum and perichondrium exhibits continuous chondrogenic activity attributed to its chondrocyte precursor cells (Cohen and Lacroix, 1955). It is believed that when a graft is laid on a full depth articular cartilage defect, these precursor cells that reside in the germinative cambial layer are capable of reactivation; and proliferative and differentiation activities trigger the cartilage repair response (Hunziker, 2001, O'Driscoll, 1999). As periosteum is more obtainable it is used more frequently than perichondrium (Beris et al., 2005). In human patients, clinical results have not been totally successful mainly due to poor integration observed at the interface between the graft and the native tissue, and the low proliferative activity of repair cells; thus failing to restore the hyaline articular cartilage. Graft calcification is also a frequent occurrence contributing to the numbers of unsuccessful treatment attempts (Minas et al., 2009). Surgical procedures have been modified to try to combat the practical problem of graft detachment using sutures or glue, however, results have varied and have been inconclusive.

1.8.4.2. Osteochondral transfer

Autogenic and allogenic transfer of osteochondral plugs forms the basis of this procedure. Autogenic osteochondral transplantation, commonly known as mosaicplasty is employed mainly for smaller sized cartilage defects (Jakob et al., 2002). The process involves removal of cylindrical plugs from non-weight-bearing regions, and their transplantation into the debrided full depth cartilage (Hangody et al., 1997). Frightfully little research went into investigating this procedure and its effectiveness and destructiveness before it was applied clinically in human patients (Hunziker, 2001). Results have suggested short term benefits, including decreased pain and increased joint function, however, there are also many problems and questions raised regarding this intervention (Jakob et al., 2002).

Allogenic transfers use tissue derived from cadavers in an attempt to repair large osteochondral defects, on the basis that large volumes of tissue can be retrieved. This approach aims to simply provide a substitute for damaged or lost articular cartilage, and does not aim to induce a repair response.

1.8.4.3. Repair of articular cartilage using tissue engineering

Tissue engineering, as described by Hunziker (2001) can be defined as the art of reconstituting mammalian tissues both structurally and functionally. Usually, there are three main components which form the basis of tissue engineering; a matrix scaffold that provides a suitable surrounding, appropriate cells, and the addition of signalling molecules, such as cytokines and/or growth factors (Kuo et al., 2006).

One of the most commonly recognised methods of cartilage repair using tissue engineering is the autologous chondrocyte transplantation method which was introduced in the 1970's by Bentley et al., (1971) using partial-thickness defects of a rabbit model, and was transferred into human clinical practice in 1994 (Brittberg et al., 1994). The procedure initially involves the excision of healthy articular cartilage from a non-weight-bearing region of the joint, which is subsequently enzymatically digested in order to release chondrocytes from the extracellular matrix. The cells are then expanded in culture until there is a sufficient concentration of cells to fill the defect. A second surgical procedure is

then carried out which involves debriding the lesion back to the point of healthy cartilage, and taking a periosteal graft from a nearby location. The graft is then sutured over the defect, creating a flap under which cells can be securely injected. Fibrin glue is also added to seal the graft and further prevent cells from floating away (Brittberg, 1999).

Results from this treatment have been fairly consistent and there is a general acceptance that reduced pain and improved joint function are achieved. Histological analysis has shown, however, that there are variations in the efficiency of inducing repair with hyaline like cartilage at different locations (Breinan et al., 1997). Other varying results suggest there may be a difference in the short term but no significant improvements in the long term. Overall, the effectiveness of this technique has been justifiably questioned, and results have been varied and inconclusive. Additionally, there is not one consistent technique but rather variations of a common theme, making comparisons and conclusions often hard to draw. Even though autologous chondrocyte transplantation (ACT) is a widely used technique for repairing cartilage there are major factors that need to be given consideration. These include donor site morbidity, chondrocyte de-differentiation *in vitro*, and fibrocartilage formation as opposed to hyaline cartilage repair (Csaki et al., 2008).
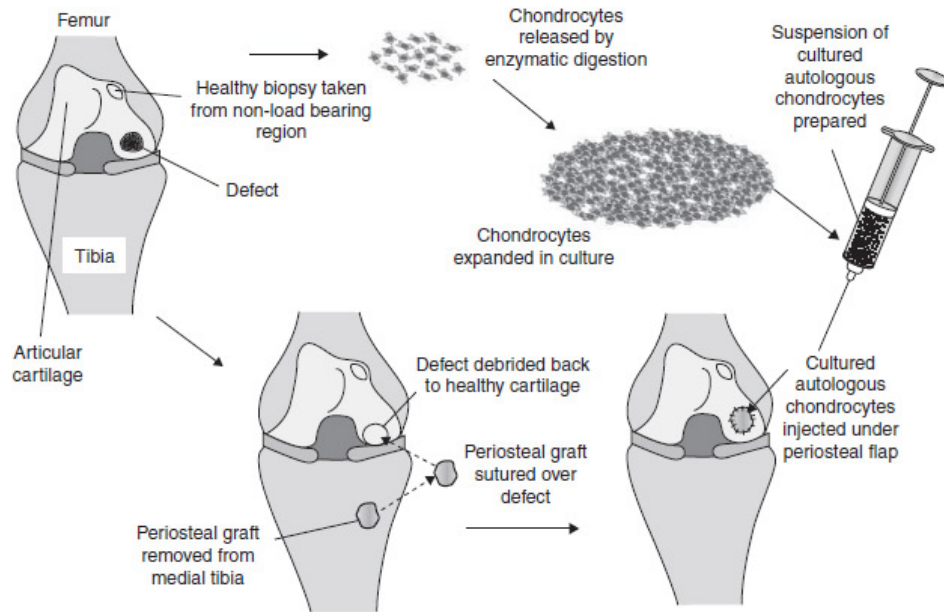
Figure 1.11. Schematic diagram showing the different stages involved in the process of autologous chondrocyte transplantation. *[Adapted from Redman et al., (2006)]*

1.8.4.4. Scaffolds

Since the introduction of the conventional ACT, there have been many developments that have aimed to improve the effectiveness of the technique, in order to achieve successful repair of articular cartilage, using biocompatible structurally and mechanically stable scaffolds. The scaffolds create a three dimensional environment, in which chondrocytes can be loaded before being re-implanted in the defect and must, therefore, be reabsorbable and non-toxic for the cells (Tuli et al., 2003). There are natural as well as synthetic substances that are suitable for scaffolds used in cartilage engineering. Among the most common natural materials are collagen- and hyaluronan based matrices as they constitute native articular cartilage. Results have been encouraging, as preliminary clinical studies using Hyalograft C, a hyaluronan based scaffold, demonstrated 96.7% of the repair tissue formed to be similar to hyaline cartilage (Pavesio et al., 2003). The advantage of synthetic scaffolds is that the problem of possible immune reactions is eliminated.

1.8.5. Stem cells for cartilage repair

It is evident that despite extensive efforts to achieve successful repair of articular cartilage, there appears to be a missing ingredient hindering the process. Stem cells provide an alternative cell source with the potential for successfully regenerating cartilage, and have largely become the focus of many studies in cartilage repair.

Whilst the term 'stem cell' is used loosely, often it encompasses progenitor cells that have limited replicative capacity and restricted differentiation potential to certain lineages. True stem cells are undifferentiated cells with endless self-renewal capacity, and the potential for multilineage differentiation. They are also easily obtainable and expandable *in vitro* making them promising candidates as the necessary vehicle for cartilage repair (Caplan and Goldberg, 1999). Stem cells reside in various 'niches' in the embryo, foetus and adults, and can be recruited to repair and replenish dying or damaged tissue, without the immunological responses that often accompany allogenic grafts (Fuchs et al., 2004).

Stem cell plasticity has been confirmed in bone-marrow-derived MSCs, which have been successfully differentiated into various specific cell lineages such as cartilage, bone, tendon, adipose tissue and muscle (Caplan, 1991, Barry, 2003, Csaki et al., 2007, Minguell et al., 2001, Pittenger et al., 1999, Short et al., 2003). MSCs have also been isolated from other sources including umbilical cord blood, adipose tissue and peripheral blood (Zuk et al., 2002, Bieback et al., 2004, Huss et al., 2000). Once *in vitro* MSCs have the capability to retain their differentiation potential for several passages (Pittenger et al., 1999). The cells are characteristically fibroblast-like in morphology, and express several adhesion molecules and receptors; allowing them to bind to adhesive proteins on the plastic under culture conditions (Conget and Minguell, 1999).

Undifferentiated progenitor cells have also been identified in articular cartilage itself, presenting a very promising source for the regeneration of cartilage. Dowthwaite et al., (2004) demonstrated successful isolation of a specific articular cartilage progenitor cell from bovine tissue, using a differential adhesion assay described by Jones and Watt in 1993.

1.8.5.1. Chondrogenic differentiation of MSCs

Stem cells reside in what is known as a niche, a microenvironment encapsulating the cells and providing local and systemic signals for their regulation and maintenance. Scadden (2006) defines a niche as a specific anatomical location that regulates how stem cells participate in tissue generation, maintenance and repair, whilst saving the cells from depletion and protecting the host from over-exuberant stem cell proliferation. Elements of the stem cell niche include cellular components such as cell–cell interactions, acellular elements such as ECM components, growth factors and membrane bound molecules, as well as the physiochemical nature of the environment. The interplay between stem cells and their niche creates the dynamic system necessary for sustaining tissues, and for the ultimate design of stem-cell therapeutics (Scadden, 2006).

Adult stem cells remain in an undifferentiated state, and therefore, it is necessary to induce chondrogenic differentiation in culture conditions to achieve chondrogenic cells, using the knowledge of stem cell–niche interactions, chondrogenic development and cartilage homeostasis and function (Mobasheri et al., 2009). Chondrogenic differentiation, as described by Johnstone et al., (1998) requires a 3D environment, and the addition of various combinations of growth factors. Of the various cytokines and growth factors used to induce chondrogenesis, isoforms of the TGF-β family are the most common (Johnstone et al., 1998). Others include specific bone morphogenetic proteins (BMPs), fibroblastic growth factor-2 (FGF-2), IGF-1, as well as synthetic dexamethasone (Pittenger et al., 1999, Johnstone et al., 1998, Awad et al., 2003, Grigoriadis et al., 1988, Nixon et al., 2000, Shea et al., 2003, Tsutsumi et al., 2001, Zhou et al., 2004). The pathways and mechanisms of action behind these signalling molecules are yet to be fully understood. The addition of FGF-2 into MSC culture conditions is also believed to stimulate chondrogenesis, as it has been demonstrated that more cartilage-specific proteoglycans are produced with the FGF-2 supplement (Solchaga et al., 2005). Dexamethasone has been shown to be a powerful supplement, inducing chondrogenesis via the glucocorticoid receptor by enhancing stimulation of the TGF-β superfamily, and consequent collagen II and cartilage-specific proteoglycan production (Derfoul et al., 2006).

1.8.5.2. Applications of MSCs for cartilage repair

There are many ongoing studies that aim to elucidate the most effective application of MSCs for the repair or regeneration of articular cartilage. Of these, several aim to develop previous theories and several propose new ideas. Perhaps the simplest technique is intra-articular injection, whereby MSCs are isolated and injected into the joint space providing a pool of cells to aid the repair of damaged tissues. MSCs have also been combined with hyaluronic acid for intraarticular injections (Murphy et al., 2003). Lee et al., (2007) postulate that hyaluronic acid facilitates the migration and adherence of MSCs to the defect, and demonstrated how this treatment was effective in inducing a repair response in a porcine model. This method, however, does not anchor the cells to the region and may result in cell migration into the marrow cavity. Consequently, the intra-articular injection may only provide very short-term responses. The use of a scaffold or periosteal flap (used in ACT) aims to eliminate this issue, and retain the cells at the site of the defect. Using the concept of conventional ACT analogous MSCs have been isolated and expanded *in vitro* before being implanted back into a defect. Long-term results have been conflicting as some studies report the formation of new cartilage and others report tissue degradation (Murphy et al., 2003, Im et al., 2001). This is possibly because the implanted cells rely on local and systemic signals to integrate and differentiate into reparative tissue. Foreign, undirected MSCs may, therefore, have little influence on the repair or regeneration of cartilage and this may be the reason for the ambiguous results.

The logical progression, as carried out by Jiang et al., (2003) focused on inducing chondrogenesis of MSCs *in vitro* and implanting these directed cells back into the defect. The data from this study however was also unsatisfactory due to inconsistent results. Matrix-assisted MSC therapies using scaffolds to provide a suitable environment, are being studied extensively as in theory they could provide suitable mechanical and biochemical properties in which MSCs can be seeded. A review by Noth et al., (2008) has summarised an ideal scaffold, which should be biocompatible and biodegradable upon tissue healing, porous (to permit cell penetration), permeable (to allow nutrient delivery and gas exchange), adaptable to the mechanical environment, conducive to cell attachment and migration, and allow appropriate ECM formation and transmission of signalling molecules. However, to date, there are no scaffolds that fulfil all these requirements whilst

achieving integrated hyaline-like repair of tissue (Mouw et al., 2005). In many studies, there have been reports of hyaline-like cartilage formation together with fibro-cartilage formation; this is not the ultimate goal in terms of producing a totally viable repair tissue and, therefore, further developments are being sought. There is also the recurring problem of integration between the repair tissue and the native cartilage. A greater understanding of the underlying mechanisms of cartilage repair is needed in order to eradicate this problem.

Despite encouraging results, the methods described above present a few common problems. As MSCs and progenitor cells are isolated in small numbers, in order for any of the techniques to be effective there needs to be sufficient number of cells and these must, therefore, be expanded *in vitro* before being placed back in the defect. This raises issues of cell de-differentiation, genetic stability and pathogen transmission.

In terms of articular cartilage progenitor cells, several research groups have been able to identify a potential population of cells within both normal and osteoarthritic human articular cartilage (Dowthwaite et al., 2004, Alsalameh et al., 2004, Fickert et al., 2004, Williams et al., 2010) presenting a source of native cells with the potential to restore damaged cartilage. If and when the cells and mechanisms of activation are fully understood, the prospects of regenerative processes are high. This may either be *in vitro*, by means of expanding and inducing the cells into a chondrogenic repair response and then implanting the cells back using an appropriate biodegradable scaffold, cell suspension, or *in vivo*. Once a deeper understanding is achieved, it is possible that these native progenitor cells may by induced or triggered *in vivo* using minimally invasive methods of delivery.

1.9. Aims of the thesis

There is clinical evidence to suggest that under permissive conditions, hyaline cartilage has the capacity for recovery. That said, there is a longstanding view that osteoarthritic cartilage is deemed irreparable. This study therefore tests the hypothesis that the joint surface deemed clinically irrecoverable contains a sub-population of viable cartilage stem cells, which have the potential to regenerate.

The overall aim of this study was to investigate progressive changes during the osteoarthritic process whilst also investigating the presence and potential of chondroprogenitor cells within osteoarthritic articular cartilage.

This thesis therefore aims to:

1) Describe a new scoring system to assess osteoarthritis severity.
2) Map out histologically the progressive changes that occur throughout progression of the disease.
3) Correlate disease severity to expression of putative stem cell markers.
4) Determine whether chondroprogenitor cells previously documented in normal hyaline cartilage also reside in osteoarthritic tissue.
5) Isolate, clone and extensively cultivate osteoarthritic chondroprogenitor cells.
6) Assess whether clonally derived osteoarthritic chondroprogenitor cells have the capability to undergo tri-lineage differentiation *in vitro*.
7) Compare chondroprogenitor cells isolated from normal and osteoarthritic tissue.
8) Assess the integration potential of chondroprogenitor cells in a 3-d environment.

NOTE

This Chapter forms the basis of a review article published in Expert Opinion on Biological Therapy. See page 316.

Chapter 2:

A novel scoring system for osteoarthritis of the knee

2.1. Introduction

The preconceived notion, which is still widely accepted, is that OA is primarily a disorder of the articular hyaline cartilage. The onset of the disease however, is still a topic of much discussion. Many believe that OA is a result of a 'wear and tear' process, which causes the cartilage to degenerate whilst denuding the joint surfaces (Radin, 1976). Others believe that it is triggered as a result of abnormal loading to joints and that the cartilage changes result from altered joint biomechanics (Englund, 2010). There is also the view that structural changes in the matrix, together with intrinsic and extrinsic growth factors, cytokines and other signalling factors mediate the response to the cartilage (Goldring and Marcu, 2009). As chondrocytes are the sole cellular component of articular cartilage, research is often focussed on their role in the pathogenesis of OA. However, it is important to remember that within the joint the articular cartilage is in direct contact with the subchondral bone, the synovial fluid and the synovium. It is widely accepted and well documented that during the course of OA, changes occur in these surrounding tissues (Martel-Pelletier and Pelletier, 2010), and the question is often raised regarding the pre-eminence of the disease; does OA initially affect the articular cartilage or are there changes within other tissues that precede these? This is a challenging question as clinical signs are not always evident at the earliest stages of the disease and so initial changes are overlooked. Similarly, investigative studies often focus on changes in the later stages of the disease; unveiling little information about early changes and capping the potential for understanding the initial responses.

Of the neighbouring tissues, changes to the subchondral bone have triggered great interest within many research groups (Karsdal et al., 2008, Lajeunesse and Reboul, 2003, Li and Zhang, 2009, Mansell et al., 1997, Westacott et al., 1997). A review by Lajeunesse et al., (Lajeunesse et al., 2003) summarises how some bone parameters such as abnormal bone mineral density, osteoid volume, and bone mechanical parameters may be indicators of bone turnover relating to OA patients, and addresses the question relating to whether growth factors, degradative enzymes and cytokines from the subchondral bone may seep through channels in the tidemark and affect the overlying cartilage. As such, there is evidence to suggest that thickening of the subchondral bone precedes fibrillation of the cartilage within some animal models, as a result of increased resistance of the bone to

compression (Bailey and Mansell, 1997). Aside from the question of whether increased bone metabolism is a primary event triggering a cascade response resulting in cartilage destruction or *vice versa*, the role of the subchondral bone throughout the pathogenesis of OA is also a topic of great interest within many research groups.

Assessing the severity of OA

In order to assess the severity of the disease, clinicians and scientists have devised many scoring systems, each focussing on different combinations of pathological features characteristic of OA. Clinically-based scoring systems have evolved using techniques including magnetic resonance imaging (MRI), X-rays and arthroscopic evaluation in attempts to assess disease progression. These systems look specifically at joint space narrowing, prevalence of osteophytes and, more recently, detection of glycosaminoglycan (GAG) levels within the articular cartilage using MRI analysis (Ling et al., 2008). Research-based scoring systems focus on histological and histochemical parameters when assessing OA severity. Early work by Collins et al., (Collins and Mc, 1960) and Mankin et al., (Mankin et al., 1971) led to a system for pathological grading of cartilage changes in relation to OA. Since then, many systems for grading cartilage have been devised to assess not only OA severity, but also *in vivo* cartilage repair and *in vitro* tissue engineering studies. The most commonly used system in assessing OA severity remains the Mankin scoring system, often referred to as the Histological-Histochemical Grading System (HHGS). This system was originally designed for grading OA in human hip articular cartilage, scoring the structure, cells, safranin O staining as well as the tidemark integrity (Mankin et al., 1971). Several other similar systems have stemmed from the HHGS and are commonly known as 'modified Mankin' systems, which tend to be adaptations for individual studies. The HHGS together with its modifications have been used extensively in human studies as well as in animal models (Ghosh et al., 1995, Goodman et al., 1991, Kim et al., 1991). In terms of cartilage repair, the O'Driscoll, Oswestry and ICRS scoring systems are amongst the most frequently used (Mainil-Varlet et al., 2003, O'Driscoll et al., 1988, Roberts et al., 2003).

More recently, the OARSI Osteoarthritis Cartilage Histopathology Assessment system was devised with the aim to provide a more useful method of assessment through 'grading' and

'staging' articular cartilage. The severity and extent of cartilage surface involvement in the local osteoarthritic process is assessed and categorised from 'normal' through to 'severe' and from 'no OA activity seen' through to >50% of articular surface affected'(Pritzker et al., 2006).

Subchondral bone and articular cartilage as a unit

Despite the abundance in the literature linking changes of the subchondral bone to the degenerative overlying cartilage, when it comes to assessing the severity of OA by means of a histopathological scoring system these correlations are often overlooked. As aforementioned, the predominant parameters focus largely on the articular cartilage, however, being in direct contact with the underlying bone, it is likely that messages or signals have an uninterrupted pathway of communication.

The primary aim of this chapter was to devise a scoring system to assess the severity of OA, which incorporates changes of the subchondral bone. We hoped to confirm that the overall score obtained through the new scoring system was indicative of the degenerative state of the tissue as a unit, including the cartilage and subchondral bone.

The second aim was to correlate changes to the subchondral bone with changes in the cartilage-based parameters, in order to establish relationships between the two tissues and obtain a greater understanding of changes that occur throughout OA.

The rationale behind including the subchondral bone into a histological scoring system was not only to grade the unit as a whole without isolating one factor from the other, but also as a potential tool to be used and translated clinically. By correlating changes of the subchondral bone to the overlying cartilage, it may be possible to establish the pattern of change that occurs within the bone throughout the progression of the disease. Clinically, this could provide a basis for a tool for early diagnosis of OA, in a minimally invasive way using bone as a sole component for grading.

The third aim of this chapter was to assess the reproducibility of the scoring system by testing inter- and intra-observer variability.

2.2. Materials

Material	Catalogue number	Supplier
DPX mounting medium	RAYLLAMB/DPX	Raymond A Lamb Medical Supplies, Eastbourne, UK
10 % Formalin solution, neutral buffered Phosphate buffered saline Ethylenediaminetetraacetic acid disodium salt dihydrate	HT501128 P4417 E4884	Sigma Aldrich, UK
Paraffin wax pastilles	298682F	VWR – Jencons, Leicestershire, UK
Polysine adhesion glass slides	MNJ-800-010F	Thermo Fisher Scientific, UK

Table 2.1. Materials and suppliers.

2.3. Methods

2.3.1. Source of material

Tibial plateaux (TPs) were obtained from OA patients who underwent partial (unicondylar) or total (bicondylar) knee replacement. OA was diagnosed following physical, radiographic and biochemical examination. Tibial plateaux from male and female patients ranging from 45 to 85 years of age were used in this study. South East Wales Research Ethics Committee safety and ethical guidelines were followed. Written informed consent was obtained from each patient and extensive precautions were taken to preserve the privacy of the participants donating tissue. Following surgery, tissue was immediately transported from the hospital to the laboratory in sterile saline solution. Only tissue from the tibial plateaux were used for this study; cartilage and bone obtained from the femoral head were omitted in order to maintain consistency.
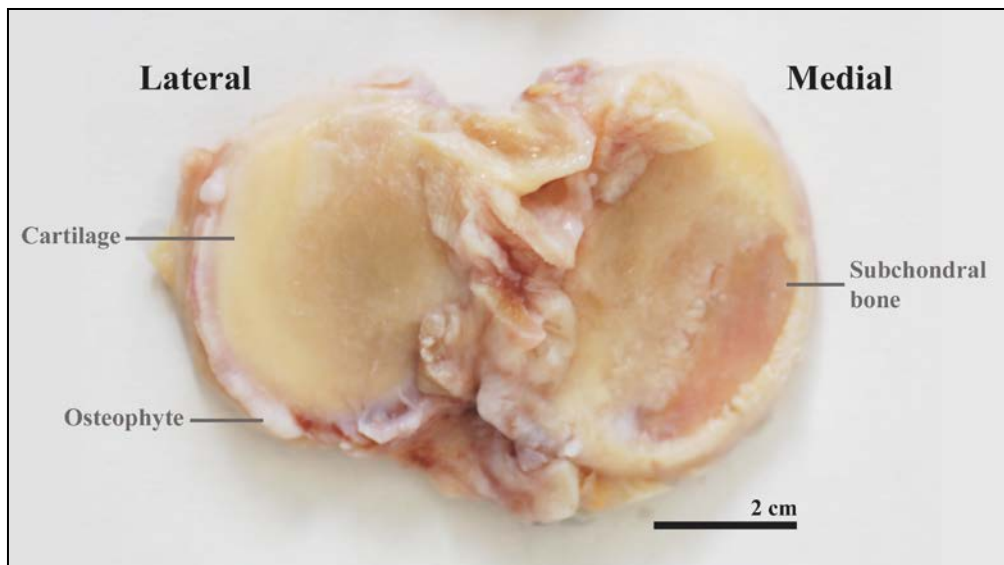
Figure 2.1. Labelled photograph of a tibial plateau excised from a total knee replacement. Scale bar = 2cm.

2.3.2. Fixation and decalcification

The tibial plateaux were fixed overnight in 10% neutral buffered formalin. Following fixation, they were washed in PBS (three changes of 10 minutes). Subsequently, they were decalcified in 12% ethylenediaminetetraacetic acid (EDTA) disodium salt dihydrate

solution at pH 7.5 for up to four weeks at 37°C. Every fifth day, the EDTA was discarded and replenished. Following decalcification, samples were washed in PBS.

2.3.3. Excision and paraffin embedding of osteochondral plugs

The tibial plateaux were assessed based on their topography; mapped and classified into regions of varying cartilage integrity (figure 2.2). These were then dissected using a sharp scalpel into osteochondral plugs (OCPs). The size of the plugs varied slightly in accordance to the size of the mapped region. From one tibial plateau approximately 4 osteochondral plugs were excised. However, this varied depending on the nature of the cartilage observed within each individual TP. The osteochondral plugs were then dehydrated in graded alcohols (70%, 95% and 100% x3) with changes of 60 minutes each before being cleared in xylene (two changes of thirty minutes), infiltrated with three changes of paraffin wax at 56°C and embedded in paraffin wax.
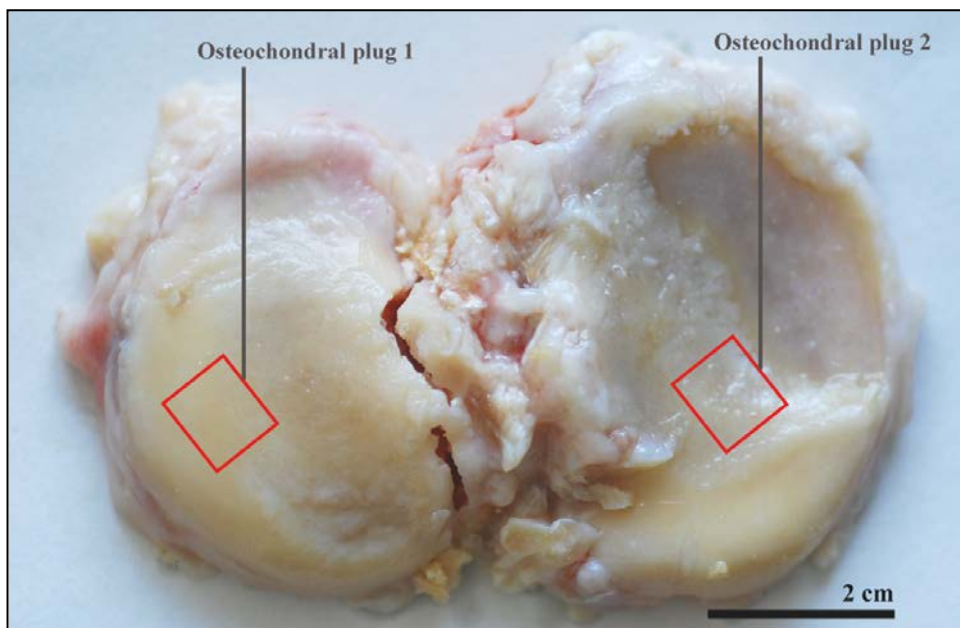
Figure 2.2. Photograph of a tibial plateau. Labelled red boxes demonstrate examples of mapped osteochondral plugs. Scale bar = 2cm.

2.3.4. Sectioning

Following embedding, serial sections were cut at 8µm on a Leitz 1512 microtome. Sections were floated on a heated water bath (45°C) before being mounted on polysine coated slides. The slides were air-dried for approximately 30 minutes on a heated rack and then dried overnight in an incubator heated to 45°C.

2.3.5. Staining of sections

Sections were dewaxed using xylene (two changes of 2 minutes) and rehydrated through a series of graded alcohols (two changes of 2 minutes in 100%, followed by one change of 2 minutes in 95% and 70%). The sections were then washed in running water for a further 2 minutes before being stained with Masson's trichrome (appendix). Following staining the sections were dehydrated through graded alcohols, cleared in xylene (two changes of 2 minutes) prior to being mounted under coverslips using DPX.

2.3.6. Microscopy and imaging

Slides were viewed using a Leica DMRB light microscope and imaged using a Moticam 2000 camera. Image processing was carried out using Adobe Photoshop (version 6.0.1).

2.3.7. Scoring the osteochondral plugs

A new scoring system was devised through which cartilage thickness, percentage of total bone area, tidemark integrity, cartilage surface integrity and cartilage morphology were assessed. Cartilage thickness and percentage of total bone area were assessed quantitatively using the method described below. This combination of features allows for a semi-quantitative assessment of the overlying cartilage together with the underlying bone. A criteria summary table for the qualitative factors can be seen in table 2.2.

2.3.7.1. Cartilage thickness

In order to determine the cartilage thickness, slides were imaged at the lowest possible magnification (x4). Three equally spaced points along the width of the section were measured in order to obtain an average thickness throughout the section. The measurement was taken from the surface of the cartilage horizontally down to the tidemark at the three locations (refer to figure 2.3). Calculating an average of the 3 measurements generates a value of cartilage thickness that can be used quantitatively.
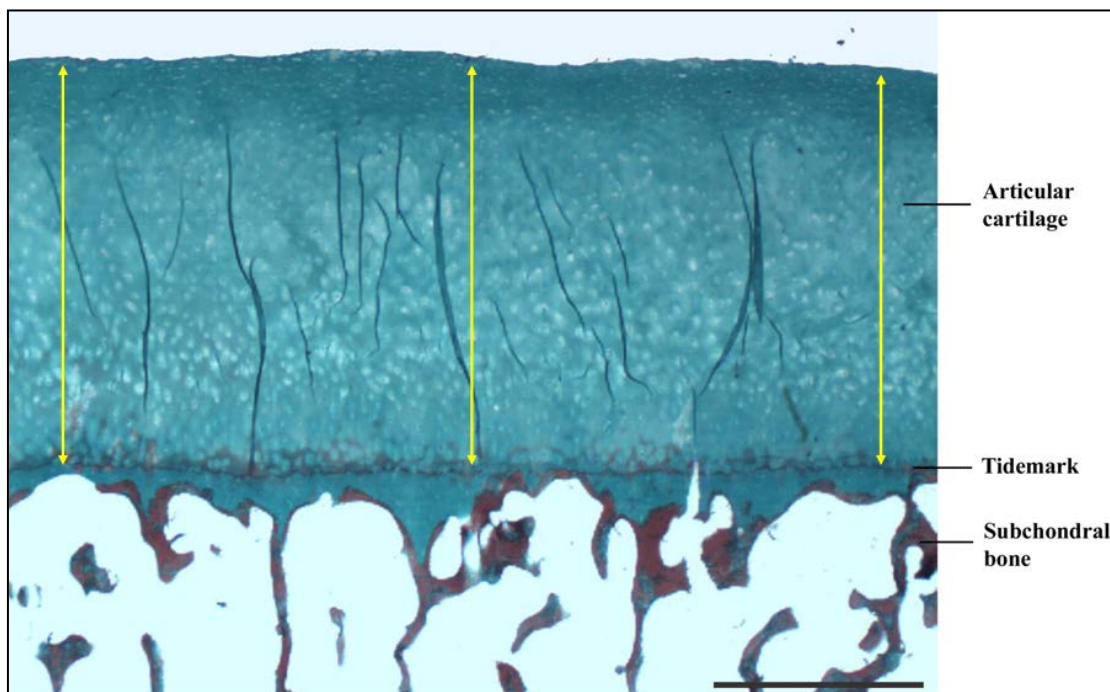
Figure 2.3. Cartilage thickness measurements were taken from three equally spaces points along the width of the section in order to obtain an average. Scale bar = 1.5mm.

2.3.7.2. Bone area

Percentage of total bone area of the imaged sections was assessed using Adobe Photoshop (version 6.0.1). By bone area, we refer to the region below the tidemark, including the bone matrix, whether mineralized or not, and osteoid. This was calculated as a percentage of the total area which includes bone marrow and other soft tissues. The bone area measurement was consistently observed from the tidemark to a depth of 2mm.

2.3.7.2.1. Method of area calculation

Using Adobe Photoshop, a line was drawn over the tidemark as a marker to delineate the region to be calculated. Under the 'Image Size' setting, the resolution was changed so that it was consistently 300 pixels per inch. The 'Magic Wand' tool (which allows for selection of part of an image based on its colour) was then used to select the area of stained bone within the 2mm region (figure 2.4). Using the Image> Histogram function, it is possible to obtain the total number of pixels in the selected region (a pixel is the smallest addressable screen element). In order to calculate the total number of pixels in the whole region including the spaces where the bone marrow and soft tissues would reside, a line was drawn around the borders so that the whole area to be calculated is defined. The 'Magnetic Lasso' tool (which automatically clings to edges of contrast objects) was then used to select the entire region so that the total number of pixels could be obtained. An area percentage was then calculated in order to ascertain a quantitative value of bone area per section.
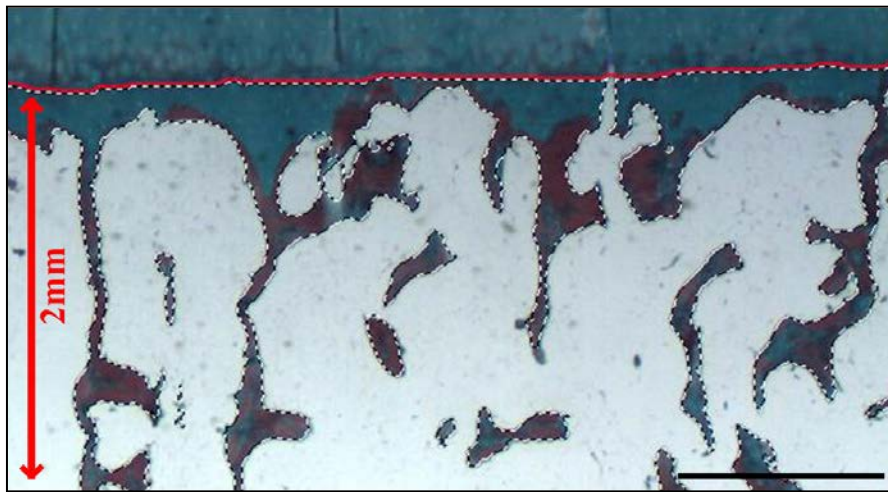
Figure 2.4. The area of bone in the subchondral region to a depth of 2mm. Scale bar = 1mm.

2.3.7.3. Tidemark integrity, cartilage surface integrity and cartilage morphology

Tidemark integrity, cartilage surface integrity and cartilage morphology was scored based on the scoring criteria (refer to table 2.2). Lower scores were indicative of a more normal state, whereas higher scores suggest a more diseased state of tissue. Tidemark integrity was scored between 0 and 4; 0 being 'normal' an 4 indicating a lack of tidemark due to the absence of cartilage. Similarly, cartilage surface integrity was also scored between 0 and 4 (4 indicating no cartilage surface integrity due to a complete lack of cartilage). Cartilage morphology was scored between 0 and 3; again, where 0 represents a 'normal' state and 3 indicating an absence of cartilage.

2.3.7.4. Overall scoring

Using the criteria described for scoring the qualitative parameters it is possible to obtain a total score between 0 and 11 for each scored slide. In order to incorporate the cartilage thickness and percentage of bone in the subchondral region into the overall scoring, they were categorised based on the following boundaries:

Cartilage thickness		Bone area	
Millimetres (mm)	**Score**	**Percentage (%)**	**Score**
0.00 – 0.49	3	10.0 – 29.9	0
0.50 – 1.49	2	30.0 – 49.9	1
1.50 – 2.49	1	50.0 – 69.9	2
2.5 +	0	70.0 – 89.9	3

This approach enables an overall sum of scores between 0 and 17 to be calculated, where the more 'normal' the sample, the lower the score.

In this study, we have used both the categorical scores and the continuous data in order to analyse quantitative data used in the scoring system.

2.3.8. Inter- and intra-observer variability

In order to assess the validity and reproducibility of the scores obtained, 10 slides were randomly picked as a sample set to be scored. These slides were graded by 5 separate individuals who had no previous connection with the scoring system.

This same sample set was also graded on 3 separate occasions by myself in order to determine the intra-observer variability.

2.3.9. Analysis

Data were analysed in several stages. Initially the mean sum of OCPs excised per patient was analysed with regards to age, sex and anatomical location. Secondly, the data were graphed in order to delineate the impact of the cartilaginous and boney parameters on the overall scores, looking into whether or not their addition resulted in significant differences or not. Thirdly, correlations between histological parameters were analysed. Fourthly, the system was tested to see whether or not the overall score could be used to differentiate between milder and more severe changes within specific tissue parameters. Lastly, inter- and intra-observer variability was assessed.

2.3.9.1. Statistical analysis

Statistical analysis was carried out using Minitab 16, SPSS 16.0 and Microsoft Office Excel (2003). Data were examined for normality using the Anderson-Darling statistic. Pearson's and Spearman's Rank correlation coefficients were calculated for parametric and non-parametric variables respectively. Student t-tests were used when comparing two sets of normally distributed data; otherwise the Mann Whitney test was used. One-way ANOVAs were carried out in order to assess the significance of the variability results.
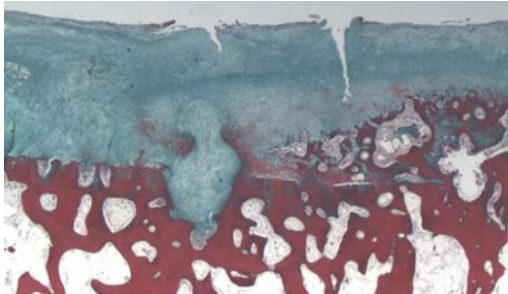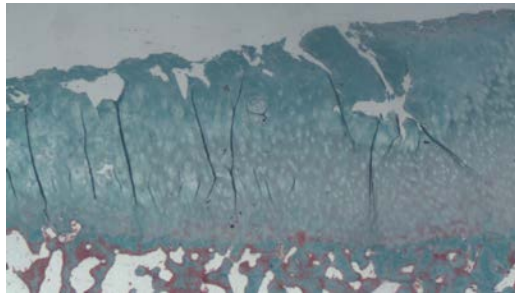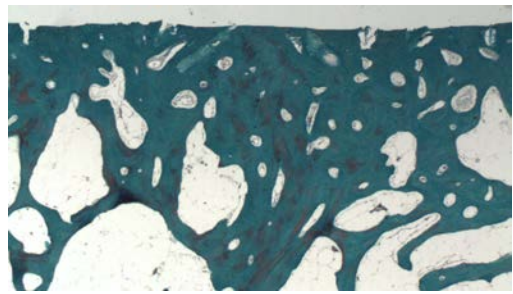
Score	Tidemark integrity:	Cartilage surface integrity:	Cartilage morphology:
0	**Tidemark normal**	**Smooth surface** : Superficial layer intact	**Normal morphology** : Organised chondrocyte arrangement
1	**Tidemark intact** : Linear : Evidence of cellular invasions	**Uneven surface** : Mild surface irregularity	**Altered morphology** = Includes 1 or more of the following : Irregular cell organisation : Cell clusters
2	**Moderate tidemark disruption** : Cellular invasions : Evidence of vascular invasions : Evidence of tidemark duplication	**Fibrillated surface** : Moderate fibrillation	**Abnormal morphology** : Exceptional difference in cellularity -Highly cellular/ acellular : Cellular organisation highly varied
3	**Complete tidemark disruption** : Non-linear : Greater cellular invasions : Numerous vascular invasions 	**Fissured surface with excessive fibrillation** : Fissure extends further than surface zone 	**No cartilage** : Denuded
4	**No tidemark** : No cartilage	**No cartilage** : Denuded	

Table 2.2. Criteria for the scoring of individual parameters namely tidemark integrity, cartilage surface integrity and cartilage morphology.

Patient #	Age	Sex	OCP #	Medial/ Lateral	Cartilage thickness mm	(0-3)	Bone density %	(0-3)	Tidemark (0-4)	Surface Integrity (0-4)	Cart. Morphology (0-3)	Sum (0-17)	Mean sum (0-17)
1	59	Female	1	Medial	0.11	3	70.07	3	2	2	1	11	6.00
			2	Lateral	2.41	1	27.63	0	0	0	1	2	
			3	Medial	1.67	1	57.61	2	1	2	0	6	
			4	Lateral	3.36	0	35.61	1	1	2	1	5	
2	73	Male	5	Lateral	0	3	66.02	2	4	4	3	16	13.75
			6	Lateral	0	3	62.99	2	4	4	3	16	
			7	Lateral	0	3	73.16	3	4	4	3	17	
			8	Medial	1.69	1	51.81	2	1	1	1	6	
3	64	Male	9	Medial	0.62	2	47.73	1	3	0	2	8	8.33
			10	Medial	1.41	2	66.89	2	3	1	2	10	
			11	Medial	3.5	0	45.29	1	1	3	2	7	
4	85	Female	12	Lateral	2.03	1	28.62	0	0	1	0	2	9.25
			13	Medial	1.92	1	39.34	1	1	1	0	4	
			14	Medial	0	3	64.13	2	4	4	3	16	
			15	Medial	0	3	32.53	1	4	4	3	15	
5	72	Male	16	Medial	0	3	59.03	2	4	4	3	16	9.17
			17	Lateral	2.32	1	30.88	1	2	0	2	6	
			18	Medial	0.44	3	74.32	3	1	1	0	8	
			19	Medial	0	3	75.36	3	4	4	3	17	
			20	Medial	1.25	2	66.95	2	0	1	1	6	
			21	Lateral	3.32	0	48.44	1	0	1	0	2	
6	45	Female	22	Lateral	1.87	1	31.52	1	0	0	0	2	4.33
			23	Lateral	3	0	48.3	1	0	1	1	3	
			24	Medial	1.99	1	50.96	2	1	3	1	8	
7	67	Female	25	Medial	1.44	2	56.6	2	0	2	1	7	9.00
			26	Medial	0.12	3	82.05	3	4	4	3	17	
			27	Lateral	1.88	1	27.47	0	1	2	1	5	
			28	Medial	0.81	2	21.13	0	2	1	2	7	
8	62	Female	29	Lateral	2.65	0	50.25	2	1	2	1	6	7.67
			30	Medial	1.08	2	52.16	2	1	1	1	7	
			31	Medial	0.61	2	55.6	2	2	3	1	10	
9	67	Male	32	Medial	0.36	3	67.73	2	0	3	1	9	6.00
			33	Lateral	1.85	1	34.81	1	2	0	1	5	
			34	Medial	1.9	1	51.51	2	1	2	1	7	
			35	Lateral	3.3	0	53.96	2	0	1	0	3	
10	69	Male	36	Medial	1.71	1	22.01	0	2	2	1	6	7.50
			37	Medial	2.25	1	48.78	1	0	1	0	3	
			38	Lateral	2.06	1	40.7	1	1	2	0	5	
			39	Lateral	0	3	50.04	2	4	4	3	16	

Table 2.3. Scores and overall sum of scores for each osteochondral plug.

2.4. Results

Based on the criteria mentioned previously the five parameters were scored and an overall sum of scores between 0 and 17 was generated for each osteochondral plug. In this study the overall scores obtained ranged between 2 and 17. Table 2.3 summarises all of the scores obtained for individual parameters together with the sum of scores for each osteochondral plug.

2.4.1. Scoring of the histological sections from the osteochondral plugs

Figures 2.5 to 2.17 show representative OCP's from each score obtained. As previously outlined, a lower score suggests a more normal state of tissue. Figure 2.5 demonstrates the lowest score obtained (score=2) when analysing the OCP's. There is a relatively thick layering of articular cartilage (cartilage thickness (CT)= 2.41mm) which falls within the range of normal articular cartilage. The OCP represents mild, initial changes that occur in osteoarthritis. The characteristic distribution of chondrocytes within the tissue can be seen; there is a flattened layer of cells in the superficial zone, accompanied by the rounded isolated cells in the mid-zone. The columns of cells which are typically seen in the deep zone are also evident. Early signs of OA include the small groups or clusters of cells. Tidemark duplication can also be observed. The articular surface, tidemark and subchondral bone are comparable to normal articular cartilage.

Figure 2.6 represents an OCP with an overall score of 3. This OCP shows close resemblance to the OCP of score 2. When comparing the two, it is apparent that the cartilage thickness is reduced (by approximately 6 percent) and that mild surface irregularities are developing. It could be argued that there is an increase in the number of cell clusters seen throughout the tissue, however, as a whole, scores 2 and 3 appear to be very similar histologically.

Following on from score 3 are scores 4-6, which can be seen in figures 2.7 to 2.9. These appear to show the next level in the progression of the disease. Despite the adequate cartilage thickness, it can be seen collectively that surface integrity is compromised in these OCP's. Fissuring of the surface is evident, combined with evidence of clustered cells

lining the fissured surfaces. In figure 2.7C, a collection of cells within a fibrous pocket appears to reside within the SZ. These do not present the typical chondrocytic features and so it could be suggested that they are a different cell type. Throughout the tissue, the chondrocyte organisation does appear to follow a general trend. However, this trend does not appear to correlate with the increasing scores. The trend is that there is an increase in cell clusters; however, as mentioned this increase varies between samples. Another observation is that the vertical columns of chondrocytes that are usually restricted to the deep zone appear to extend beyond this deep zone and into the mid-zone. The tidemark between scores 4 and 6 also show great similarities in that they are linear, with moderate cellular and vascular invasions threatening the area. Figure 2.8D illustrates a breach of the tidemark where cells from the subchondral bone, accompanied by vasculature, are migrating into the deep zone of the articular cartilage.

Progressively, scores 7 and 8 depict the next stages in the advancement of the disease. At a glance it can be seen that there is still cartilage covering the underlying bone, however the quality of the cartilage is severely compromised. The OCP representing score 7 (figure 2.10) shows excessive fibrillation, comprising deep fissures throughout the articular surface. A higher power view of what would be named the superficial zone shows a cellular lining throughout the fissured surface. This population appears to be a mixture of chondrocyte-like and non chondrocyte-like cells. Examining the tidemark in figure 2.10A and D, it can be seen that there are numerous tidemark breaches into the deep zone. Interestingly, in the specific case, on the right side of figure 2.10A (higher power can be seen in figure 2.10E), an unusual structural arrangement can be seen. There appears to be a pocket which is enclosed by a circular fibrous ring (outlined by the X's) which appears to be partly detached from the surroundings. Within this ring is a combination of cells and what appears to be vascular vessels anchored into a thick fibrous sheet. This is not only interesting because it is atypical, but is also suggests a phenomenon which questions the structure of cartilage; as cartilage is renowned for its aneural and avascular composition.

The OCP which represents score 8 depicts another case whereby a cartilaginous layer is apparent; however this layer does not appear to represent the usual structure of cartilage. In figure 2.11, it can be seen that the cartilage and subchondral bone show little resemblance to what would be seen in a normal articular unit other than the two tissues

being in proximity to one another. The overlying cartilage resembles fibrocartilage rather than hyaline cartilage and this seems to cover the whole surface (as indicated by the white star in figure 2.11B). The red stars in figures 2.11B and C pinpoint small regions in what would be classified the deep zone where the organisation resembles remaining hyaline cartilage; it appears that this region is engulfed by the fibrocartilagenous covering. The tidemark is also an interesting factor as it is difficult to delineate. The chondro-osseo interface in this OCP is a mesh with several large passages interconnecting the two. The black arrows in figures 2.11B and C draw attention to regions within the cartilage where vascularisation is occurring, similar to what was seen in the OCP of score 7. The vascular regions in figure 2.11B look as though they have resulted from the flow of cells that have breached what would have been the tidemark. As a whole, it is interesting to note however that the articular surface looks smooth and it would not be fair to say that there is any fibrillation present, despite the overall state of the tissue.

Scores 9 and 10 (figures 2.12 and 2.13) represent OCPs illustrating the progression into the latter stages of cartilage degradation involved in OA. The cartilaginous layering does not cover the entire surface; there are areas where degradation has extended down to the subchondral bone. In what remains of the cartilage, fissuring and fibrillation extend beyond the surface. The chondrocytes reside largely in clusters and there is only a small proportion of isolated cells. Looking at the tidemark, it is evident that established vascular canals have been formed. In figure 2.13B an accumulation of cells are located below a deep fissure, extending to the tidemark. It is difficult to say whether these cells have extended from the surface down, or if they have emerged from the subchondral bone and are moving upwards. Looking at figure 2.12D it can be seen that there are multiple tidemarks below the original one. A marked difference between scores 9 and 10 is the bone thickness. It can be seen that there are far fewer marrow cavities in score 10 and, therefore, a higher bone density.

From score 11 to 17, the remaining tissue comprises predominantly of bone. The OCP representing score 11 (figure 2.14) has a small region with a very thin (approximately 200μm) covering of cartilage, however the other OCPs up to score 17 have no cartilage at all. A closer look at figure 2.14B shows that despite only a thin layer of cartilage, there are still tidemark breaches and, in this case, it can be seen that the breach is an extension of a

bone marrow cavity. Interestingly in figure 2.14C, a pocket of soft tissue is outlined by X's and extends from the surface and into the bone. The cells within this region appear to be within lacunae, similar to what would be seen in hyaline cartilage. Surrounding this pocket are large marrow cavities, suggesting remodelling of some sort.

In this study, no OCPs achieved a score of 12, 13 or 14. This indicates that once the degradation has reached a certain point, there are fewer intermediate points; once there is no cartilage the bone adapts to the new conditions and there are no in-between stages. Having said that, in this study, the difference between OCPs from scores 15 to 17 are that the higher the score the greater the bone density. It can be seen in figure 2.15, that there are marrow cavities filling up a large proportion of the bone, whereas in figure 2.17, the area occupied by marrow cavities is remarkably smaller. The articulating surface of the OCP from score 17 appears to be eburnated bone.

Score 2:

Figure 2.5. A representative osteochondral plug from tibial plateau with an overall score of 2.

Figure A. Low power view of a Masson's stained OCP with an overall score of 2. The articular cartilage (AC) is separated from the underlying subchondral bone (SCB) by the tidemark (TM). Scale bar = 1.5mm.
Figure B. The superficial zone (SZ) of the OCP with a score of 2. The arrows indicate clusters of cells forming in the superficial-mid zone. The top arrow indicates a group of cells in a horizontal columnar arrangement. Scale bar = 200 µm.
Figure C. The deep zone (DZ) of the OCP with a score of 2. The top left arrow indicates the characteristic vertical column as seen in normal hyaline cartilage. The bottom arrow indicates tidemark duplication. Scale bar = 200 µm.

Score 3:

Figure 2.6. A representative osteochondral plug from tibial plateau with an overall score of 3.

Figure A. Low power view of a Masson's stained OCP with an overall score of 3. The linear tidemark (TM) separates the cartilage from the underlying subchondral bone. The fissure seen is a processing artefact. Scale bar = 1.5mm.

Figure B. The superficial zone (SZ) of the OCP with a score of 3. Top arrow highlights slight fibrillation of the surface. There is also evidence of cells clusters forming in the superficial zone as indicated through the lower arrow. Scale bar = 200 μm.

Figure C. The mid-zone (MZ) of the OCP with a score of 3. There are relatively low numbers of the characteristic isolated, rounded chondrocyte usually found in normal articular cartilage (top arrow). The lower arrows indicate the abundance of cell clusters. Scale bar = 200 μm.

Figure D. The deep zone (DZ) of the OCP with a score of 3. There is a continued presence of clusters of chondrocytes within the deep zone. Although there are columns of cells, it does not appear to be the predominant chondrocyte organisation within this region. There is evidence of cellular migration towards the linear tidemark. Scale bar = 200 μm.

Score 4:

Figure 2.7. A representative osteochondral plug from tibial plateau with an overall score of 4.

Figure A. Low power view of a Masson's stained OCP with an overall score of 4. The tidemark (TM) separates the cartilage from the underlying subchondral bone. Scale bar = 1.5mm.
Figures B & C. The superficial zone (SZ) of the OCP with a score of 4. Arrow in Figure B highlights increased surface fibrillation. Characteristic flattened surface chondrocytes are absent. Top arrow in figure C indicates a highly cellular region in the superficial zone. Chondrocyte clustering is evident in both figures B and C. Scale bar = 200 μm.
Figure D. The mid-zone (MZ) of the OCP with a score of 4. The arrow indicates presence of chondrocyte clusters in this region. Scale bar = 200 μm.
Figure E. The deep zone (DZ) of the OCP with a score of 4. The top two arrows highlight the presence of clusters as well as columns. Clusters appear to be more numerous when compared to the deep zone of OCPs with lower overall scores. Lower arrows highlight the presence of tidemark breeches. Tidemark duplication is also evident. Scale bar = 200 μm.

77

Score 5:

Figure 2.8. A representative osteochondral plug from tibial plateau with an overall score of 5.

Figure A. Low power view of a Masson's stained OCP with an overall score of 5. The tidemark (TM) separates the cartilage from the underlying subchondral bone. Overall reduction in cartilage thickness is apparent. Scale bar = 1.5mm.

Figure B. The superficial zone (SZ) of the OCP with a score of 5. The top arrow indicates greater surface fibrillation relative to the lower scores. Lower arrow indicates a characteristic flattened surface zone chondrocyte. Cell clusters are apparent yet sparse. Scale bar = 200 μm.

Figure C. The mid-zone (MZ) of the OCP with a score of 5. The arrow indicates vertical columns normally seen in the deep zone of articular cartilage. Scale bar = 200 μm.

Figure D. The deep zone (DZ) of the OCP with a score of 5. Top arrow highlights the presence of typical vertical columns. Lower arrows highlight the presence of cellular and vascular tidemark breeches. Scale bar = 200 μm.

Score 6:

Figure 2.9. A representative osteochondral plug from tibial plateau with an overall score of 6.

Figure A. Low power view of a Masson's stained OCP with an overall score of 6. The linear tidemark (TM) separates the cartilage from the underlying subchondral bone. Bone thickening is apparent. Scale bar = 1.5mm.

Figure B. The superficial zone (SZ) of the OCP with a score of 6. Moderate fibrillation can be seen in superficial zone. Cell clusters as indicated by the arrows are evident near the fissured surfaces. There is an absence of cells in the transitional region between the surface and the mid zone. Scale bar = 200 μm.

Figure C. The mid-zone (MZ) of the OCP with a score of 6. The arrows highlight the presence of chondrocyte clusters as well as vertical columns in the mid-zone. There are few rounded isolated cells as would be seen in the normal articular cartilage. Scale bar = 200 μm.

Figure D. The deep zone (DZ) of the OCP with a score of 6. Top arrow highlights the presence of columns that appear at a tangent rather than vertical. Lower arrows indicate the cellular migration towards the tidemark as well as the cellular and vascular breaches of the tidemark. Scale bar = 200 μm.

Figure 2.10. A representative osteochondral plug from tibial plateau with an overall score of 7.

Figure A. Low power view of a Masson's stained OCP with an overall score of 7. The linear tidemark (TM) separates the cartilage from the underlying subchondral bone. Bone thickening is excessive and surface fibrillation apparent. Scale bar = 1.5mm.

Figure B. The superficial zone (SZ) of the OCP with a score of 7. Fibrillation extending deeper than the surface zone is evident. Fissured surfaces appear to be highly cellular as indicated by the arrow. Scale bar = 200 μm.

Figure C. The mid-zone (MZ) of the OCP with a score of 7. The arrow indicates the presence of cell clusters. Scale bar = 200 μm.

Figure D. The deep zone (DZ) of the OCP with a score of 7. The top arrows highlight the presence of characteristic vertical chondrocyte columns. The lower arrow exemplifies the cellular breaches of the tidemark. Scale bar = 200 μm.

Figure E. Part of the mid zone (MZ). An abnormal pocket is evident as outlined by the X's. There appears to be a circular fibrous covering surrounding the abnormal region containing vascular vessels. Scale bar = 400 μm.
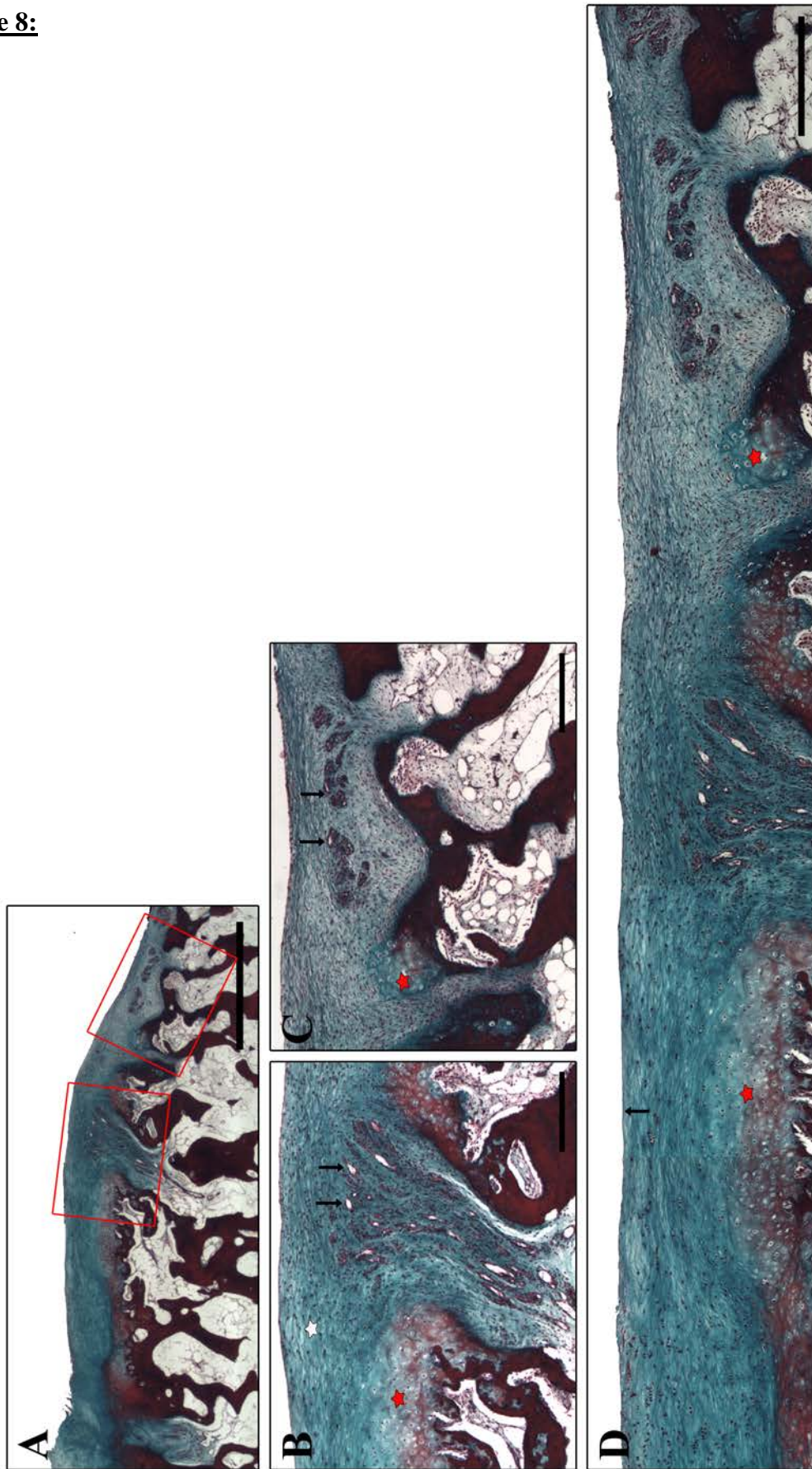
Score 8:

Figure 2.11. An osteochondral plug from tibial plateau with an overall score of 8.

Figure 2.11. An osteochondral plug from tibial plateau with an overall score of 8.

Figure A. Low power view of a Masson's stained OCP with an overall score of 8. The reduced thickness of the articular cartilage is apparent. The tidemark is barely recognisable as there are numerous extensive breeches. There is no distinction between the zones of articular cartilage. Scale bar = 1.5mm.

Figure B. The region highlighted by the left red box in figure A. Tissue appears highly cellular with a fibrous organisation (indicated by the white star). Black arrows point toward a major breech from the subchondral bone, where vascularisation is evident. The red star indicates a different region which appears to be hyaline cartilage-like, with chondrocytes located within lacunae. Scale bar = 200 μm.

Figure C. The region highlighted by the right red box in figure A. Black arrows indicate vascularisation within the cartilaginous region, surrounded by the fibrous covering. The red star indicates a hyaline-like region encapsulated by the thick fibrous covering. Scale bar = 200 μm.

Figure D. A panoramic view of the articulating surface. Cellular organisation is not representative of hyaline cartilage and there is extensive tidemark disruption. The surface does not appear to be fissured. Red stars correlate to those in figures B and C. Scale bar = 400 μm.
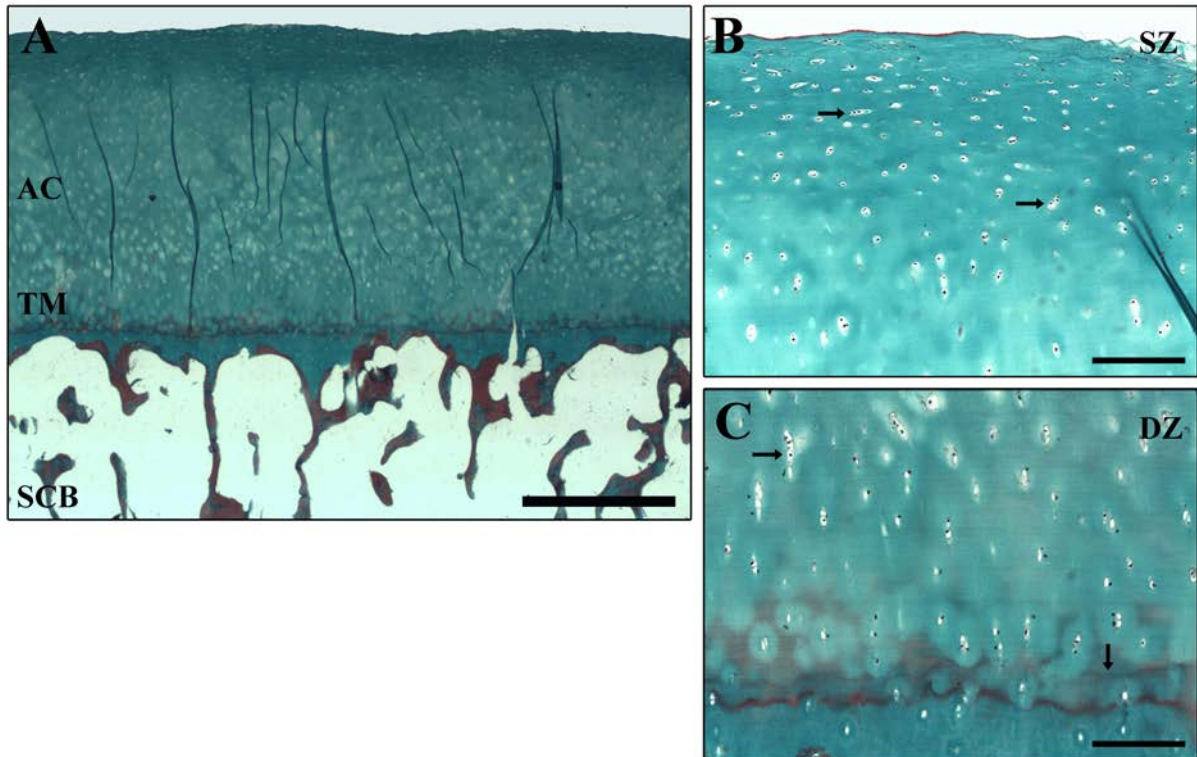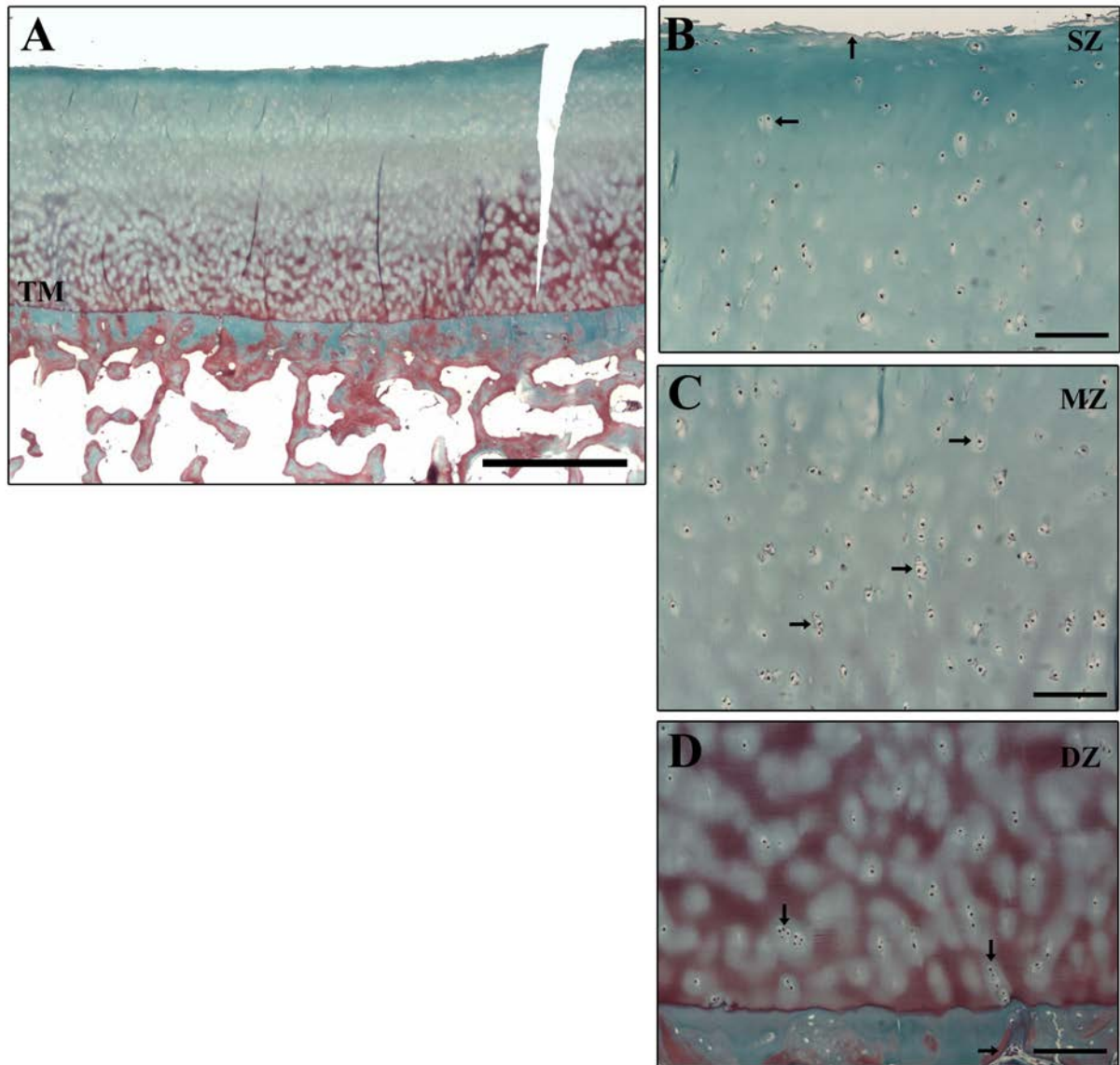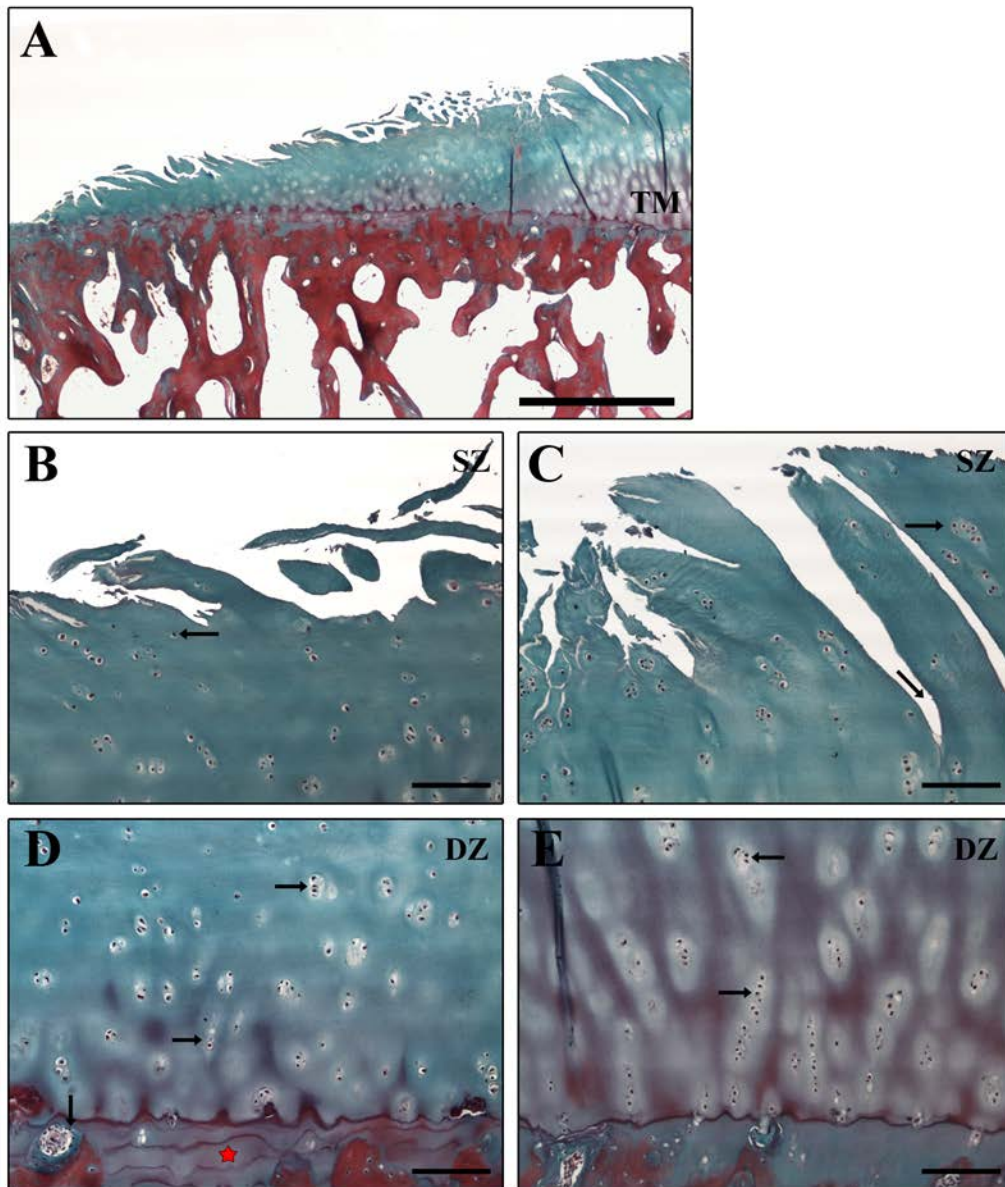
Score 9:

Figure 2.12. A representative osteochondral plug from tibial plateau with overall score of 9.

Figure A. Low power view of a Masson's stained OCP with an overall score of 9. The linear tidemark (TM) separates the cartilage from the underlying subchondral bone. Regression in cartilage thickness is evident, together with fissuring throughout the whole surface. Bone thickening below the tidemark is apparent. Scale bar = 1.5mm.

Figures B & C. The superficial zone (SZ) of the OCP with a score of 9. Cell clusters are predominant. However, there are few remaining single cells as indicated by the arrow in figure B. Figure C demonstrates the excessive surface fissuring, with the surrounding clusters of cells. Scale bar = 200 μm.

Figures D & E. The deep zone (DZ) of the OCP with a score of 9. Through figure D it can be seen that the majority of the chondrocytes in this region are located within clusters. In figure E, as well as clusters, there are a greater proportion of cells orientated in the typical columnar arrangement (indicated by the arrows). Vascular and cellular invasions are also apparent, together with great tidemark duplication as indicated by the red star in figure D. Scale bar = 200 μm.
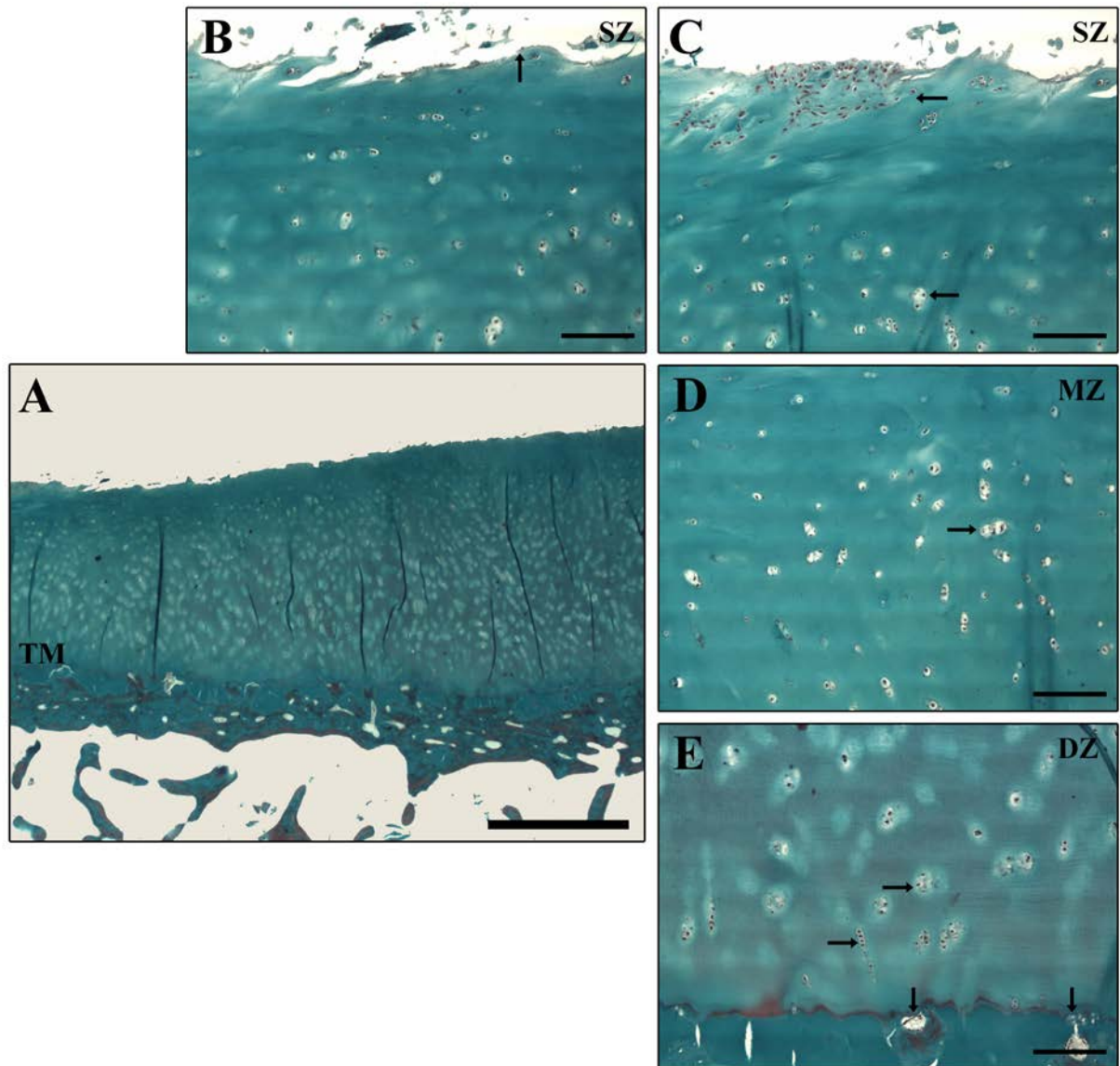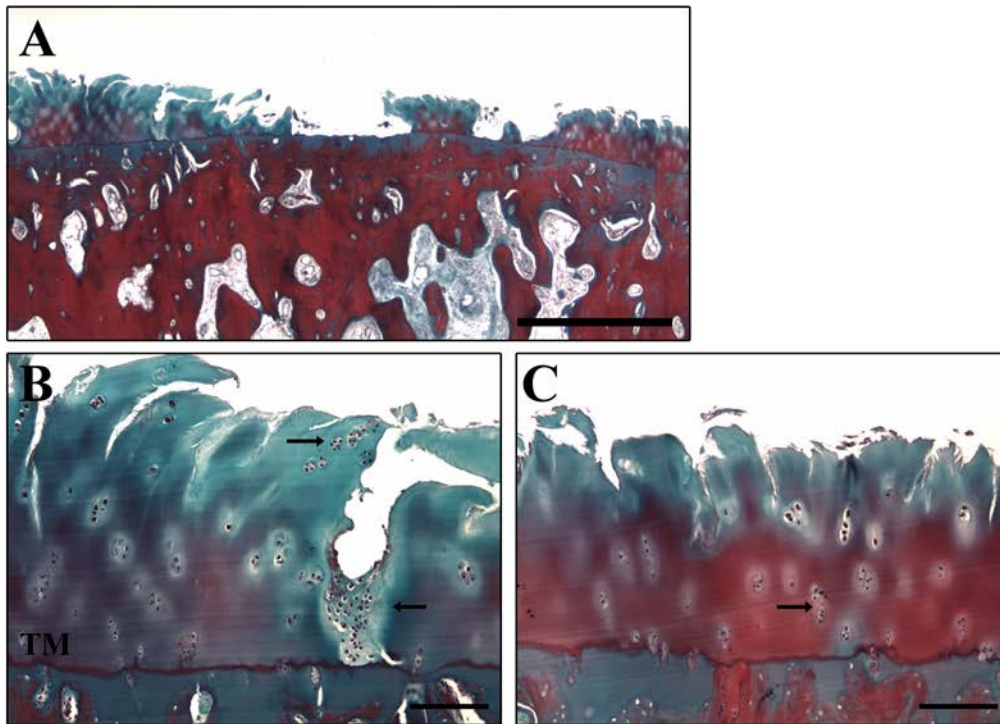
Figure 2.13. A representative osteochondral plug from tibial plateau with an overall score of 10.

Figure A. Low power view of a Masson's stained OCP with an overall score of 10. The residual overlying cartilage is minimal. The subchondral bone is thick and contains blood vessels and bone marrow cavities. Scale bar = 1.5mm.
Figures B & C. The remaining cartilage and tidemark from the OCP with a score of 10. Chondrocytes are all located within clusters as indicated by the arrows. The articular surface is highly fissured. Figure B shows an accumulation of cells located below a deep fissure. Scale bar = 200 µm.
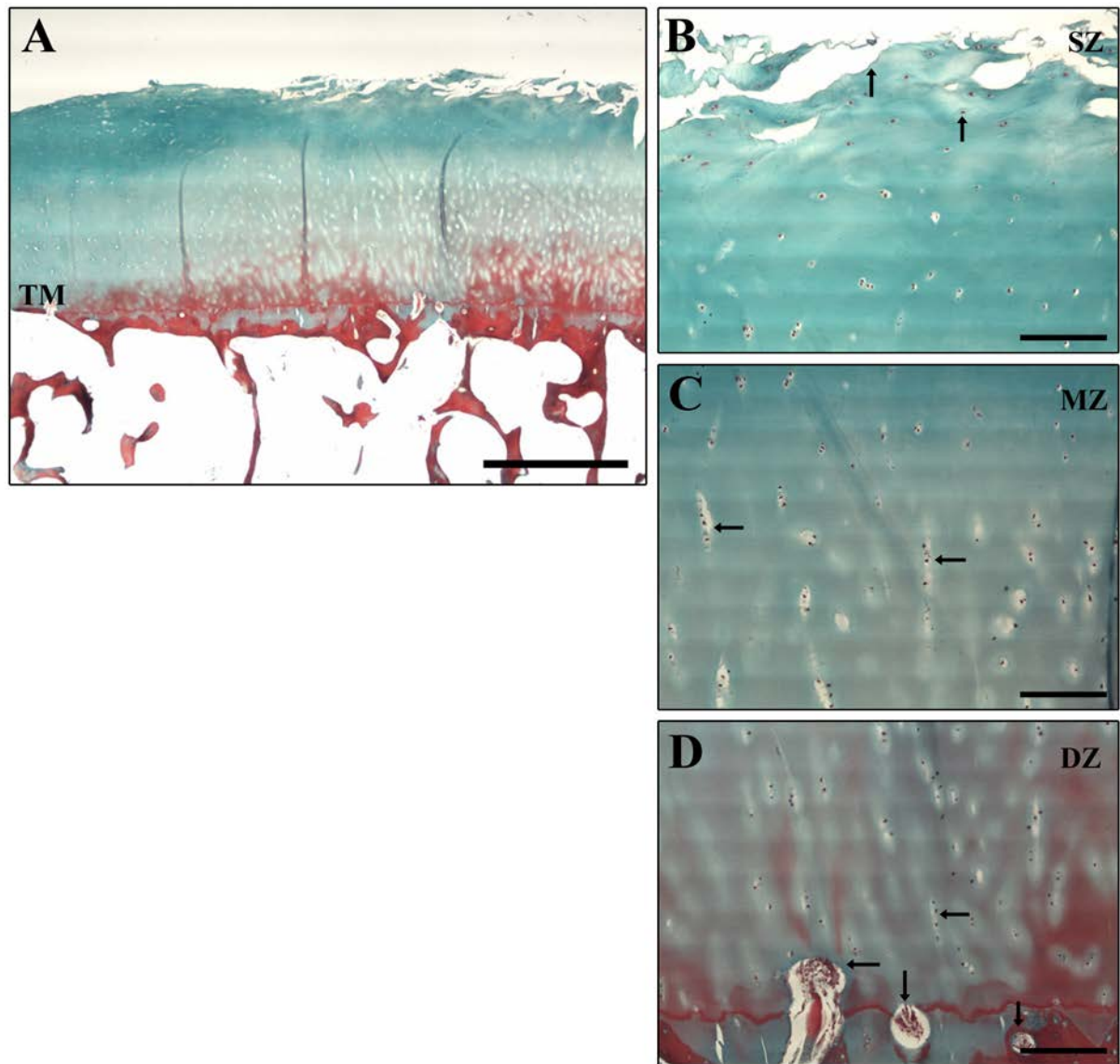
Score 11:
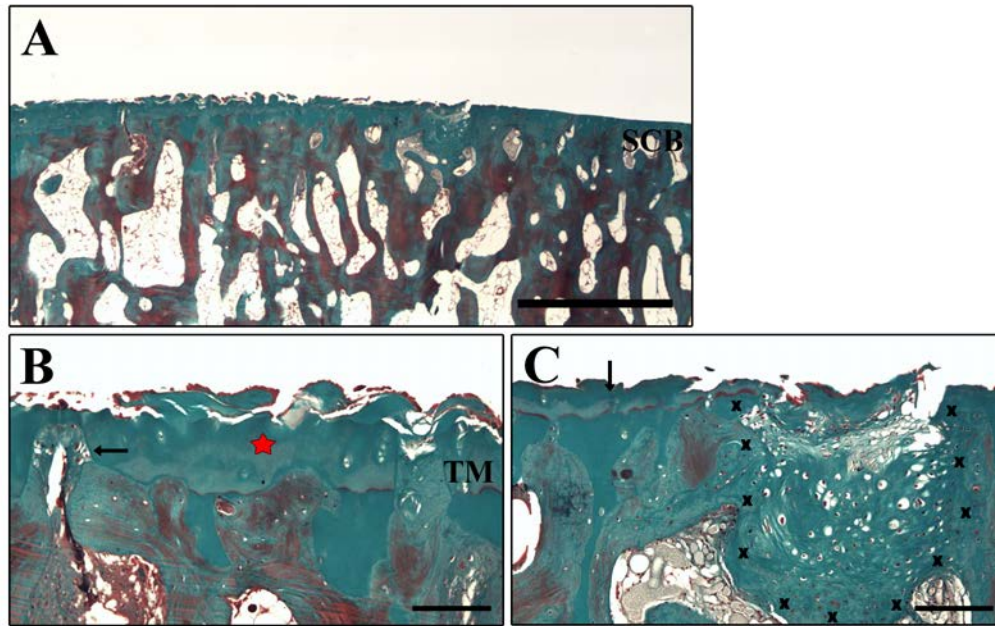
Figure 2.14. A representative osteochondral plug from tibial plateau with an overall score of 11.

Figure A. Low power view of a Masson's stained OCP with an overall score of 11. There is a very thin covering of cartilage over two thirds of the OCP. The subchondral bone has numerous blood vessels near the articular surface. There is an abnormal pocket of cells (imaged in figure C). Scale bar = 1.5mm.
Figure B. The remaining articular cartilage from the OCP with a score of 11. The surface is fissured. Multiple tidemarks are illustrated by the red star. There is evidence of vascularisation and cellular breeches at the tidemark as indicated by the arrow. Scale bar = 200 μm.
Figure C. An abnormal pocket is evident as outlined by the X's. There appears to be a highly cellular region extending from the surface into the bone or *vice versa*. Large regions of marrow cavity surround the abnormal pocket. Arrow indicates tidemark duplication. Scale bar = 200 μm.
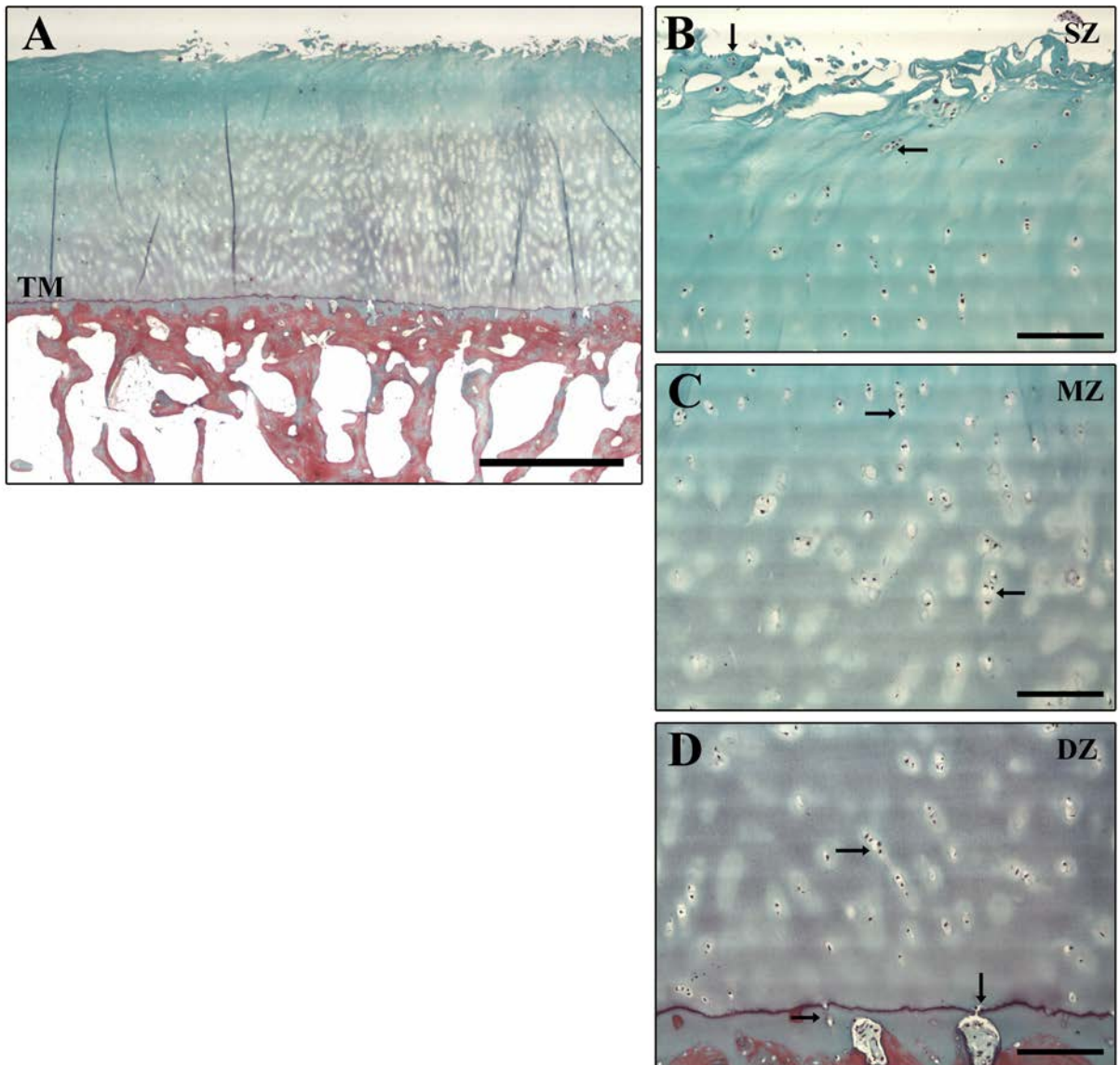
Score 15:
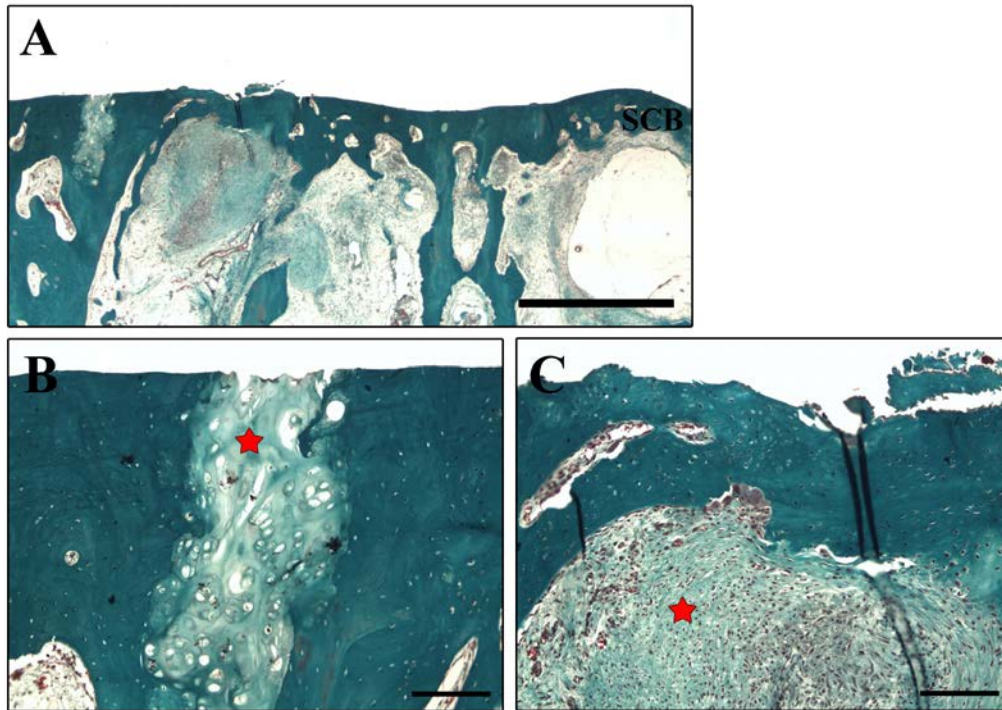
Figure 2.15. A representative osteochondral plug from tibial plateau with an overall score of 15.

Figure A. Low power view of a Masson's stained OCP with an overall score of 15. There is no overlying articular cartilage. Large marrow cavities reside within the subchondral bone. Scale bar = 1.5mm.

Figure B. A cellular pocket extending from the surface into the bone. Cells located within lacunae are characteristic of chondrocytes. Vascular channels can be seen within the bone. Scale bar = 200 μm.

Figure C. A highly cellular region of a marrow cavity extending towards the surface of the articulating bone is indicated by the red star. A vascular channel can also be seen between the surface of the bone and the highly cellular cavity. Scale bar = 200 μm.

Score 16:
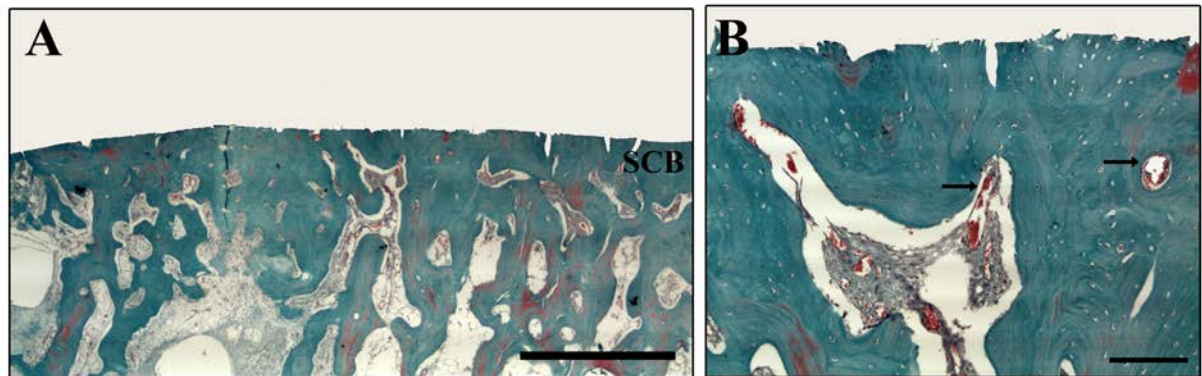
Figure 2.16. A representative osteochondral plug from tibial plateau with an overall score of 16.

Figure A. Low power view of a Masson's stained OCP with an overall score of 16. There is no overlying articular cartilage. The bone area is more dense than in the lower score as a result of smaller marrow cavities. Scale bar = 1.5mm.
Figure B. A vascular/marrow cavity within the bone. Arrows are indicative of vascular channels. A cellular region sits within the bone cavity. Scale bar = 200 μm.
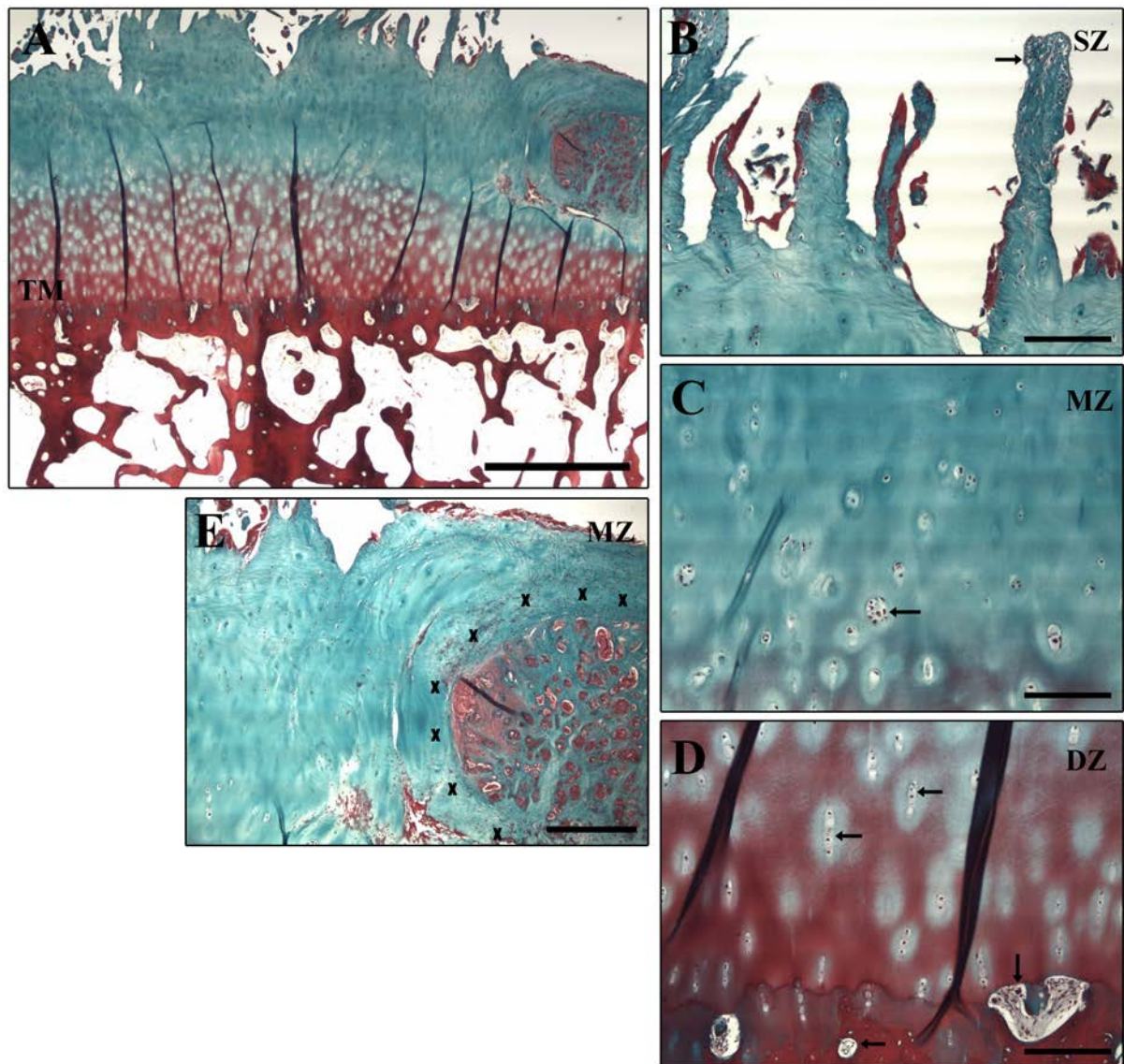
Score 17:
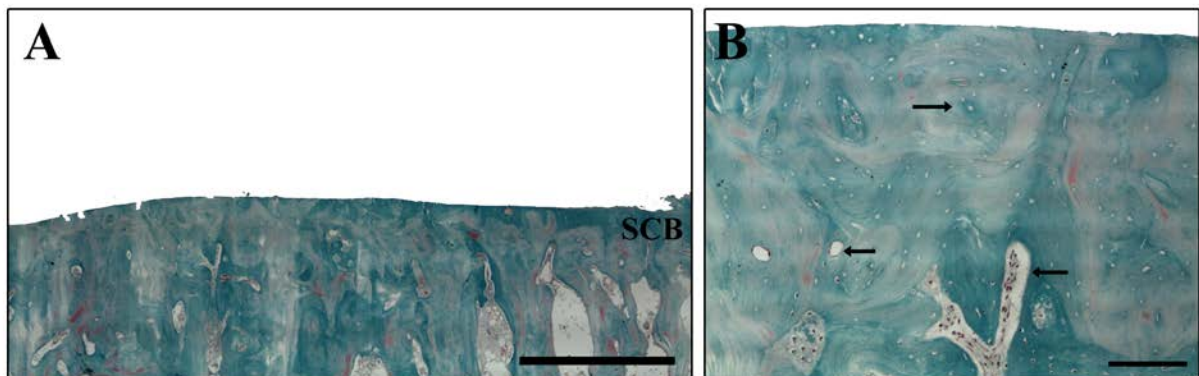
Figure 2.17. A representative osteochondral plug from tibial plateau with an overall score of 17.

Figure A. Low power view of a Masson's stained OCP with an overall score of 17. There is no overlying articular cartilage and the bone is very dense. Scale bar = 1.5mm.
Figure B. A higher power image of the bone. Vascular channels are indicated by the arrows. The size of the cavity is smaller in relation to the lower scores. Scale bar = 200 μm.

2.4.2. Scoring of osteochondral plugs

Having assembled all of the scores for the OCPs (table 2.3) it was possible to examine data between parameters. For each patient, several OCPs were excised representing the topographically different regions within the medial and lateral compartments. Using the overall scores obtained from each OCP, a mean sum of overall scores was calculated for each patient in order to give an indication of the severity of the tibial plateau as a whole. Figure 2.18 demonstrates the relationship between patient age and the mean sum of overall scores obtained for the patient. The blue line indicates the positive regression line which suggests that as age increases, the severity of OA also increases. Pearson's correlation test showed a significant correlation between the two parameters ($p < 0.05$).

Using the mean sum of scores, differences in sex were examined in order to ascertain whether or not sex is a variable factor affecting the severity of OA. The mean sum of scores in the females ranged from 4.3 to 9.3. In the males this was slightly higher ranging from 6 to 13.75, however this difference was not statistically significant when tested using a student t-test (figure 2.19).

Figure 2.20 is a box plot comparing scores obtained from medial and lateral OCPs. It can be seen that despite the range of scores being similar, the median in the medial side is 8, which is higher than the median in the lateral side which is 5. This suggests that as a whole, the medial side is more severely affected than the lateral side. Using the Mann-Whitney test statistical significance was confirmed ($p < 0.02$).
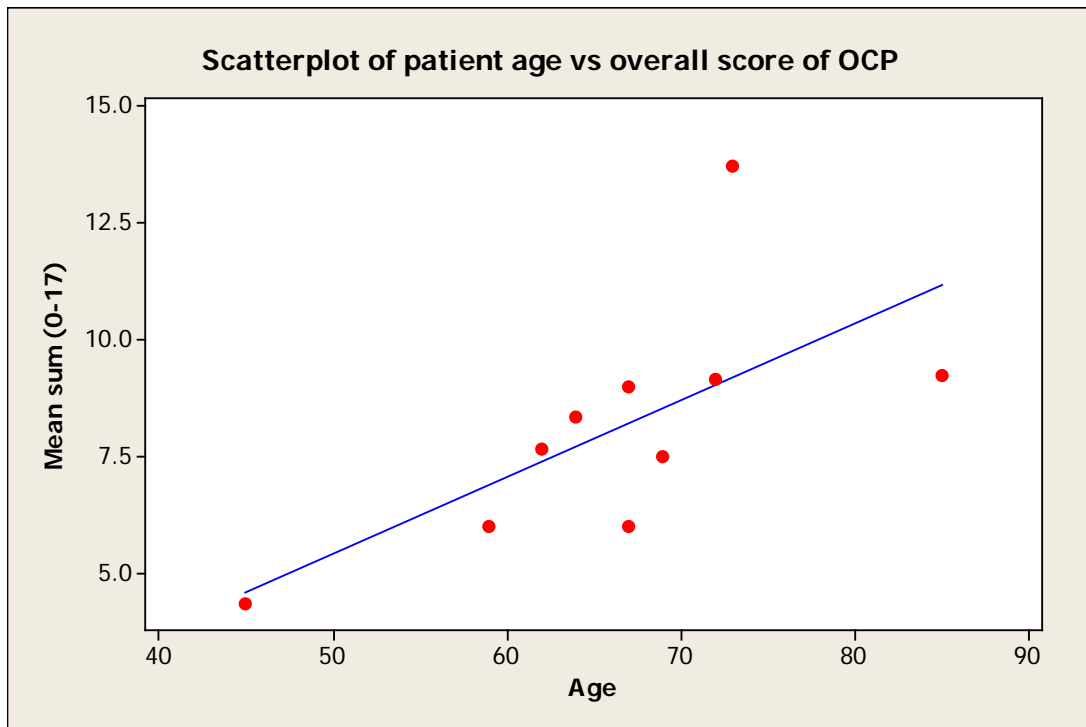
Figure 2.18. A scatter-plot illustrating the relationship between the patient age and the mean sum of scores obtained through the scoring system (n=10). Blue line indicates the trendline. Pearson's correlation test confirmed that there is a significant relationship between the parameters (p<0.05).
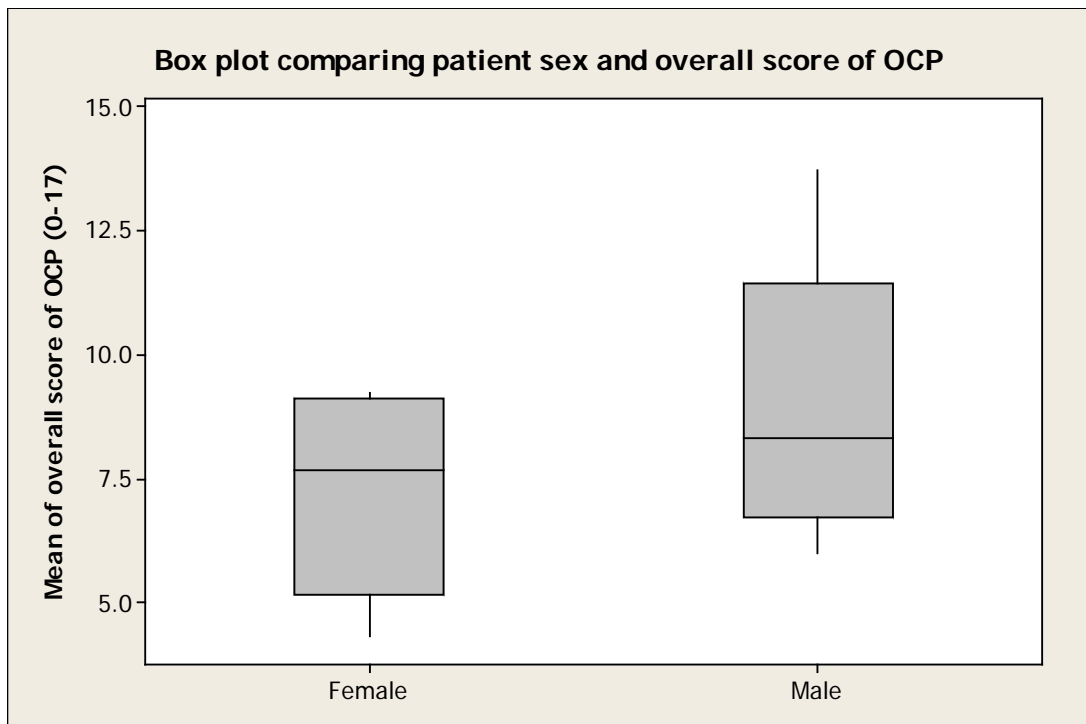
Figure 2.19. A box-plot showing the distribution of mean overall scores obtained from OCP's between female (n=5) and male (n=5) patients. The midline of the box-plot is representative of the median value (f=7.67, m=8.33), the second and third quartiles are displayed as a box and the first and third quartiles as whiskers. Student t-test confirmed that there were no statistical differences between these two groups (p>0.05).
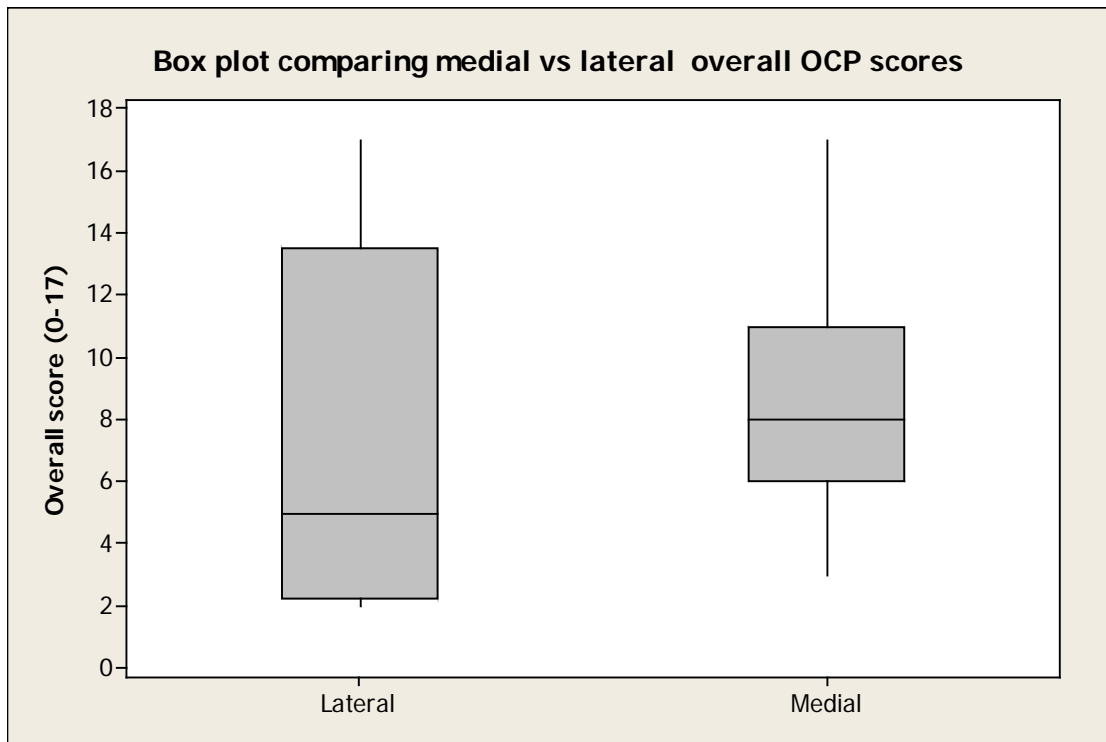
Figure 2.20. A box-plot comparing the differences in overall scores of OCPs excised from the medial (n=23) and lateral (n=16) tibial condyles. The midline of the box-plot is representative of the median value (l=5, m=8), the second and third quartiles are displayed as a box and the first and third quartiles as whiskers. Mann Whitney test was used to confirm that the differences between the two groups was significant (p<0.02).

Moving on more specifically to the parameters used for scoring the OCPs, figures 2.21 and 2.22 are scatter graphs showing the relationship of scores obtained when looking solely at the cartilage parameters, or solely at the bone parameters, in relation to the score obtained when combining both the cartilage and bone. In these graphs the adjusted score represents the score as a percent of the maximum possible score. This was calculated in order to keep constant the overall score; without a percentage of the total it would be unfair to compare a score out of 17 to a score out of 10 as it is for the cartilage parameters alone. Figure 2.21 shows the relationship between scores obtained with and without bone factors. The blue line indicates the trend line which suggests that as the combined cartilage and bone score increases, the cartilage parameters alone also increase at a similar rate. These findings were confirmed using Spearman's rank correlation coefficient where $p<0.01$. This suggests that by including the bone based parameters does not significantly alter the score which would have otherwise been achieved using solely the cartilage based parameters. Figure 2.22 is a similar scatter graph which shows the relationship between scores obtained with and without cartilage parameters. Again, a positive relationship can be seen between the two which was confirmed by Spearman's rank correlation coefficient $p<0.01$. Studying this graph it can be concluded that including the cartilage parameters does not alter the score trend which would have otherwise been obtained from only the bone based scores. It can also be noted from the graph that the progression in bone scores occurs in line with the progression achieved when scoring the unit as a whole. In this way it can be said that the bone changes are just as significant and happen together with the changes observed in the cartilage.
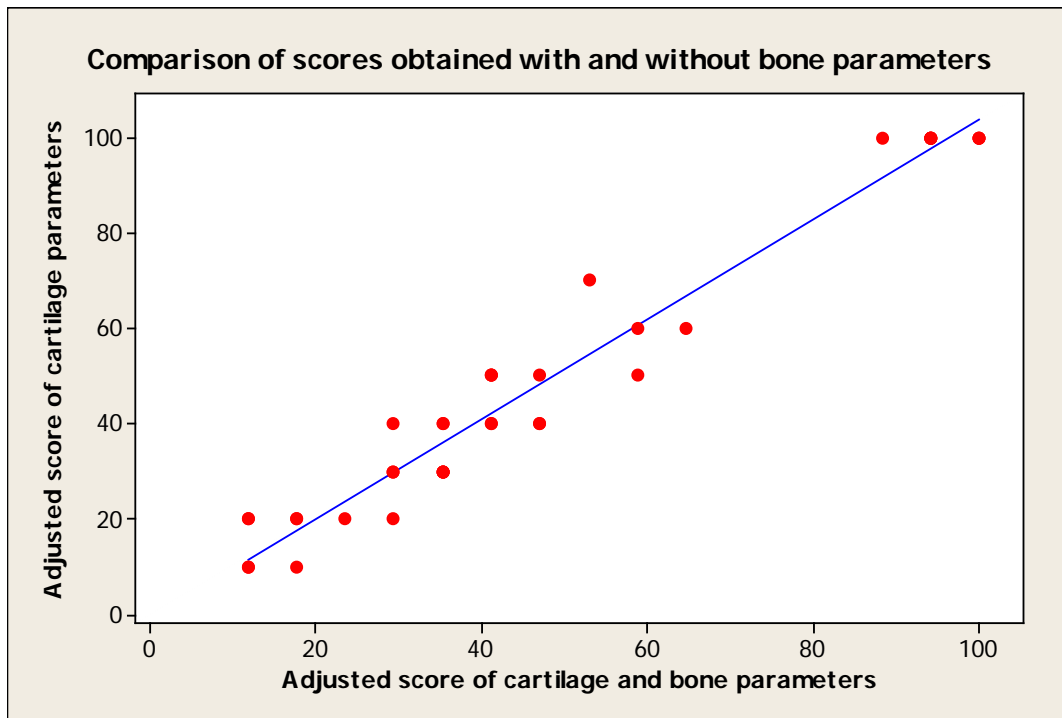
Figure 2.21. A scatter-plot demonstrating the relationship of scores (n=39) when comparing those obtained using only the cartilage parameters to the scores obtained using both the cartilage and the bone parameters. Blue line is indicative of the trendline. Spearman's rank correlation coefficient confirmed that the two variables showed a significant correlation (p<0.01).
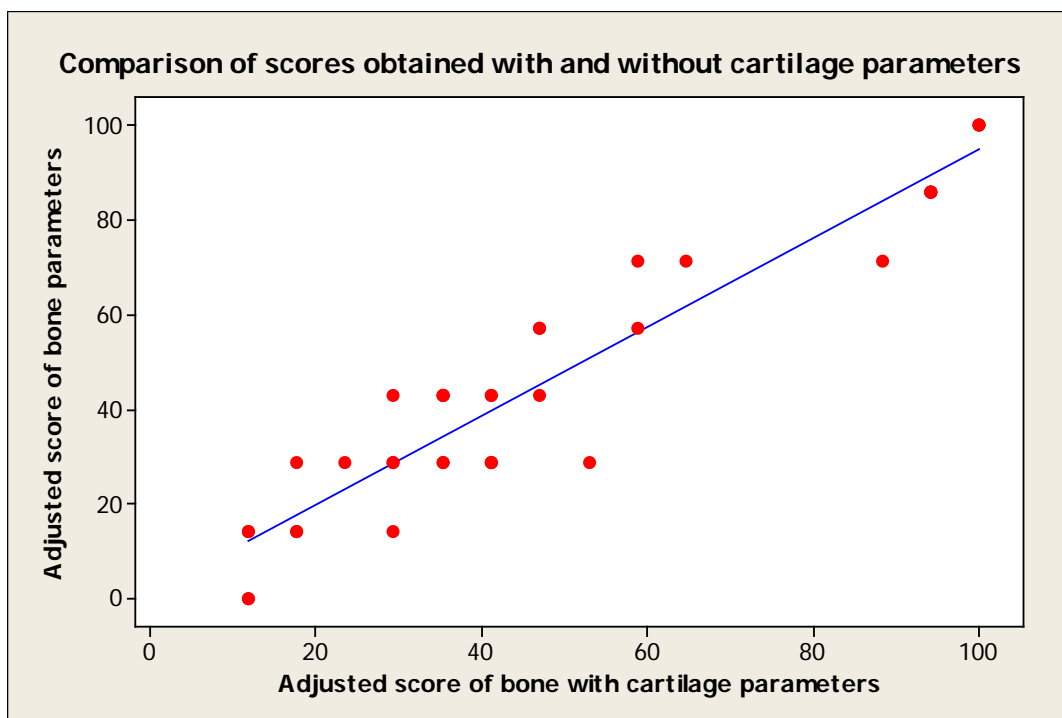
Figure 2.22. A scatter-plot demonstrating the relationship of scores (n=39) when comparing those obtained using only the bone parameters to the scores obtained using both the bone and the cartilage parameters. Blue line is indicative of the trendline. Spearman's rank correlation coefficient confirmed that the two variables showed a significant correlation (p<0.01).

2.4.3. Correlations between histological parameters

Using the whole data set correlation coefficients were produced. Cartilage thickness was significantly and negatively correlated with percentage bone area, tidemark integrity, surface integrity and cartilage morphology ($p<0.05$). The cartilage thickness and tidemark integrity showed the greatest correlation coefficient (results not shown).

Bone area was also significantly correlated with all parameters. The percentage of bone correlated negatively with the cartilage thickness and demonstrated positive correlations with the tidemark, surface and morphology parameters. Pearson's and Spearman's rank correlation coefficients in all cases produced a significant $p<0.05$ value. Figure 2.23 illustrates the negative regression line produced when correlating the percentage of bone to the cartilage thickness.

The bar charts seen in figures 2.24 to 2.26 demonstrate frequencies of the categorical parameters in relation to the categorical bone scores. Looking specifically at figure 2.24 it is evident that with increasing bone score there is an increasing number of samples that had a tidemark score of 4 (highest score). The low tidemark scores (scores 0 and 1) are abundant in the lower bone score categories. It is also possible to suggest that the bone scores appear to become higher (suggesting a more diseased state) prior to the changes to the tidemark. In other words, with the increasing bone scores, there remains an abundance of lower tidemark scores whilst also seeing an increase in the numbers of higher tidemark scores. It is only when the state of the bone appears at its worst (score 3) that the lower tidemark scores reduce. As mentioned, this may indicate that changes to the subchondral bone precede the tidemark changes. Interestingly, there is a lack of tidemark score 3 in the highest bone score category. A possible reason for this may be that once changes do begin to occur in the tidemark, it then deteriorates rapidly and, as a consequence, falls into the highest scoring category rather than score 3. Data were computed using the crosstabulation method on SPSS, showing statistical significance when analysed using Spearman's rank correlation for ordinal variables ($p<0.01$).

Figures 2.25 and 2.26 show similar trends when compared to figure 2.24. When the bone achieves the highest score (score 3), the most frequent score obtained for the surface

integrity and cartilage morphology is also the highest score. In figure 2.25, the low surface integrity scores are restricted to the low bone scores. As the state of the bone progresses, it seems that the changes to the surface are variable in that there are samples whose surface integrity deteriorates at what seems to be a relatively similar rate to the bone. However, there are also many samples whose bone scores are high but whose surface scores remain low. It is important to note however, that data in figure 2.26 did not generate a significant correlation despite following the general trend (p>0.05).
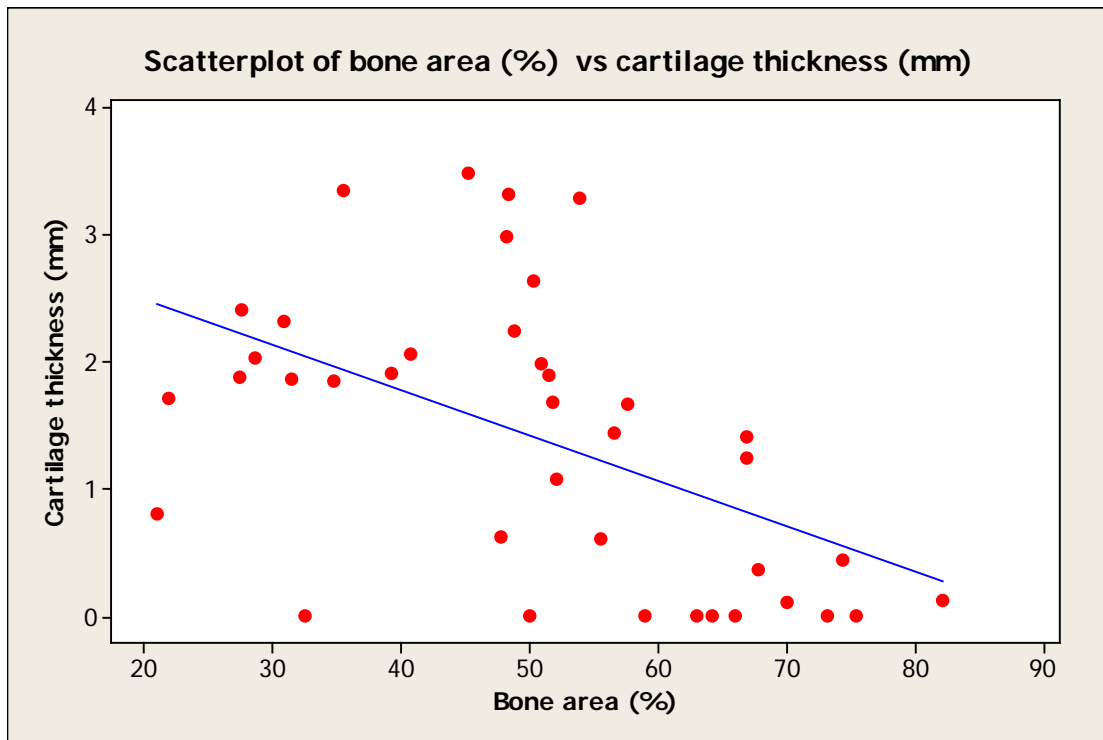
Figure 2.23. A scatter-plot showing the correlation between the amount of bone (%) and the cartilage thickness (mm) within the whole data set (n=39). Blue line is indicative of the trendline. Pearson's and Spearman's correlation tests demonstrate a significant difference between the parameters ($p<0.01$).
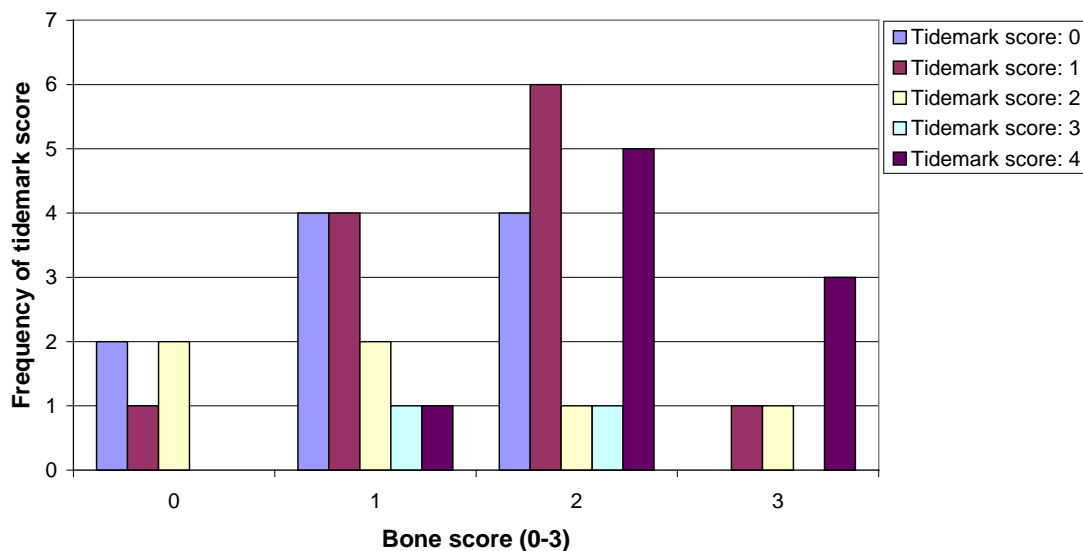
Figure 2.24. Frequency bar charts showing tidemark integrity scores obtained relative to the bone scores within the whole data set (n=39). Lower scores are indicative of a more normal state. Spearman's rank correlation for ordinal variables suggest a significant trend ($p<0.05$).

Frequency chart for bone area vs surface integrity scores
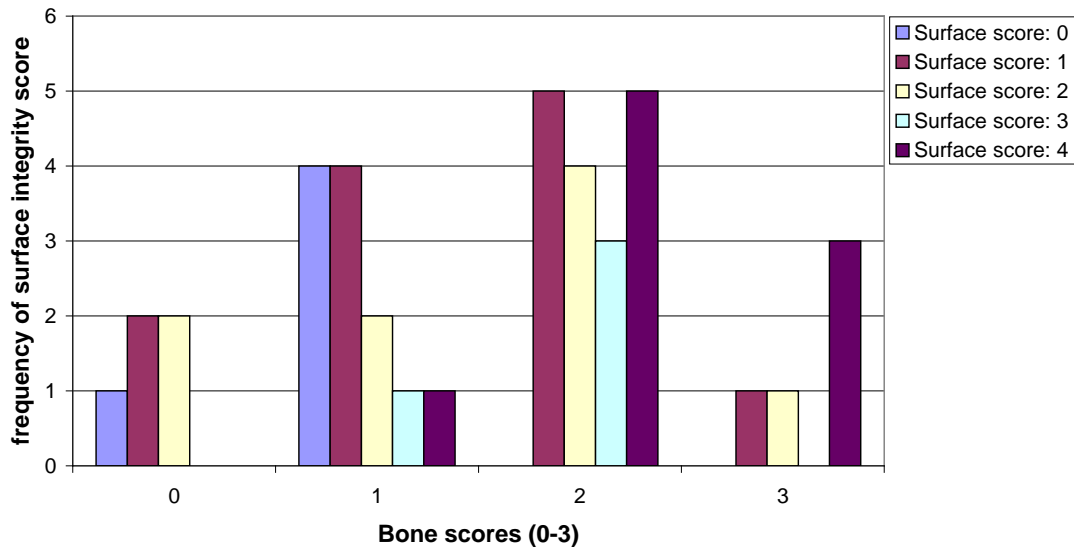
Figure 2.25. Frequency bar charts showing surface integrity scores obtained relative to the bone scores within the whole data set (n=39). Lower scores are indicative of a more normal state. Spearman's rank correlation for ordinal variables suggest a significant trend (p<0.01).

Frequency chart for bone area vs cartilage morphology scores
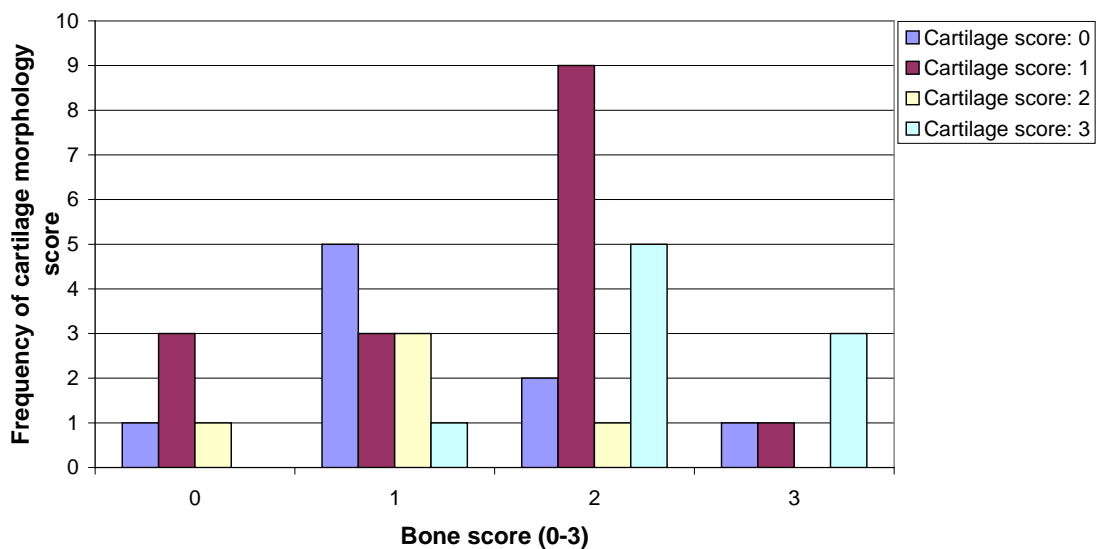
Figure 2.26. Frequency bar charts showing cartilage morphology scores obtained relative to the bone scores within the whole data set (n=39). Lower scores are indicative of a more normal state. Spearman's rank correlation for ordinal variables did not suggest a significant trend (p>0.05).

2.4.4. Using the scoring system to distinguish 'mild' and 'severe' samples of OA

Obtaining a score between 0 and 17 represents the overall state of tissue, as the more 'normal' the sample, the lower the score. The system was tested to see whether or not these overall scores could be used to distinguish between 'mild' from 'severe' OA samples. Within the data set, as previously mentioned, the overall scores ranged from 2 to 17, and the mean of all scores was 8.26. Based on this observation, the overall scores were used to group the milder cases from the more severe cases of OA. Scores between 0 and 8 were categorised under 'mild OA' and scores between 9 and 17 were categorised under 'severe OA'. Figure 2.27 illustrates the difference between the two groups. It can be seen that in the mild category, the median score is 6 where as in the severe category the median is 16. The difference between the two groups was shown to be statistically significant ($p<0.01$) when analysed using a Mann-Whitney test for non-parametric data.

Using these two separate groups, the individual parameters were analysed to see whether the overall sum was accurate in distinguishing mild from severe OA groups. Table 2.4 shows the breakdown of frequencies within the individual categorical parameters, enabling us to assess whether scores obtained through the scoring system was representative of individual parameters (figures 2.28 – 2.32).

For cartilage thickness and bone area, the continuous data was used rather than the categorical data (figures 2.28 and 2.29). The median cartilage thickness in the mild group was 1.91mm, whereas in the severe group the majority of the samples were denuded resulting in a thickness of 0mm. This demonstrates a great difference between the two groups which was statistically confirmed using a Mann-Whitney test ($p<0.01$). This result confirms that the overall scores obtained from the scoring system can be used to distinguish 2 significantly different groups (mild and severe); in this case within the cartilage thickness parameter. Similarly, figure 2.29 illustrates the bone area box-plot. The median bone area within the mild group was 48 percent, compared to the median within the severe OA group which was 66 percent. Student t-tests confirmed that the two groups were significantly different ($p<0.01$).

The categorical parameters are represented in figures 2.30 to 2.32. Figure 2.30 shows the tidemark integrity scores within the mild OA and the severe OA groups. The mode in the

mild group is 1, whereas the mode in the severe group is 4. This pattern of results is consistent within the other parameters namely, surface integrity and cartilage morphology as shown in figures 2.31 and 2.32. Mann Whitney tests carried out on all sets of data confirmed that the mild and severe OA groups could be classed as two significantly different groups based on the scores obtained (p<0.01).
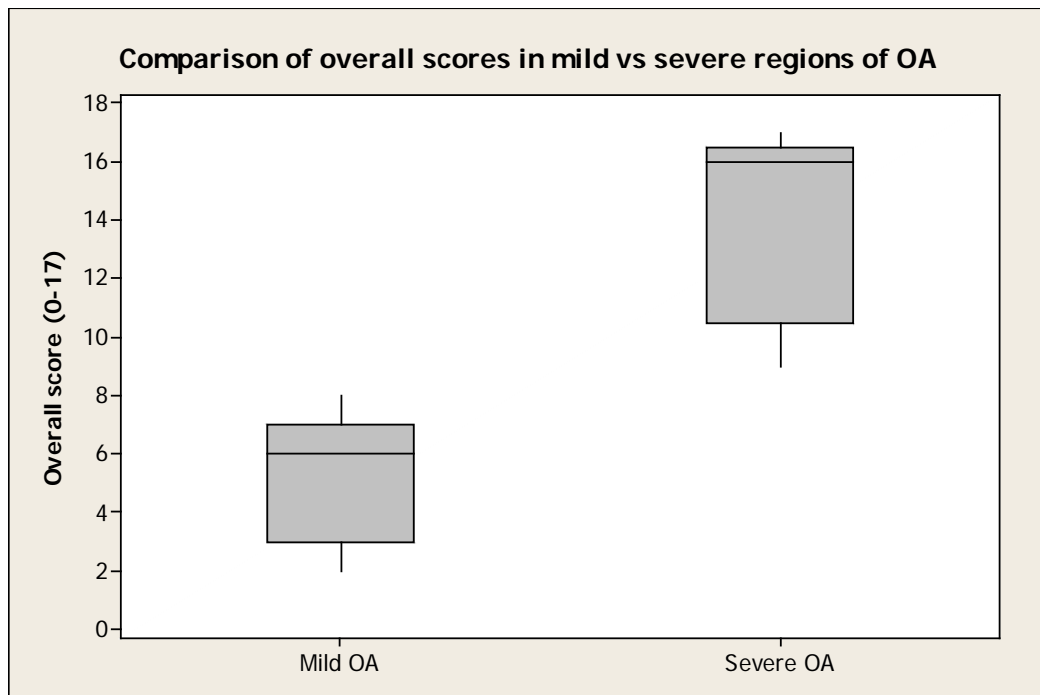
Figure 2.27. A box-plot showing the differences in overall scores for the mild OA group compared to the severe OA group. The midline of the box-plot is representative of the median value (m=6, s=16), the second and third quartiles are displayed as a box and the first and third quartiles as whiskers. Mann Whitney test shows that the difference between these two groups is significant (p<0.01).

Tidemark integrity				Surface integrity		
Score	Mild OA	Severe OA		Score	Mild OA	Severe OA
0	9	1		0	5	0
1	12	0		1	11	1
2	4	2		2	8	1
3	1	1		3	2	2
4	0	9		4	0	9

Cartilage morphology			Cartilage thickness			Bone area		
Score	Mild OA	Severe OA	Score	Mild OA	Severe OA	Score	Mild OA	Severe OA
0	9	0	0	6	0	0	5	0
1	13	3	1	14	0	1	11	1
2	4	1	2	5	2	2	9	8
3	0	9	3	1	11	3	1	4

Table 2.4. Frequency table summarising the distribution of scores within each parameter, between the 'mild OA' and the 'severe OA' groups.
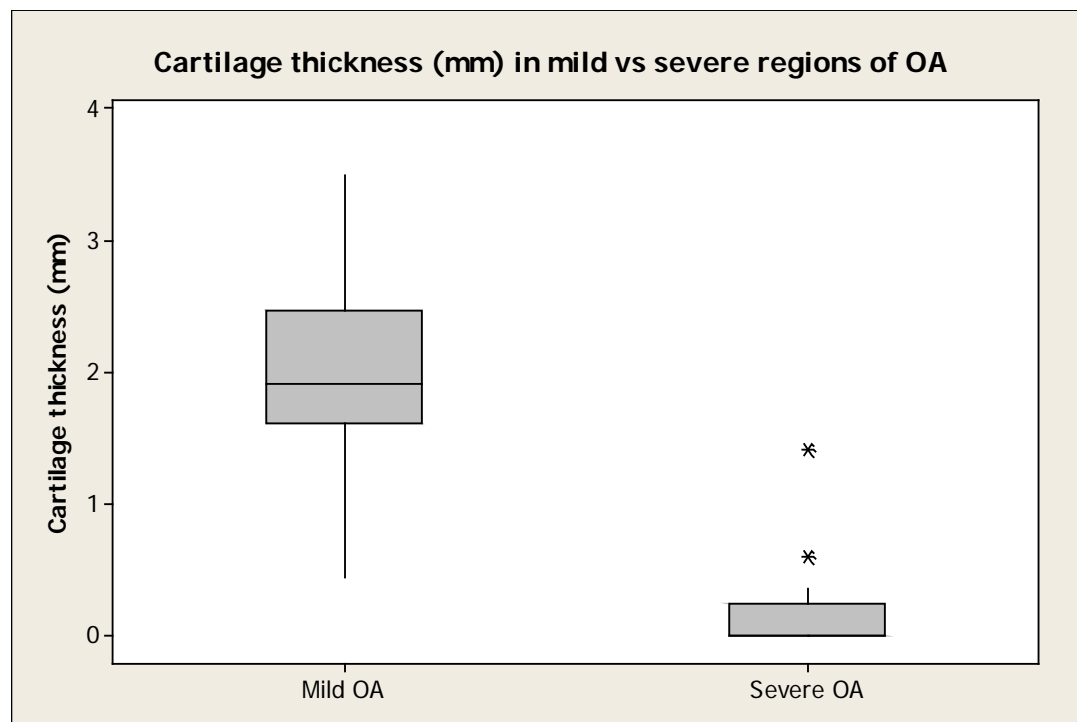
Figure 2.28. A box-plot showing the differences in cartilage thickness (mm) between the mild and severe OA groups. The median in the mild group is 1.91 mm and in the severe group is 0.00mm. Mann Whitney test shows that the difference between these two groups is significant (p<0.01). Suspected outliers are represented by an asterix (*).
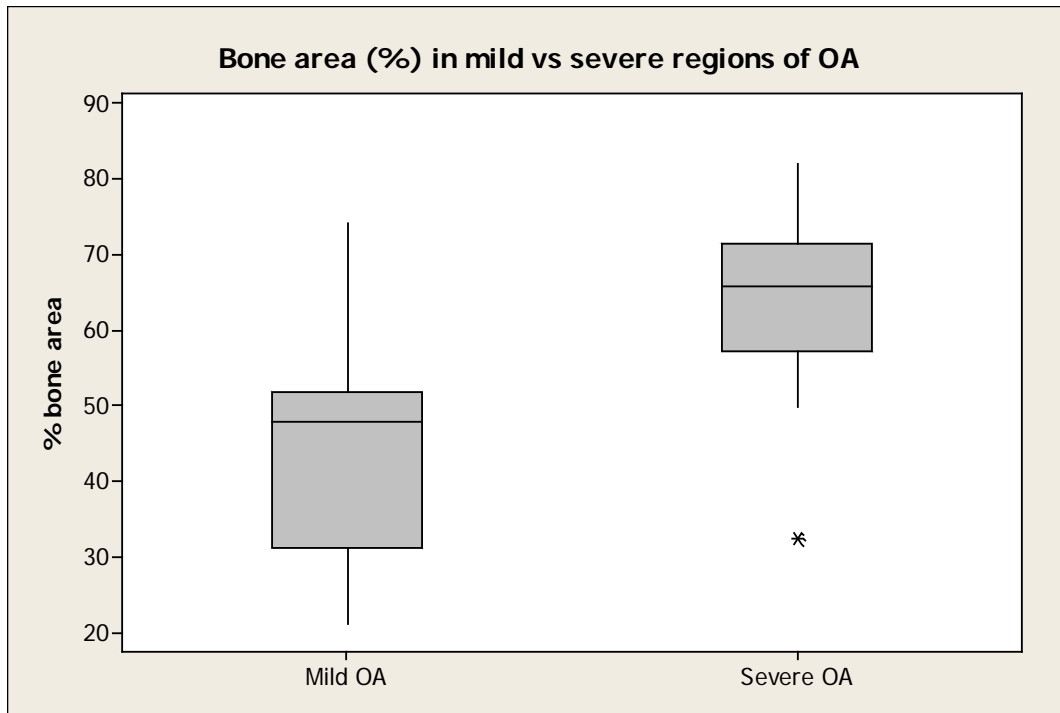
Figure 2.29. A box-plot showing the differences in bone area (%) between the mild OA group compared to the severe OA group. The median in the mild group is 48.02 and 66.02 in the severe group. Student t-test shows that the difference between these two groups is significant (p<0.01).
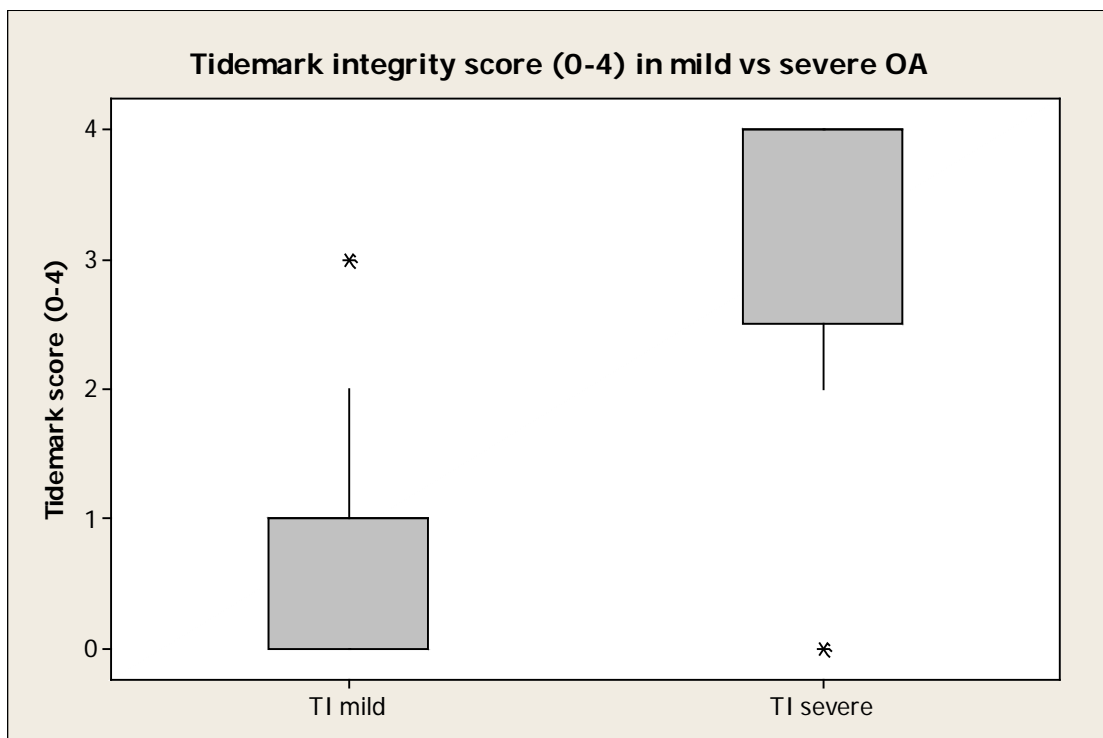
Figure 2.30. A box-plot showing the differences in tidemark integrity (TI) in the mild OA group compared to the severe OA group. The median in the mild group is 1 and 4 in the severe group. Mann Whitney test shows that the difference between these two groups is significant (p<0.01).
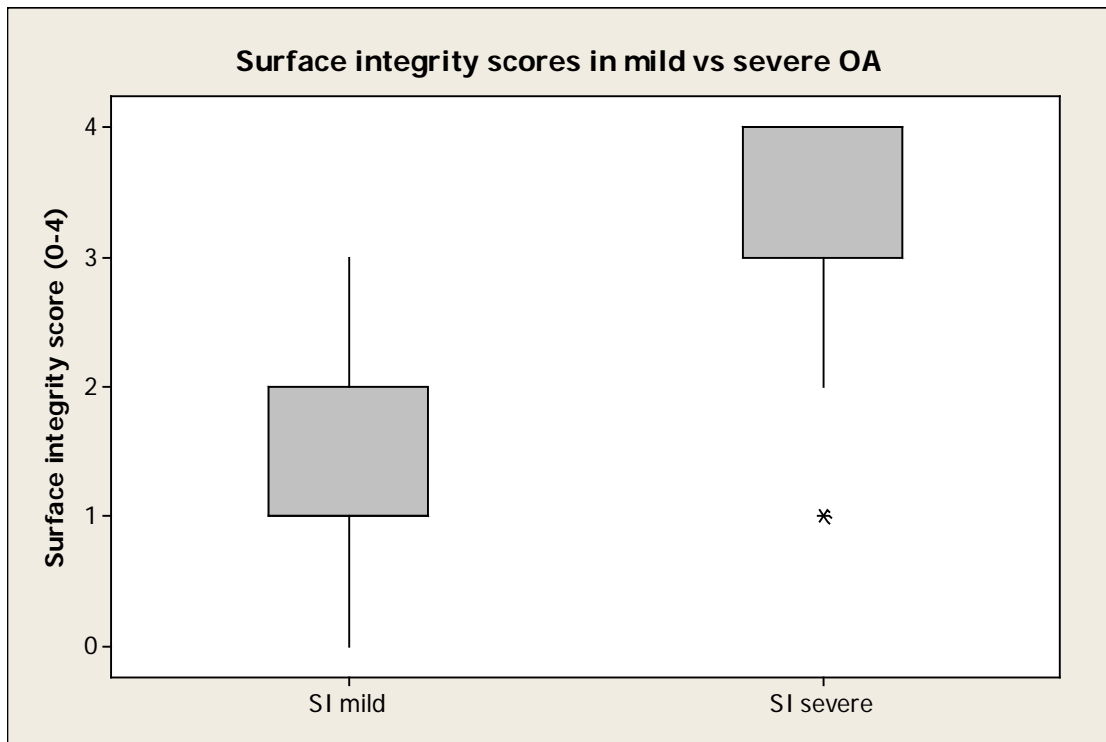
Figure 2.31. A box-plot showing the differences in surface integrity (SI) in the mild OA group compared to the severe OA group. The median in the mild group is 1 and 4 in the severe group. Mann Whitney test shows that the difference between these two groups is significant (p<0.01).
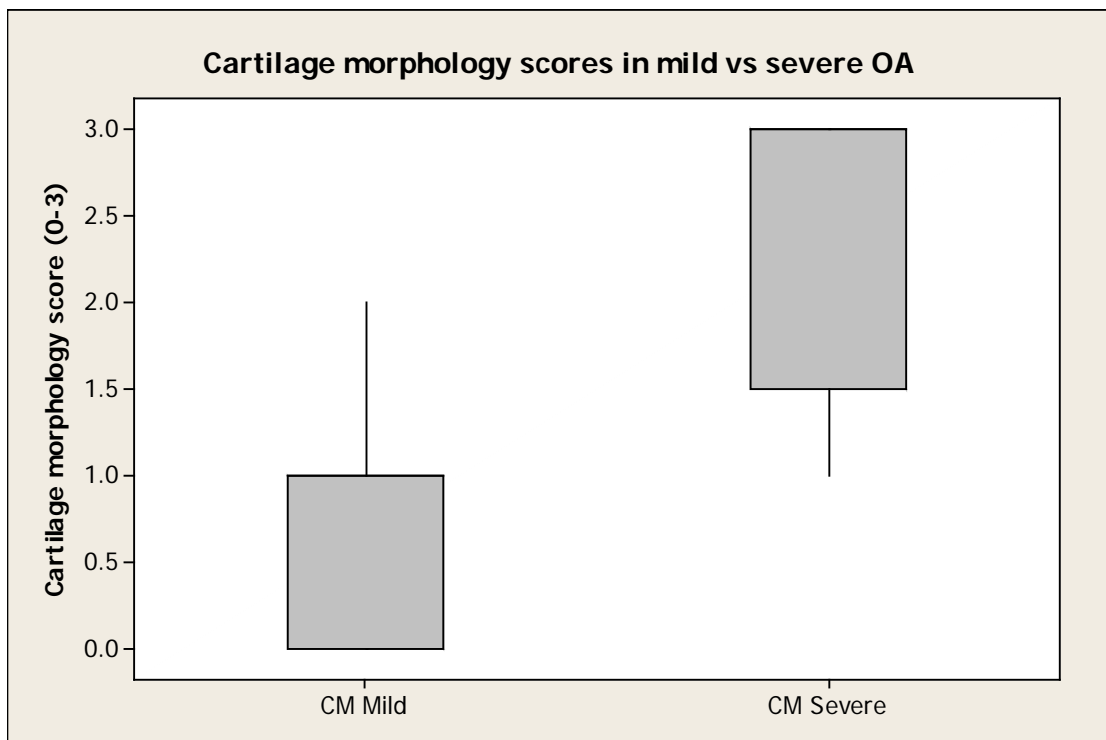
Figure 2.32. A box-plot showing the differences in cartilage morphology (CM) in the mild OA group compared to the severe OA group. The median in the mild group is 1 and 3 in the severe group. Mann Whitney test shows that the difference between these two groups is significant (p<0.01).

2.4.5. Variability

Inter- and intra-observer variability was examined in order to assess the validity and reproducibility of the results. Studying the inter-observer results, figure 2.33 illustrates the sum of scores of the 10 OCPs. It can be seen that the combined scores range between 64 and 71. The standard deviation for individual OCPs should not be regarded as relevant information as this is based on the varying scores of the different plugs. What should be observed, however, is how the standard deviation varies between OCPs as this is what gives the indication on how much variation there was between the OCPs. This information is also summarised in table 2.5. One way ANOVAs confirmed that there was no significant variation between observers.

Figure 2.34 shows the mean scores of OCPs scored by the different observers, ranked in order of severity. In this case, the error bars demonstrating standard deviations are indicative of the variation that each OCP obtained. It is evident through looking at this chart that there was greatest variation in the lowest score (SD=1.13), and that with increasing scores and, therefore, more diseased tissue. There was no variation between observer scores (indicated by the fact that SD=0).

Intra-observer variability results show very similar trends when compared to the inter-observer results. Relating to figure 2.35 which illustrates the combined sum of scores achieved on the 3 separate occasions, it can be seen that there is a smaller range of scores (64-67). The range of standard deviation is also smaller indicating that intra-observer scoring demonstrate more reproducibility than the inter-observer scoring.

Similar to figure 2.34, figure 2.36 shows that within the intra-variability scores, there is greater variability in the lowest scores OCP, and that the highest scores show no variation (SD=0). In 60 percent of the OCPs, there was no variation in the overall score obtained on the 3 separate occasions.

2.4.5.1. Inter-observer

Combined sum of inter-observer scores
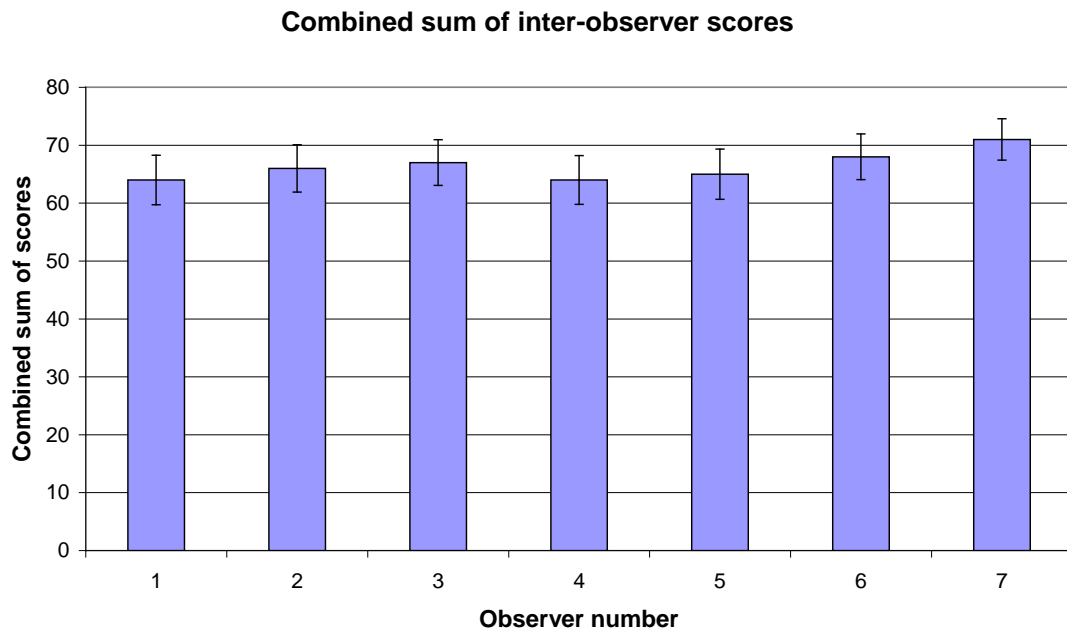
Figure 2.33. A Bar chart illustrating the combined overall scores obtained between observers. The combined scores ranged between 64 and 71 when grading 10 OCPs. Error bars are indicative of standard deviation. One way ANOVA confirmed that there was no significant difference between observer scores (p=0.99).

Mean inter-observer OCP score
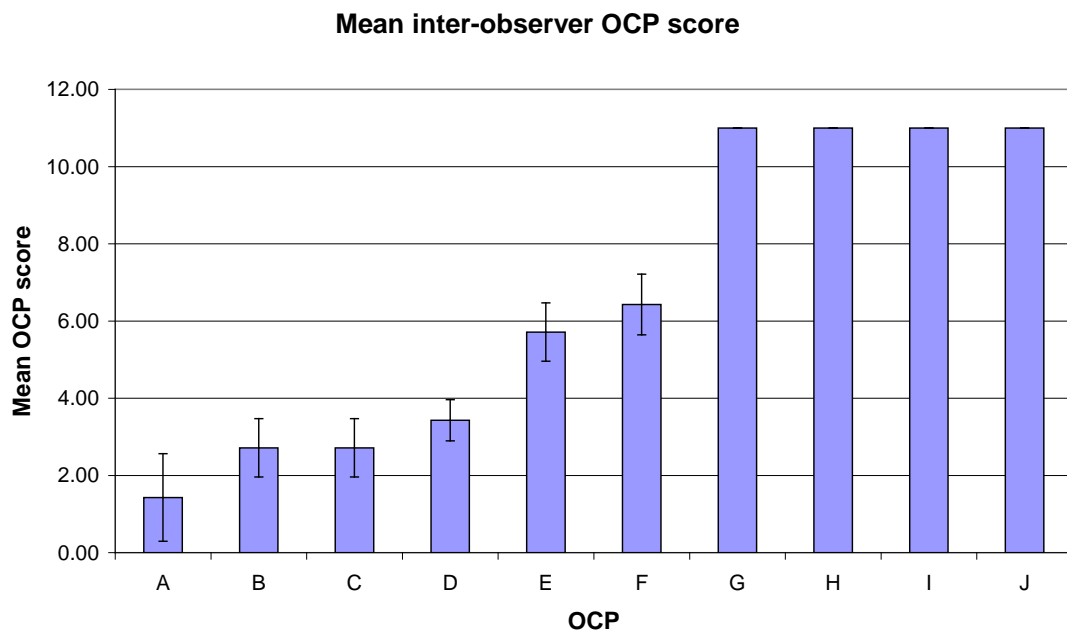
Figure 2.34. A bar chart showing the mean scores of OCPs scored on 7 occasions by different people, ranked in order of severity. The error bar shows the standard deviation (SD) of scores, indicating the level of variability between observers for each OCP. OCPs G-H show no error bars as the SD was 0.

OCP	Observer							MEAN	SD
	1	**2**	**3**	**4**	**5**	**6**	**7**		
A	0	1	2	2	0	2	3	1.43	1.13
B	2	3	3	3	2	2	4	2.71	0.76
C	3	3	3	1	3	3	3	2.71	0.76
D	4	3	3	3	3	4	4	3.43	0.53
E	5	5	5	6	6	6	7	5.71	0.76
F	6	7	7	5	7	7	6	6.43	0.79
G	11	11	11	11	11	11	11	11.00	0.00
H	11	11	11	11	11	11	11	11.00	0.00
I	11	11	11	11	11	11	11	11.00	0.00
J	11	11	11	11	11	11	11	11.00	0.00
TOTAL	64	66	67	64	65	68	71		
SD	4.27	4.09	3.95	4.20	4.33	3.94	3.57		

Table 2.5. Summary of inter-observer scores for 10 OCPs. The mean score for each OCP is shown, as well as the total combined score achieved from each observer. SD = standard deviation.

2.4.5.2. Intra-observer

Combined sum of intra-observer scores
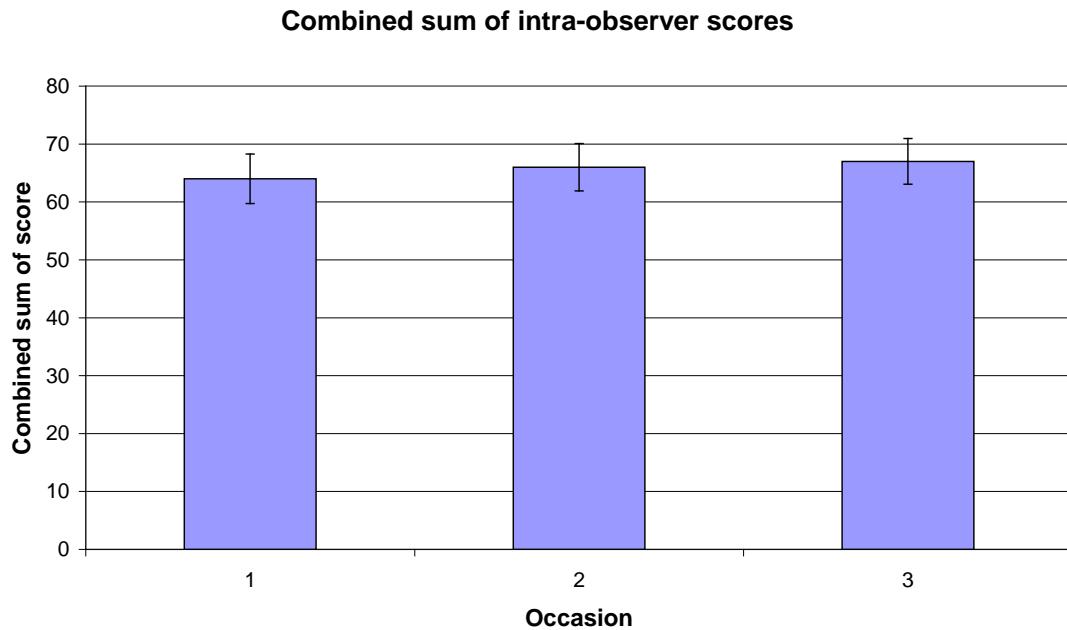
Figure 2.35. A Bar chart illustrating the combined overall scores obtained on three separate occasions by the same observer. The combined scores ranged between 64 and 67 when grading 10 OCPs. Error bars are indicative of standard deviation. One way ANOVA confirmed that there was no significant difference between observer scores ($p=0.99$).

Mean intra-observer OCP score
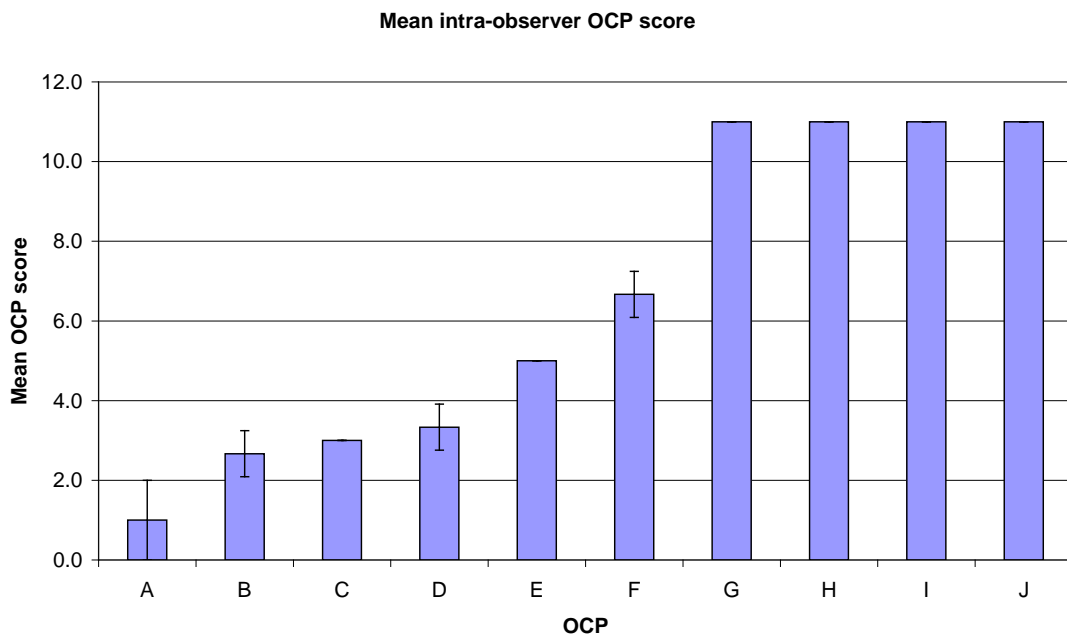
Figure 2.36. A bar chart showing the mean scores of OCPs scored on 3 occasions by myself, ranked in order of severity. The error bar shows the standard deviation (SD) of scores, indicating the level of variability between scores obtained throughout the 3 occasions. OCPs C, E and G-J show no error bars as the SD was 0.

OCP	Occasion			MEAN	SD
	1	2	3		
A	0	1	2	1.0	1.0
B	2	3	3	2.7	0.6
C	3	3	3	3.0	0.0
D	4	3	3	3.3	0.6
E	5	5	5	5.0	0.0
F	6	7	7	6.7	0.6
G	11	11	11	11.0	0.0
H	11	11	11	11.0	0.0
I	11	11	11	11.0	0.0
J	11	11	11	11.0	0.0
TOTAL	64	66	67		
SD	4.27	4.09	3.95		

Table 2.6. Summary of intra-observer scores for 10 OCPs. The mean score for each OCP is shown, as well as the total combined score achieved from each observer. SD = standard deviation.

2.5. Discussion

The relationship between the overlying cartilage and the subchondral bone has been observed for decades. Radin et al., (1986) stated that "the health and integrity of the overlying articular cartilage depends on the mechanical properties of its bony bed, and that alterations of the bony bed occur before the cartilage changes". Despite this heavily sited article and the abundance in literature emphasising the involvement of the subchondral bone in and throughout the course of OA, the articular cartilage remains in the spotlight when assessing the severity of diseased tissue. The cartilage is not only isolated from all other tissues to be used as the sole tool for judgement, but the cartilage is also stripped from its core; the subchondral bone, to which it is directly anchored. The process of detaching the cartilage from the bone has been questioned by many; a recent study by Amin et al., (2009) addressed this issue and went on to suggest that the condition of the underlying bone significantly influenced chondrocyte survival in the overlying cartilage. So the question to be raised is 'why is the subchondral bone overlooked when its involvement is so widely accepted?'.

A new scoring system: a histological view

The purpose of this new scoring system was not only to incorporate the subchondral bone, but also to obtain overall scores for the graded tissue that was indicative of the diseased state. Figures 2.5 to 2.17 demonstrate the increasing scores, mapping out stages in the progression of OA. The range of possible scores obtained from this scoring system is 0-17, however within these data sets the lowest obtained score was 2. As the patients who underwent total knee replacement surgery were diagnosed with OA, it would be surprising to find normal (score=0) OCPs, as this would suggest that the tissue was unaffected by the disease and surgery would, therefore, be unnecessary. Relating once again to the range of scores, another interesting point to note was that within the OCPs, scores 12-14 were absent. As briefly discussed in the results section, this could indicate that once the degradation has reached a certain point, the changes occur at a much quicker rate and so there are fewer intermediate points.

Addressing specifically the changes within the cartilage morphology, it appears that in

general, cell clustering was a feature throughout all stages of the disease where cartilage was present, varying between OCPs but not following any general trend. It could be said that clusters were larger and/or more abundant in more severe OCPs but this was not always the case. It is widely discussed in the literature that clustering of chondrocytes is indicative of mitotic activity resulting in cell proliferation, however it has also been proposed that clustering may be a result of cellular migration (Kouri et al., 1996, Morales, 2007). It would be interesting to know whether the chondrocyte clusters resulted from cell migration, or cell proliferation as this would give an indication of the mechanisms involved in the changes that occur. The typical structured organisation of cartilage was also ambiguous as there were some severe cases where there was evidence of an organised matrix, as well as some milder cases with little structural organisation. Based on this finding, it could be argued that the overall cartilage morphology does not necessarily represent the overall state of disease within OCPs. This theory however, challenges many of the current scoring systems as they are heavily weighted on the cartilage structure and morphology (Collins and Mc, 1960, Mankin et al., 1971).

The cartilage surface integrity as well as the tidemark integrity do appear to follow a general trend based on the histological sections, in that the higher scores show more severe changes. Having said that, duplication of the tidemark and/or multiple tidemarks do not seem to represent the severity as a whole, as they were seen sporadically throughout the OCPs.

The OCP of score 7 (figure 2.10) showed in interesting feature within the articular cartilage which can be seen outlined by X's. As aforementioned, there is a region which appears to be encapsulated by a circular fibrous covering, containing an unfamiliar variety of components. Further analysis confirmed that within this pocket vascular channels had accumulated in this area. This is intriguing as articular cartilage is renowned for its avascular structure. The question to be raised is 'where did this accumulation originate from'? It could be a result of down-migration from the synovial fluid, or it could be up-migration from the subchondral bone via invasions through the tidemark. The fibrous covering also appears to be partly detached from the surrounding tissues suggesting that it is a separate unit residing within the articular cartilage. The assumption that could be made is that a repair response is occurring within the tissue, however, the problem that this raises

relates to the process that occurs in endochondral ossification. Following vascularisation, mineralisation occurs leading to collagen type X production and eventual terminal differentiation and ossification. This would be detrimental to the cartilage whose structure and function is aimed to enable low-friction movement.

The OCP of score 8 (figure 2.11) could be referred to as an anomaly. Despite a relatively smooth articular covering, the characteristics of the tissue are hugely altered when compared to the normal composition of articular cartilage. Clinically, this could be misleading as the articular surface is often examined prior to TKRs by arthroscopy, and the surface of this OCP is relatively smooth with no fissures or fibrillation. Within the cartilage, there are regions (which are indicated by the red stars), which resemble hyaline cartilage, representing a very small portion of the tissue as a whole. In saying so, it appears that another cell type has taken over the tissue and the hyaline-like areas are the 'last standing' areas. A question to ask, is 'given time would those remaining regions also have been displaced'? The invading fibrous connective tissue appears to be the result of a repair response, and there is evidence of cellular infiltration totally destructing the tidemark. It could be hypothesised that the invading cells are mesenchymal stem cells (MSC's) which are being triggered into producing a repair tissue. As well as the cellular influx, vascularisation was also apparent, and this could follow on as a consequence of the MSCs entering the area. The non-characteristic cartilage and vascularisation brings to mind the thought that the repair tissue being formed may be a 'pannus-like' tissue. Pannus is an inflammatory response normally seen in rheumatoid arthritis, however, a pannus-like tissue has previously been reported in OA (Shibakawa et al., 2003). This is important to note as it may signify cross-relations between rheumatoid and osteoarthritis, and also supports reports which state that OA does in fact have an inflammatory response.

With regards to the 'pannus-like' tissue, there were other OCPs with small, highly cellular, fibrous regions (scores 4, 7, and 10; refer to figures 2.7C , 2.10B and 2.13B respectively). Although these regions are insignificant in comparison to the OCP in score 8 (figure 2.11), they may be indicative of an early stage in the process. In the figures mentioned, the regions in question were indicated with a black arrow.

Moving through the scores to the more severe cases, it could be suggested that within the

scoring system, scores 9-10 represent the time frame in which the last of the cartilage remains. That said, the cartilage is highly fissured, and the tissues possess few of the characteristics that normal articular cartilage should. The subchondral bone appears to have thickened, and at this point one could assume that the cartilage was doing little in terms of transmitting the high compressive/tensile forces which would be imposed on the weight bearing joint. Scores 11 through to 17 are representatives of the remaining underlying bone. The increasing scores show the progression from a relatively porous bony area with pockets extending to the surface, to a more compact structure with few marrow cavities.

Analysing the differences in patient data

OA is a degenerative joint disease commonly characterised by progressive erosion of the articular cartilage. The correlation between increasing age and prevalence of OA has been heavily documented (Aigner et al., 2007) and there has been evidence to show that age-related changes in the function of chondrocytes may contribute to the development and progression of OA (Buckwalter and Mankin, 1997). In saying that, results from these data sets adhere to this general trend. It is important to note however, that the scatter graph in figure 2.18 represents the age at which the patient underwent TKR, and this does not indicate the initial age at which the patient was diagnosed with OA. In terms of gender differences in OA, there is mixed information in the literature as some authors have found no differences (Davis et al., 1988), whereas others have described a 1.5-4 times higher risk in women than in men (Tsai and Liu, 1992). The data sets used in the present study (figure 2.19) showed no significant gender differences; this could, however, be verified by increasing the patient number in the study.

In relation to compartmental differences, there was significant evidence in this study to suggest that the medial compartment is more severely affected than the lateral compartment. This is in line with previous findings by Ledingham et al., (1993) who found that the medial compartment disease was 4 times more common than the lateral.

Relevance of bony parameters as components in OA scoring

Scoring systems to date focus largely on the state of the hyaline cartilage when assessing the severity of OA. In this scoring system, the subchondral bone and tidemark integrity were added as components to assess the articular unit as a whole. In doing so, scatter graphs were produced so that it was possible to see the impact of the bone based scores when they were added to the cartilage scores. Similarly, we tested to see whether or not adding the cartilage based scores to the bone scores made a difference to the overall output (figures 2.21 and 2.22). In both cases, it was found that there was a significant correlation between the two scores. This not only suggests that the changes to the bony parameters are happening congruent to the cartilaginous changes, but potentially, suggests that the bony parameters alone may be sufficient to assess the severity of OA, as the score obtained when grading only with the bone parameters correlated to the score obtained when assessing the unit as a whole. This could open a pathway for clinicians in assessing the severity of changes in OA prior to TKRs, as a less invasive method of examination using imaging techniques such as MRI.

Correlating the histological parameters

Correlating the histological parameters established that the bone area was a parameter that serves as an indicator as well as any of the other parameters, the difference being that the bone area can be assessed quantitatively. The bone area correlated negatively with the cartilage thickness, and positively with the tidemark and surface integrity parameters. This ties in with the hypothesis of the subchondral bone involvement in OA, as the changes occur parallel, or possibly even prior, to the changes in the other parameters, based on the finding that while the bone scores appeared to be high, there were still high frequencies of low-scoring cartilage parameters (refer to figure 2.25). Interestingly, there was not a significant trend found when comparing the bone score to the cartilage morphology score. This was not surprising as, histologically, it was shown that there were large variations in the cartilage at all levels of severity. However, it does challenge the current scoring systems which rely largely on the assessment of the cartilage morphology.

Using the scoring system to distinguish between 'mild' and 'severe' OA

Using the mean as the midpoint to distinguish between the milder and the more severe OA samples, the overall sum was successful in generating two significantly different states of severity. This was further confirmed by studying individual parameters. The difference between the cartilage thickness was more apparent than the difference between the bone area within the two groups. However, the mechanisms involved differ between the two and, therefore, it is not possible to conclude that the cartilage is being affected to a greater extent. The important point to note is that the changes within the bone parameter were significant and that these differences did correlate with the mild/severe group as categorised through the overall sum.

The qualitative parameters which include the tidemark, the articular surface and the whole cartilage morphology, as previously mentioned, showed similar trends in that there was a significant difference in the distribution of scores obtained in the mild versus the severe samples. This re-established the point that the scores assigned when assessing the tissue as a whole do indeed match up with scores from the individual qualitative parameters, and that the scoring system can successfully separate the milder cases from the more severe cases.

On a separate note, the parameters were assigned based on the fact they are not influenced by the fixation and staining process. Most current scoring systems incorporate matrix staining as a variable to be assessed, based on the level of proteoglycan staining achieved. It is well documented however, that proteoglycan leaching is often associated with fixation methods and so the reliability of the staining is questionable (Pousty et al., 1975). In addition, matrix staining is not consistent throughout the articular cartilage; the distribution differs between the surface and deep layers and so the question of staining intensity becomes subjective. For these reasons we have chosen to omit matrix staining from our new scoring system.

Variability

Inter- and intra-observer variability was tested, indicating the precision of the measurements and also the reproducibility of the results. The results showed that there was greater consistency within intra-observer scores when compared to inter-observer scores, however the scores as a whole did not reveal great variation. The trend that was observed in both the inter- and intra-observer variabilities was that the lowest overall scores (i.e. the milder cases which may be verging on normal) demonstrated the most variation. The severe cases were less sensitive as there was no variation in the inter- and intra-observer scores. A reason for this may be due to the ambiguous nature of the initiation and early progression of the disease.

Conclusion and clinical relevance

The involvement of subchondral bone in OA has been a topic of much discussion in the past decades, however it has been greatly ignored in scoring systems. Here we have incorporated this 'bystander' into the assessment process and have shown that there are significant correlations between changes to this parameter compared to other more commonly used parameters. Inter- and intra-observer variability confirmed that this scoring system provides a promising new devise for the histopathological assessment of OA.

In order for the devised scoring system to be more widely accepted it should undergo a validation process. As such, it would be interesting to score the same tissue samples using the Mankin scoring system to establish whether the results obtained through this scoring system differ from what would be achieved through currently validated scoring systems. It would be of interest to show that despite the different parameters, the result is not radically different from what would have otherwise been obtained. One may then ask 'why bother going to the effort when the end result is no different?'. The answer to this question is that this scoring system highlights changes in the bone that occur congruent to the more widely recognised changes in surrounding tissues, and by validating this scoring and showing the progressive bone changes, a diagnostic tool may be developed providing a more robust method for earlier identification of the disease process.

Within this study, the location of the OCPs excised was based on the topography, where the tibial plateaux were mapped and classified into regions of varying cartilage integrity. It would be of interest to carry out a similar study limiting the analysis to specific anatomical sites within the joint, as this would provide further insight into the locations of the observed progressive disease changes. As a means of further enhancing the scoring system, it would also be beneficial to include the use of molecular targets such as denatured type II collagen epitopes. Hollander et al., (1994) developed an immunoassay to detect denatured type II collagen in osteoarthritis and demonstrated its significant increase particularly in the superficial zone of OA cartilage. As such, it would be interesting to incorporate this technique into the new scoring system to add greater value and further distinguish it from previous methods.

Confirming the relationship between the subchondral bone changes with the overlying hyaline cartilage changes is an exciting prospect as it opens doors for clinical translation. We can hypothesise that quantifying subchondral bone will give the clinician an indication of hyaline cartilage degradation. This will ultimately assist the clinician in identifying cartilage damage or deterioration, thereby facilitating the early diagnosis and the ability to monitor OA in a minimally invasive way.

Chapter 3:

Correlating disease severity with expression of matrix markers, proliferation and stem cell markers in osteoarthritic tissue

3.1. Introduction

As previously outlined, OA is a disease characterised by a loss of articular cartilage components, accompanied by remodelling and a repair attempt carried out by the resident cells. Despite the array of knowledge which has been elucidated from studies throughout the decades, studies commonly focus on the comparative differences between normal or early stage OA and end stage diseased specimens giving little insight into the progressive changes that occur as the disease develops (Ostergaard et al., 1999, Ostergaard et al., 1997).

3.1.1. Matrix markers

Early in development, the cartilage anlagen is predominantly made up of collagen type I, and together with the process of chondrogenic differentiation, there is a gradual transition from type I to type II collagen synthesis (von der Mark, 1980). As such, type I collagen is often referred to as a developmental marker within articular cartilage.

In osteoarthritic cartilage, type I collagen is re-expressed and it is, therefore, regarded as a factor involved in the pathogenesis of the disease (Goldwasser et al., 1982, Nerlich et al., 1993, Miosge et al., 2004). Type I collagen is also associated with fibrocartilage which is referred to as a form of repair tissue following disease or injury within hyaline cartilage (Miosge et al., 1998).

Collagen type IIA is temporarily expressed early in chondrogenesis as a procollagen prior to collagen type II synthesis, and it is thought to have roles other than purely structural (Nah and Upholt, 1991, Oganesian et al., 1997, Sandell et al., 1991). Expression of this protein in later stages of cartilage maturation and under pathological conditions have been observed by several authors, however the expression in these stages aren't clearly understood. In osteoarthritic cartilage, the expression of type IIA procollagen has led to the assumption that OA chondrocytes reverse their phenotype towards a chondroprogenitor phenotype whilst undergoing hypertrophic changes (Aigner et al., 1999, Nah et al., 2001). Despite the acceptance of collagen type IIA in osteoarthritic cartilage, human studies predominantly compare end-stage of the disease to normal specimens and, as such,

information regarding the progressive expression of collagen type IIA throughout the progression of the disease is not known.

Together with the detection of collagen type IIA in osteoarthritic cartilage is the detection of collagen type X, a marker for terminally differentiated hypertrophic chondrocytes. A study by Nah et al., (2001) demonstrated that in the same upper zone of osteoarthritic cartilage where type IIA labelling is evident, collagen type X was also detected. Both collagens type IIA and X were absent from the corresponding regions in normal, mature articular cartilage. There are several other studies which have shown the presence of type X collagen in diseased cartilage (Girkontaite et al., 1996, Walker et al., 1995); however, Rucklidge et al., (1996) detected collagen type X labelling in the surface of normal, human articular cartilage and it is therefore difficult to draw any solid conclusions from the literature. Type X collagen is more commonly renowned for its presence in the deep zone and the zone of calcified cartilage in normal articular cartilage where the cells may become involved in mineralisation; and this labelling has been shown to be consistent in osteoarthritic cartilage (Nah et al., 2001, Rucklidge et al., 1996, von der Mark et al., 1992).

3.1.2. Proliferation marker: Proliferation cell nuclear antigen

Proliferation cell nuclear antigen (PCNA) is an essential component for eukaryotic chromosomal DNA replication, and is, therefore, often used as a marker for cell proliferation (Paunesku et al., 2001). Chondrocytes in normal articular cartilage have a stable phenotype when compared to immature or growth plate cartilage; however, as Pfander et al., (2001) describes; "the possible expression of proteins which are normally produced by chondrocytes during various stages of differentiation in growth plate cartilage, by chondrocytes in OA cartilage could lead to the altered functional activities and loss of their ability to maintain a functional articular cartilage matrix." As such, PCNA which is undetectable in normal human articular cartilage, has been shown to be present in moderately affected OA cartilage, as well as in clusters (chondrones) in severely affected OA cartilage (Pfander et al., 2001).

3.1.3. Stem cell markers

Stem cells in synovial joints are mesodermal by origin, and, as such, are referred to as mesenchymal stem cells (MSCs). Unlike hematopoietic stem cells however, there is no single marker for MSCs at present and thus combinations of cell surface molecules are often employed to identify the cells. According to the International Society for Cellular Therapy (ISCT), MSCs are characterised by their adhesion potential in monolayer culture, their tripotent differentiation potential *in vitro*, and the expression of surface markers CD73, CD90 and CD105 (Dominici et al., 2006). The ISCT have also defined certain surface markers, including CD45 and CD 34 which MSCs should lack. In addition to the cell surface markers listed, many other publications have employed other surface markers to identify progenitor cells in *in vitro* and *in vivo* studies including CD44, CD90, CD166; as well as Stro-1 and Notch-1 (Artavanis-Tsakonas et al., 1999, Baron, 2003, Dennis et al., 2002, Diaz-Romero et al., 2005, Simmons and Torok-Storb, 1991).

Stro-1 is a cell surface protein most widely known for its expression by bone marrow stromal cells (Simmons and Torok-Storb, 1991). Work by Dennis et al., (2002) demonstrated that a subset of Stro-1 positive cells were capable of differentiating into multiple mesenchymal lineages. As such, Stro-1 is regarded as a valuable marker for the identification of human bone marrow stromal precursors, and more generally, a mesenchymal progenitor cell marker. A recent study by Grogan et al., (2009) identified Stro-1 positive cells within normal and increased activation in OA cartilage. Karlsson and Lindahl (2009) have hypothesised that the increased activation of certain cell surface markers, including Stro-1, in OA cartilage could indicate signalling from a regenerative response, and a sign of activated progenitor cells.

Notch-1

The notch signalling pathway plays a crucial role during cell fate assignment, cell differentiation and proliferation, and also in maintaining a stem cell population in many tissues throughout life. Notch receptors are 300-kDa transmembrane proteins with a large extracellular domain containing epidermal growth factor repeats essential for ligand-receptor interactions. In mammals, there are four Notch homologues (Notch 1-4) that

interact with ligands of the Notch receptor, namely Jagged 1 & 2, and Delta 1,3 & 4 (Sassi et al., 2011).

The Notch activation cascade is initiated by cleavage of the receptor in the trans-Golgi network. Through cell-cell contact, the active Notch receptor can then bind with one of its ligands (Gering and Patient, 2010). The canonical pathway consists of a series of cleavages which lead to the release of the intracellular domain of the receptor, which then interacts in the nucleus with the transcription factor CSL (CBF1, Su [H], Lag-1) to regulate the expression of downstream target genes including HES and HERP (Iso et al., 2003, Schweisguth, 2004). Other studies including Matrinez Arias et al., (2002) however, have also suggested that CSL-dependent signalling does not mediate all functions of Notch, and that there is also a CSL-independent signalling pathway.

Extensive research has implicated the Notch pathway in numerous cell fate decisions throughout development; and in particular its role in limb development and chondrogenesis (Artavanis-Tsakonas et al., 1999, Austin et al., 1995, Conlon et al., 1995, Jiang et al., 1998, Williams et al., 2009). Prior to birth, data suggest that the presence of Notch is required for cell differentiation and proliferation, whilst during the late stages of development and post-birth, the expression of Notch instead allows the terminal differentiation and maturation of chondrocytes; favouring the process of endochondral ossification. As summarised by Sassi et al., (2011); "One of the most relevant hypotheses is that Notch may act as an on/off switch, either enabling maturation of the articular cartilage by promoting cell proliferation or acting as a terminal differentiation potential leading to bone formation."

More recent studies have demonstrated that the Notch signalling pathway also promotes the maintenance of a progenitor cell phenotype; a hypothesis supported by Dowthwaite et al., (2004), who showed that Notch was expressed on the surface of articular cartilage of a 7-day-old calf by a progenitor cell population. The authors describe how these cells exhibit increased colony forming efficiencies compared with chondrocytes not expressing Notch, suggesting a primordial role for the receptor in controlling the clonality of the surface zone chondrocytes. Studies by McCarthy et al., (2011) have also confirmed similar findings in chondroprogenitors isolated from equine cartilage.

In relation to human cartilage, studies have demonstrated the presence of chondrocytes in the surface zone of the articular cartilage which positively label for Notch-1 in healthy and OA specimens, which has raised the issue of involvement of the Notch signalling pathway in the pathogenesis of OA, especially with regards to the changes that the chondrocytes undergo during the process (Grogan et al., 2009, Karlsson et al., 2008, Ustunel et al., 2008, Williams et al., 2010).

It was, therefore, the aim of this study to correlate disease severity with the expression of various matrix, stem cell and proliferation markers in order to determine patterns of change that occur as the OA progresses. The scoring system devised in the previous chapter was used to identify specimens at varying stages of disease progression.

3.2. Materials

Material	Catalogue number	Supplier
Procollagen type IIA (003-02) antibody	Ab17771	Abcam, UK
Dako pen Mouse immunoglobulins PCNA (PC-10) antibody	S2002 X0931 M0879	Dako, UK
Aggrecan (5C5) antibody	ALX-803-311-R100	Enzo Life Sciences, UK
DPX mounting medium Haemalum (Mayer) Methylated spirit industrial 0.89 S.G. 74 O.P. Polysine adhesion glass slides Xylene	LAMB/DPX LAMB/170-D M/4450/17 MNJ-800-010F X/0200/17	Thermo Fisher Scientific, UK
Type X collagen antibody	Gift	Klaus von der Mark
Stro-1 antibody	MAB1038	R & D Systems Europe Ltd, UK
Notch-1 (M-20) antibody	SC-6015	Santa Cruz Biotechnology, Inc, USA
Chondroitinase ABC from Proteus vulgaris Hyaluronidase from Streptomyces hyalurolyticus Hydrogen peroxide, 30% (w/w) Phosphate buffered saline Proteinase K from Tritirachium album Toluidine blue Tween$^®$ 20 Type I collagen (COL-1) antibody	C2905 H1136 H1009 P4417 P6556 89640 P1379 C2456	Sigma Aldrich, UK

Antigen unmasking solutions R.T.U Vectastain Universal Quick Kit DAB Peroxidase Substrate Kit, 3,3'-diaminobenzidine	H-3300 PK-7800 SK4100	Vector Laboratories, UK
Safranine O Gurr 'Certistain'	343122N	VWR – Jencons, Leicestershire, UK

Table 3.1. Materials and suppliers.

3.3. Methods

3.3.1. Source of material

Osteochondral plugs (OCPs) from tibial plateaux were excised and processed as described in Chapter 2.3.2 – 2.3.4. This included fixation and decalcification of the tissue prior to wax embedding and sectioning at 8µm.

3.3.2. Scoring

The OCPs were scored using the scoring system that was outlined in Chapter 2 incorporating the articular cartilage and the subchondral bone. A possible score between 0 and 17 was obtained, indicating the degree of change seen within the tissue -higher scores represent more severe changes. The tissue sections were then ranked according to overall score.

The scores of the OCPs ranged from 2-17; in order to see progressive changes in the tissue sections, representatives from score 2, 4, 6, 8, 10, 11, 16 and 17 were analysed. As there were no OCPs scored between 12 and 15 it was not possible to include them. For this reason it was decided that 'score 11' should be presented. Score 17 is important as it is the highest possible score.

3.3.3. Immunohistochemistry: peroxidase labelling

Tissue sections were dewaxed and rehydrated as above. Indirect immuno-histochemistry was then performed in a light-proof, humidified chamber. Using a 'DAKO' pen, a hydrophobic ring was drawn around the tissue sections in order to retain solutions on the slide. Sections were subsequently rinsed in 0.1M PBS containing 0.01% Tween 20 (PBS-T), a wetting agent used to increase penetration and permeability of the antibody. For subsequent washes PBS-T was used. At this point, certain primary antibodies required antigen retrieval techniques. Where required these are outlined in table 3.2. Sections that did not require pre-treatment were maintained in PBS until required. Endogenous peroxidise activity was blocked with 0.3% hydrogen peroxide in distilled H_2O for 5

minutes. Sections were then rinsed. The following steps utilised the R.T.U Vectastain Universal Quick Kit in which reagents (excluding primary antibodies) are contained and instructions outlined. Briefly, tissue sections were incubated in prediluted normal horse serum for 20 minutes. This step is species-specific; appropriate to the species in which the secondary antibody was raised in order to block any non-specific binding to epitopes on the secondary antibody. Following incubation, excess serum was tipped off and primary antibodies diluted in PBS-T were directly applied and incubated; either at room temperature for one hour, or at 4°C overnight. Sections were subsequently washed in PBS (three changes of 5 minutes) and then incubated for 15 minutes in prediluted biotinylated pan-specific universal secondary antibody at room temperature. Following further washes, sections were incubated in a streptavidin/peroxidase complex for 5 minutes. Sections were washed again and developed using a 3,3'Diaminobenzidine (DAB) substrate kit, for 2 to 3 minutes. Subsequently, slides were rinsed in distilled H_2O and immersed in filtered Mayer's haematoxylin for 90 seconds and then washed under running water. The slides were then dehydrated in graded alcohols, cleared in xylene and mounted in DPX. Specific antibodies, incubation times, concentrations and temperatures are summarised in table 3.2.

3.3.3.1. Controls

Negative controls

Primary antibody was omitted and:

- replaced with isotype specific immunoglobulins to demonstrate that the secondary antibody is binding specifically to the primary antibody.
- replaced with PBS to confirm that the secondary antibody is not binding non-specifically to the tissue.

Where possible positive controls were also used to demonstrate that the antibodies were reactive and specific to their antigens.

3.3.3.2. Primary antibody concentration

It was essential that the primary antibodies were optimised by antibody titration so that the best possible results could be obtained.

3.3.4. Microscopy

Labelling was viewed using a Leitz DMRB Leica (Leitz, Wetzlar, Germany) light microscope and images were captured using a moticam 2000 (Motic China Group Co. Ltd.) and subsequently processed using Adobe Photoshop.

3.3.5. Quantification of immunolabelling

Determining the percentage of immunolabelled cells involved systematic counting of positive and negative cells in three 400 x 530µm grids (20x field), starting from the cartilage surface down. The average of the three counts was used for statistical analysis. Comparisons between different scores were made via one-way analysis of variance (ANOVA) followed by Fishers A Priori and Student t-tests to test between individual means (Minitab16). *P* values less that 0.05 were considered significant.

Primary antibody	P/M	Detects	Antigen retrieval	IgG	Incuba-tion time	Optimal working dilution/concent-ration
Type I	M	Collagen type I	Chondroitinase (0.25U/ml) & hyaluronidase (2U/ml). 1h30min @ 37°C	Mouse	1 hour	1:800
Procollagen type IIA	M	Procollagen type IIA	Chondroitinase (0.25U/ml) & hyaluronidase (2U/ml). 1h30min @ 37°C	Mouse	1 hour	1:300 3.3μg/ml
Type X	M	Type X collagen	Proteinase K (2μg/ml) 1h @ 37°C followed by Chondroitinase (0.25U/ml) & hyaluronidase (2U/ml). 30min @ 37°C	Mouse	1 hour	1:3 dilution
5C5	M	Aggrecan	Hyaluronidase (2U/ml) 1hr30 @ 37°C	Mouse	1 hour	1:100
M-20	P	Notch-1	None	Goat	Overnight	10μg/ml
PC-10	M	Proliferating cell nuclear antigen	Antigen unmasking solution (1:100). Bring to boil and put over sections for 1 min. Rinse in cold water	Mouse	Overnight	5μg/ml
STRO-1	M	Human Stro-1	None	Mouse	Overnight	1:50 10μg/ml

Table 3.2. Primary antibodies including antigen retrieval methods used and dilution factors. M – Monoclonal, P – Polyclonal.

3.4. Results

3.4.1. Collagen type I

Collagen type I was detected in all OCPs to varying degrees of intensity. Regionally, there was a trend observed in which the extracellular matrix protein was mostly restricted to the superior aspects of the OCPs; emerging from the surface zone and extending into the middle zone. In figure 3.1A illustrating an OCP of score 2, type I collagen labelling is detected predominantly in the surface zone, accompanied by regions of hypercellularity, and the intensity of the label is gradually reduced inferiorly. As such it appears that a reparative process has been activated through which chondrocytes are altering the ECM. Looking at the detectable labelling in scores 2 and 4 compared to scores 6 & 8, it appears that collagen I is more widespread in the lower scores. In the OCP of score 6 (figure 3.1C) there is clear delineation approximately $300\mu m$ below the articular surface where type I collagen labelling diminishes. Similarly, in the OCP of score 8 (figure 3.1D), within the deep fissures type I collagen labelling in the interterritorial matrix is more sparse. Having said that, it can be seen in figure 3.1D that despite the reduction of ECM labelling, there is evidence of cellular up-regulation within individual cells as well as cell clusters. In most cases, there was no apparent labelling in the deep zones of the various OCPs as demonstrated through figure 3.1H. The 'anomalous' OCP is described below.

Figures 3.1E and F show collagen type I label in an OCP which achieved score 10. Within this OCP, an abundance of collagen type I was seen throughout the entire tissue. Mid-zone chondrocytes labelled positively and deep zone labelling surrounds the pericellular matrix. The fibrous orientation of the fibres within this OCP is also highlighted through the collagen type I labelling, particularly in the surface zone. There appears to be a lack of cellular presence in the surface zone of this OCP as demonstrated by the empty lacunae in the surface zone. Associated with subchondral remodelling is the increased synthesis of type I collagen which can be seen surrounding cell clusters in regions which may have originated from the bone marrow spaces.

Through figure 3.1G (score 11) it can be seen that inferior to the tidemark in the region of calcified cartilage, there is collagen type I labelling which appears reduced in the neighbouring bone.

3.4.2. Procollagen type IIA

The overall distribution of procollagen type IIA labelling throughout OCPs of varying scores was comparable to that seen when labelling for collagen type I. In the OCPs of scores 2 through to 6 (figures 3.2A-C), the surface zones labelled positively throughout the ECM, whereas the middle and deep zones elicited no signs of detectable procollagen type IIA synthesis. There was evidence of cellular labelling as demonstrated in figure 3.2C in some but not all chondrocytes, regardless of whether they were in clusters. Figure 3.2D demonstrates the fissured surface containing many chondrocyte clusters in an OCP achieving score 8. Upon procollagen type IIA labelling, it could be said that there was a lack of definitive cellular and extracellular labelling found.

Figures 3.2E to H highlight the major features seen in the 'anomalous' OCP of score 10 labelled for procollagen type IIA. The surface and middle zones can be seen in figure 3.2E. Figure 3.2F illustrates a higher power image of the cells in the mid-zone through which it can be seen that there is a high percentage of positively labelled cells. It appears that the surface zone cells comprise large lacunae, which are absent in the population of cells in the middle zone perhaps suggesting that there may be a heterogeneous population of cells within the OCP. Similar to the images seen in figure 3.1, the fibrous orientation of the cartilage is highlighted through the procollagen type IIA label. Figure 3.2G is a low power image demonstrating the changes in procollagen type IIA distribution between the different regions. There is an arched delineating line that spans through the middle zone, inferiorly towards the deep zone on the left of the image. Superior to this line, the ECM has labelled positively, and inferiorly there is a reduction in labelling. Having said that, through the central aspect of the non-labelled region there is a zone of cells which appear to be approaching from the subchondral region, showing more positive labelling than the surrounding matrices. This region is shown at a higher power in figure 3.2H. A distinct change in cellular morphology was also observed, as chondrocytes surrounding this region appear to be larger and rounder than the cells within the unidentified region of cells.

Figure 3.2I portrays an OCP of score 11 showing procollagen type IIA labelling within the thin region of remaining articular cartilage.

3.4.3. Aggrecan

Aggrecan labelling is a distinctive feature of articular cartilage as it is typically highly abundant in the ECM. Indeed, in this study it was widely distributed throughout the OCPs of varying scores. Figures 3.3A to C show aggrecan labelling detected in and OCP of score 2. Figures 3.3A and B are images of separate regions along the surface, highlighting the presence of atypical regions within low scoring tissue. It can be seen in figure 3.3B that there is a surface pocket lacking aggrecan, suggesting reduced tissue integrity. Figure 3.3C confirms the presence of aggrecan in the middle and deep zones.

With scores increasing between 2 and 8, the pattern of labelling is continued. Aggrecan was detectable throughout all regions in OCPs of scores 4 and 6 as shown in figures 3.3D to H. One notable observation however, was that the labelling shifted from predominantly extracellular, as seen in figures 3.3A - C to both cellular and extracellular in the higher scores. Between scores 6 and 8 it was noted that there were various regions in which aggrecan labelling diminished; particularly on the surface of the fissures in the OCP of score 8 as seen in figure 3.3I.

Figures 3.3K to P demonstrate the results of aggrecan labelling in the OCP which achieved score 10; previously described for its unusual collagen I and collagen type IIA labelling. A low power image can be seen in figure 3.3K where remarkable changes in aggrecan distribution throughout the tissue was observed. Superiorly in the surface region, aggrecan labelling is reduced when compared to the intensity of label seen in the neighbouring middle region, as illustrated in figures 3.3M and N. However, similar to the procollagen type IIA labelling previously described, there is an imaginary line spanning through the middle zone and progressing inferiorly delineating the regions of positive and negative ECM labelling. The chute-like structure which was previously mentioned for apparent procollagen type IIA label also appears to have heavily labelled for aggrecan as seen in figure 3.3P. The region inferior to the middle zone shows a distinct lack of extracellular aggrecan labelling, despite eliciting cellular labelling as illustrated in figure 3.3O.

3.4.4. Collagen type X

In articular cartilage, collagen type X is usually restricted to the deep zones and the zone of calcified cartilage where terminal differentiation occurs. In the OCPs examined, between scores 2 and 8 there were no unusual differences observed and results are shown in figures 3.4A to C. Figure 3.4D portraying an OCP of score 10 demonstrates evidence of increased label extending into the middle zone. It is also apparent in this image that the tidemark is not linear and has been breached by cell clusters arising from the subchondral bone, a possible contributing factor to the altered type X collagen expression.

Figures 3.4E to I demonstrates the anomalous type X labelling which was detected in the OCP of score 10, highlighting the extent of remodelling and terminal differentiation occurring within this OCP. The distinguishable zones observed previously were maintained; type X collagen synthesis was noticeably up-regulated in the region spanning between the middle zone and the subchondral bone; diminishing to the left of the image. As such, the region which lacked aggrecan labelled positively for type X collagen. Interestingly, however, the chute-like structure previously observed was not apparent when labelling for type X collagen. Higher power views of specific areas are shown in figures 3.4F to I. Within figure 3.4F, a region lacking type X collagen can be seen neighbouring a region with extensive labelling. A population of invading cells can be seen in the right side of the image, shown in higher power in figure 3.4H. Figure 3.4G shows the surface region lacking type X collagen expression. An interesting observation was that at the presumptive tidemark, the overlying tissue appears to have detached from the bone on which it sits, and this detachment can be seen throughout the majority of the OCP when looking at figure 3.4E. In addition, looking at the left side of figure 3.4I where there is no apparent detachment, it appears instead that cells are arising from the bone and spreading through the overlying tissue in a fan-like manner.

3.4.5. PCNA

Figures 3.5A to D demonstrate the presence of proliferating cells in OCPs of varying scores. It can be seen that the labelled cells vary from individual cells to cell clusters, predominantly at the surface and surrounding fissure edges. Interestingly, however, no

PCNA labelling was evident in the lowest scoring OCP. As a general trend, middle and deep zones showed no PCNA labelling within chondrocytes, other than in the anomalous OCP of score 10 (figures 3.5C and D). Through the low power image, it can be seen that the demarcation of labelled regions follows a similar pattern to what was seen previously with the procollagen type IIA and aggrecan labelling. As such, whether in the surface, middle or deep zones, a great proportion of the cells have labelled positively for PCNA, whereas the counterpart elicits virtually no positive labelling.

Figure 3.6 shows the percentage of total cells in the surface zone that labelled positively for PCNA, as an average of 3 random snapshots. What is clear initially by looking at the histogram is that the lower score (score 4) has a significantly reduced proportion of labelled cells when compared to the higher scores, and this was confirmed using one way ANOVA and Student t-tests. Between scores 6 and 10 there was no significant difference between the proportion of labelled cells as they all ranged between 55 and 65 percent. Another interesting point to note is that the error bars are the greatest at score 6, suggesting the greatest variation. With increasing severity, the error appears to reduce in size suggesting that the high proportion of labelled cells is more consistent throughout the surface of the tissue.

In line with the increased proportion of labelled cells in the surface zone was a general trend that became apparent, in that there was also a general increase in the sheer number of cells with increasing scores. This ties in with the finding that there is increased PCNA labelling in OCPs of higher scores.

3.4.6. Stro-1 and Notch-1

Similar to the pattern seen in PCNA labelling, Stro-1 and Notch-1 was localised in OCPs of varying scores as shown in figures 3.7 and 3.9 respectively. Individual cells and cell clusters were shown to have labelled positively. In these OCPs, Stro-1 labelling was restricted to a region approximately 200μm from the surface (figure 3.7C), whereas Notch-1 labelling extended further, into the middle zone (figures 3.9B to D). There was no label detected for either Stro-1 or Notch-1 in the OCP with the lowest score (score 2).

Figures 3.7D to G illustrate the Stro-1 labelling detected in the anomalous OCP of score 10. In this particular case, the area containing positively labelled cells extends beyond the surface zone. It can be seen in figure 3.7G that the Stro-1 labelled region corresponds with the previous findings, spanning throughout the width of the tissue. Again there is a clear demarcation between the non-labelled and the labelled regions as shown in figure 3.7E. Interestingly, it was observed that upon Stro-1 labelling, dendritic-like cells with long 'tails' could be seen particularly in the middle zone (figure 3.7D). Cellular invasions highlighted in figure 3.7F also labelled extensively for Stro-1.

Notch-1 labelling in the anomalous OCP of score 10 showed a similar pattern to the Stro-1 labelling however, the transition between the labelled and non labelled regions was not as clearly defined. As such, the cells in the 'non-labelled' region in the Stro-1 did show signs of Notch-1 labelling albeit to a lesser extent (figure 3.9D).

Figures 3.8 and 3.10, similar to figure 3.6 show the percentage of total cells in the surface zone that labelled for Stro-1 and Notch-1 respectively, as averages of 3 random snapshots. Looking specifically at figure 3.8, the histogram relating to Stro-1 it can be seen that there is no apparent trend in the proportion of cells labelled between the varying scores, and this observation was confirmed statistically using the one way ANOVA test. The proportion of labelled cells in the surface zone as a whole ranged between 67 and 81 percent, with varying degrees of standard error in accordance to the variability seen. On the other hand, Notch-1 labelling in the surface zone did show significant difference between the varying scores, as confirmed using one way ANOVAs and Student t-tests (figure 3.10). Score 4 showed a significantly reduced proportion of labelled cells (approximately 48 percent) when compared to higher scores, and score 6 elicited the highest proportion of labelled cells, at 97 percent. The higher scores (8 and 10) also comprised a large proportion of labelled cells when compared to score 4, at approximately 85 percent. Notably, the greatest variation seen in Notch-1 labelling was in the score 10, where the error levels are over double those from the other scores.
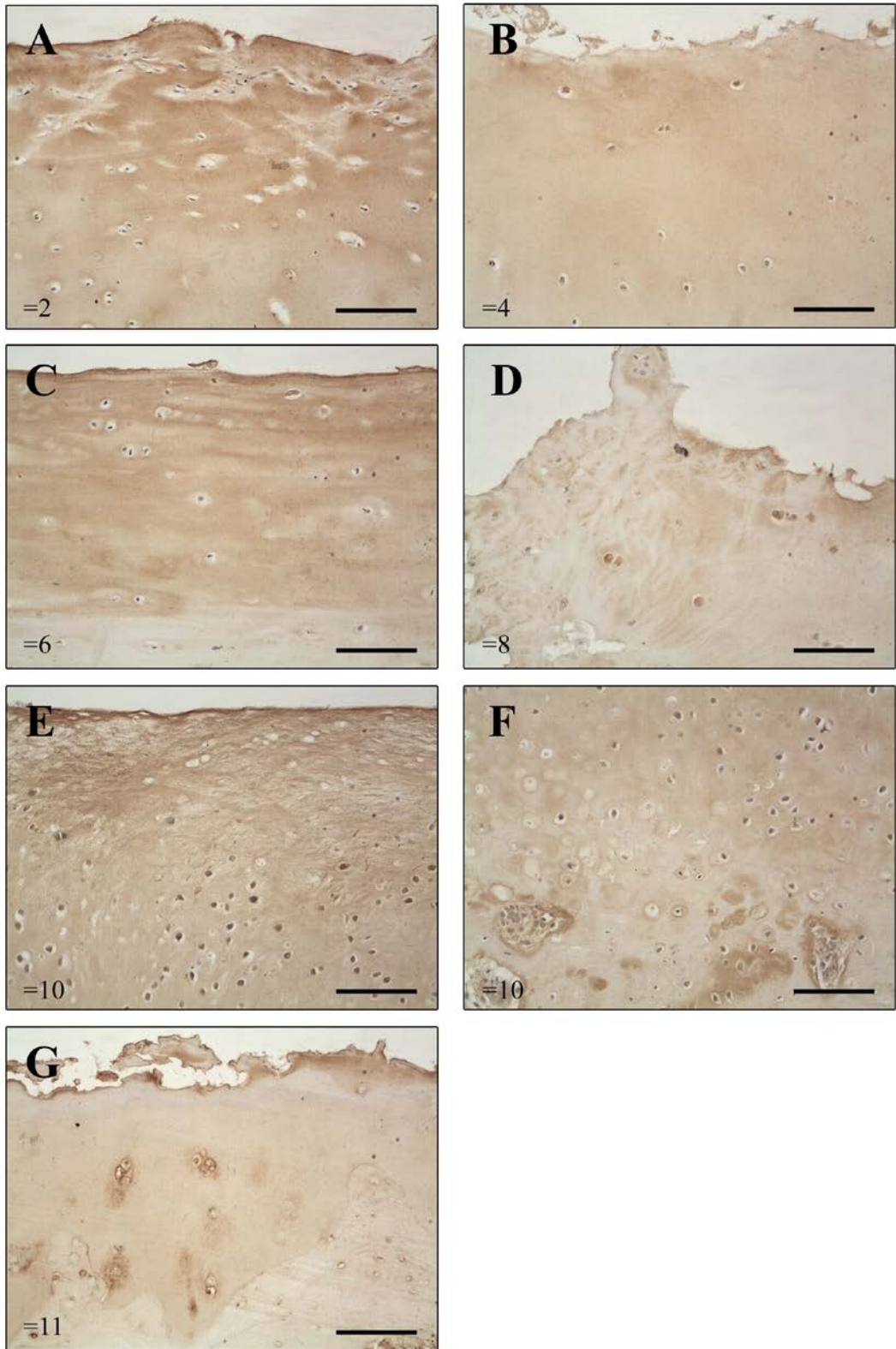
Figure 3.1. Type I collagen labelling in OCPs of varying scores.
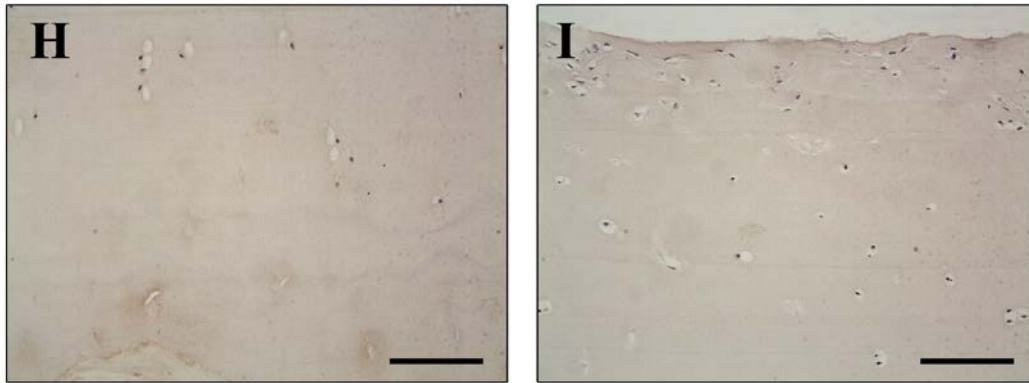
Figure 3.1. Type I collagen labelling in OCPs of varying scores.

Figure A. Surface region of OCP with score 2. Collagen type I labelling throughout the ECM, with more intense labelling superficially. No cellular label apparent. Hypercellularity in the surface zone is indicative of a repair process. Scale bar = 100μm.

Figure B. Surface region of OCP with score 4. Collagen type I label evenly distributed throughout imaged area. There is evidence of cellular labelling in the superficial cells. Scale bar = 100μm.

Figure C. Surface region of OCP with score 6. Collagen type I label in the surface only. A visible reduction can be seen on entering the mid zone. A lack of cellular and pericellular labelling was observed. Scale bar = 100μm.

Figure D. Surface region of OCP with score 8. Weak collagen type I labelling can be seen in the interterritorial matrix. Evidence of cellular labelling in individual cells as well as cell clusters. Scale bar = 100μm.

Figures E & F. Type I collagen labelling in an OCP of score 10. Figure E illustrates the surface zone extending into the mid zone, whilst figure F demonstrates the deep zone with evidence of subchondral bone remodelling. ECM labelling is apparent throughout the regions. Cellular labelling is restricted to the mid and deep zones. Scale bar = 100μm.

Figure G. Type I collagen labelling in an OCP of score 11. A thin layer of articular cartilage covering the subchondral bone labelled positively for collagen type I. Label is also apparent in the calcified cartilage and bone regions. Scale bar = 100μm.

Figure H. The deep zone of an OCP demonstrating an absence of type I collagen labelling in this region. Multiple tidemarks can be seen. Scale bar = 100μm.

Figure I. Negative control showing no non specific labelling of type I collagen in the surface region. Scale bar = 100μm.
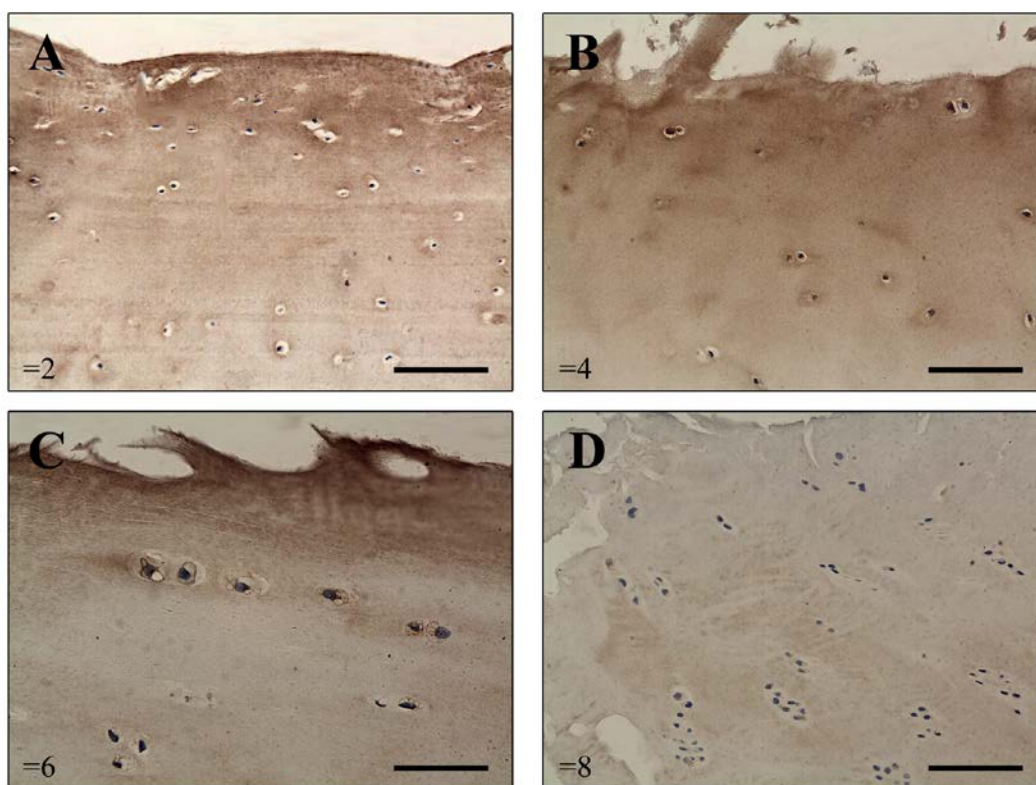
Figure 3.2. Procollagen type IIA labelling in OCPs of varying scores.

Figure A. Procollagen type IIA labelling in an OCP of score 2. Label apparent throughout the matrix. Increased label intensity is apparent in the surface zone and in the pericellular matrix region. Scale bar = 100µm.

Figure B. Procollagen type IIA labelling in an OCP of score 4. Labelling can be seen in the ECM of the surface zone extending into the mid zone. Evidence of cellular labelling in the surface zone chondrocytes. Scale bar = 100µm.

Figure C. High power view of procollagen type IIA labelling in the surface zone of an OCP of score 6. Cellular labelling evident in some but not all cells. Interterritorial matrix labelling observed in the most superficial regions. Scale bar = 50µm.

Figure D. Fissured surface of an OCP with score 8 labelled for procollagen type IIA. There is an absence of labelling in the superficial region. Very weak labelling was detected in the mid zone. Cellular labelling was apparently absent. Scale bar = 100µm.
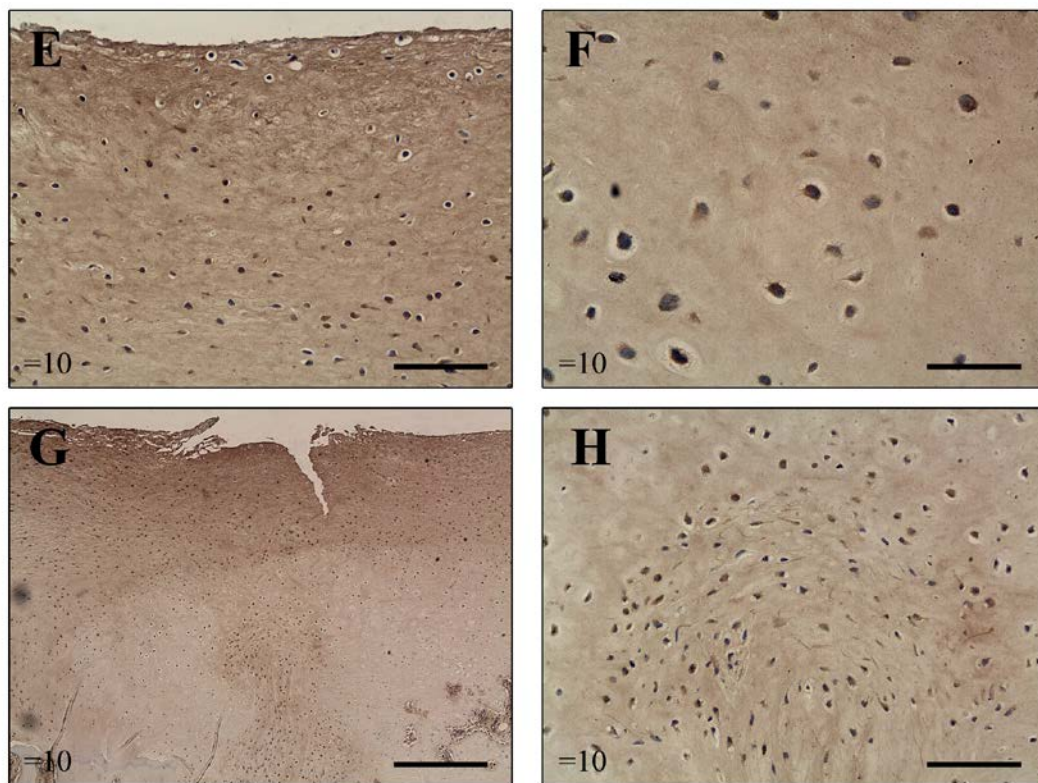
Figures 3.2. E – H. Procollagen type IIA labelling in an OCP of score 10.

Figure E. Demonstrates the surface and mid zones where label was detected in the matrix regions. Cellular labelling is evident in the middle zone chondrocytes, and was largely undetectable from the surface zone. The fibrous nature of this tissue sample can also be seen. Unlabelled cells appear to have large surrounding lacunae which are absent from the labelled cells. Scale bar = 200µm.

Figure F. High power image of the cells in the mid zone as seen in Figure E. Cellular and territorial matrix labelling apparent in some cells. Scale bar = 50µm.

Figure G. Low power image demonstrating the overall distribution of detectable procollagen type IIA labelling. There is a line delineating a region of positive labelling seen in the mid/surface zones, which extends through to the deep zones on the left. Within the deep zone there is also a region of positively labelled cells forming a chute-like structure coming from the subchondral region. Scale bar = 400µm.

Figure H. High power image demonstrating the chute-like feature highlighted in Figure G. Weak labelling is apparent and there is evidence of cellular labelling. Cells in this region appear to be different in shape and size. Scale bar = 100µm.
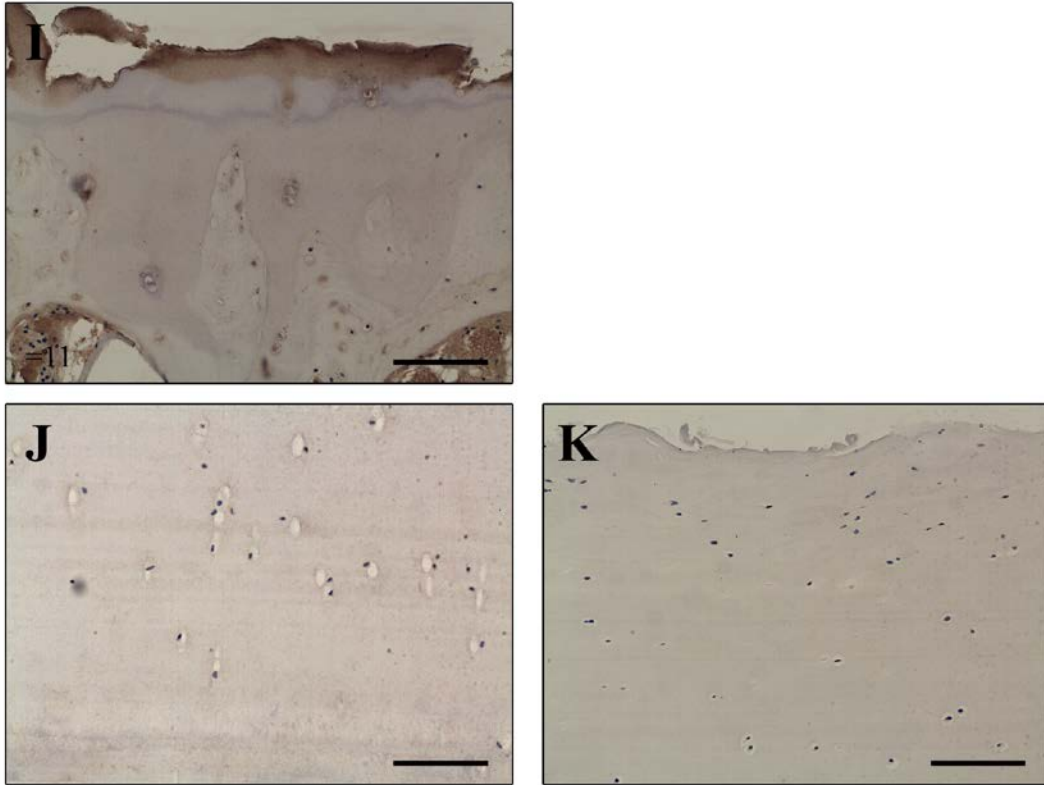
Figure 3.2. Procollagen type IIA labelling in OCPs of varying scores.

Figure I. Procollagen type IIA labelling in an OCP of score 11. Positive labelling is evident within a thin region of remaining articular cartilage. Labelling is also evident in the calcified cartilage and bone regions. Scale bar = 100µm.

Figure J. Demonstrates the absence of procollagen type IIA labelling in the middle/deep zones. Scale bar = 100µm.

Figure K. Negative control showing no non specific labelling of procollagen type IIA in the surface region. Scale bar = 100µm.
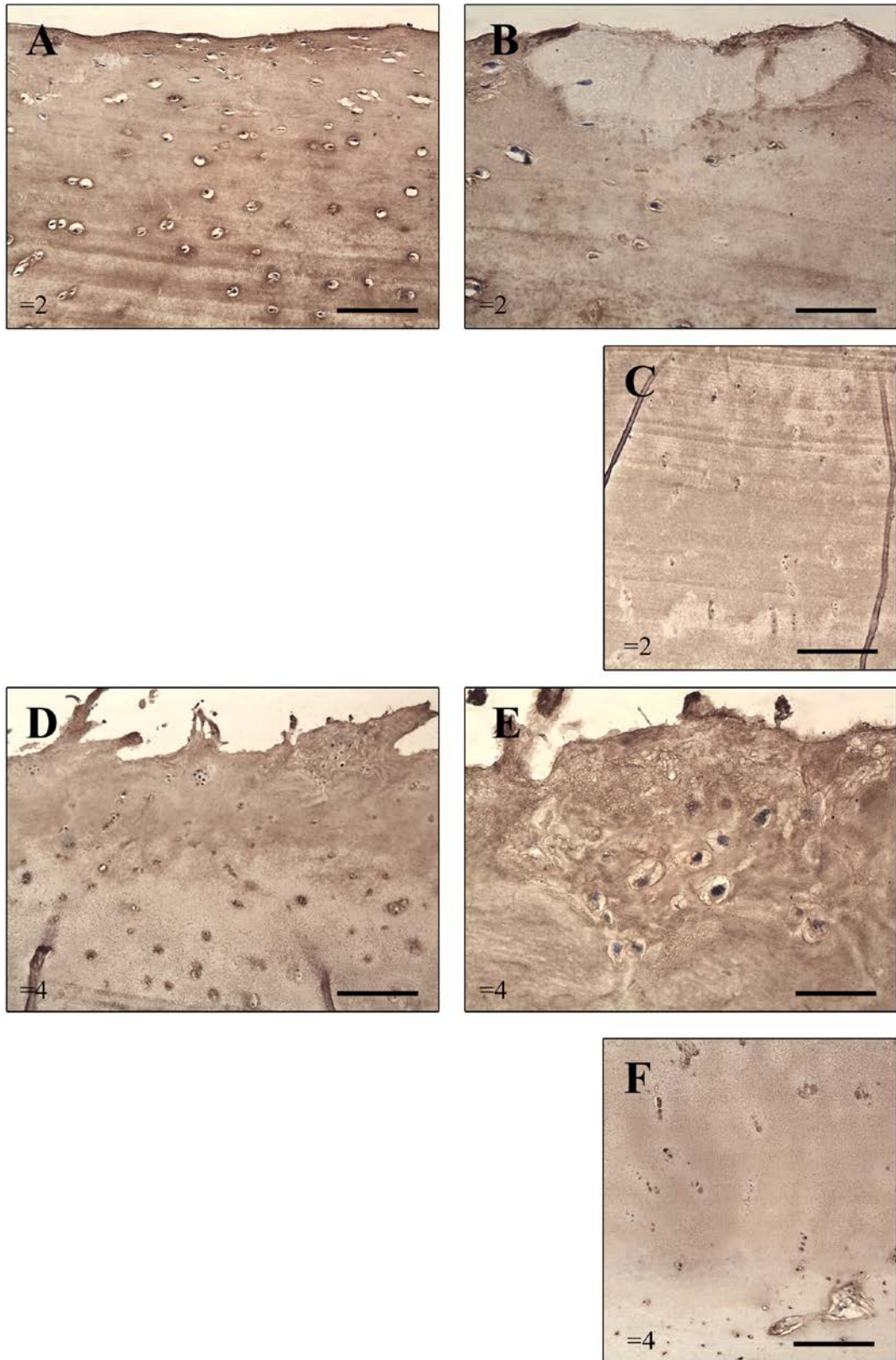
Figure 3.3. Aggrecan labelling in OCPs of varying scores.
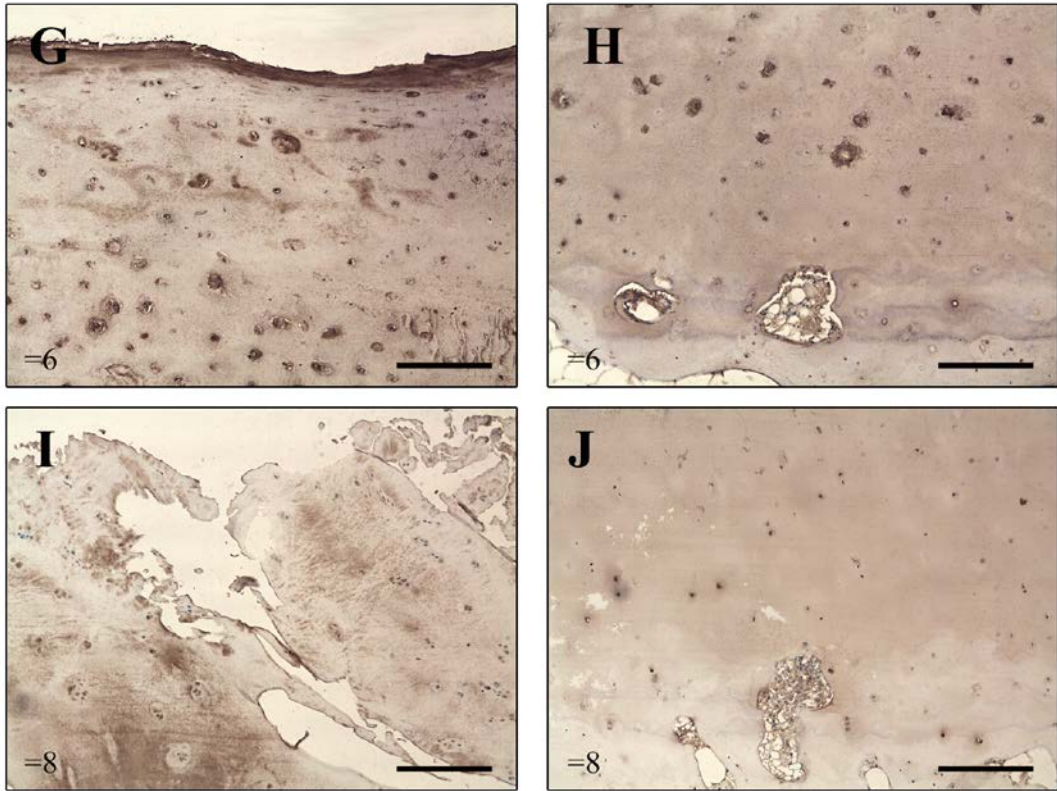
Figure 3.3. Aggrecan labelling in OCPs of varying scores.

Figures A – C. Aggrecan labelling in an OCP of score 2. The surface zone is demonstrated in Figures A & B. Figure A shows the typical distribution of labelling (scale bar = 100µm) and figure B shows an atypical region where pockets in the surface show a distinct lack of labelling (scale bar = 50µm). Figure C confirms the presence of aggrecan labelling in the mid-deep zones (scale bar = 200µm).

Figures D-F. Aggrecan labelling in an OCP of score 4. The surface zone shoes positive cellular and extra cellular labelling as seen in figures D and E. Territorial labelling was evident in chondrocytes from the middle zone as seen in Figure D. Positive labelling also evident in the deep zone as seen in figure F. Scale bar (figures D & F) = 200µm. Scale bar (figure E) = 50µm.

Figures G & H. Aggrecan labelling in an OCP of score 6. Figure G illustrates the superficial and mid zones and figure H the deep zones. Labelling in the interterritorial matrix appears reduced throughout, with exception of the surface zone. However, there also appears to be increased production of aggrecan as seen by the intense label immediately surrounding the chondrocytes. Scale bar = 200µm.

Figures I & J. Aggrecan labelling in an OCP of score 8. Figure I illustrates the superficial and mid zones and figure J the deep zones. Matrix breakdown resulting in fissures extending into the mid zone is confirmed by a marked reduction of aggrecan labelling in the superficial zone. Inferiorly, aggrecan labelling was observed in the deep regions and surrounding the chondrocytes. Scale bar = 200µm.

Figure 3.3. K. A low power image of aggrecan labelling in an OCP of score 10. An unusual distribution of aggrecan spans the OCP as a result of marrow invasions and subchondral remodelling. High power images on following page. Scale bar = 400µm.
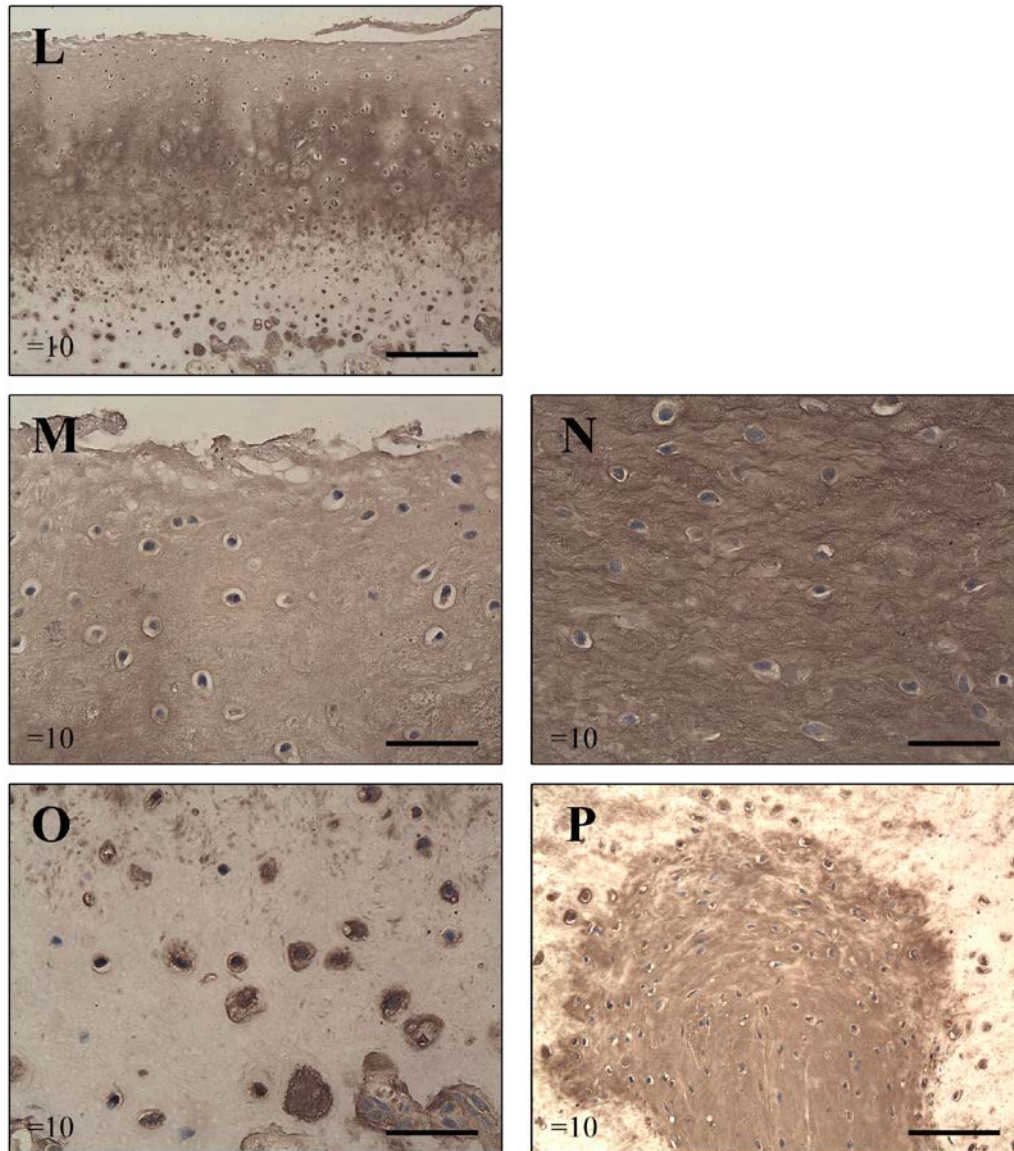
Figures 3.3. L – P. Higher power images of figure 3.3 K, an OCP of score 10 labelled for aggrecan.

Figure L. A region extending from the surface to the mid zone illustrating. There is reduced labelling in the articular surface accompanied inferiorly by a region of more pronounced labelling. The deep region elicits a lack of extracellular labelling, despite evidence of cellular and pericellular labelling. Scale bar = 200µm.

Figure M. The surface zone of an OCP of score 10 demonstrating chondrocytes with large lacunae. Aggrecan label is detectable in the extracellular label. Scale bar = 50µm.

Figure N. Mid zone of an OCP of score 10 highlighting the increased intensity of labelling compared to the surface zone (figure M). The chondrocytes appear to be immersed between a thick fibrous matrix, and lack the typical lacunae as seen in figure M. Scale bar = 50µm.

Figure O. A region where the deep zone appears to be terminally differentiating and remodelling, forming a part of the subchondral bone as a result of endochondral ossification. Scale bar = 50µm.

Figure P. A highly labelled region spreading from the subchondral bone through the deep zone and towards the middle zone. The cells within this region appear to be smaller than the cells from the surface and middle zones. Scale bar = 100µm.
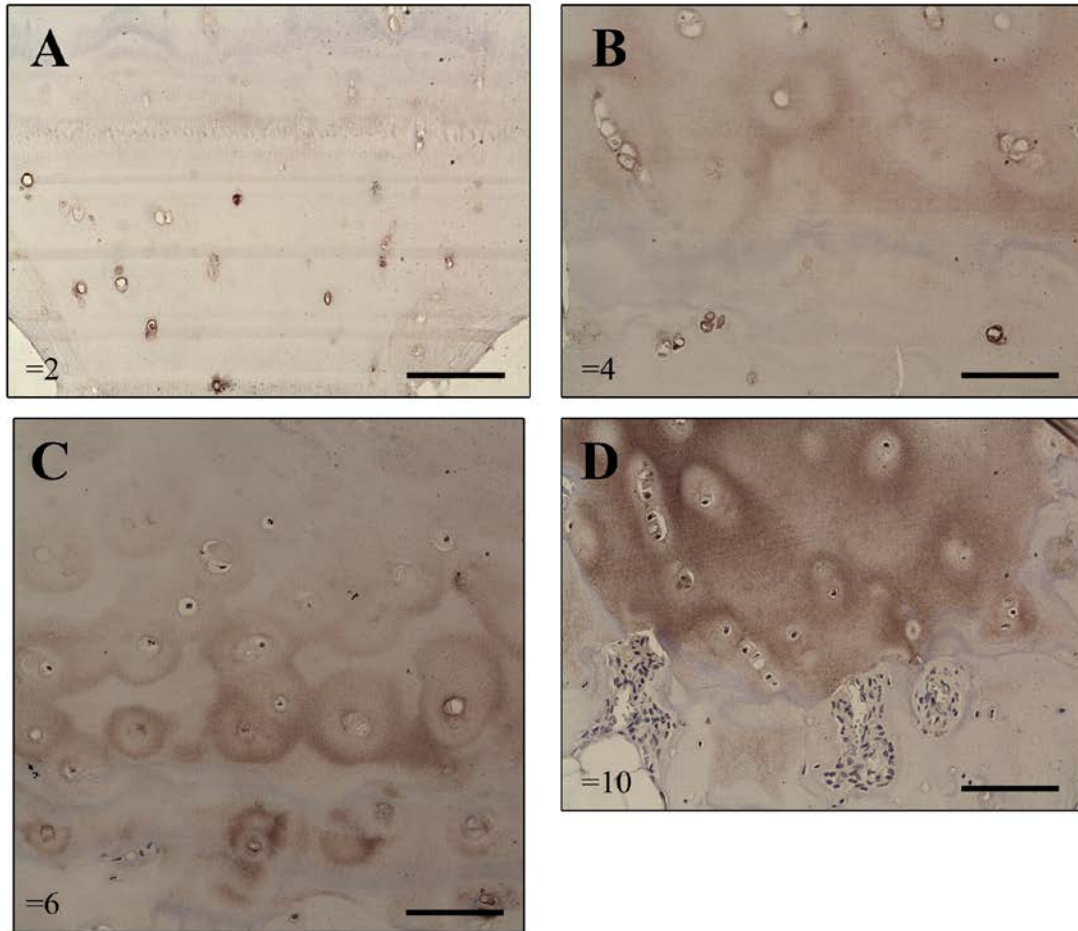
Figure 3.4. Type X collagen labelling in OCPs of varying scores.

Figure A. Tidemark and calcified cartilage in an OCP with score of 2. A number of type X positive cells in the calcified cartilage region. Scale bar = 100µm.

Figure B. Superior to the tidemark, territorial labelling of type X collagen was detected surrounding individual cells and cell clusters in an OCP of score 4. Inferior to the tidemark, positively labelled cells are also evident. Multiple tidemarks can also be observed. Scale bar = 100µm.

Figure C. Territorial labelling of type X collagen extends further into the deep zone in an OCP of score 6. Multiple tidemarks observed with increased type X labelling in this region. Scale bar = 100µm.

Figure D. Heightened type X collagen labelling in the deep zone of an OCP of score 10. Non-linear tidemark is observed together with cellular invasions emerging from the subchondral region and breaching the tidemark. Scale bar = 100µm.
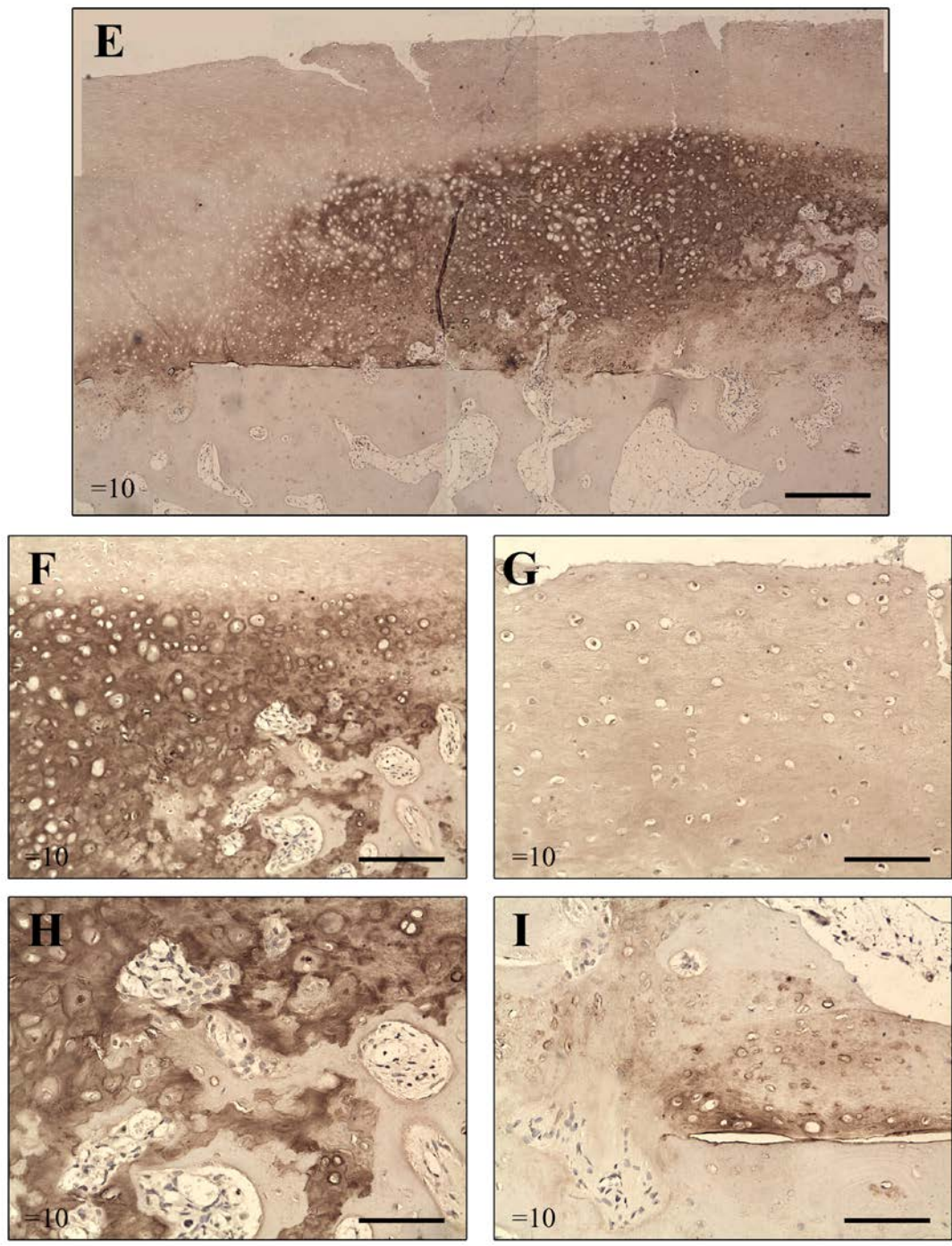
Figures 3.4. E – I. Type X collagen labelling in the corresponding OCP of score 10.
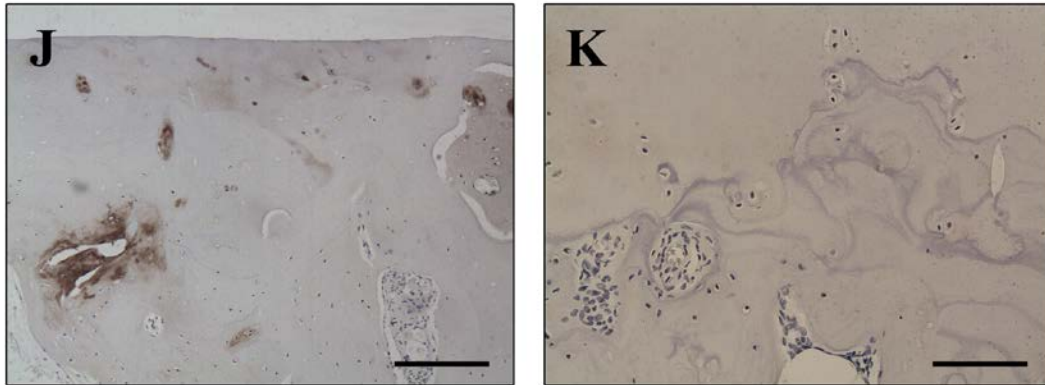
Figures 3.4. E – I. Type X collagen labelling in the corresponding OCP of score 10.

Figure E. A low power image of type X collagen labelling in the corresponding OCP of score 10. An inverse relationship with the pattern of aggrecan labelling was observed. A region of extensive remodelling below the surface zone can be seen. Cellular and vascular invasions from the underlying bone are prominent. There is a clear boundary in the mid zone where the type X collagen labelling terminates. Scale bar = 400µm.

Figure F. The transition between the region with no type X labelling and the region of extensive type X labelling. Cellular invasions on the left side of the image are accompanied by regions of no collagen type X (figure H). The fibrous nature of the ECM is highlighted by the type X labelling. Scale bar = 100µm.

Figure G. A high power image of the surface region demonstrating the lack of detectable type X collagen. Scale bar = 100µm.

Figure H. A high power image of figure F highlighting the transition zone where bone formation has proceeded following type X collagen formation in the presumptive deep zone of articular cartilage. The cellular invasions can be seen protruding further into the deep zone. Scale bar = 50µm.

Figure I. A high power image of the deep zone. Extensive remodelling in the cartilage resulting in the total detachment of the cartilage from the underlying bone. Marrow invasions breaching through the cartilage appear to fan out in an organised arrangement, presumably attempting to repair the damaged cartilage. Scale bar = 100µm.

Figure J. Demonstrates the presence of type X collagen in the underlying bone of confirming the continued remodelling in the latter stages of the disease. Scale bar = 200µm.

Figure K. Negative control showing no non-specific binding of type X collagen in the deep regions. Scale bar = 100µm.
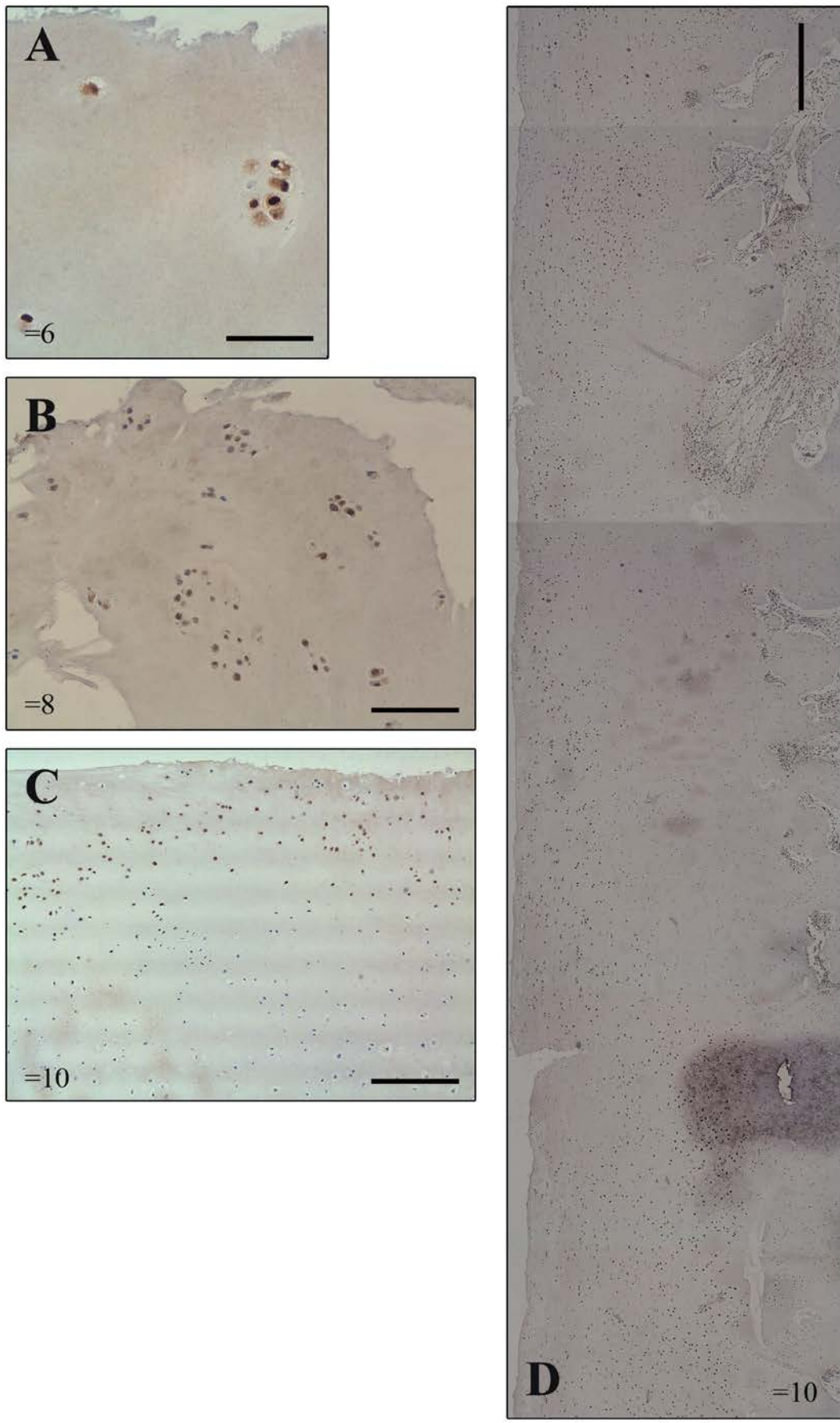
Figure 3.5. PCNA labelling in OCPs of varying scores.

Figure 3.5. PCNA labelling in OCPs of varying scores.

Figure A. Individual cells and cell clusters in the surface of articular cartilage in an OCP of score 6. Within the cluster there are positively and negatively labelled cells. Scale bar = 50µm.

Figure B. A high number of chondrocyte clusters on the fissured articular surface labelling positively for PCNA, accompanied by a small number of cells that exhibit no labelling. Scale bar = 100µm.

Figure C. PCNA labelling in an OCP of score 10. The distribution of positively labelled cells can be spanning the surface zone of the articular cartilage. Inferiorly there is a lack of detectable PCNA. Scale bar = 200µm.

Figure D. A low power image of PCNA labelling in the corresponding OCP of score 10. Positively labelled cells are located in the regions lacking collagen type X and eliciting positive aggrecan labelling. On the right side of the image, this region is restricted superiorly, and spans through the mid zone and into the deep zone on the left side of the image. Scale bar = 400µm.

Percentage of cells labelling positive for PCNA in the superficial zone
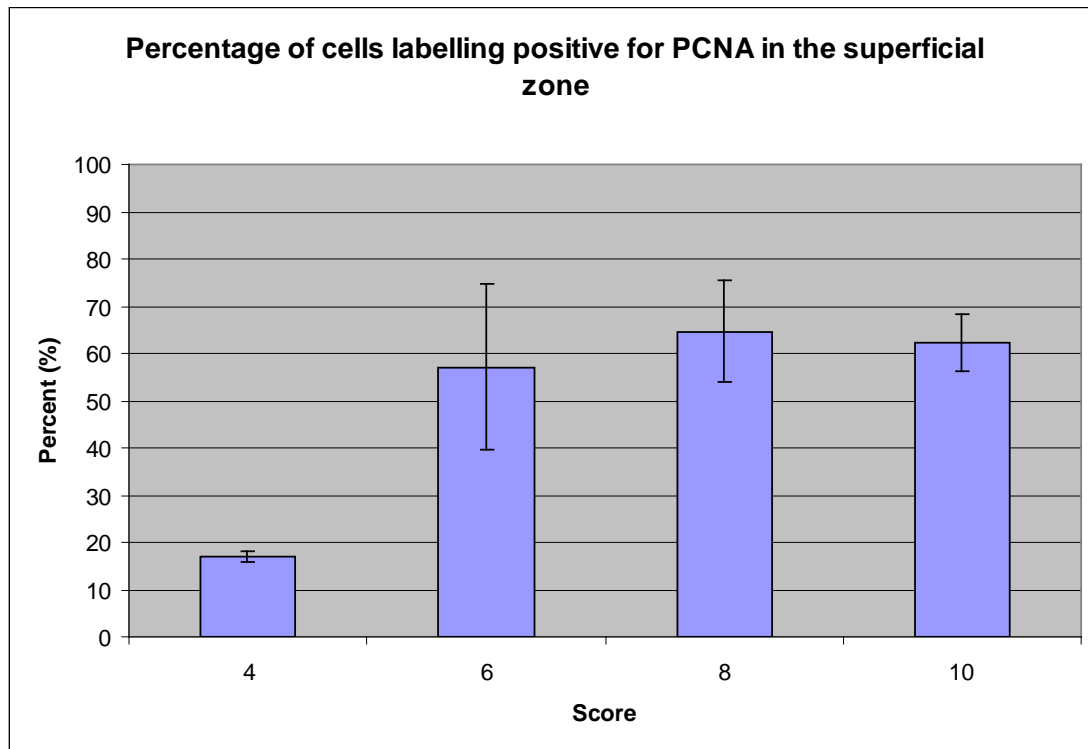
PCNA

Score	No. positive	Total no.	% positive	Standard Error
4	5.33	32.33	16.94	1.08
6	10.00	22.00	57.15	17.61
8	26.00	42.33	64.56	10.78
10	59.67	98.33	62.33	6.07

Figure 3.6. Histogram and corresponding table showing the percentage of total cells that labelled positive for PCNA in the superficial zone of OCPs of varying scores.

Data are expressed as the mean (n=3) $\pm$ SE of the percentage of total cells which show cell-associated labelling. Score 4 showed a significantly reduced proportion of labelled cells when compared to the higher scores as confirmed by one way ANOVA and Student t-tests ($p < 0.05$).
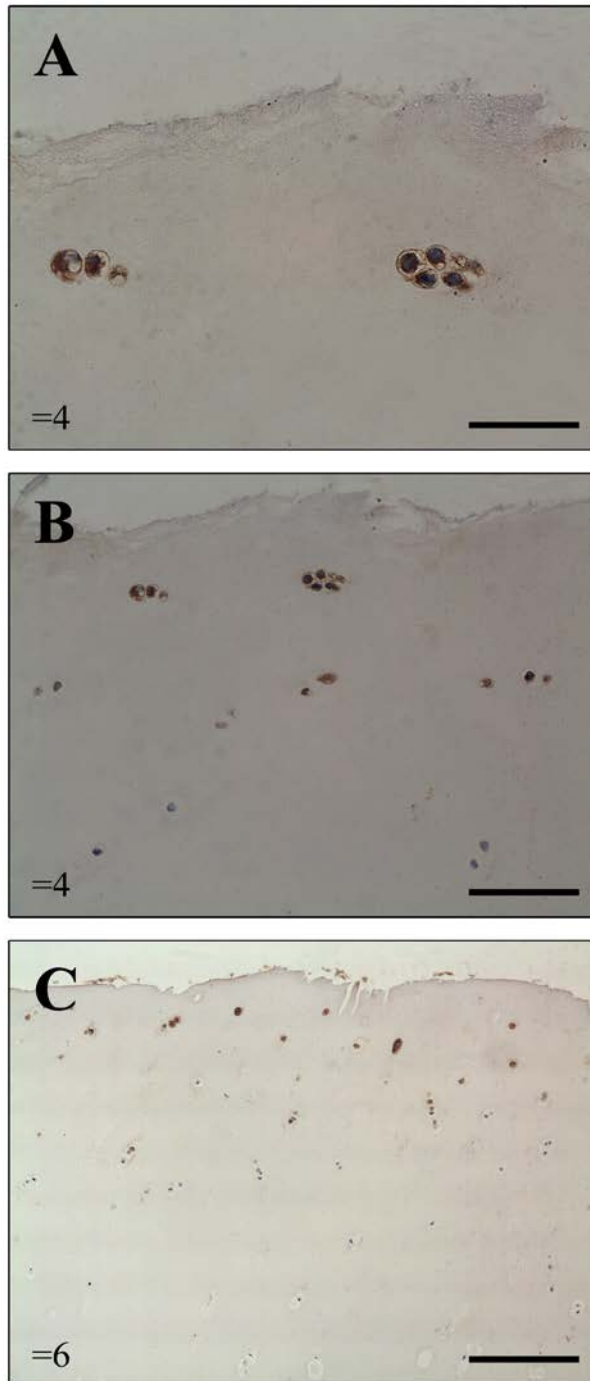
Figure 3.7. Stro-1 labelling in OCPs of varying scores.

Figures A & B. Stro-1 labelling in an OCP of score 4. Figure A is a high power image of chondrocyte clusters in the surface of articular cartilage demonstrating positive cytoplasmic labelling for Stro-1. Scale bar = 50µm. Figure B demonstrates the transition from the positively labelled surface zone cells to the negatively labelled middle zone cells. The cells in the mid zone are individuals or pairs where as in the surface there is a balance between individual cells and cell clusters. Scale bar = 100µm.

Figure C. Stro-1 labelling in an OCP of score 6. A similar pattern of labelling is seen whereby the surface layer of cells show detectable PCNA. The middle and deep zones lack detectable PCNA. Scale bar = 200µm.
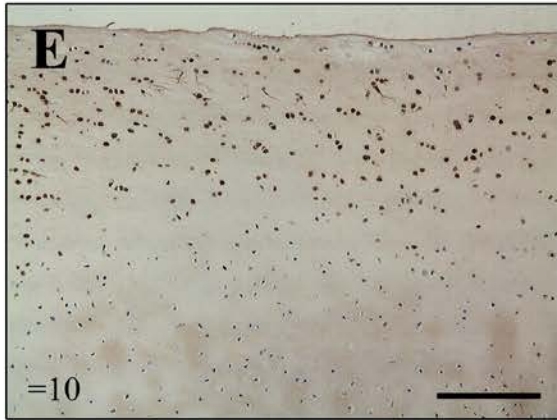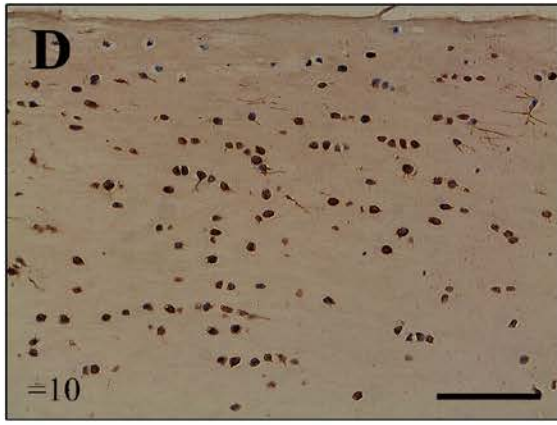
Figure 3.7. Stro-1 labelling in an OCP of score 10.

Figure 3.7. D – G. Stro-1 labelling in an OCP of score 10.

Figure D. Stro-1 labelling in the surface and middle regions of the corresponding OCP of score 10. Abundant Stro-1 labelling can be seen in the majority of the cells. Dentritic-like cells are evident. Scale bar = 100µm.

Figure E. Demonstrates the distribution of positively labelled cells and the distinct transition in the mid zone to non Stro-1 expressing cells. The presence of dentritic-like cells is further emphasised in this image. Scale bar = 200µm.

Figure F. Cellular invasion protruding from the underlying bone presents positively for Stro-1 label. Blood vessels are also evident in this frame. Scale bar = 200µm.

Figure G. A low power image of Stro-1 labelling in the corresponding OCP of score 10. The distribution is comparable to that seen in the PCNA labelling (figure 3.5D). Scale bar = 400µm.

Percentage of cells labelling positive for Stro-1 in the superficial zone
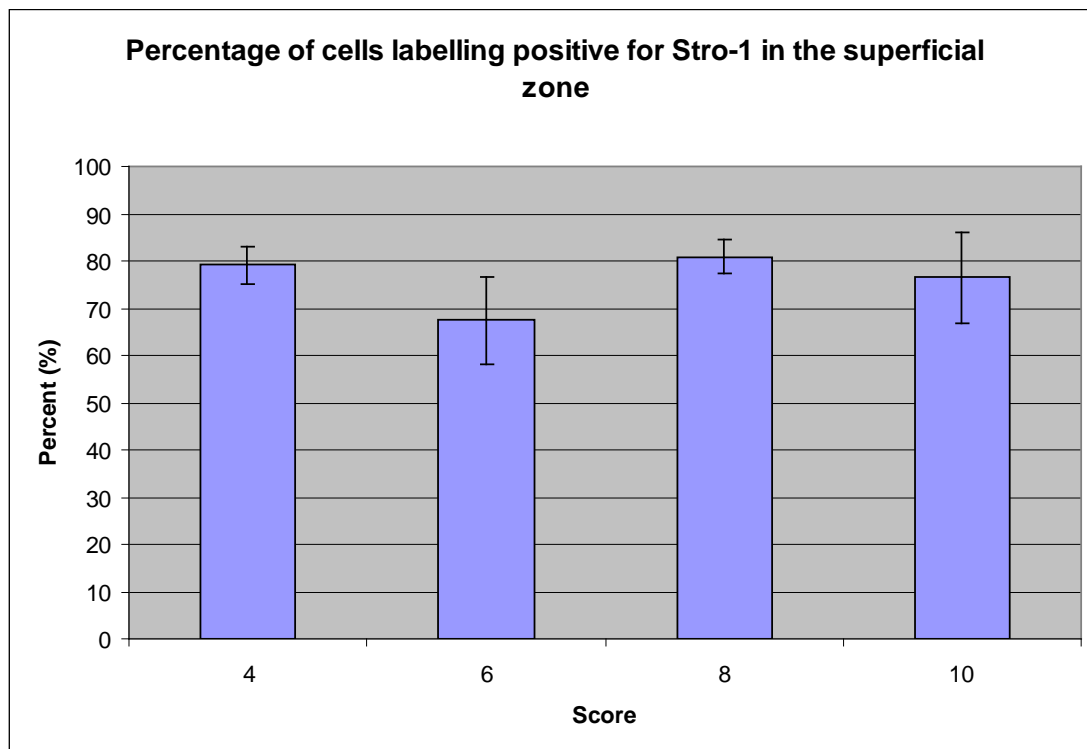
Stro-1

Score	No. positive	Total no.	% positive	Standard Error
4	16.33	20.67	79.13	4.02
6	11.33	17.33	67.41	9.21
8	28.67	36.00	80.85	3.51
10	91.00	117.33	76.46	9.53

Figure 3.8. Histogram and corresponding table showing the percentage of total cells that labelled positive for Stro-1 in the superficial zone of OCPs of varying scores.

Data are expressed as the mean (n=3) $\pm$ SE of the percentage of total cells which show cell-associated labelling. One way ANOVAs and Student t-tests suggested that there was no significant difference in the proportion of labelled cells between the varying scores (p>0.05).
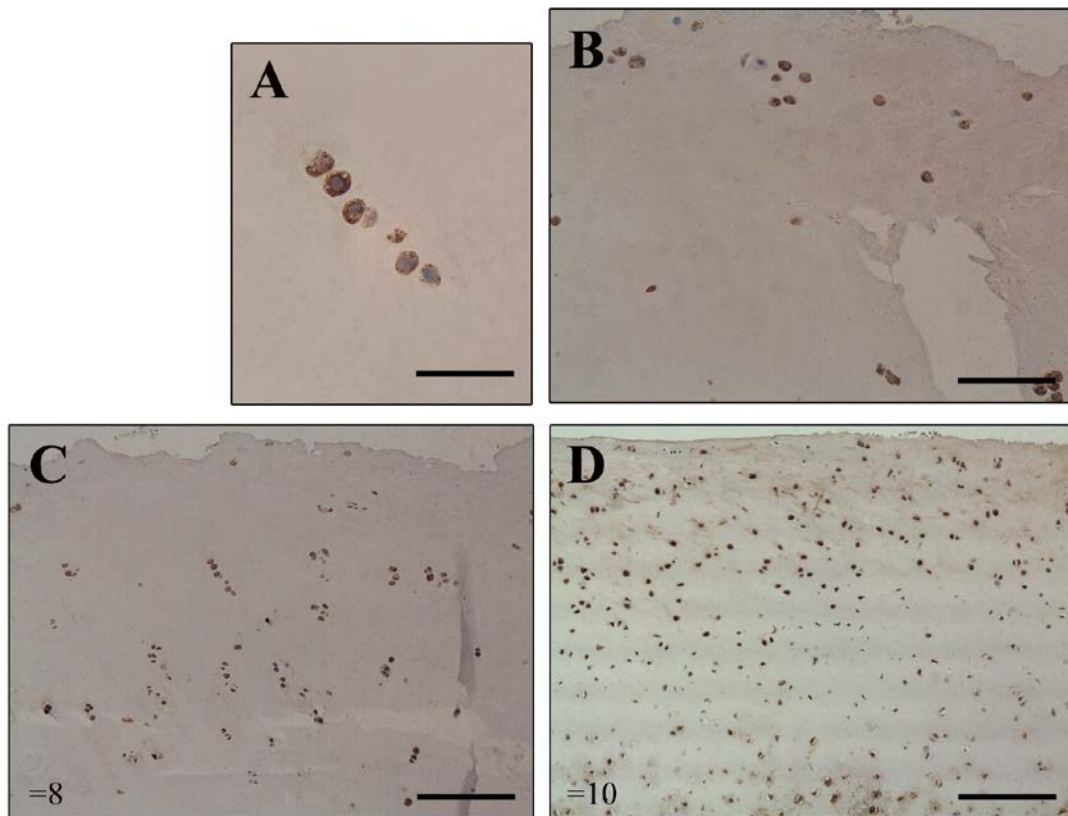
Figure 3.9. Notch 1 labelling in OCPs of varying scores.

Figure A. High power of a cluster of cells in the articular surface showing cytoplasmic labelling of varying degrees. Scale bar = 50µm.

Figure B. Distribution of Notch 1 labelling across the articular surface. Cells are negatively and positively labelled regardless of whether they are in clusters. Scale bar = 100µm.

Figure C. Notch 1 labelling in an OCP of score 8 illustrating the abundance of positively labelled cells and cell clusters. Notch 1 labelled cells extend beyond the surface zone into the middle zone. Scale bar = 200µm.

Figure D. Notch 1 labelling in the corresponding OCP of score 10 elicits similar labelling to that seen in figure 3.7 of Stro-1, however the transition between the labelled and non labelled zones was not as clearly defined. Labelling extends inferiorly to the lower aspect of the image. Dendritic-like cells evident. Scale bar = 200µm.

Percentage of cells labelling positive for Notch-1 in the superficial zone
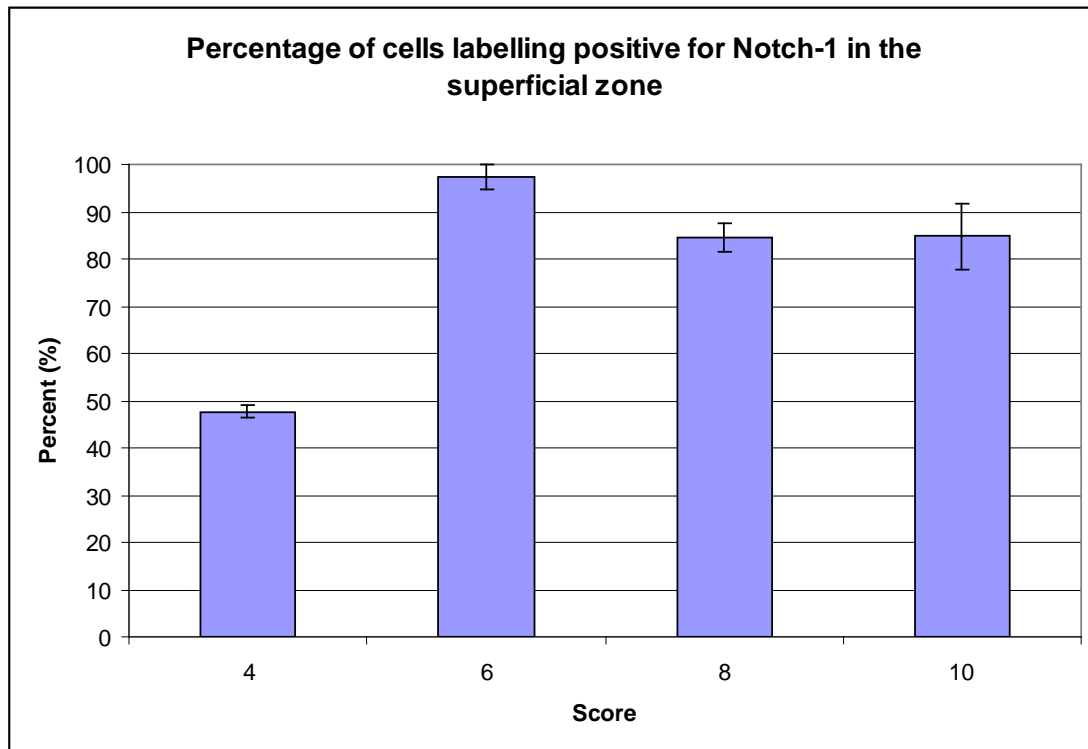
Notch 1

Score	No. positive	Total no.	% positive	Standard Error
4	9.33	19.33	47.61	1.32
6	18.67	19.00	97.44	2.56
8	24.00	28.00	84.54	3.06
10	55.67	66.33	84.75	6.84

Figure 3.10. Histogram and corresponding table showing the percentage of total cells that labelled positive for Notch-1 in the superficial zone of OCPs of varying scores.

Data are expressed as the mean (n=3) ± SE of the percentage of total cells which show cell-associated labelling. Score 4 showed a significantly reduced proportion of labelled cells when compared to the higher scores as confirmed by one way ANOVA and Student t-tests (p<0.05). Score 6 showed a significantly greater proportion of labelled cells when compared to scores 4 & 8 as confirmed by one way ANOVA and student t-tests (p<0.05).

3.5. Discussion

The purpose of this study was to map out changes in ECM components relative to disease severity in osteochondral plugs excised from tibial plateaux. Research into osteoarthritis often focuses on end stages and the differences between the state of tissue 'before' and 'after' the disease, however, there is little insight into the progressive changes that occur as the disease develops. Is there one common factor that precedes the changes that follow? There are several studies that do look into relative changes in gene expression between normal and/or early stage OA compared to late stage OA (Brew et al., 2010, Martin et al., 2001, Young et al., 2005), however, gene expression does not necessarily relate directly to protein synthesis; just because a gene is present or even up-regulated it does not signify that it is activated.

As such, using the scoring system devised in the previous chapter, a range of different scores were assessed using antibodies to localise synthesis of major ECM proteins, stem cell and proliferation markers. The aim was to reveal changes and identify trends within the shifting tissue, giving an insight into the mechanisms behind the changes that occur throughout this mysterious disease. Whilst displaying the results the choice was made not to omit the 'anomalous' OCP which achieved an overall score of 10. The reason for this was because despite it being an anomalous result within the small study which was carried out, it may indeed be representative of processes that occur more widely and are not recognised or distinguished from the usual changes which are more commonly reported. It is, therefore, imperative that a similar study is carried out on a larger scale so that one can verify whether or not an 'anomalous result' is indeed anomalous on a greater scale. Similarly, many of the trends observed throughout this study would be more heavily supported in a study of greater magnitude, as inevitably variation and inconsistencies are two of the common hindrances encountered when doing osteoarthritic studies on human patients.

Collagen type I production was evident in all of the OCPs to varying degrees of intensity. In OCPs of lower grade (lesser extent of severity), where the surface zone often remained, labelling was restricted to this region. This is concurrent with previous reports which suggest that collagen type I labelling is evident as an independent layer residing in the

154

superficial region of normal articular cartilage (Pfander et al., 1999, Teshima et al., 2004). As such, it is not uncommon to find collagen type I labelling in normal articular cartilage, supporting the case that lower grade OCPs from this study resemble normal, un-diseased hyaline cartilage.

Interestingly, collagen type I labelling in the surface zone was often accompanied by regions of hypercellularity in the form of cell clusters, in low scoring OCPs. This could, therefore, be indicative of cellular changes preceding ECM changes in the early phases of cartilage degradation in OA.

Converse to the general consensus, in this study the trend lent towards a reduction in type I collagen in the ECM, with increasing severity of the tissue. Previous reports have suggested that a thicker band of type I collagen is seen in OA cartilage (Pfander et al., 1999), and there is great ongoing speculation regarding the presence of type I collagen formation in cartilage repair tissue. The question addresses the issue of whether the type I collagen-rich tissue is the end-product of the repair mechanism; producing a fibrocartilagenous tissue in place of the original hyaline cartilage, or if the presence of type I collagen is merely a moment captured in time, of a long process that recapitulates early cartilage development.

This question fails to be answered as the integrity of the tissue as a whole diminishes, resulting in further erosion and degradation. If the type I collagen is indeed a precursor to type II collagen formation, it may be a case of a 'race against time' in that the process of maturation from a type-I rich tissue to a type-II rich tissue is not given enough time, and the degradative process occur at a more rapid rate overriding the repair process before it has had the chance to impact the tissue integrity. The slow rate of collagen synthesis, particularly in adult articular cartilage is well documented (Maroudas, 1980).

As mentioned, in this study no marked increase in type I collagen was found in the ECM of OCPs of increasing severity. However, it was observed that there was cellular up-regulation in individual cells as well as cell clusters. As such, it may be that the changes to the ECM were not yet apparent despite the well documented mechanism of collagen type I activation being switched on.

Aside from the trend of little type I collagen which has been discussed, the OCP of score ten which has been termed the 'anomalous' OCP reared very different results when immunohistologically labelled for collagen type I. In this OCP, an abundance of collagen type I was seen throughout the entire tissue, spreading from the surface through the mid- and into the deep zone. The distinct fibrous features suggest a well established fibrocartilagenous tissue (Roberts et al., 2001). In this instance, large clusters of cells appear to be localised at and around the presumptive tidemark region. It may be that a mass infiltration of cells pierced through the tidemark as a result of subchondral remodelling resulting in the highly cellular type I positive tissue.

Type II collagen is synthesised by chondrocytes as a procollagen which is cleaved before being incorporated into the forming fibril and, as such, can be used as a more direct measure of type II collagen synthesis (Lee et al., 1996). It was found that procollagen type IIA labelling in this study correlated to the regions of type I collagen synthesis. In OCPs of lower scores the surface zone labelled positively, yet middle and deep regions elicited no positive label. Cellular and extracellular procollagen type IIA therefore suggests an active metabolic state within the osteoarthritic tissue, particularly in earlier stages of disease progression. Aigner et al., (1999) proposed that procollagen type IIA could be used as a marker of OA as its presence is congruent with the apparent onset of the disease. Similarly, other studies have accrued similar results; Khan et al., (2008) demonstrated the presence of procollagen type IIA in bovine articular cartilage in mild lesions of OA tissue, whilst commenting on the reduction of labelling in overtly fibrillated tissue. These reports are in accordance with the findings of this study; whereby OCPs of scores higher than 8 lacked procollagen type IIA labelling.

Relating these findings to those of the collagen type I results, it would appear that the matched labelling is indeed indicative of the developmental state being recapitulated. If the type I collagen rich tissue was the end state of the repair tissue, one could assume that procollagen type IIA collagen would not be present. As the type II collagen precursor is present, the conclusion may be drawn that type I rich fibrocartilage is not the intended end-state of the tissue. It could instead be more a case of the equilibrium between degradation and synthesis being disturbed, resulting in a quicker rate of degradation and

thus capping the potential for the newly formed tissue to reach the desired composition and integrity.

Procollagen type IIA labelling in the 'anomalous OCP' does not directly correlate to the collagen type I results. A demarcation between labelled and non-labelled regions was evident dividing the mid-zone, with a positively labelled chute-like structure extending from the subchondral bone. By the stature of the structure it appears as though it is an invasion of cells from the subchondral region; more specifically an invasion of stromal cells from the marrow regions. As such, these undifferentiated BMSCs have the capacity to differentiate into articular cartilage *in vivo* (Han et al., 2008), and so an unknown mechanism may have been activated in this case to trigger the onset of new articular cartilage formation in this region. It could be hypothesised therefore, that within this OCP two different repair mechanisms are occurring; one at the surface where the surface zone cells are responding like the other OCPs by recapitulating the developmental phase in a repair attempt, and the second mechanism is through the vast infiltration of BMSCs from the subchondral region.

The presence of aggrecan in articular cartilage ECM endows the tissue with its characteristic water imbibing properties and as such, is a distinctive feature of the tissue (Bayliss et al., 2000). It was, therefore, expected that aggrecan would be present throughout the OCPs, particularly in the lower scoring specimens. Indeed, it was found this component was widely present throughout the matrix of the OCPs assessed.

Within the low scoring OCPs, atypical pockets along the surface of the tissue lacked aggrecan and cellular presence. As such, it could be hypothesised that these pockets are areas of weaknesses which develop into fibrillated surfaces as the disease progresses. It is well renowned, however, that chondrocyte clusters are a histological hallmark of OA (Lotz et al., 2010), particularly localised around fissured surfaces in the upper regions of the cartilage. Through this study, it was seen that aggrecan labelling in pockets along the surface occur prior to chondrocyte cluster formation and as such, it can by hypothesised that tissue integrity is initially compromised through aggrecan degradation, and the formation of chondrocyte clusters is a secondary effect.

Cellular labelling of aggrecan was detected in some OCPs of higher scores, which suggested anabolic mechanisms resulting in renewed synthesis of the macromolecule prior to its exportation out of the cell. This, however, was not seen in all of the OCPs of higher scores, and this may in part be due to OCPs being excised from patients of different ages; it is known that the rate of aggrecan synthesis is dependent on the age of the specimen from which the tissue was obtained (Bayliss et al., 1999). In the OCP of score 8, where large fissures extend into the mid-zone, a marked reduction of aggrecan was observed accompanied by typical chondrocyte clusters. This finding supports the hypothesis that aggrecan loss occurs initially, followed by tissue degradation prior to the formation of cell clusters which attempt to repair and relay new matrix (Lotz et al., 2010).

In the anomalous OCP, intriguingly, substantial labelling was evident alongside regions that clearly lacked positive labelling in the ECM. Concurrent with the other OCPs, the surface zone lacked aggrecan; which became more abundant in the middle region. However, in this OCP, a clear separation exists between regions of the mid-zone. Inferior to the line, aggrecan labelling is absent in the ECM however cellular labelling was observed. Superior to the line the tissue was rich in aggrecan throughout the ECM. This discrepancy very clearly highlights the altered composition of the tissue which would ordinarily contain aggrecan throughout the depth of the tissue. It appears that the non-labelling, chute-containing deep region may not be of a cartilaginous nature, and may be indicative of a region in which endochondral bone formation is occurring. This finding reinforces the well known dogma that unknown mechanisms occur throughout the progression of OA. Again, it is important to elucidate whether this is a unique case or if this is common on a grander scale. It is important to understand the difference between what is occurring in this case compared to 'traditional' OA, as it also highlights the issue that perhaps patients are being misdiagnosed; perhaps this is a different disease which has not been detected and thus categorised as OA.

The chute-like structure seen in this OCP which labelled positively for collagen type I and procollagen type IIA also demonstrated substantial aggrecan labelling. This again reinforces the view that infiltrating cells emerged from the subchondral region in an attempt to produce a hyaline-like repair tissue in response to the tissue damage.

Despite literature reporting the increased presence of type X collagen in OA cartilage (Walker et al., 1995), as whole OCPs between scores 2 and 8 showed no distinctive pattern or difference. This highlights the issue that, in many cases, the patterns of change that evolve in articular cartilage as a result of OA, are not always consistent with one another and vary from patient to patient. These inconsistencies, in part, are why assessing the severity of OA has become a subjective issue.

With regards to inconsistencies, the 'anomalous' OCP of score 10 did indeed present with remarkable type X labelling extending beyond the zone of calcified cartilage and deep regions of the tissue. Having said that, concomitant with the findings with regard to this OCP, a distinct line can be seen separating the labelled and non-labelled regions. This further amplifies the evidence to suggest that within this OCP, hyaline cartilage has been replaced by a region in which endochondral bone formation is occurring. As type X collagen is a marker of hypertrophic chondrocytes which form prior to angiogenesis and subsequent mineralisation (Kronenberg, 2003), it fits the hypothesis that this region is no longer a region of hyaline, articular cartilage.

Upon further examination using CD34 to identify endothelial cells of blood vessels, it was observed that indeed, on the right aspect, the noted cellular invasions were accompanied by blood vessels, further supporting the suggested theory.

Upon type X collagen labelling in this OCP, the chute-like region which was previously distinguishable, could not be seen. It was previously suggested that these cells may have originated as BMSC from the bone marrow region. Studies have demonstrated that BMSCs, when chondrogenically induced *in vitro*, present with type X collagen (McCarthy et al., 2011) and as such, it is understandable that this previously identifiable region does not stand out under these conditions.

Typically, chondrocytes in mature articular cartilage have low mitotic activity when compared to other cell types, and an increase in proliferative cells may be suggestive of a reparative attempt (Pfander et al., 2001). Concurrent to this, in our study, it was shown that in the lowest scoring OCP no mitotic activity in the form of PCNA labelling was detected. OCPs of score 4 plus did show evidence of PCNA labelling, agreeing with other studies

that report of increased mitotic activity in OA specimens (Hellio Le Graverand et al., 2001, Pfander et al., 2001).

Quantitative investigation (figure 3.6) suggested that there was a marked increase in PCNA in OCPs achieving a score of 6 or more, although no obvious trend between these higher scores (6 to 10) in relation to relative numbers of labelled cells was noted. More specifically, between the scores of 6 and 10, the proportion of labelled cells in the surface of the tissue ranged between 55 and 65 percent. Interestingly, error bars were greatest at score 6, suggesting the greatest level of variation at this score. With increasing severity, error levels reduced in size suggesting that the high proportion of labelled cells was more consistent throughout the surface of more severely diseased tissues.

A review by Lotz et al., (2010) also confirmed the consensus that PCNA labelling, and more generally, cell proliferation is increased with OA. Unfortunately, however, within this study there was no progressive trend that was observed, in that PCNA labelling did not steadily increase with increasing severity and, as such, it is difficult to use this information to further decipher mechanisms of disease progression.

Relating back to the 'anomalous' OCP, cells which labelled positively for PCNA were present throughout the hyaline-cartilage like tissue yet absent in the inferior region demonstrating endochondral bone characteristics. As such, hypercellularity throughout certain regions of the tissue is accounted for due to the actively proliferating cells; however, the phenomenon which segregates the two congruent regions of tissue is not explained. Migratory cells have been reported in OA cartilage (Khan et al., 2009, Koelling et al., 2009) which may have played a role in creating this divide between the tissue but again it is difficult to elucidate the mechanisms behind this change.

The labelling of stem cell markers Stro-1 and Notch-1 was examined qualitatively and quantitatively. Qualitative data confirm previous findings of increased synthesis of the two putative stem cell markers within OA (Grogan et al., 2009), however particularly within Stro-1, no pattern was observed between increasing severity of disease within tissue and Stro-1 positive cells. In addition, the volume of labelled cells within the surface zone was significant in that over 65 percent of cells demonstrated positive (Stro-1) label. These were

not only individual cells, but also cell clusters, and interestingly, within clusters it was seen that there were, at times, a mixture of labelled and unlabelled cells. Numerically, the proportion of labelled cells is remarkably high which brings into question the reliability of Stro-1 as a marker for stem/progenitor cells. Studies by Giurea et al., (2006) have shown that alongside the articular cartilage, Stro-1 positive cells are also significantly increased in the neighbouring synovium and this may have a cascade effect onto the exposed fibrillated surface of the articular cartilage. Concurrent with this, Grogan et al., (2009) agree that despite demonstrating clear involvement in the process of OA, Stro-1 should not be used as a sole representative indicator of stem cells within human articular cartilage.

Notch-1 has been shown to promote the maintenance of a progenitor cell phenotype in normal articular cartilage (Dowthwaite et al., 2004). However, in diseased articular cartilage, its reliability as a stem cell marker has also been questioned (Grogan et al., 2009). Within this study, the lack of Notch-1 labelling in the lowest scoring OCPs was accompanied by an increase in labelling in OCPs of score 4, suggesting that there is a progressive correlation between severity of disease and Notch-1. Having said that, within OCPs of scores 6 and above, no distinct trend was detected; once OCPs reached a 'threshold' level, Notch-1 labelling was notably elevated in relation to OCPs of low scores. With over 80 percent of the surface/mid zone cells of OCPs with severe OA labelling positively for Notch-1, it again brings to light the issue of whether or not Notch-1 can be used generally as a sole marker for stem cells within articular cartilage. These results do, however, confirm that Notch-1 signalling is dysregulated in OA, although we have been unable to make any direct correlations between severity of OA and Notch-1 labelling due to variability seen within the results.

As a whole, the aim of this study was to map out progressive changes in OCPs of varying scores. As such, no obvious trend or direct correlation was found. This reinforces the fact that there are clearly many unknown mechanisms involved in OA which may interact at varying degrees not only within different people but also within different joints of one particular person. It is important to remember that OA is a disease that not only affects the articular cartilage, and that mechanisms of disease progression may be intricately intertwined between contributing factors from the surrounding environment.

Oxygen tension is one environmental factor that several authors have shown to have an effect on cartilage homeostasis. More specifically, studies have demonstrated that chondrocytes favour hypoxic conditions when compared to normoxic ($\approx$20%) conditions (Buckley et al., 2010), and so a vicious cycle may generate when a fibrillated surface begins to form in the early stages of OA. The increased surface area results in increased exposure to the joint capsule and its constituents. The detrimental effects of the increased oxygen levels may be due to the fact that chondrocytes are not usually exposed to high levels of oxygen being an avascular tissue, and as a result the change/increase in oxygen alters the metabolism of the cells. Similarly, molecular oxygen is required for the production of nitric oxide and other reactive oxygen species (ROS) which also have been shown to be involved in the pathogenesis of OA (Khan et al., 2008, Pelletier et al., 2000, Yudoh et al., 2005, Ziskoven et al., 2010). Furthermore, a study by Altindag et al., (2007) suggested that decreased collagen metabolism may also be related to oxidative stress, which would further enhance the degradative cycle resulting in compromised tissue integrity alongside deranged cells.

Previous studies have demonstrated the presence of cytokines and MMPs in the neighbouring subchondral bone and synovial fluid, which not only further contribute to the web of mechanisms leading to the progression of OA, but also are indicative of the pro-inflammatory condition of OA pathology (Hulejova et al., 2007, Scanzello et al., 2009). This is of importance as it was evident in this study that the 'anomalous' OCP of score 10 could perhaps be a case of a misdiagnosed specimen. Indeed many of the features seen within this OCP could be linked to rheumatoid arthritis (RA), a chronic, systemic inflammatory disorder (Allard et al., 1988). Within RA, a typical feature is pannus; a 'cloth-like' soft tissue which appears as an invasive granulation tissue covering the articular cartilage, and tissue described in the OCP of score 10 did indeed bear great resemblance to this archetypal pannus. Several reports in the literature do report of a pannus-like tissue evident in OA cartilage (Shibakawa et al., 2003, Yuan et al., 2004); however, its occurrence is not heavily documented. A more recent article by Furuzawa-Carballeda et al., (2008) linked the similarities between pannus in OA and RA by describing similar metabolic characteristics and pro-inflammatory cytokine responses. As such, these similarities highlight issues that clinicians face when diagnosing a patient and prescribing relevant treatments, in that many diseases present in comparable ways.

Similarly, as each case is unique and symptoms of the disease vary between patients, the need for a deeper understanding of OA is further emphasized. Misdiagnosing patients as a result of similarities between diseases could be of further detriment and as such it is imperative that mechanisms are understood in order to be able to improve on diagnostic tools.

Chapter 4:

Isolation and characterisation of chondroprogenitor cells in osteoarthritic articular cartilage

4.1. Introduction

Chondroprogenitor cells are cartilage derived stem cells that originate from pluripotent MSCs. They have a limited replicative capacity and restricted differentiation potential to certain lineages. The terms progenitor cell and stem cell are often used interchangeably however and it is important that their differences are recognised. True stem cells (introduced in Chapter 1) are undifferentiated cells with endless self-renewal capacity and the potential for multi lineage differentiation. According to the International Society for Cellular Therapy (ISCT), MSCs are further characterised by their adhesion potential in monolayer culture and their differentiation potential into chondrocytes, osteocytes and adipocytes *in vitro* (Dominici et al., 2006). The ISCT has also listed several markers that MSCs should exhibit or lack. Markers that MSCs should exhibit include CD105, CD73 and CD90, whereas CD45 and CD34 are amongst the markers that MSCs should lack.

As outlined in Chapter 1, surgeons have begun to implement cell therapies for articular cartilage repair using chondrocytes and/or MSCs as these are natural and logical choices for repair applications. However, chondrocytes pose problems due to the limited capacity of donor sites to provide the necessary quantities for ACT (Andriamanalijaona, 2010), as well as donor site morbidity, chondrocyte dedifferentiation *in vitro* and other major impediments that have been encountered from this treatment (Csaki et al., 2008). Treatments using MSCs offered a promising progression, following their use with a variety of techniques including intra-articular injections and matrix assisted therapies. However, it has come to light that foreign, undirected MSCs may have little influence on the repair or regeneration of cartilage leading to ambiguous results (Murphy et al., 2003, Im et al., 2001, Jiang et al., 2003). Furthermore, evidence of fibrocartilage formation has superseded hyaline cartilage formation in several cases, and integration problems have also been apparent, suggesting that there is room in the market for an improved technique. An added challenge that has been raised with regards to MSCs is their tendency to demonstrate type X collagen expression during *in vitro* chondrogenesis (Barry et al., 2001). While type X collagen is usually used as a marker for hypertrophic chondrocytes, Pelttari et al., (2006) revealed that upregulation of type X collagen during *in vitro* chondrogenesis leads to strong matrix calcification accompanied by vascular invasion –a process similar to that occurring during endochondral ossification which ultimately leads

to the development of new bone. Therefore, the predisposition of MSCs towards osteogenesis and matrix calcification is an unfavourable aspect of using MSCs to produce a hyaline like repair tissue in articular cartilage defects (Andriamanalijaona, 2010).

More recent advancements in cell therapies for articular cartilage repair have moved onto investigating the potential of using a population of native cells to repair defective cartilage. These cells may offer a source of cells that would not be accompanied by 'baggage' in the form of problems that surgeons currently face when treating damaged or diseased hyaline cartilage: donor site morbidity, genetic instability and poor integration. As such, if and when the native cells and methods of activation are fully understood, the prospects of regenerative processes are high.

In view of using a native cell source, work in our laboratory demonstrated the presence of a stem/progenitor cell population in bovine articular cartilage in 2004 (Dowthwaite et al., 2004b). Successful isolation of these chondroprogenitors was achieved using a differential adhesion assay described by Jones and Watt in 1993 involving rapid adhesion to fibronectin (Jones and Watt, 1993). Fibronectin plays a major role in regulating many cellular processes including adhesion and migration, regulation of cell growth, differentiation and homeostasis (Pierschbacher and Ruoslahti, 1984). In their original article, Jones and Watt showed that a subpopulation of human epidermal keratinocytes were epidermal stem cells; distinguishable by their adhesive properties and high levels of $\alpha5\beta_1$ integrins, and these cells correlated to the cells with the highest colony forming efficiencies (CFEs). The fibronectin adhesion assay outlined by Jones and Watt was pursued by Dowthwaite et al., (2004) who enzymatically digested cartilage to release the resident chondrocytes and investigated the adhesion and CFEs using a bovine model. The authors investigated relative differences in chondrocytes from different zones and found that the chondroprogenitor cell population was localised to the surface zone where the cells not only exhibited significantly higher CFEs but the mean number of cells per colony was also significantly increased in the cohort.

Progressing from the work carried out by Dowthwaite et al., (2004), Williams et al., (2010) and McCarthy et al., (2011) investigated the possibility that a sub-population of chondroprogenitor cells may reside within normal human and equine articular cartilages

respectively. Williams et al., (2010) demonstrated that it was possible to isolate and expand clonal cell lines using determined growth medium to supplement the cells *in vitro*. This cohort of cells elicited a restricted differential potential during chondrogenic induction in a 3D pellet culture system as well as demonstrating further multipotent differentiation capacity.

These results are of major interest due to the potential for therapy and implications to clinical practise. Traditionally, chondrocytes that are enzymatically released and cultured in monolayer at low densities undergo phenotypic modulation, whereby synthesis of cartilage specific macromolecules are down-regulated and the cells acquire a fibroblast-like morphology. Given the right conditions and a chondrogenically permissive environment; chondrocytes are able to retain their chondrogenic potential (and redifferentiate or re-establish the original phenotype) up to 7 population doublings and sometimes beyond depending on medium additives. Due to the relatively low numbers of resident chondrocytes in articular cartilage, this tends to pose a problem when large numbers of cells are required to fill an articular defect. As a result, several research groups have focussed on the use of growth factors and 3D culture systems to maintain chondrogenic potential of cells (Benya and Shaffer, 1982, Jakob et al., 2001, Li et al., 2004, Wolf et al., 2008). As Williams et al., 2010 summarises "Although these modifications, to some extent, have proved successful they would be unsuitable as a method of expanding cells for use in cell-based repair therapies and as such, monolayer culture is a limiting factor for chondrocyte efficacy. Additionally, when chondrocytes are used in cell based tissue engineering, the resulting repair tissue is unpredictable and often fibrocartilagenous." A way to overcome this cell source limitation is to use a cell type that maintains its inherent proliferative capacity and possesses the 'developmental repertoire' of the native tissue. As such, the identification and characterisation of this cartilage progenitor population resident in normal human cartilage of varying ages presents a potential cohort of cells suitable for advancing cell based tissue repair therapies for cartilage defects.

In support of data presented by Dowthwaite et al., (2004), Williams et al., (2010) and McCarthy et al., (2011) not only demonstrated the presence of a congruent chondroprogenitor population resident in equine articular cartilage; but also compared the

chondroprogenitor cells to bone marrow-derived stromal cells (BMSCs) as potential cell sources for cartilage repair in the horse. Results were promising as data from this paper suggested that the chondroprogenitor cells may be considered superior to BMSCs in producing a functional repair tissue. The article demonstrated that following 3D chondrogenic induction, collagen type X labelling was not detected in the progenitor cell pellets whereas distinct labelling was evident in the BSMC pellets. This study reiterates the problem highlighted earlier regarding the tendency of MSCs to undergo terminal differentiation with an endochondral phenotype, potentially limiting the cartilage repair processes; and conversely presents the articular cartilage progenitor cells as a more viable cell source.

Work highlighted thus far focuses on progenitor cells within normal articular cartilage. However, with repair and regeneration in mind several research groups have directed their work towards looking into progenitor cells within osteoarthritic cartilage. As described in Chapter 1, there are many conservative and invasive surgical methods that are currently used which may either be palliative, or result in inconsistent results; and as such, no single treatment has been established as truly successful one. Total joint replacements are often used in patients where the tissue is deemed irrecoverable, however, this procedure does not rectify the problem; it provides an alternative solution through an invasive procedure that does not last a life-time and incurs many other implications. A native source of progenitor cells within diseased articular cartilage, therefore, presents with high prospects of regenerative processes; however this requires a deeper understanding of said cells and mechanisms of activation.

Alsalameh et al., (2004) was the first to describe the presence of a mesenchymal progenitor cell population in human osteoarthritic cartilage, using flow cytometry to demonstrate a significant increase in CD105+/CD166+ cells compared to the primary cell cultures from normal cartilage. Fickert et al., (2004) published an article shortly after Alsalameh et al., which was agreeable despite using a different selection of CD markers (CD9+, CD90+ and CD166+) to conclude that within human osteoarthritic cartilage, there are cells with mesenchymal progenitor cell characteristics. More recently, Koelling et al., (2009) has described the presence of migratory chondrogenic progenitor cells within human osteoarthritic cartilage which are believed to be migrating in response to

chemoctactic signals. A review by Khan et al., (2009) suggests that despite being present, these cells fail to receive local differentiation cues and thus, retain their native phenotypic state within OA cartilage instead of differentiating into fully committed chondrocytes.

The purpose of this study was to elucidate whether or not it is possible to isolate progenitor cells from human OA cartilage using the established Jones & Watt/Dowthwaite method of isolation and to examine whether these clonally derived populations had the potential for chondrogenic induction. Further investigations were carried out in order to establish the *in vitro* expansion potential of these cells and to determine their plasticity potentials into osteogenic and adipogenic lineages.

4.2. Materials

Material	Catalogue number	Supplier
anti-CD105 FITC Conjugate anti-CD166 R-PE Conjugate	326-040 393-050	Ancell, USA
40µm mesh cell strainer	352340	BD Falcon™, UK
CellTrics 30 µm filters	04-004-2326	Partec, UK
Dulbecco's modified eagles medium Dulbecco's modified eagles medium F12 + glutamax Fetal calf serum Gentamicin L-glutamine 200mM Hepes buffer Insulin transferrin selenium Rabbit serum Trypsin-EDTA 0.05%	41965-062 31331-093 10106-169 15750-045 25030-024 15630-056 41400-045 16120107 25300-062	Gibco, UK
SafeView Nucleic Acid Stain	NBS-SV1	NBS Biologicals Ltd, UK
Low Molecular Weight DNA Ladder Quick-Load 1 kb DNA Ladder	N3233S N0468	New England Biolabs, UK
Human FGF - basic Human TGF - β2	100 - 18B 100 – 35B	Peprotech, UK
Agarose GoTaq® Flexi DNA Polymerase M-MLV Reverse Transcriptase, RNase H Minus Random primers Recombinant RNasin Ribonuclease Inhibitor Set of dATP, dCTP, dGTP, dTTP TBE Buffer	V3125 M8301 M5301 C1181 N2511 U1240 V4251	Promega, USA

Pronase from *Streptomyces griseus*	11 459 643 001	Roche, UK
Accutase	A6964	Sigma Aldrich, UK
Albumin from bovine serum	A8022	
L-Ascorbic acid 2-phosphate	A8960	
Cloning rings	C7983	
Collagenase from clostridium histolyticum	C0130	
Dexamethasone	D8893	
Dimethyl sulfoxide	D5879	
Fibronectin from bovine plasma	F1141	
Formalin solution, neutral buffered, 10%	HT501320	
D-(+)-Glucose	G6152	
β-Glycerophosphate disodium salt hydrate	G9422	
Indomethacin	I7378	
Insulin solution, human	I9278	
3-Isobutyl-1-methylxanthine	I7018	
B-Mercaptoethanol	M3148	
Oil Red O	O9755	
Paraformaldehyde	P6148	
Phosphate buffered saline	P4417	
Silver nitrate	S6506	
Sodium carbonate	S2127	
Sodium thiosulfate pentahydrate	S7143	
Water (RNase free)	W4502	
Ethanol	E/0650DF/17	Thermo Fisher Scientific, UK
Propan-2-ol	P/7500/15	
Sodium hydroxide	S/4920/60	
Paraffin wax	298682F	VWR – Jencons, Leicestershire, UK
RNase-free DNase set	79254	Qiagen, UK
RNeasy Mini Kit	74104	
Qiashredder	79654	

Table 4.1. Materials and suppliers.

4.3. Methods

4.3.1. Tissue digestion & chondrocyte isolation

Following TKRs, tibial plateaux (TPs) were immediately transported in saline solution to the laboratory. Under sterile conditions, cartilage was excised from the TPs by fine dissection using a scalpel, ensuring where possible, that no other tissues (meniscus, ligament or osteophyte) were included in the digestion process. The cartilage was collected in a sterile 50ml tube and the chondrocytes were released from their matrix by sequential enzyme digestion using 70U ml^{-1} pronase in supplemented Dulbecco's Modified Eagles Medium F12 (DMEM/F12) plus Glutamax, [DMEM/F12 + Glutamax with 100mg ml^{-1} Gentamicin, 50µg ml^{-1} L-ascorbic acid 2-phosphate, 1mg ml^{-1} glucose, 2mM L-glutamine and 5% foetal calf serum (FCS)], for 30 minutes at 37˚C on a roller. Subsequently, the pronase was removed and replaced with 300U ml^{-1} collagenase (type I) in supplemented media for 3 hours at 37˚C on a roller. Following digestion, the chondrocytes were passed through a 40µm mesh cell strainer to ensure that any undigested tissue was eliminated, and the remaining cell suspension was centrifuged at 2000 rpm x g for 5 minutes. The supernatant was then removed and the pellet was re-suspended in supplemented DMEM/F12 without FCS and counted using a haemocytometer.

4.3.2. Fibronectin adhesion assay to isolate cartilage progenitor cells

Studies by Jones and Watt in 1993 demonstrated a method to identify epidermal stem cells using differential adhesion to fibronectin *in vitro*. Since then, Dowthwaite et al., 2004 expanded on this method and utilised fibronectin in an *in vitro* adhesion assay to identify bovine articular cartilage progenitor cells. This method is now an accepted method to isolate articular cartilage progenitor cells, and Williams et al., in 2010 described the presence of these cells within human articular cartilage. In this chapter, the fibronectin adhesion assay was utilised to see whether cartilage progenitor cells were evident in diseased articular cartilage.

Chondrocytes were re-suspended at a concentration of 4000 cells ml^{-1} in supplemented DMEM/F12 and seeded onto 6-well plates that had been pre-treated with fibronectin (10µg ml^{-1} in PBS containing 1mM MgCl$_2$ and 1mM CaCl$_2$) for 24 hours at 4˚C. Cells were incubated for 20 minutes at 37˚C, after which the media and non-adherent cells were removed. Fresh media (DMEM/F12 + 10% FCS) was then added to the dish and the cells were incubated and maintained in culture in a humidified chamber containing 5% CO$_2$ at 37˚C. Twenty four hours later, the media was changed once again to ensure that any non-binding cells were removed.

4.3.3. Colony isolation

Colonies consisted of clusters of 32 plus cells derived from an initial cell adhering as a result of the fibronectin assay. The bottom of the tissue culture plastic was marked in order to locate the colonies and allow for colony isolation. Subsequently, the media was removed and dishes were washed with serum-free media. Sterile polystyrene cloning rings were then dipped into Vaseline using sterile forceps and placed over the marked colony. One hundred microlitres of trypsin-EDTA was then added to the cloning ring, and the dish was placed at 37˚C for 3-5 minutes until the cells had rounded. The cells were then lifted by gentle pipetting and added to 1ml supplemented DMEM/F12 + 10% FCS containing 1ng ml^{-1} TGF-β2 and 5ng ml^{-1} FGF-2 in a fresh 24-well plate.

4.3.4. Expansion in monolayer culture

The cultures were maintained in a humidified CO$_2$ incubator at 37˚C, and supplemented media (DMEM/F12 + 10% FCS containing 1ng ml^{-1} TGF-β2 and 5ng ml^{-1} FGF-2) was changed 3 times a week. Once the cells reached confluence, they were washed in serum-free media and incubated in trypsin-EDTA for 6-8 minutes at 37˚C. The lifted cells in trypsin were then transferred to a 50ml centrifuge tube and an equal volume of DMEM/F12 + 10% FCS was added to the tube in order to deactivate the trypsin. The cell suspension was then centrifuged at 2000 rpm x g for 5 minutes. The supernatant was removed and the pellet was re-suspended and counted so that population doublings (PDs) could be monitored, using the following formula:

PD = [log (N) – log (N$_0$)] / 0.301

Where N is the number of cells recovered at the end of the passage and N_0 is the number of cells initially plated. Day 1 was considered the day in which the cells were initially plated and the initial number of cells was 1. PDs were analysed using Microsoft Excel.

If there was a surplus of cells, they were frozen down in 100µl dimethyl sulfoxide (DMSO) and FCS making the total volume up to 1ml in a sterile microcentrifuge tube, and stored at -80˚C until necessary.

4.3.5. Pellet cultures

In order to establish the chondrogenic potential of the cells 3D pellet cultures were generated. Confluent flasks were washed in serum-free media before being trypsinised for 6-8 minutes at 37˚C. The cell suspension was then transferred to a centrifuge tube and equal volumes of DMEM/F12 + 10% FCS added. The cell suspension was centrifuged at 2000 rpm x g for 5 minutes, the supernatant removed and the pellet re-suspended and counted. Half a million cells were added to a sterile 1.5ml Eppendorf tube containing chondrogenic media (DMEM/F12 + Glutamax with 2% FCS, 100mg ml^{-1} Gentamicin, 50µg ml^{-1} ascorbic acid, 1mg ml^{-1} L-glucose, 2mM L-glutamine, 1% hepes, and supplemented with 1% insulin transferring selenium (ITS), 0.1µM dexamethasone and 5ng ml^{-1} TGF-β2). The Eppendorf tube containing cells was then centrifuged at 2000 rpm x g for 5 minutes and incubated at 37˚C. Pellets were fed every second day for either 3 weeks or 6 weeks after which they were processed for analysis.

4.3.6. Processing pellets for paraffin wax embedding

Following the incubation period, the pellets were washed in PBS and then fixed in 4% paraformaldehyde or 70% ethanol for 20 minutes. The pellets were dehydrated in graded alcohols (70%, 95% and 100% x 2) with changes of 20 minutes each before being cleared in xylene (one change of 20 minutes), infiltrated with paraffin wax at 56˚C for one hour and finally embedded in paraffin wax. Following embedding, the pellets were sectioned as outlined in Chapter 2.3.4.

4.3.7. Pellets for RNA extractions

Following the incubation period the pellets were washed in sterile PBS. Three hundred and fifty microlitres of Buffer RLT containing $10\mu l$ ml^{-1} β-mercaptoethanol from the Qiagen RNeasy Mini Kit was then added to the Eppendorf tube and the pellet was disrupted by gentle pipetting. The lysed pellet was then either immediately used or was stored at -80˚C until needed.

4.3.8. Phenotypic plasticity

Osteogenic differentiation

Pellet cultures were established as described above. Osteogenic differentiation medium comprised DMEM + 10% FCS, 10mM β-glycerophosphate, 10nM dexamethasone and 0.1mM L-ascorbic-acid-2-phosphate, 500mg ml^{-1} Gentamicin and 1% Hepes. Pellets were incubated at 37˚C and 5% CO_2 and media was changed every second day for either 3 or 6 weeks, after which they were processed as above.

von Kossa staining for calcium mineral deposits

Once pellets were embedded and sectioned, they were dewaxed using xylene (2 changes of 2 minutes) and rehydrated through the graded alcohols (see Chapter 2.3.5). The sections were washed for a further 2 minutes in order for the von Kossa silver impregnation technique to be carried out. The sections were stained with fresh 5% aqueous silver nitrate for 30 minutes under bright light, and then rinsed 3 times in distilled water. Subsequently, the stain was developed using 5% sodium carbonate in 10% neutral buffered formalin solution (NBFS) for 5 minutes. Sections were then rinsed in distilled water again before being fixed in 5% sodium thiosulphate for 2 minutes. Examination and images were recorded using the Leitz DMRB light microscope.

Adipogenic differentiation

Adipogenic differentiation was induced in monolayer cultures using a modified protocol described by Koch et al., (2007). In brief, cells were seeded in 6-well plates at 5×10^4 per

well and cultured until sub-confluent, at which point they were treated with DMEM + 10% FCS containing 10µg ml^{-1} insulin, 1µM dexamethasone, 100µM indomethacin, 500µM 3-isobutyl-1-methyl xanthine (IBMX) and 15% normal rabbit serum. The medium was changed every 48 hours for 6 days after which the cells were either fixed for 10 minutes with 10% NBFS and stained with Oil red-O for the presence of lipid droplets, or washed in PBS and lifted using Buffer RLT using the method described above, for RNA extraction.

Oil red-O staining for adipogenic differentiation

Following fixation in 10% NBFS, the cells were rinsed and maintained in PBS whilst fresh Oil red-O was prepared (0.3% Oil red-O in 60% isopropanol) immediately prior to staining. (A stock solution of 0.5% Oil red-O was made up in 100% isopropanol and then diluted in distilled water). The stain was added to the plates for 1 hour at room temperature before being washed thoroughly in distilled water, examined using a Nikon Eclipse TS100 microscope and imaged using a Nikon E4500 camera.

4.3.9. Histological stains

Sections were dewaxed using xylene (two changes of 2 minutes) and rehydrated through a series of graded alcohols (two changes of 2 minutes in 100%, followed by one change of 2 minutes in 95% and 70%). The sections were then washed in running water for a further 2 minutes before being stained with either safranin O (2 mins) or toluidine blue (1 min). Following staining, sections were washed in running water for 2 minutes (or until water was clear). Toluidine blue stained sections were air-dried overnight and mounted under coverslips using DPX the following day. Safranin O stained sections were dehydrated in graded alcohols (one change of 1 minute in 70% and 95%, followed by two changes of 2 minutes in 100%), cleared in xylene (two changes of 2 minutes) and mounted under coverslips using DPX.

4.3.10. Immunohistochemistry

Immunoperoxidase labelling was carried out as described in Chapter 3 using antibodies against collagens type I, II and X, and aggrecan. A summary table of antibodies and concentrations is shown in table 3.2.

4.3.11. Total RNA extraction using the RNeasy Mini Kit (Qiagen)

The protocol used for extracting RNA was from the RNeasy Mini Handbook supplied within the RNeasy Mini Kit (materials supplied).

A simple outline of the protocol that was used is described below.

Initially, the cells were lysed in 350µl of Buffer RLT containing 10µl ml^{-1} β-mercaptoethanol. The lysate was then transferred onto a QIAshredder spin column in a 2ml collection tube and centrifuged for 2 minutes at maximum speed (13,000 rpm x g). Three hundred and fifty microlitres of 70% ethanol was then added to the homogenized lysate, and mixed well by pipetting. Seven hundred microlitres were transferred into an RNeasy spin column placed in a 2ml collection tube and centrifuged at 10,000 rpm x g for 15 seconds. To eliminate genomic DNA contamination, additional On-column DNase digestion steps were carried out. Three hundred and fifty microlitres of Buffer RW1 was added to the spin column and centrifuged for 15 seconds at 10,000 rpm x g. Ten microlitres of DNase I stock solution was added to 70µl Buffer RDD and placed directly on the RNeasy spin column membrane and left for 15 minutes at room temperature. Subsequently, 350µl Buffer RW1 was added to the spin column and centrifuged for 15 seconds at 10,000 rpm x g. Five hundred microlitres of Buffer RPE were then placed onto the RNeasy column and centrifuged for 15 seconds at 10,000 rpm x g. Another 500µl of Buffer RPE was added to the RNeasy column and centrifuged for a further 2 minutes at 10,000 rpm x g. After every step, the flow-through was discarded. To elute the total RNA, the RNeasy column was transferred to a new 1.5ml collection tube, and 30µl of RNase-free water was placed onto the RNeasy silica-gel membrane and centrifuged for 1 minute at 10,000 rpm x g. The total RNA was stored at -80°C.

4.3.12. Estimation of RNA concentration and purity

Total RNA was quantified by measuring the absorbance at 260nm and 280nm in a NanoDrop ND-100 Spectrophotometer associated with Nano-Drop 3.0.1 software (NanoDrop Technologies, UK) against a blank of molecular biology grade water. The ratio of absorbance provides an indication of the purity of the RNA with respect to contaminants that absorb in the UV spectrum such as proteins. Pure RNA has an A_{260}/A_{280} ratio of ~2.0.

4.3.13. Complimentary DNA synthesis

Total RNA was reverse transcribed to prepare complimentary DNA (cDNA). The mass of RNA used was kept constant where possible at 100ng. Reverse transcription was carried out in a 50µl volume and reagents were from Promega, UK. Total RNA was mixed with 10µl 5x M-MLV RT buffer, 1µl random hexamers, 1µl deoxyribonucleotide triphosphate (dNTPs) (at 20mM), 1µl rRNasin RNase inhibitor and 0.5µl M-MLV reverse transcriptase. RNase free water was added to make the reaction volume up to 50µl. The mixtures were placed in RNA-free dome cap tubes and incubated for 10 minutes at 25˚C, 60 minutes at 48˚C and a further 10 minutes at 95˚C on a Techne TC-3000 thermal cycler (Techne, Cambridge, UK). Samples were then held at 4˚C before being stored at -20˚C until the cDNA was required.

4.3.14. Reverse transcriptase polymerase chain reaction (RT-PCR)

Standard PCR amplification of cDNAs of interest was carried out in a reaction containing 2.5mM $MgCl_2$, 200nM of each forward and reverse primer, Go*Taq* Flexi buffer, pH8.5 and 1 unit of Go*Taq* Flexi DNA polymerase in the presence of 200µM dNTPs (reagents from Promega, UK). Reaction volumes were scaled to a 12.5µl with the following quantities.

Reagent	Volume (µl)
5x GoTaq buffer	2.50
MgCl$_2$ (25mM)	1.25
Forward primer (10µM)	0.25
Reverse primer (10µM)	0.25
dNTPs (10mM each)	0.25
GoTaq Polymerase	0.06
dH$_2$O/cDNA	7.94
TOTAL	**12.50**

Table 4.2. Reaction volumes for reverse transcriptase polymerase chain reaction (RT-PCR).

Samples were initially denatured at 95˚C for 3 minutes and then amplified for 40 cycles at 95˚C for 30 seconds, primer specific annealing temperature (Tm) for 30 seconds, and the extension phase was held for 30 seconds at 72˚C (refer to table 4.3 for annealing temperatures). A final extension was held at 72˚C for 10 minutes. Samples were then stored at 4˚C prior to the analysis of products by agarose gel electrophoresis.

4.3.15. Agarose gel electrophoresis

Nucleic acid was resolved on 2% (w/v) agarose gels containing SafeView nucleic acid stain at 5µl 100ml^{-1} prepared in 1x Tris Borate EDTA (TBE) buffer. DNA ladders were run alongside the products. Gels were visualised and documented using a transilluminator on a Bio-Rad Gel Doc 2000.

Gene of interest	Primers (5'-3')	Annealing temp (˚C)	Product size (bp)
18S Ribosomal RNA	Fwd - GCA ATT ATT CCC CAT GAA CG Rev – GGC CTC ACT AAA CCA TCC AA	60	125
Sox 9	Fwd - AAT CTC CTG GAC CCC TTC AT Rev – GTC CTC CTC GCT CTC CTT CT	62	198
Notch-1	Fwd - GAG GCG TGG CAG ACT ATG C Rev - CTT GTA CTC CGT CAG CGT GA	60	117
Lipoprotein lipase (LPL)	Fwd - AGG AGC ATT ACC CAG TGT CC Rev - CCA AGG CTG TAT CCC AAG AG	60	130
Osteonectin	Fwd - AAA TAC ATC CCC CCT TGC CT (Exon 6/7) Rev - CCA GGA CGT TCT TGA GCC AG (Exon 7)	60	78
Osteocalcin	Fwd - GGC AGC GAG GTA GTG AAG AG (Exon 3) Rev - GAT CCG GGT AGG GGA CTG (Exon 4)	60	73

Table 4.3. Summary table of primer sequences for specific genes used for generating PCR products. Annealing temperature and product size also included in table.

4.4. Results

4.4.1. Chondroprogenitor cell isolation and expansion

4.4.1.1. Morphology

Chondroprogenitor cells were successfully isolated from osteoarthritic tibial plateaux and cultured until clonally derived primary cell lines were established. The number of days required for colonies to form ranged from 8 days up to 14 days; after which they were disregarded. The morphological appearance of the colonies formed showed a large degree of variation. Figures 4.1 A-H demonstrates the differences in these variations. Differences seen related to the size of the colony (figure 4.1A compared to H), how condensed the cells within the colonies were (figure 4.1C compared to E), and also to the size and shape of the cells within the colonies. It was observed that larger cells often correlated with the looser colonies and smaller cells with the tighter ones. The cell shape typically seen was fibroblast-like, however flatter cells with numerous protrusions were also identified, as were spindle-like cells.

Using cloning rings, colonies were isolated to enable clonal cell lines to be expanded independently. Figures 4.2 A-C are representatives showing the typical appearance of the expanded chondroprogenitor cell lines isolated from osteoarthritic tissue. Figure 4.2A demonstrates the cells at sub-confluence and Figure 4.2B is a representative photograph of the cells at confluence. These images are from cells at population doubling (PD) 28-30. Figure 4.2C illustrates a clonal cell line at over 60PDs and it can be seen that the cells retain a similar morphology at this late stage. It was generally observed that the cells had a tendency to increase in size with longer culture periods.

Crucially, it was noted that many cell lines would initially proliferate and pass the point of colony formation, after which mitotic activity was curbed and proliferation ceased. Morphological changes in the cells were apparent at this stage and representatives of unsuccessful cell lines are shown in figures 4.3 A & B.

4.4.1.2. Population doublings

Growth kinetics of the clonally derived chondroprogenitor cells lines from 9 tibial plateaux were investigated (figure 4.4). It was observed that there was a large amount of heterogeneity between the different cell lines from the different patients; however, different cell lines from the same patient appeared to adopt similar proliferation rates. A large number of cell lines did not survive past the initial phase of exponential growth (up to 20 PDs), which in certain cases resulted in limited cell lines being analysed per patient. From the chart (figure 4.4) it can be seen that after the initial surge, the tendency was for proliferation rates to slow. In some cases this reduction eventually plateaued, however, in other cases, following the initial reduction in growth rate, a second surge was apparent where proliferation rates increased again. The furthest that any of the cell lines were expanded to was to 67.4 PDs and this was achieved in 157 days.

As previously mentioned, many of the chondroprogenitor cell lines that initially appeared to be proliferating normally showed a sudden arrest in their proliferation. Based on the number of cell lines initially cultured passed 20PDs, a substantial 48% of these failed to reach 30PDs (figure 4.5). As such, of the initial clonally derived chondroprogenitor cell lines originally cultured, only 14 successfully reached 30 PDs from 6 different patients (figure 4.6). The time taken to reach 30 PDs ranged between 34 and 75 days and this significant difference highlights the heterogeneity in cells isolated and cultured in the same way, from different patients. Interestingly, the clonal variation (variation between clones from the same patient) was less pronounced and no statistical significance was found between these cells.

Seven cell lines from 4 different patients were successfully cultured to 40 PDs and the time taken to reach this stage ranged between 50 and 98 days; as such, the retarded cell lines were slower by 2-fold (figure 4.7) highlighting again that there is a distinct difference in cell behaviour and proliferation rates under the same conditions. The diminishing numbers and lack of consistency again highlights the heterogeneity throughout the chondroprogenitor cell lines isolated from osteoarthritic tibial plateaux.

Comparisons of PDs per day can be seen in figures 4.8 and 4.9. PDs per day allows for a direct measure of proliferation rate within a defined amount of time. Using the cell lines that reached 40 PDs, PDs per day up to 30 PDs and up to 40 PDs were investigated in order to establish whether or not the rate of proliferation slowed in the latter stages of culture. Figure 4.8 allows for a direct comparison between the two time points to be visualised and it can be seen that in most cases (6 out of 8) the PDs per day up to 30 PDs were slightly greater than those up to 40, this trend suggesting that the cell proliferation slows after extended periods in culture. There were 2 anomalies noted however; in one case the PDs per day increased after 30 PDs, and in the second instance, PDs per day did not appear to change after 30 PDs were reached. The PDs per day up to 30 PDs ranged from 0.42 to 0.88, and the PDs per day up to 40 PDs ranged from 0.41 to 0.79. For both of those data sets however, the initial phase of exponential growth was included and as such, this phase is likely to have the greatest impact on PDs per day. Consequently, figure 4.9 illustrates the PDs per day for the duration between 30 and 40 PDs thus eliminating the early phase so that a comparison can be made to how the rates really differ in the former and latter stages of culture. Between 30 and 40PDs, the rate of PDs per day ranged between 0.29 and 0.81. Statistically, there was no significant difference observed due to the varied behaviours of the different cell lines - some cell lines showed a reduction in proliferation whereas others demonstrated an increase in proliferation. As such, no definitive conclusion can be drawn as to whether the proliferation rates slow in later stages of culture; more so each cell line has its own behavioural pattern.

A linear regression line was plotted in order to establish whether or not there was a relationship between proliferation rates (PDs per day) and patient age. This dot plot was based on the cell lines that surpassed 30 PDs and the dots represent cell lines rather than individual patients. Interestingly it was found that proliferation rates were higher in cell lines of older patients (P<0.05 using Pearsons correlation test), however a low R^2 value brings to question the significance of the regression line.

4.4.2. Chondrogenic 3D pellet formation

Chondroprogenitor cells were chondrogenically induced into 3D pellets containing 5×10^5 cells (figures 4.11 A-E). These pellets were smooth and iridescent, resembling a typical

hyaline cartilage surface. The pellets formed varied in size between clonal cell lines and between patients but were typically between 600µm and 1.0mm. Figures 4.11 A-C illustrate pellets from clonal cell lines from 3 separate patients, expanded to 24-26 PDs. Despite varying slightly in size their physical appearance is comparable. Figure 4.11 D illustrates a pellet formed following expansion in culture to 60PDs. Again the difference observed was in size (500µm) however it cannot be assumed that this difference is due to the long culturing period. When forming the pellets for each clonal cell line, a minimum of 3 replicates were maintained. As such, it was apparent that within one particular cell line, the resultant pellets were homologous to one another (figure 4.11 E). The size and gross appearance of the pellets were consistent within the clonal cell lines. In terms of gross morphology, it was noted on several occasions that outgrowths sporadically formed off the main pellet. Although not featured in figure 4.11 they are apparent in several of the sectioned pellets for histology and immunohistochemistry.

4.4.2.1. General histology

The ECM present in pellets was visualised by safranin O and toluidine blue staining (figure 4.12 & 4.13 respectively). Four pellets were imaged to illustrate the variation between clonal cell lines from different patients after culturing the cells in monolayer for 24-26 population doublings (A – D). Figure 4.12/13 E represents a pellet formed after culturing in monolayer for 35 PDs and figure F illustrates a pellet formed following extended culture in monolayer, furthering 60 PDs. In all cases GAG deposition was evident, to greater or lesser extents. In the PD24-26 pellets, safranin O was most abundant in pellet A and, incidentally, the pellet also appears to be more intact; a coherent pellet with a retained structure when removed for analysis. In pellet C it can be seen that there are areas that lack GAG deposition particularly around the centre of the pellet, and similarly this pellet appears to have the least amounts of integrity. The pellets from PD 35 and 60 (E & F) demonstrated GAG deposition again, to differing degrees.

Toluidine blue staining (figure 4.13) demonstrated very similar results however it appears to have been a more sensitive stain as there are regions that elicit positive toluidine blue stain that apparently lacked GAG deposition when looking at the safranin O results.

Having said that, pellet C maintained its apparently poor ECM, as was found with the safranin O.

In all cases, safranin O and toluidine blue staining for sulphated GAGs was most abundant around the periphery of the pellet, where an apparently more fibrous outer coating appears to surround the pellet.

4.4.2.2. Immunohistochemistry

The sectioned pellets were labelled with a panel of antibodies to ECM components. These were carried out on pellets formed from cells expanded to PD 24-26, 35 & 60 and cultured in 3D for 21 days. To see whether time influenced expression of ECM components, pellets were cultured for 21 and 41 days respectively. These pellets originated from cells expanded to 24-26 PDs.

All pellets labelled for collagen type II (figure 4.14). Although it is not possible to quantify labelling, it is apparent that labelling is more continuous in pellets A and C, compared with E and G, and this also correlates with the integrity of the pellets assessed. Pellets I and K, formed from later PDs do not show any marked difference in the level of collagen type II labelling. Looking at the pellets that were cultured for different lengths of time (M-S), no distinct differences were detected in the first pellet (M/O) however the longer culture period did appear to yield more collagen type II in the second pellet (Q/S). As such, culturing the pellets for longer periods of time did not elicit a distinct response on the resultant tissue.

Aggrecan labelling was not consistent throughout the pellets (figure 4.15). In certain pellets, labelling was evident throughout the tissue and, in particular, around the periphery (pellet A). However, in other pellets (pellet C) despite having a sound histological appearance, very little aggrecan was detectable. Pellets with less integrity demonstrated lower levels of aggrecan particularly in the core of the pellet (E and G). No major difference was found in pellets cultured from cells at later PDs; the trend that was generally observed was that the more aggrecan detected, the more intact the pellet, regardless of PDs at the point of pellet formation. Similar to the collagen type II result, the

185

effect of incubation time on aggrecan expression appeared to be cell-line specific as in one instance the 6 week incubation time made no difference and in the other pellet an increase in aggrecan expression was observed (figure 4.15 M-S).

Collagen type I expression was evident in the ECM of all the pellets (figure 4.16). In some pellets it was more prominent in the core when compared to the periphery (pellets A and G). No distinct pattern, however, was observed in relation to the distribution of type I collagen and there more no marked difference in expression between the 3 and 6 week cultures.

Labelling for type X collagen demonstrated the greatest variation between the pellets (figure 4.17). Some demonstrated a distinct lack of type X collagen, whereas in other pellets from different clonal cell lines, the ECM component was detected (pellet A). This is interesting as it demonstrates clear heterogeneity between the pellets. Pellet G represents the pellet cultured from cells expanded to 60 PDs and it is evident that in that particular case extended culturing did not increase the propensity of type X collagen expression. Pellets I to O demonstrate no marked effect of 3 versus 6 week incubation times whilst in pellet culture.

4.4.3. Plasticity

Following adipogenic induction, the cells adopted different morphologies in that they developed projections and resembled a more dendritic phenotype when compared to the controls (figures 4.18 and 4.19). Histological examination using oil red O revealed the presence of numerous lipid vacuoles surrounding the cells. This was consistent between all the clonal cell lines (figure 4.18 A-C). No lipid vacuoles formed in the corresponding controls (figure 4.19). Real-time reverse transcriptase polymerase chain reaction (RT-PCR) analysis of the expression of mRNA for lipoprotein lipase (LPL), a member of the lipase gene family found in adipose tissue, in cultures exposed to adipogenic treatment verified the histological observation seen within the clonal cultures. Figure 4.23 B illustrates the absence of LPL in the chondroprogenitor cultures (C) compared to the positive bands seen in the adipogenic cultures (A).

Osteogenic differentiation was induced in a similar 3D pellet culture system used for chondrogenic induction. Gross morphology of the osteogenic pellets after 3 weeks closely resembled that of the chondrogenic pellet. The smooth, white structures are pictured in figure 4.20. Sectioned pellets were stained using the von Kossa technique to demonstrate deposits of calcium, indicative of a mineral rich matrix. Results were cell-line specific as varying levels of deposits were apparent after the 3 week incubation time (figure 4.21). Pellet A showed abundant staining throughout the pellet, pellet B showed signs of mineral deposits particularly in the core region of the pellet; and pellet C apparently lacked any calcium deposits after 3 weeks. Pellet D however is the same clonal cell line as pellet C, cultured under the same conditions for 6 weeks rather than 3, and here it was evident that after 6 weeks the mineral deposits formed and were abundant throughout. No positive stain was detected in any of the corresponding controls (figure 4.22). RT-PCR was carried out in order to demonstrate gene expression of osteogenic markers, however no particular gene was found to be exclusive to the osteogenic pellets whilst being absent from the chondrogenic pellets.
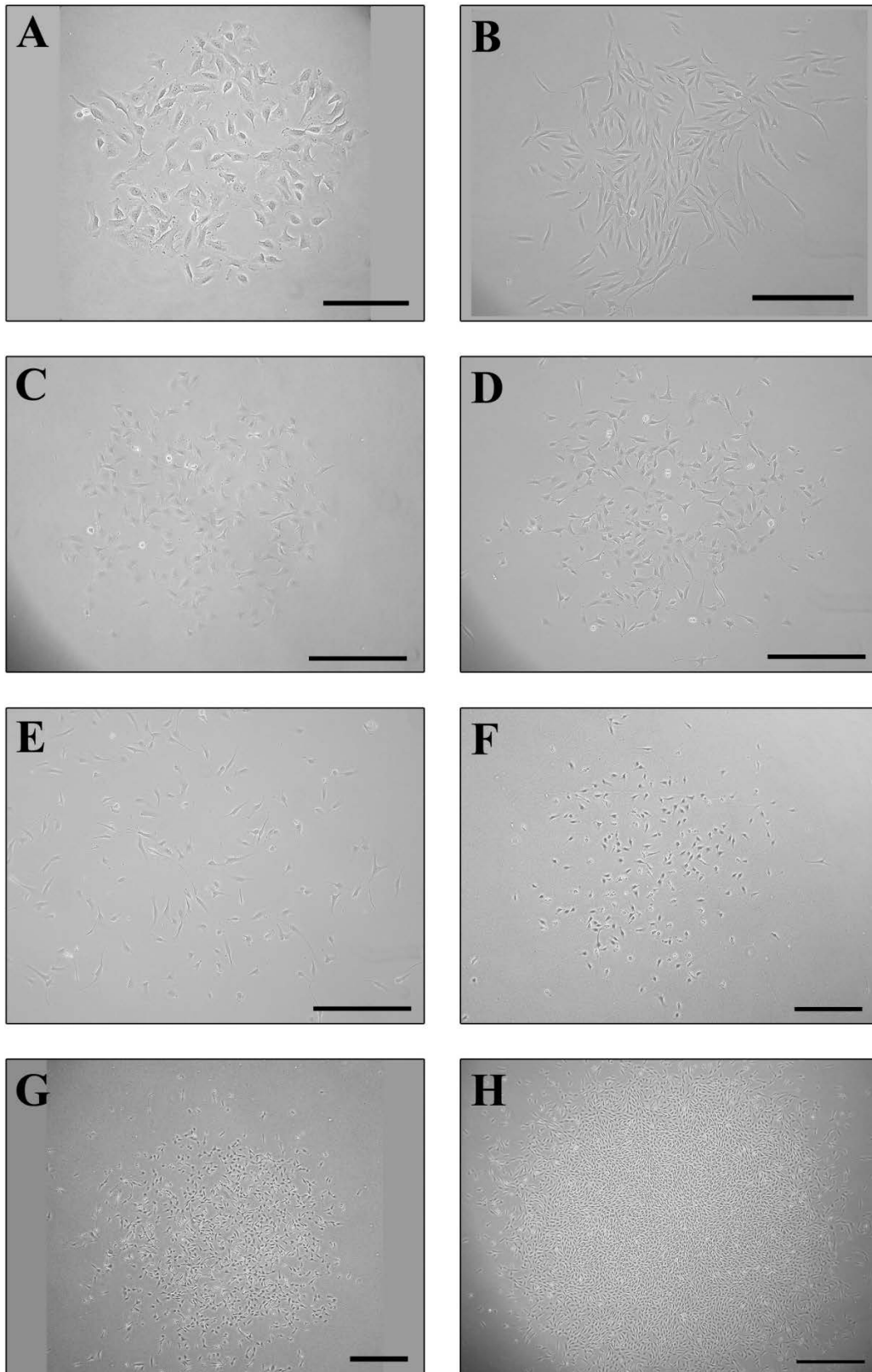
Figure 4.1. Comparative morphology of chondroprogenitor cell colonies isolated from osteoarthritic cartilage.

Pictured colonies were cultured between 8 – 14 days in conditioned medium. Cells displayed a typical fibroblast-like phenotype of dedifferentiated chondrocytes. Colonies varied both in size and density. Scale bars: A-B = 200µm; C-E = 400µm, F-G = 500µm, H = 700µm.
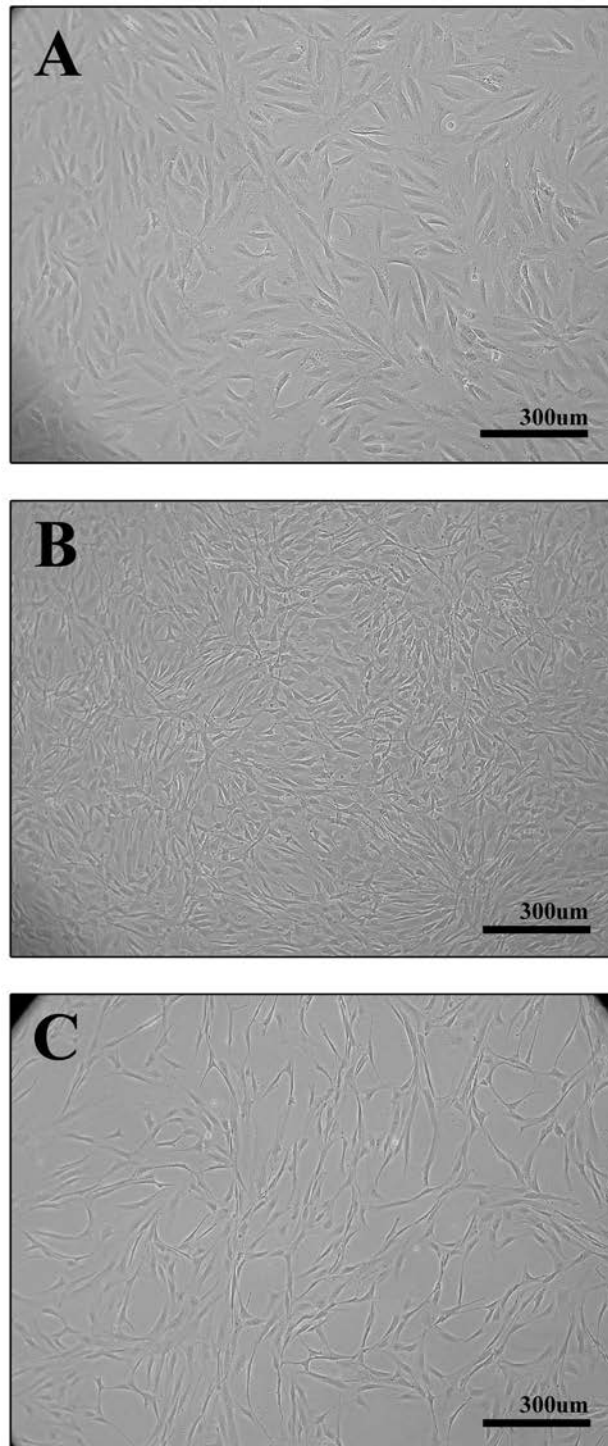
Figure 4.2. Representative images of chondroprogenitor cells expanded in monolayer culture at sub-confluent stages (A) and at confluence (B).

Cells cultured passed 60PDs retained they typical fibroblast-like morphology (C) throughout the extended culture period.
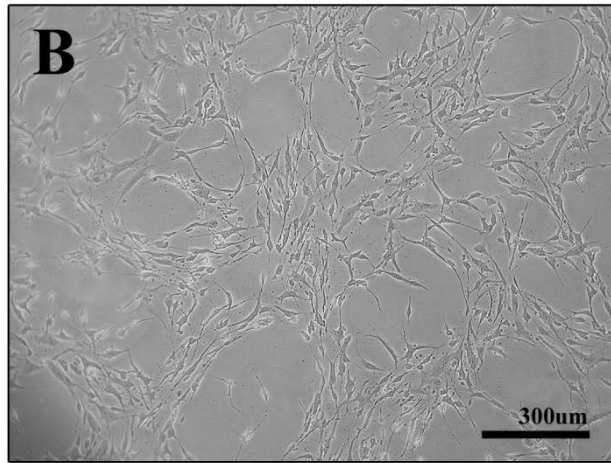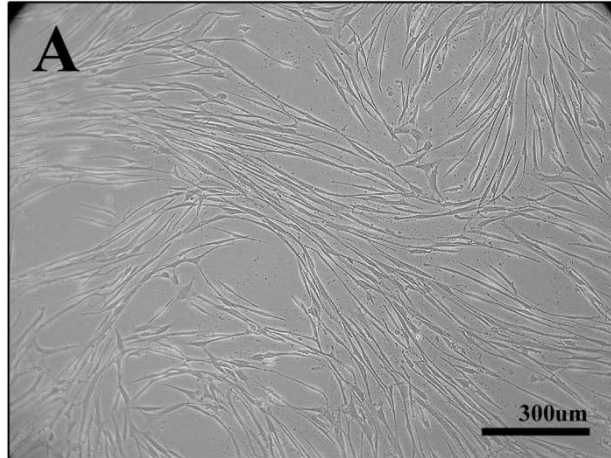
Figure 4.3. Representative images of chondroprogenitor cell lines that failed to continue proliferating.

Cell morphology became altered; they adopted either a long thin appearance (A) or an irregular, straggly appearance (B). In all cases, these 'unsuccessful' cells showed a greater affinity to each other; clustering together forming networks of non-proliferating cells.
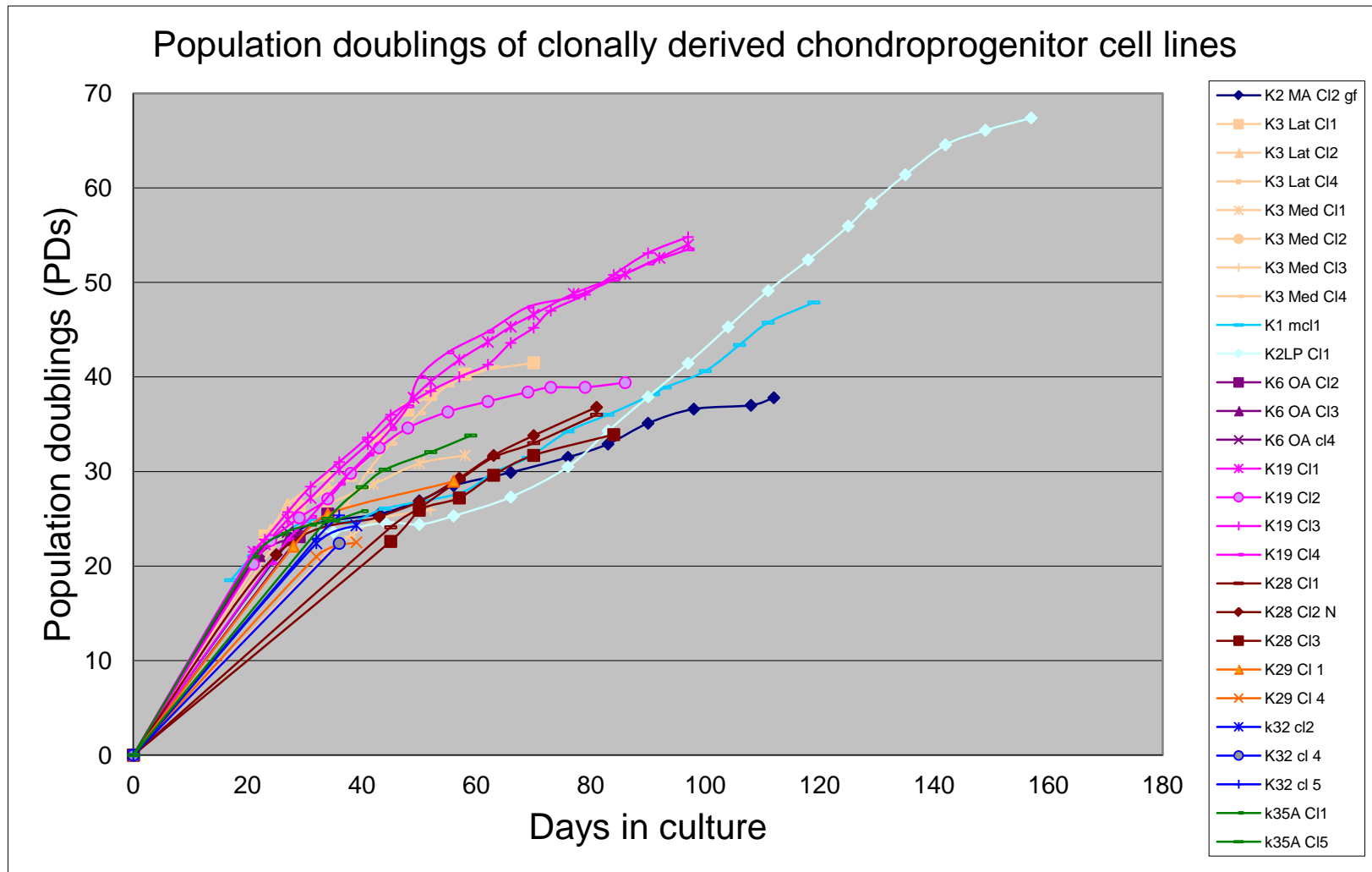
Figure 4.4. Chart to illustrate population doublings of clonally derived primary chondroprogenitor cell lines isolated from human osteoarthritic knee cartilage.
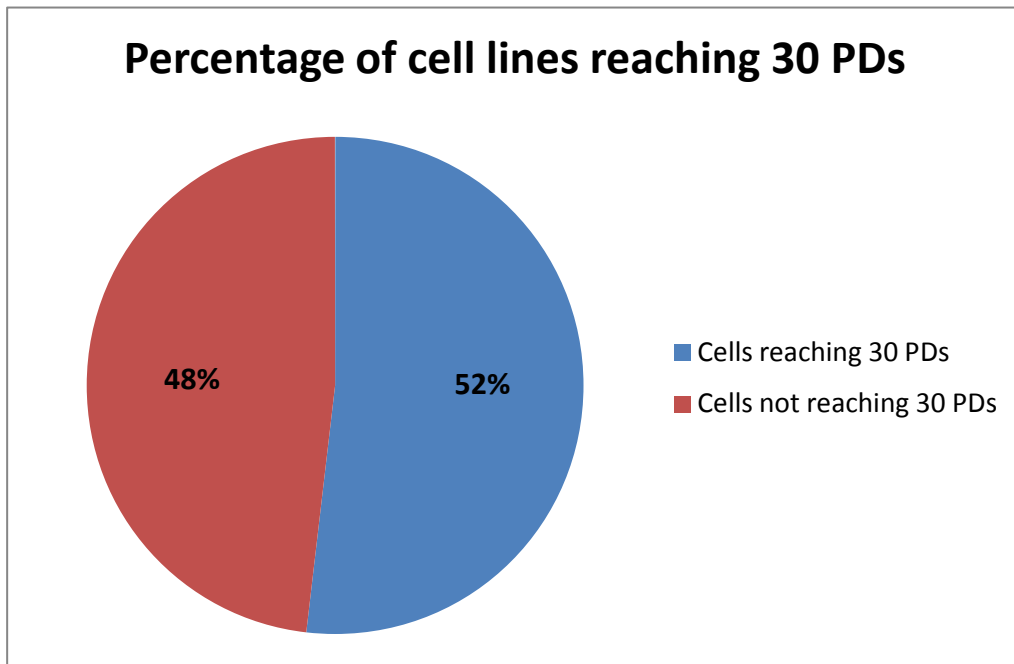
Figure 4.5. Pie chart displaying the proportion of cell lines that were successfully expanded passed 30 PDs.

Fifty-two percent of the total number (n=27) successfully reached 30PDs.
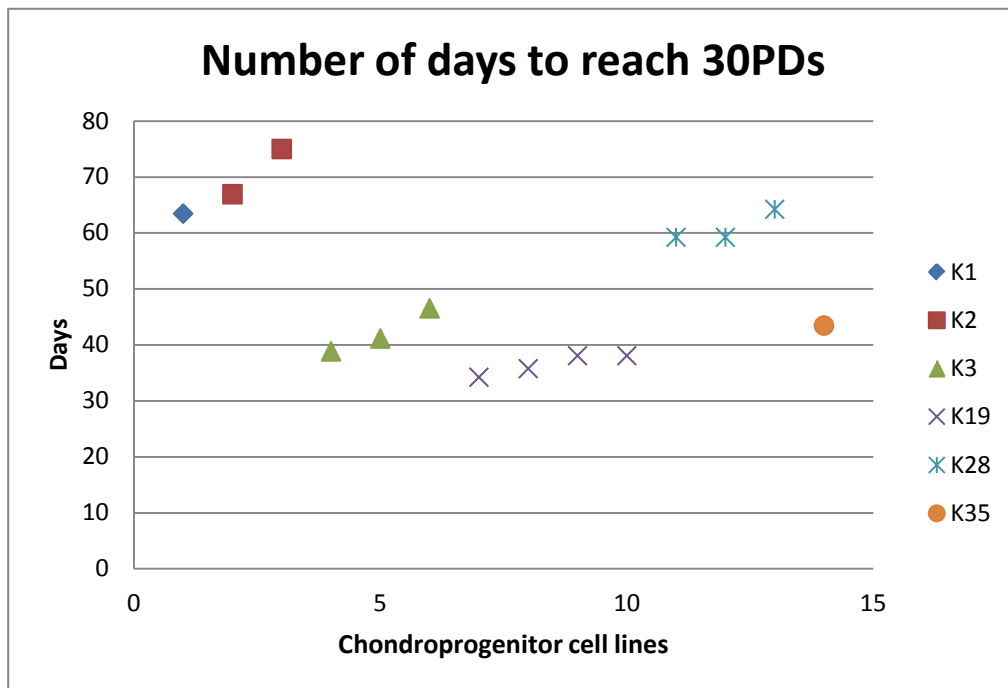
Figure 4.6. Dot plot representing the range of number of days in culture before clonally derived chondroprogenitor cell lines reached 30 population doublings.

One-way ANOVAs confirmed that there was a statistical significance (P<0.001) between days taken to reach 30PDs in different patients. No significance was found between clones of the same patient, however this does not consider the cell lines that failed to reach 30PDs.
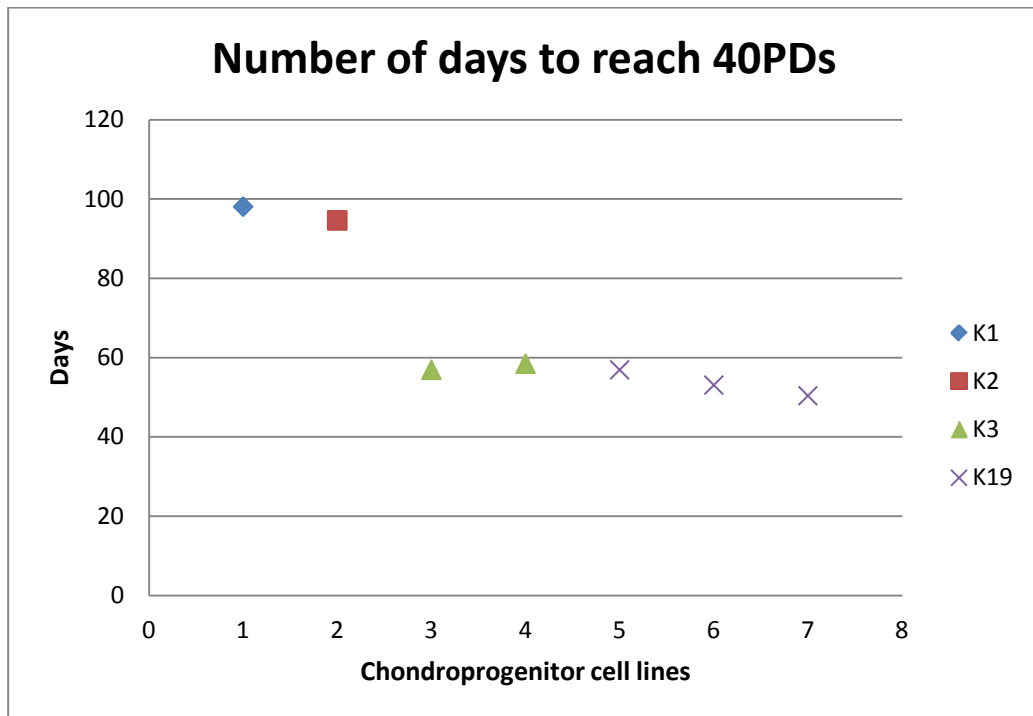
Figure 4.7. Dot plot representing the range of number of days in culture before clonally derived chondroprogenitor cell lines reached 40 population doublings.

One way ANOVAs confirmed a significant difference (P≤0.001) between days taken to reach 40PDs in different patients.
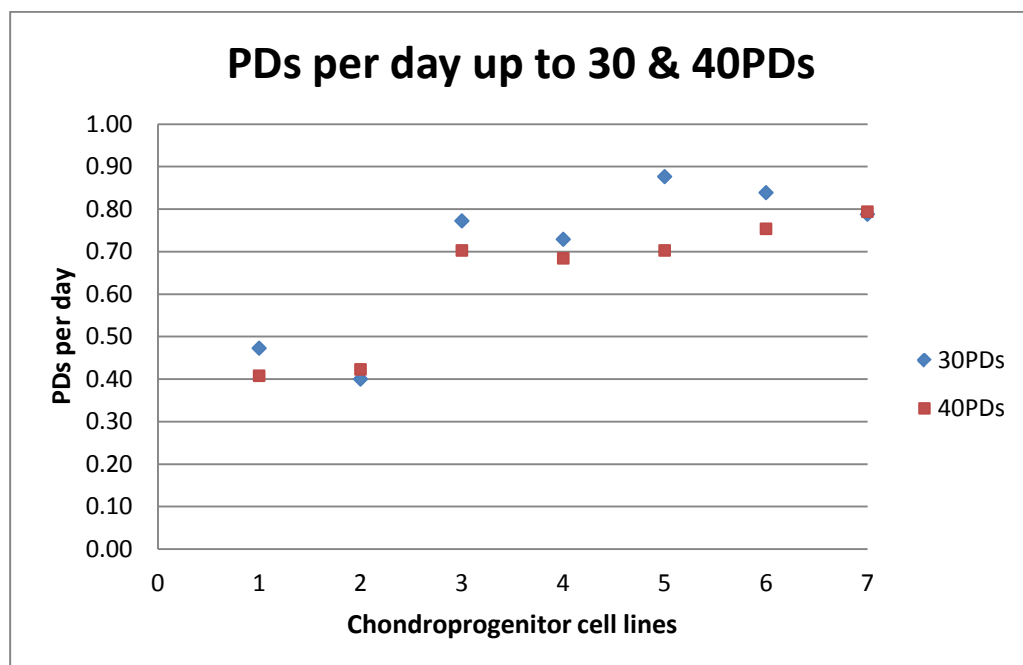
Figure 4.8. Dot plot demonstrating the rate of population doublings per day up to 30 (blue) and 40 (red) PDs in clonally derived chondroprogenitor cell lines reaching this proliferative stage.
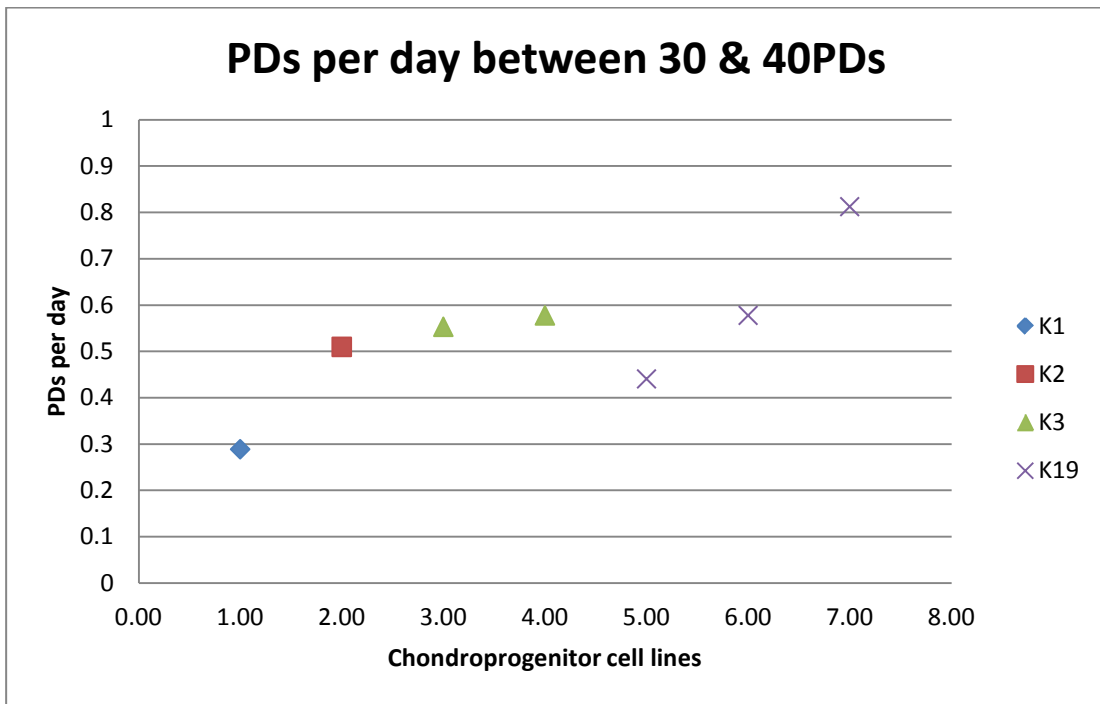
Figure 4.9. Dot plot demonstrating the rate of population doublings specifically between 30 and 40PDs in clonally derived chondroprogenitor cell lines.

A paired t-test was used to establish whether or not there was a difference between proliferation rates at 0-30 PDs and 30-40PDs; as such no difference was found ($p > 0.05$).
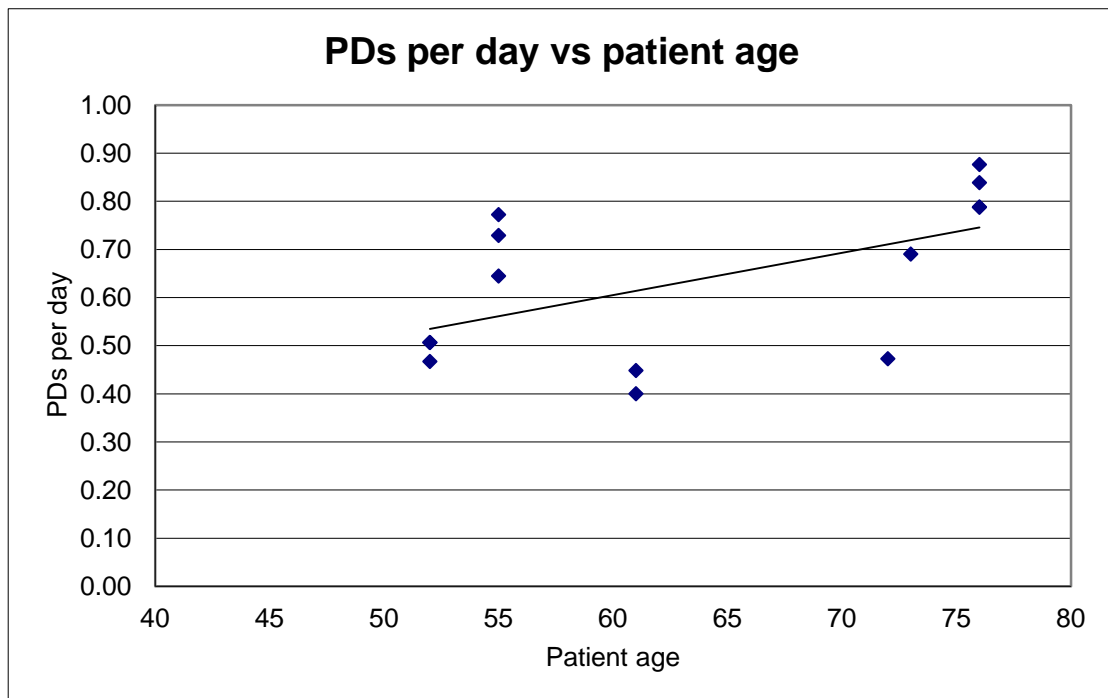
Figure 4.10. Dot plot demonstrating the correlation between population doublings per day in relation to patient age in clonal cell lines that reached 30 PDs.

Pearson's correlation test demonstrated a positive relationship ($p < 0.05$).

194
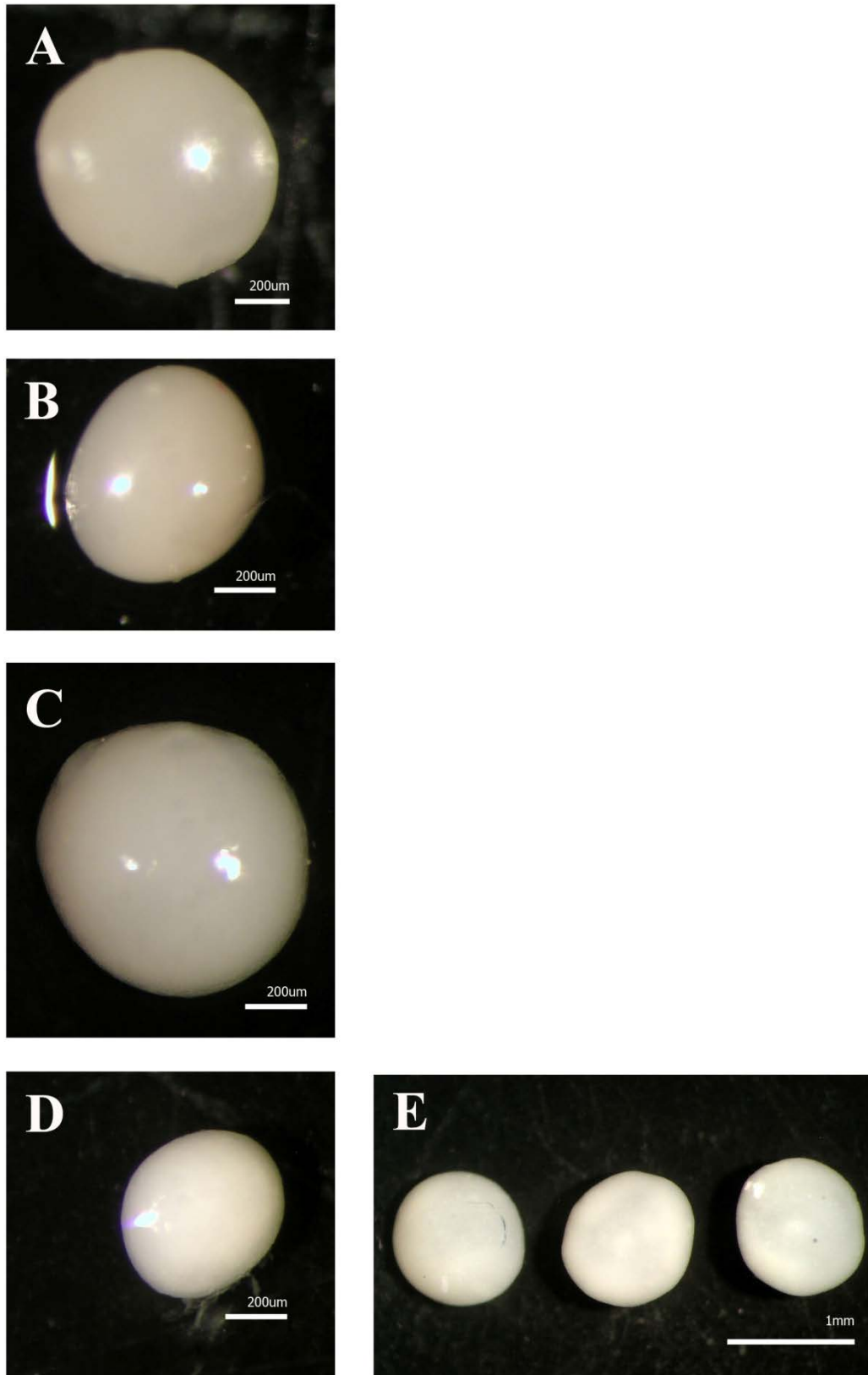
Figure 4.11. Photomicrographs of the gross morphology of chondrogenic pellets.

Cell lines from different patients were used (A-C) displaying consistent characteristics. The major difference observed was size related. After long term expansion (beyond 60PDs) cells maintained the capacity to form pellets (D). Replicates within cell lines demonstrated consistency in pellet size (E).
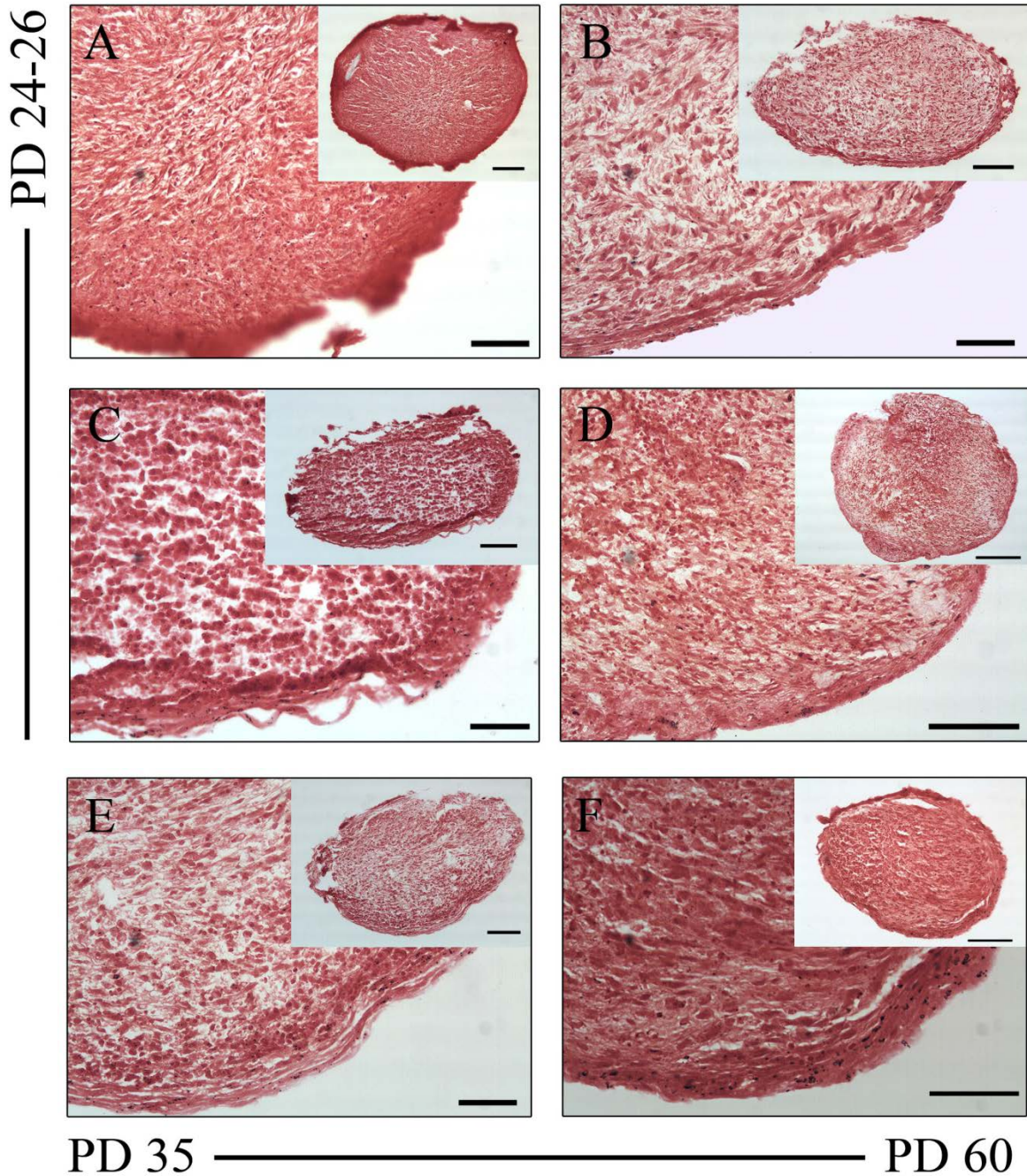
Figure 4.12. Photomicrographs of chondrogenic pellets stained with Safranin O for GAGs.

Varying amounts of GAG was observed in pellets from clonal cell lines derived from different patients at PD 24-26 (A-D). Detectable GAG was particularly evident around the periphery of the pellet. GAG was also evident in pellets formed after longer culture periods; at PD 35 (E) and PD 60 (F). Scale bars: A-C, E-F = 50µm (insert = 100µm), D =100µm (insert = 200µm).
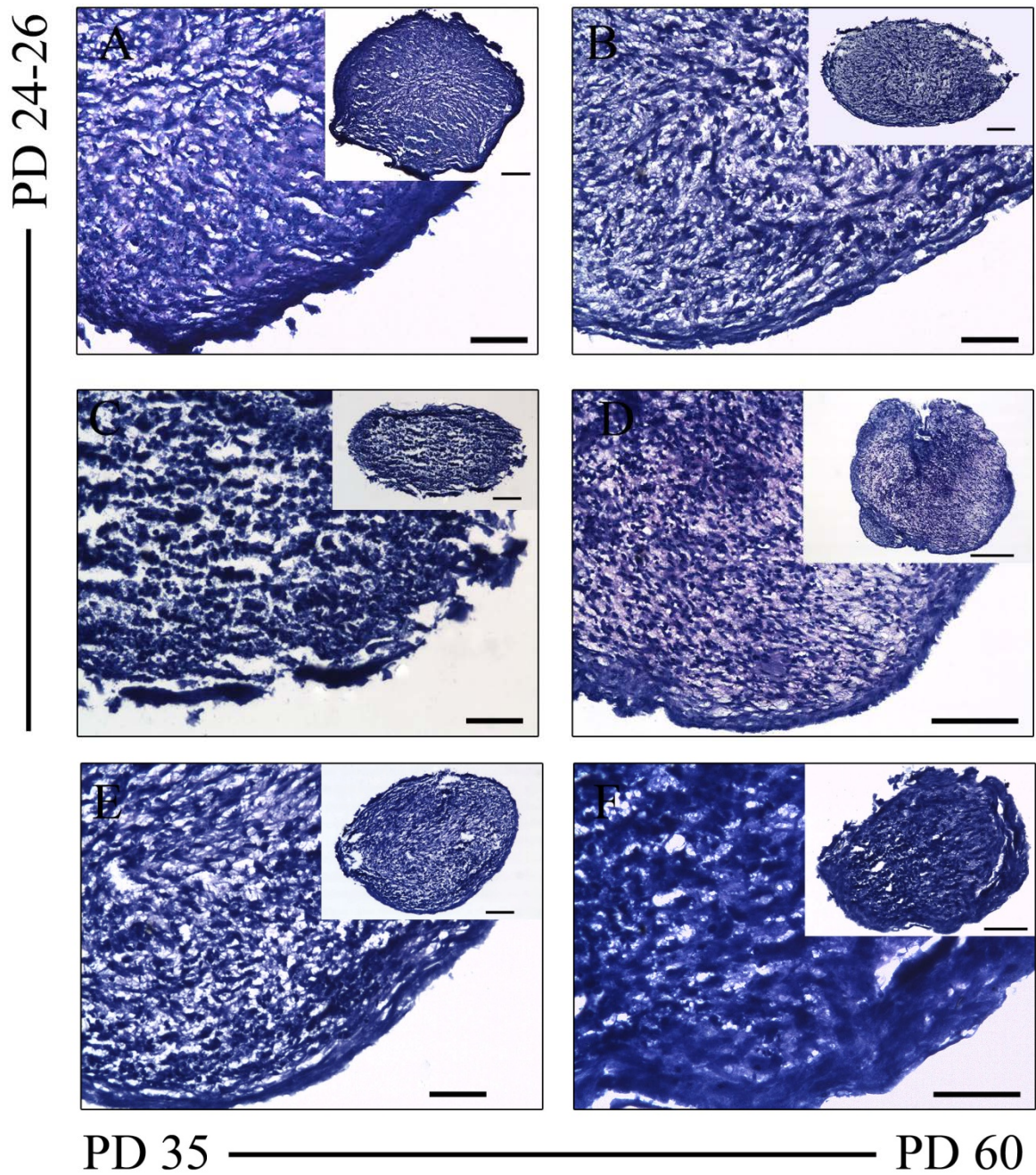
Figure 4.13. Photomicrographs of chondrogenic pellets stained with toluidine blue.

Varying amounts of GAG was observed in pellets from clonal cell lines derived from different patients at PD 24-26 (A-D). Detectable GAG was particularly evident around the periphery of the pellet. GAG was also evident in pellets formed after longer culture periods; at PD 35 (E) and PD 60 (F). Scale bars: A-F = 50µm (insert = 100µm).

PD 24-26

Figure 4.14. Collagen type II expression in chondrogenic pellets formed from chondroprogenitor cells isolated from osteoarthritic tibial plateaux.

Figure 4.14. Collagen type II expression in chondrogenic pellets formed from chondroprogenitor cells isolated from osteoarthritic tibial plateaux.

A-H: Pellets from cells expanded to PD 24-26. I-J: Pellets from cells expanded to PD 35. K-L: Pellets from cells expanded beyond 60PDs. Collagen type II labelling was evident throughout the sectioned tissue.

M-R: Pellets incubated for 3 (M+ P) or 6 (O+R) weeks. Collagen type II labelling evident in pellets at both time periods. In P/R there is an increase in intensity of the stain in the 6 week pellet.

Control pellets displayed on the right side (B, D, F, H, J, L, N, and Q). Scale bars: A-D = 150µm (insert = 300µm). E, G, I-K = 100µm (insert = 200µm). F, H, L = 200µm.

Figure 4.14. Collagen type II expression in chondrogenic pellets formed from chondroprogenitor cells isolated from osteoarthritic tibial plateaux.

Figure 4.15. Aggrecan (5C5) expression in chondrogenic pellets formed from chondroprogenitor cells isolated from osteoarthritic tibial plateaux.
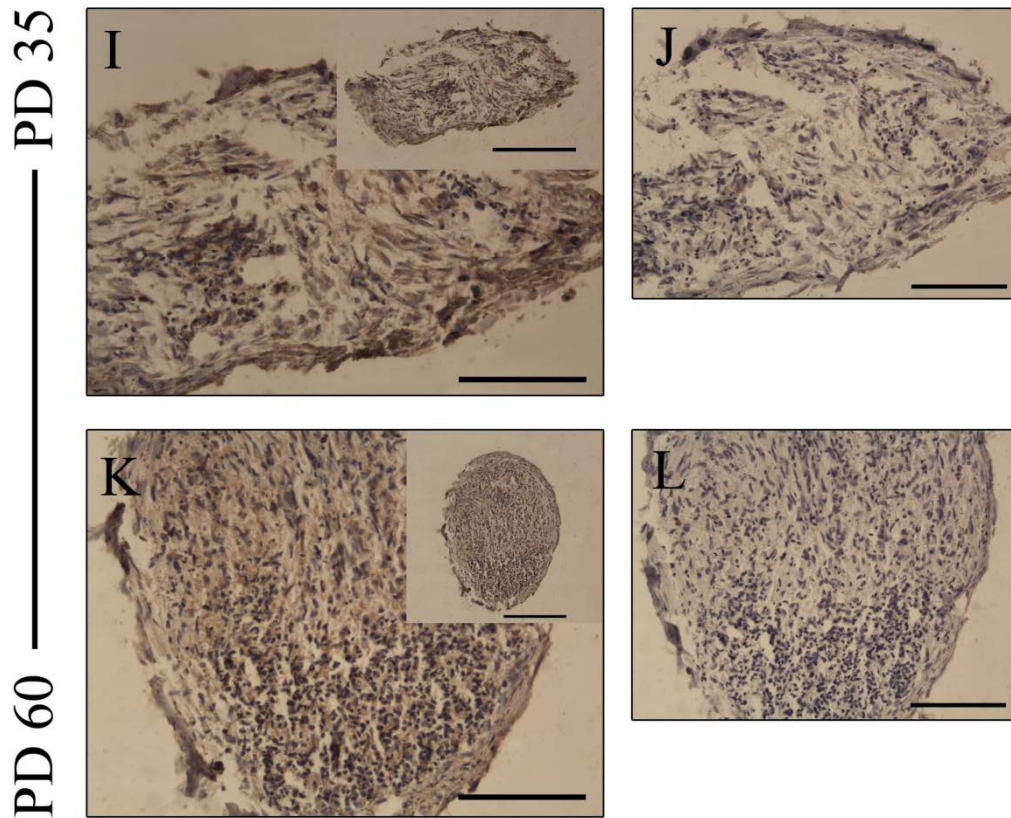
Figure 4.15. Aggrecan (5C5) expression in chondrogenic pellets formed from chondroprogenitor cells isolated from osteoarthritic tibial plateaux.

A-H: Pellets from cells expanded to PD 24-26. I-J: Pellets from cells expanded to PD 35. K-L: Pellets from cells expanded beyond 60PDs. Aggrecan labelling was evident throughout the sectioned pellets.

M-T: Pellets incubated for 3 (M+ Q) or 6 (O+S) weeks. Aggrecan was detected in pellets at both time periods. No consistent pattern relating to expression in relation to incubation time was observed.

Corresponding control pellets displayed on the right side (B, D, F, H, J, L, N, P, R and T). Scale bars: A-L = 100µm (insert = 200µm). M-T = 150µm (insert = 300µm).
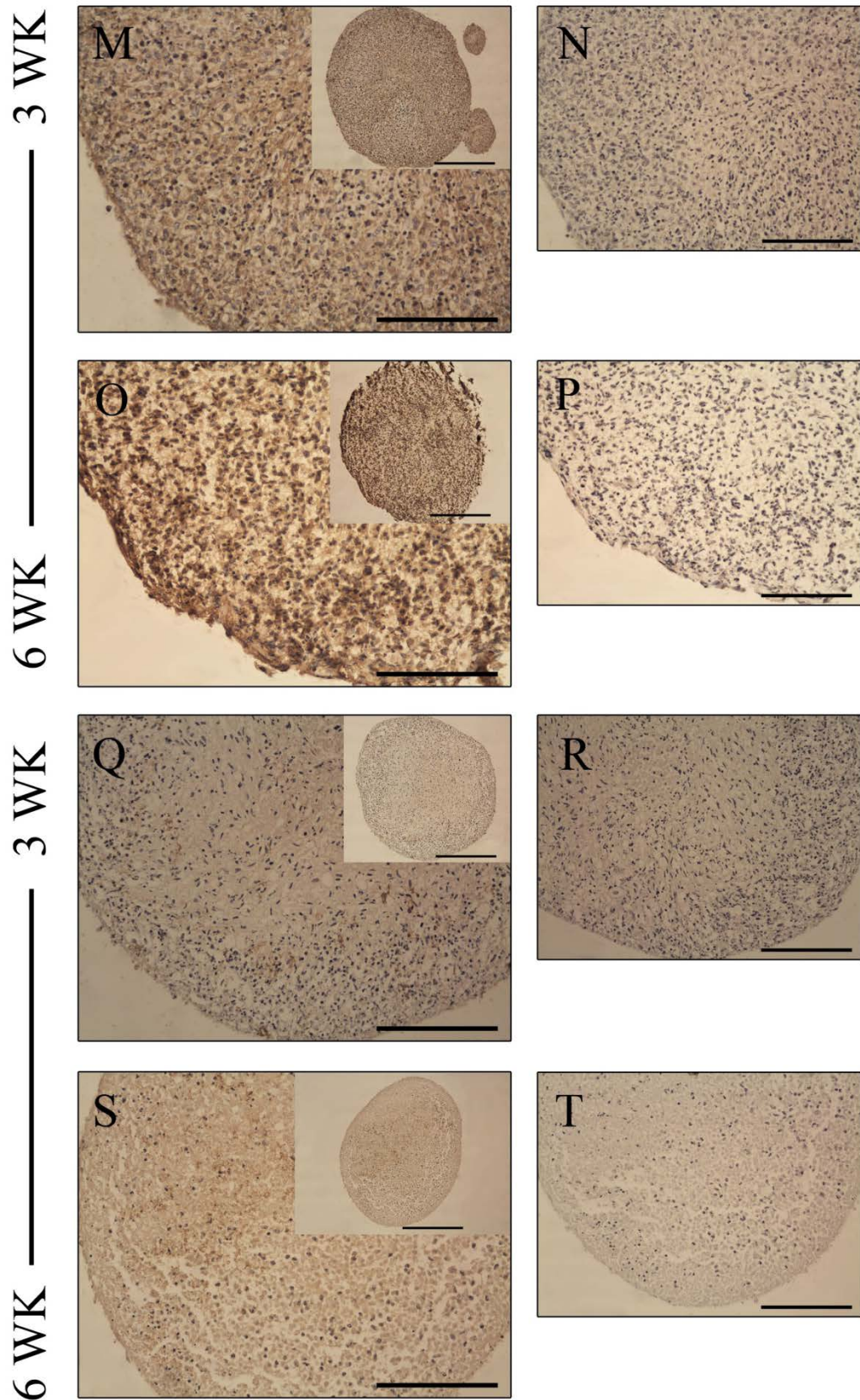
Figure 4.15. Aggrecan (5C5) expression in chondrogenic pellets formed from chondroprogenitor cells isolated from osteoarthritic tibial plateaux.

Figure 4.16. Collagen type I expression in chondrogenic pellets formed from chondroprogenitor cells isolated from osteoarthritic tibial plateaux.
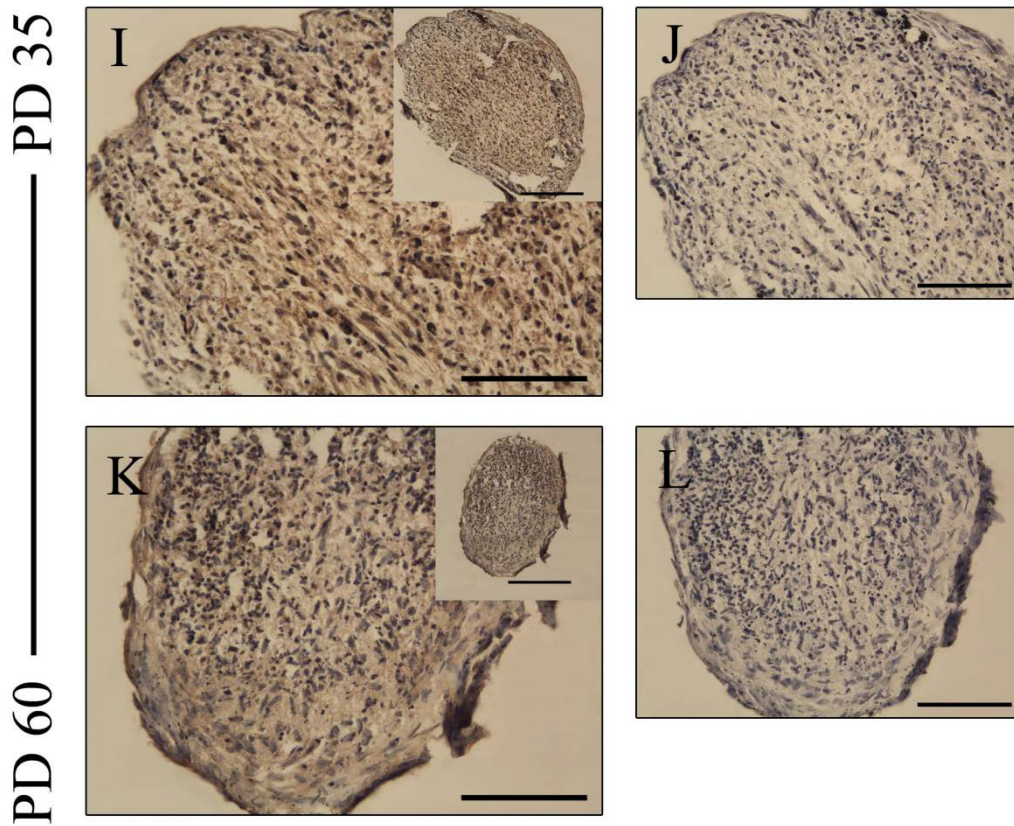
Figure 4.16. Collagen type I expression in chondrogenic pellets formed from chondroprogenitor cells isolated from osteoarthritic tibial plateaux.

A-H: Pellets from cells expanded to PD 24-26. I-J: Pellets from cells expanded to PD 35. K-L: Pellets from cells expanded beyond 60PDs. Collagen type I labelling was detected in all pellets.

M-S: Pellets incubated for 3 (M+ P) or 6 (O+R) weeks. Collagen type I labelling evident in pellets at both time periods.

Control pellets displayed on the right side (B, D, F, H, J, L, N, Q and S). Scale bars: A-D, I-L = 100µm (insert = 200µm). E-H, M-S =150µm (insert = 300µm).
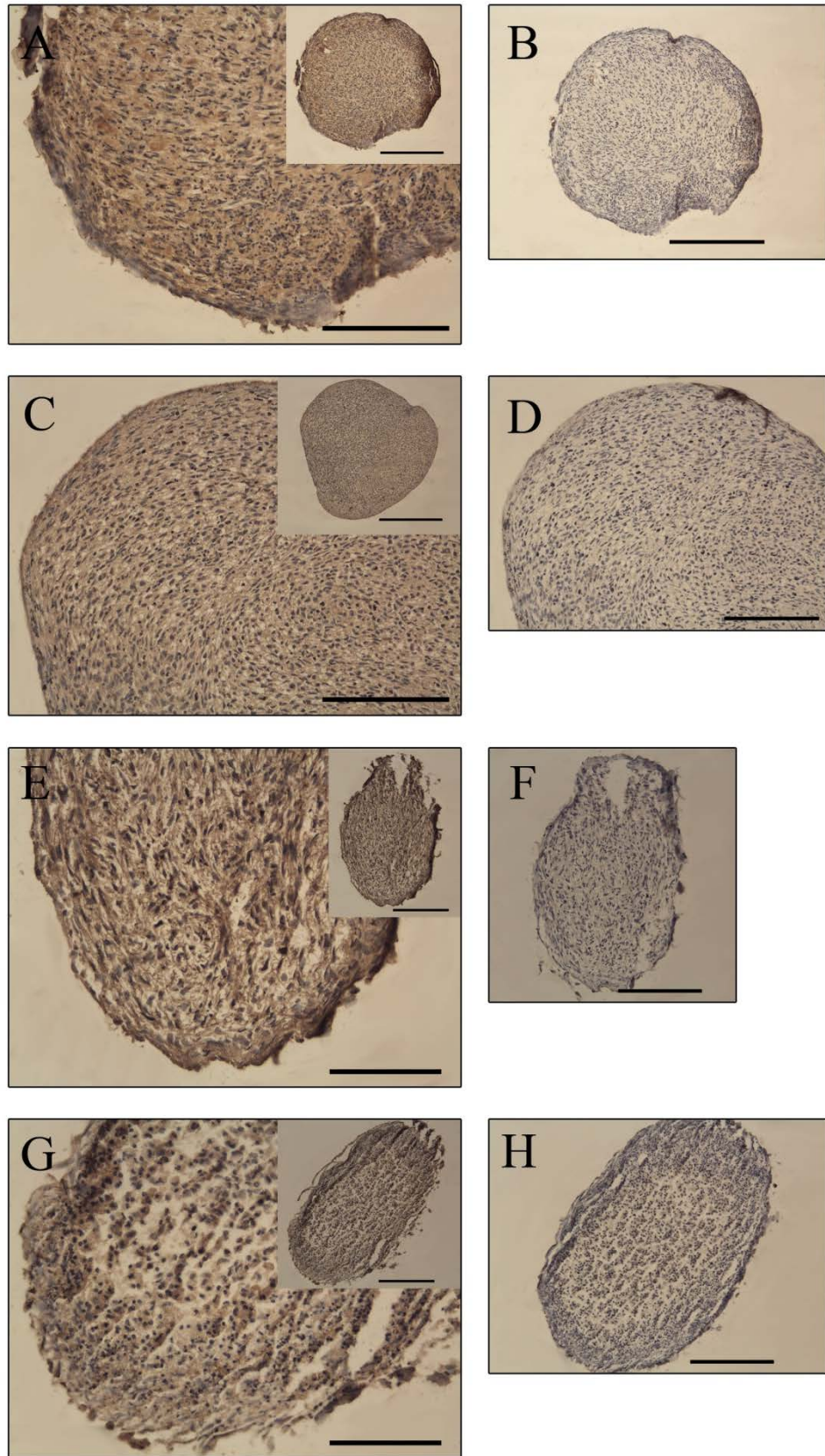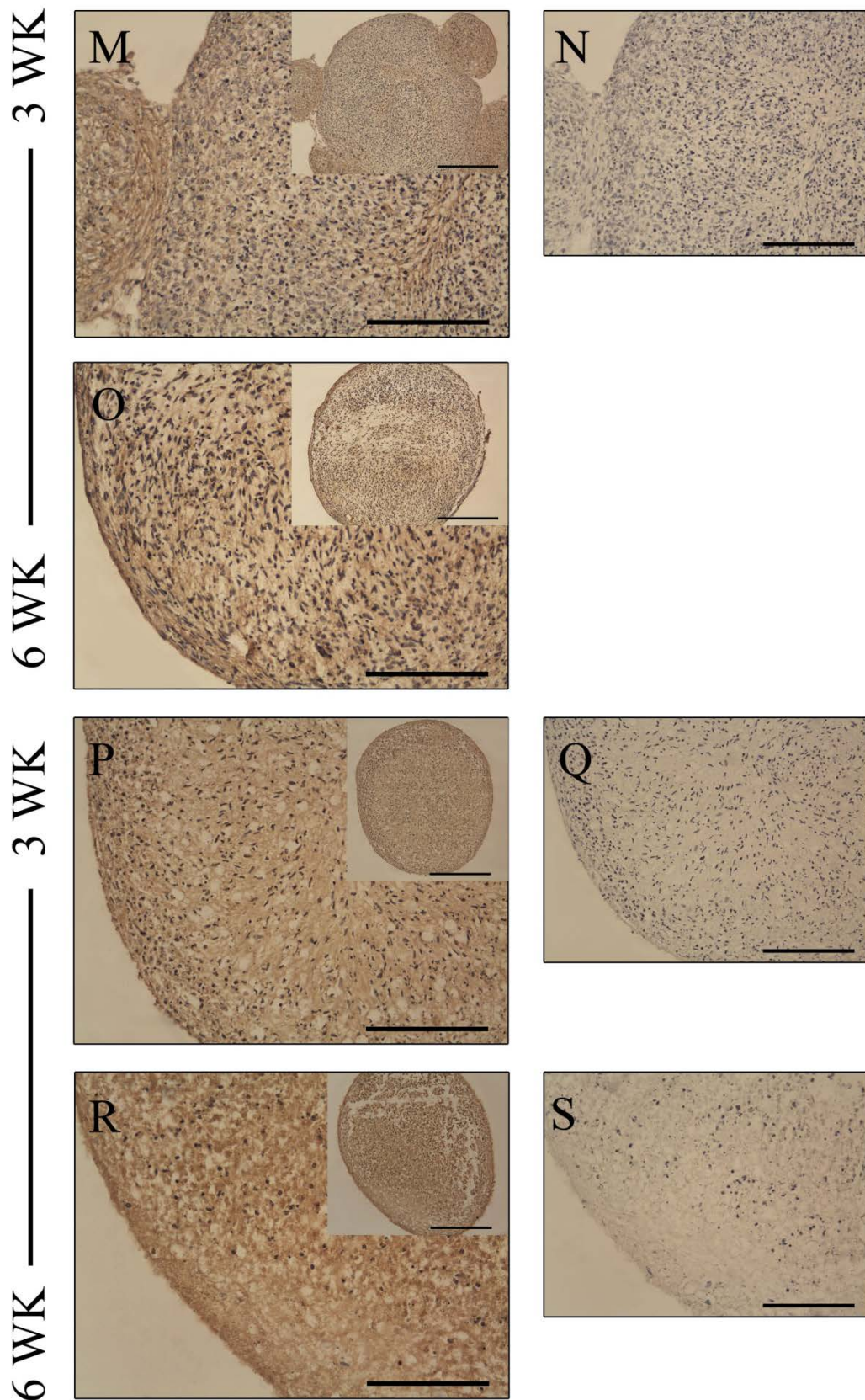
Figure 4.16. Collagen type I expression in chondrogenic pellets formed from chondroprogenitor cells isolated from osteoarthritic tibial plateaux.

Figure 4.17. Collagen type X expression in chondrogenic pellets formed from chondroprogenitor cells isolated from osteoarthritic tibial plateaux.
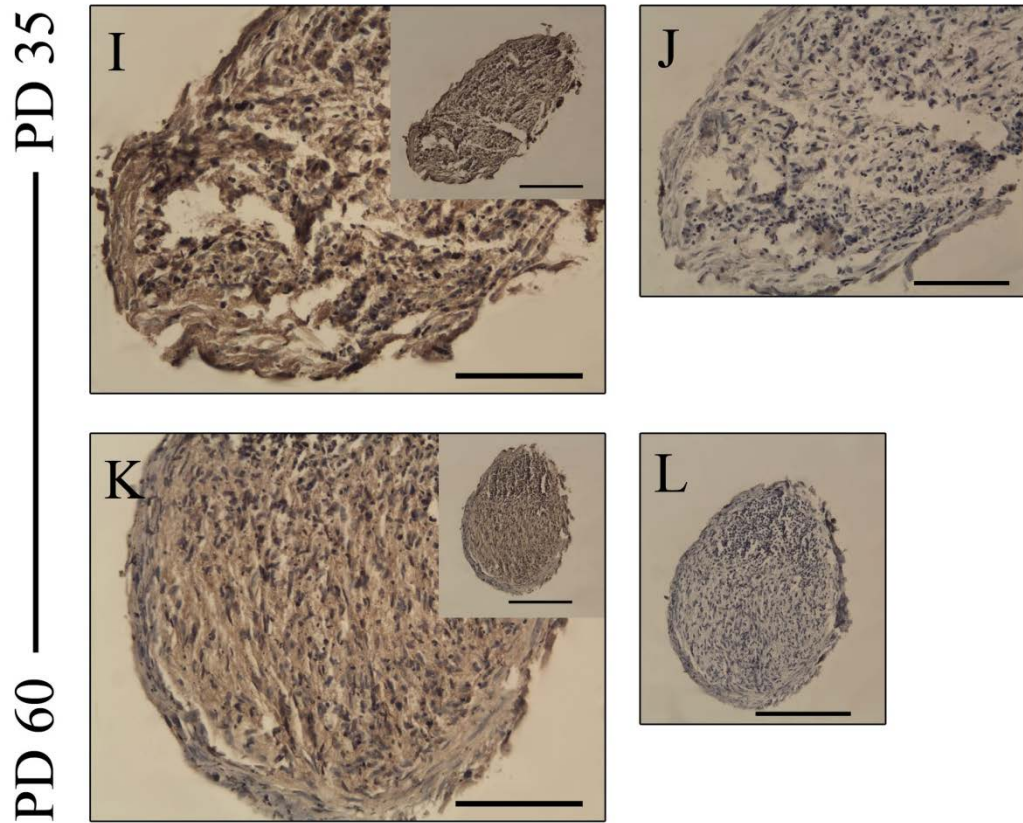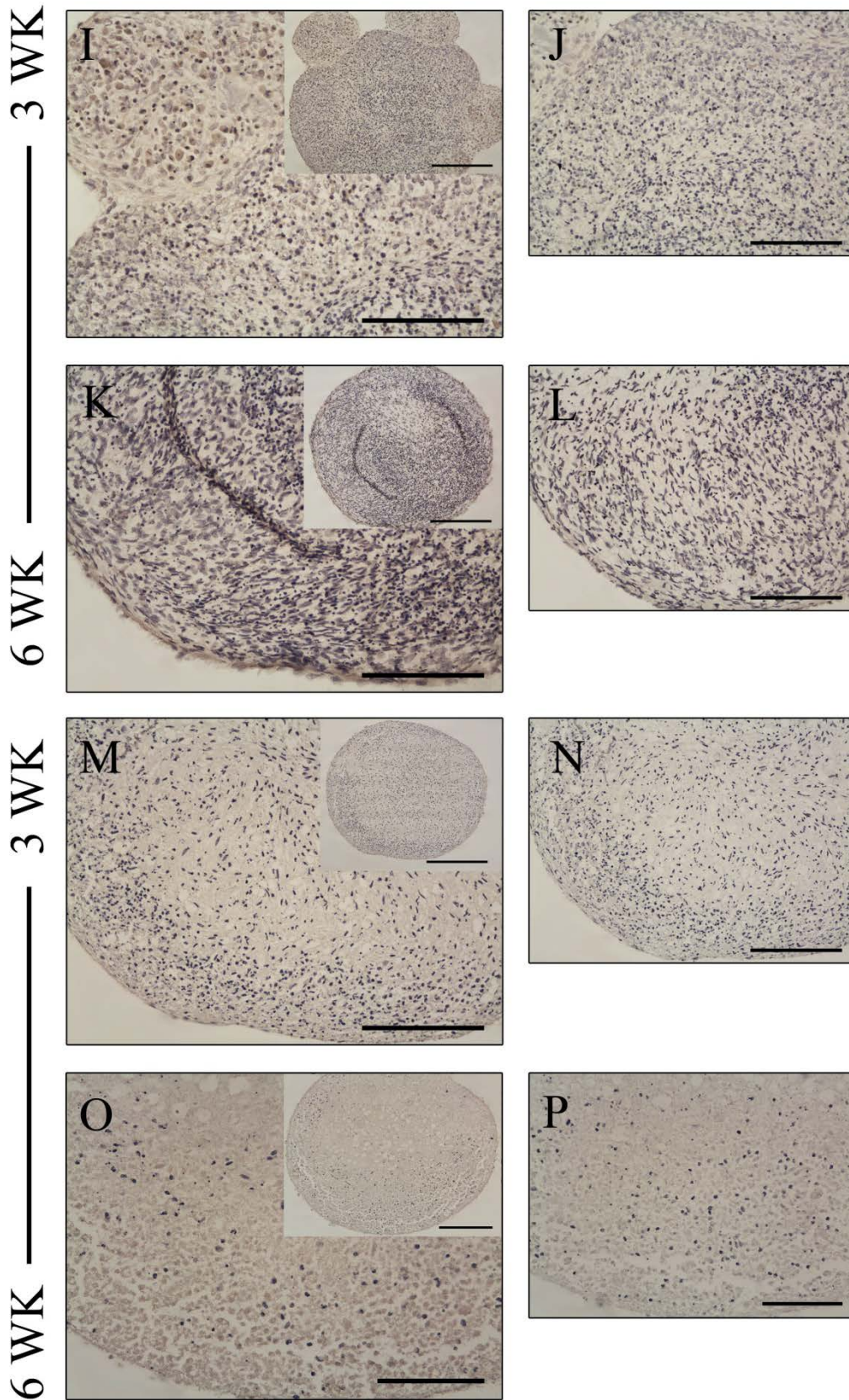
Figure 4.17. Collagen type X expression in chondrogenic pellets formed from chondroprogenitor cells isolated from osteoarthritic tibial plateaux.
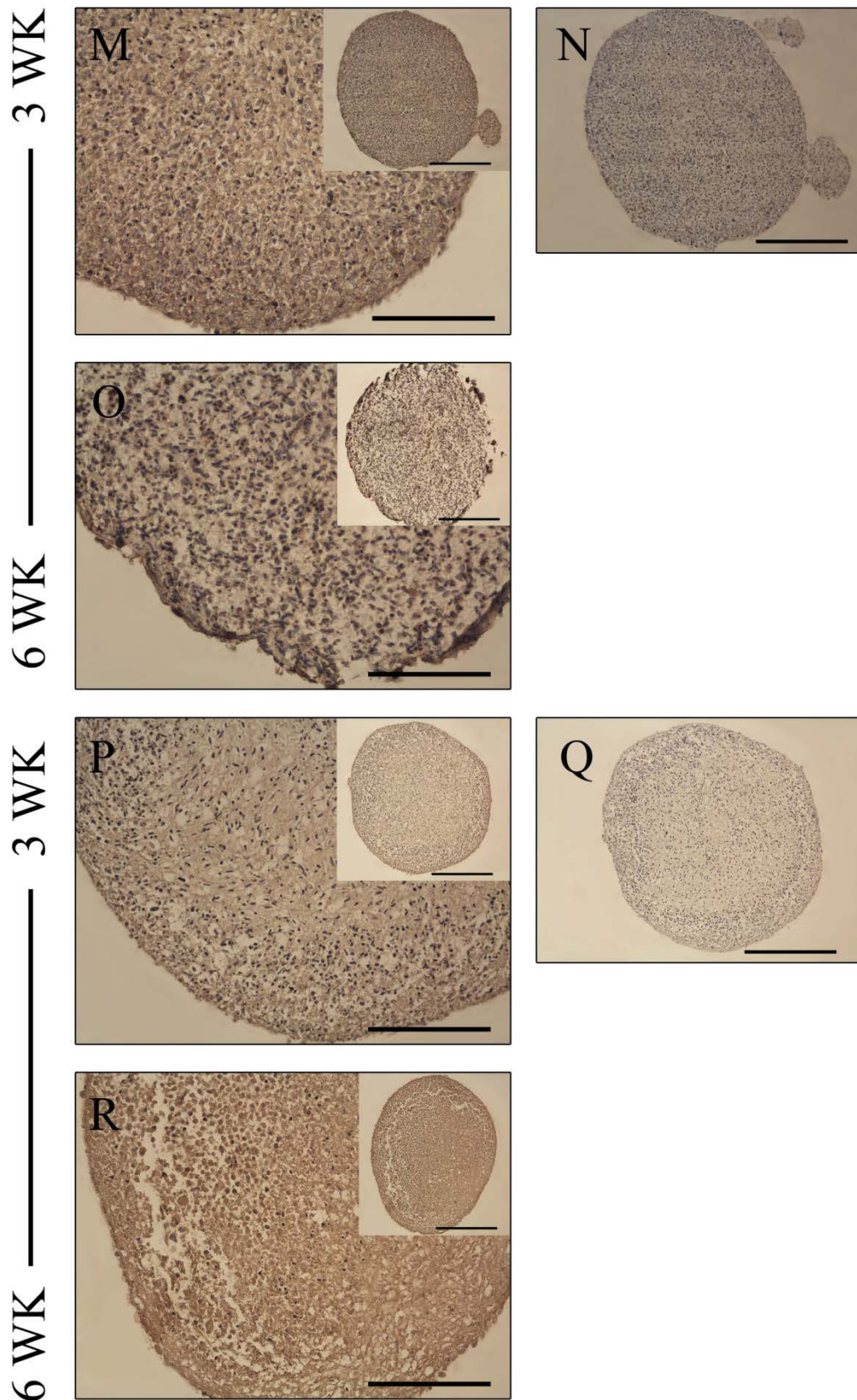
Figure 4.17. Collagen type X expression in chondrogenic pellets formed from chondroprogenitor cells isolated from osteoarthritic tibial plateaux.
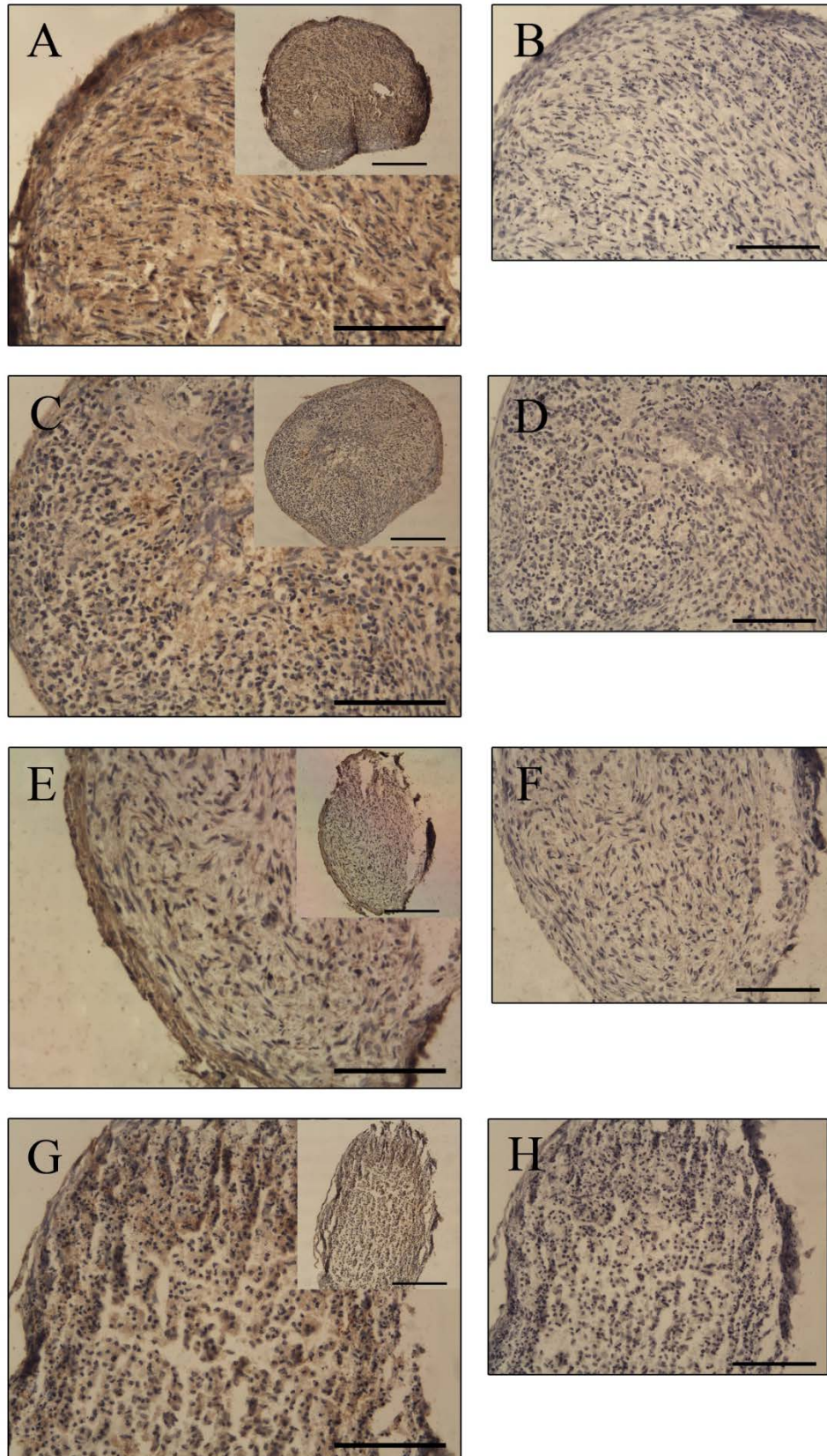
A-F: Pellets from cells expanded to PD 24-26. G-H: Pellets from cells expanded beyond 60PDs. Collagen type X labelling was not consistent between pellets. Pellet A displays positive labelling whereas no detectable collagen type X is seen in pellet E. No collagen type X was observed in the pellets formed following extended expansion (60+ PDs) in monolayer (G).

I-P: Pellets incubated for 3 (I + M) or 6 (K + O) weeks. No marked difference in collagen type X expression was observed between the different incubation times.

Control pellets displayed on the right side (B, D, F, H, J, L, N, and P). Scale bars: A – H, O - P =100µm (insert = 200µm). I - N =150µm (insert = 300µm).
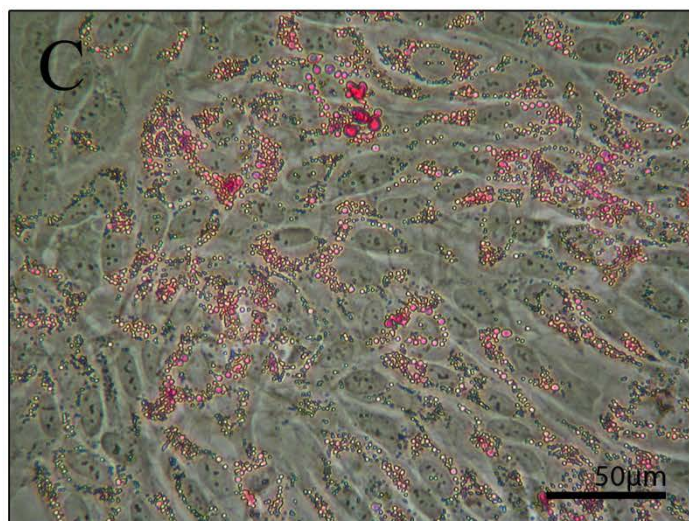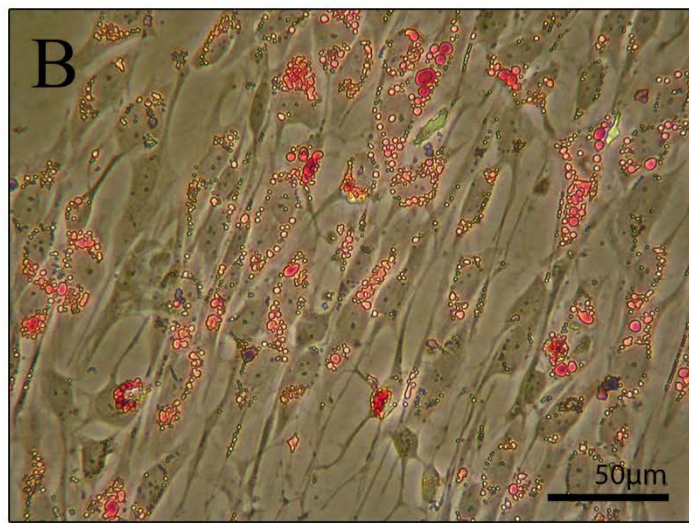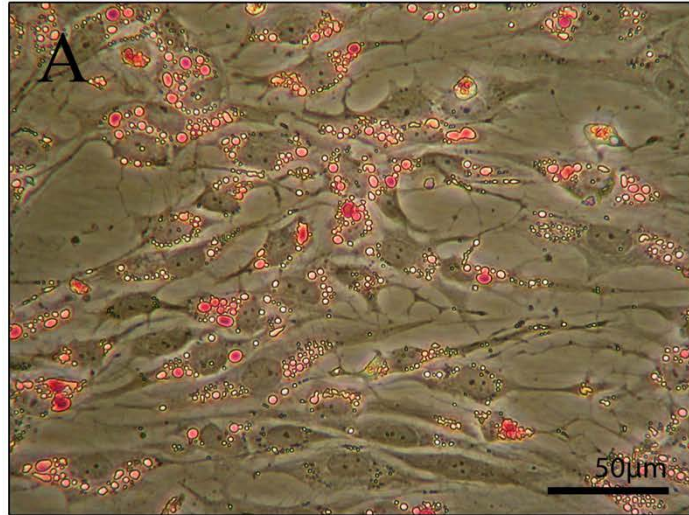
Figure 4.18. Photomicrographs of monolayer cultures following adipogenic induction in clonally-derived cell lines from several patients.

Cells were stained using oil red-O to highlight lipid vacuole formation.
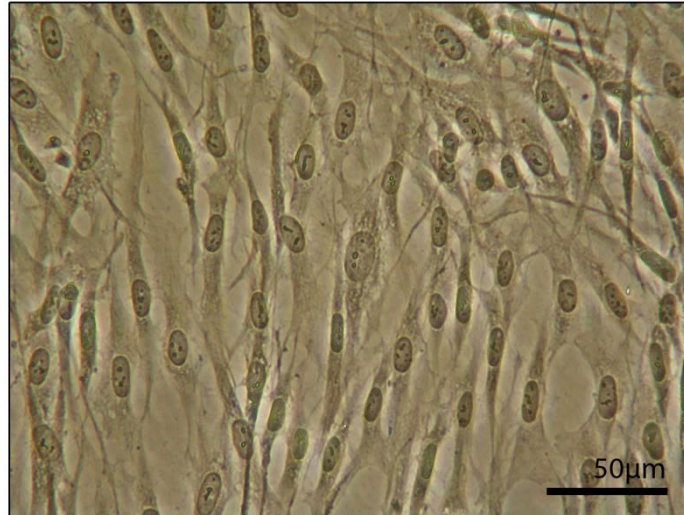
Figure 4.19. Photomicrograph of monolayer culture demonstrating comparative control following adipogenic induction.

Lipid formation is absent in chondroprogenitors when treated with oil red-O.
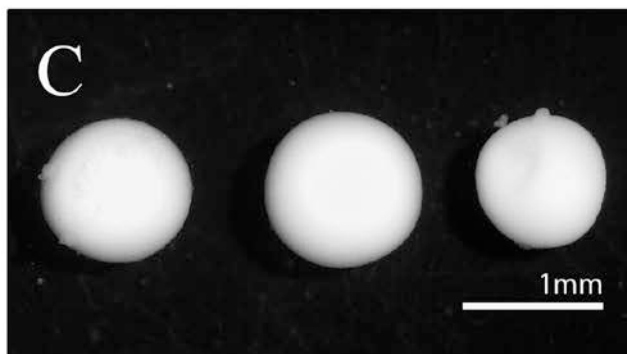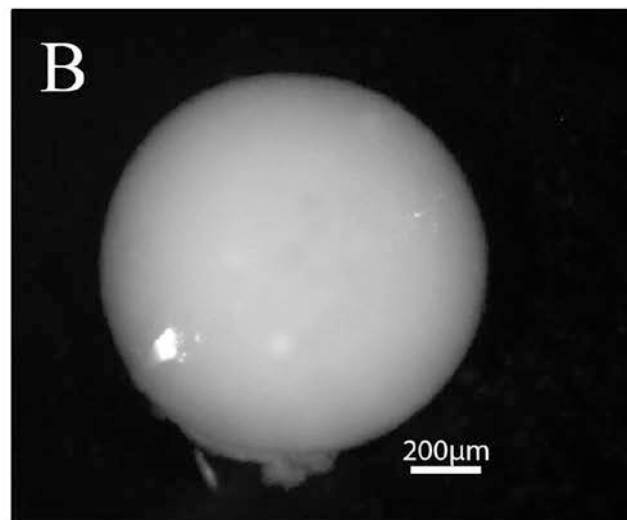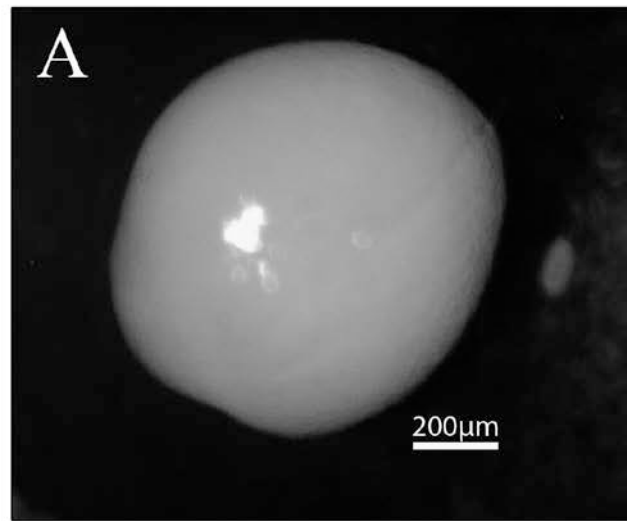
Figure 4.20. Photomicrograph of osteogenic pellets from clonally derived cell lines from different patients (A-C).

Gross morphology of the pellets showed a smooth white surface similar to chondrogenic pellets previously displayed. Variation was found in pellet size from different clonal cell lines and patients however, consistency in size was seen within replicates from a particular cell line (C).
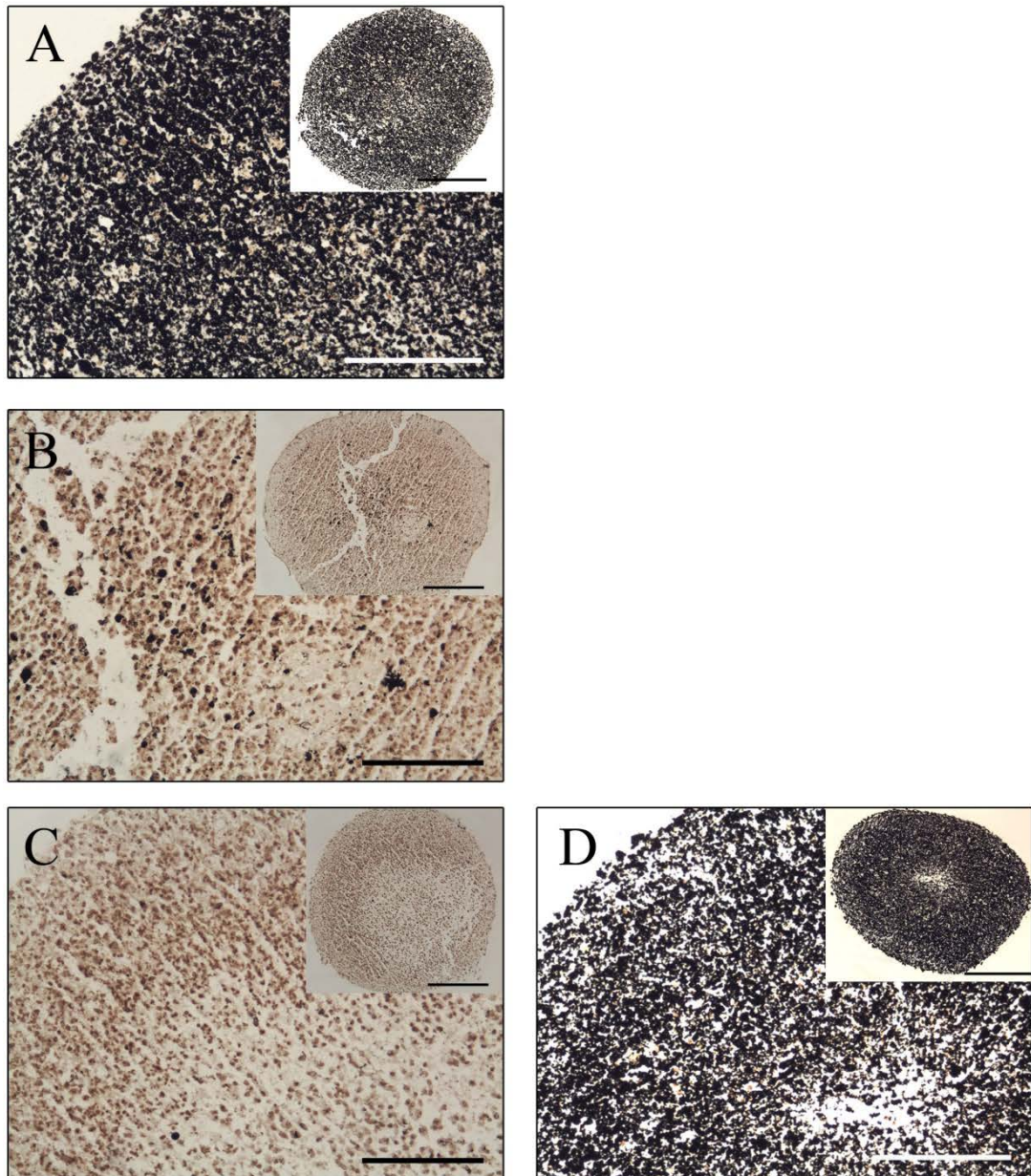
Figure 4.21. Photomicrographs of sectioned osteogenic pellets stained using the von Kossa technique for mineral deposits.

Great variation was found between pellets from different cell lines; in certain pellets (represented by A) strong positive labelling was detected throughout the pellet, in other pellets (B) evidence of mineral deposits were detected particularly in the core of the pellet; and there was a third category of pellets which demonstrated no sign of mineral deposition (C), following a 3-week incubation period. The experiment was repeated where pellets were incubated for 6 weeks to test whether changes observed were time dependent. Image D is from the same cell line as image C- after 3 weeks no mineral deposition was detected, however, after 6 weeks mineral deposition was abundant. This result however was not consistent and in some cases no difference in deposition could be detected. Scale bars: A & D = 150μm (insert = 300μm), B-C = 100μm (insert = 200μm).
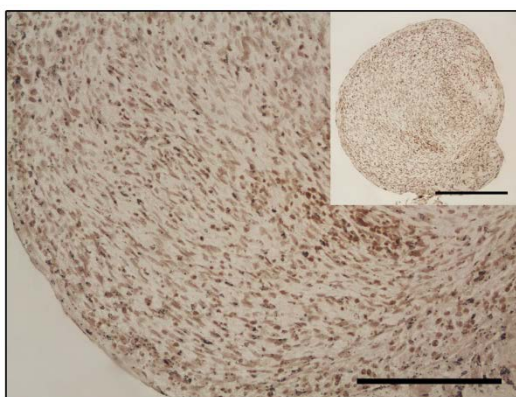
Figure 4.22. Photomicrograph of a sectioned pellet representing a comparative control following von Kossa staining.

No positive labelling was detected signifying no detectable mineral deposits in control pellets. Scale bar: 150µm (insert = 300µm).
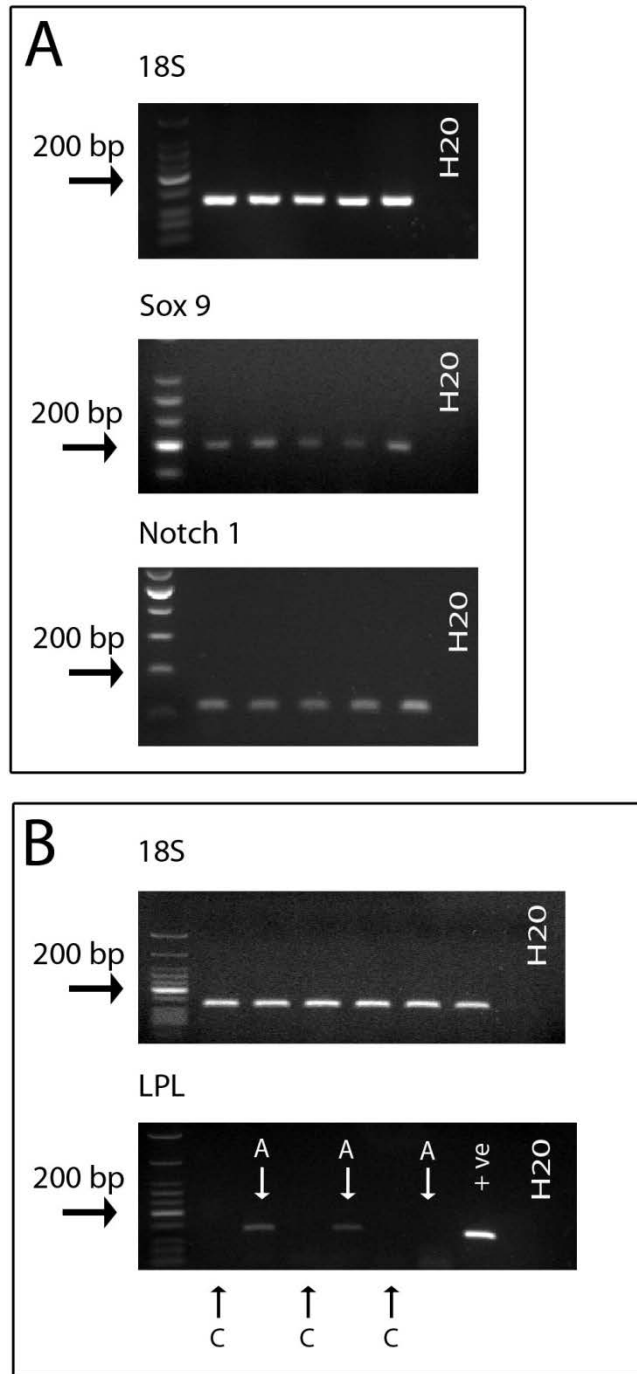
Figure 4.23. Expression of sox 9, notch 1, LPL and 18S genes were investigated by RT-PCR following multi-lineage induction of chondroprogenitor cells.

Chondrogenic pellets expressed sox 9 and notch 1 genes (A) and adipogenic cultures expressed LPL (B). A = adipogenic cultures & C = comparative controls.

4.5. Discussion

The presence of articular cartilage stem/progenitor cells is now a concept that has become increasingly accepted with various research groups reporting on their occurrence (Alsalameh et al., 2004a, Dowthwaite et al., 2004a, Khan et al., 2009a, Koelling et al., 2009a, McCarthy et al., 2011a, Pretzel et al., 2011, Williams et al., 2010a). Previous work from our laboratory has demonstrated in normal bovine, equine and human tissue that these cells can be isolated and expanded in culture whilst retaining their cartilage-specific characteristics *in vitro* in permissive conditions. Other research groups have identified tissue-specific progenitor cells using other methods of identification including CD markers and migratory capacities; and using these, investigators have also demonstrated the existence of progenitor cells in normal and diseased, osteoarthritic tissue.

Within this study we have demonstrated for the first time the presence of a progenitor cell population isolated from human osteoarthritic cartilage using the Jones & Watt/Dowthwaite method that relies specifically on α5β1 integrin interactions within a twenty minute timeframe.

Colonies of cells formed from single cells. However, there was great variation seen in the time taken for the colonies to appear, in the density of colonies and in the morphology of the cells within the colonies. The reason for these discrepancies remains unknown and it was not possible to assess whether or not these early differences had implications on the cultures at later stages of expansion. Of the initially seeded cells that formed colonies of over 32 cells, three different categories were observed. There was i) a group which initially surpassed 32 cells and then almost immediately stopped proliferating, ii) a cohort of cells that reached the region of 25-30 population doublings, and iii) a group which could be cultured beyond 30 population doublings; in one case reaching up to 60 population doublings. Colonies selected for expansion were picked at random and therefore, it is possible that disparities in results could stem back to these early differences in colony morphology and it would be interesting to pursue this finding further as it may have major implications on the potential of the cells used for regenerative purposes. In a recent paper by Pevsner-Fischer et al., (2011), the author discusses the possibility that "long-term culture of MSCs leads to the selection of specific clones overtaking the culture. Since

MSCs may be a priori heterogeneous, functionally divergent MSC cultures could simply be an outcome of specific culture conditions that select particular type of MSCs". This is a view that raises the point of certain cells taking over others within long term culture, a reasonable rationale, however the differences in this case were not a result of culture conditions as all cells were isolated and expanded in culture in the exact same conditions.

Only 52% of the cell lines cultured reached 30 PDs, a substantial figure implying that approximately half of the chondroprogenitors isolated have the capacity to be cultured long term. It was also interesting to observe the varied proliferation rates following the initial exponential phase. Some cell lines slowed down, some remained constant, and intriguingly others sped-up upon reaching the 30 PD mark. Again these differences highlight a discrepancy in the cells isolated suggesting that despite the constant $\alpha5\beta1$ integrin interactions, there is heterogeneity within this cell population.

Understanding the proliferation mechanisms of chondroprogenitors is an issue that has been addressed by Martin et al., (2005) who state that optimal proliferation rates of chondroprogenitor cells are achieved in the presence of 40% fetal bovine serum. However, this high percentage of serum results in a high level of 'unknown' combinations of substances acting on the cells; an issue that would be raised if this method was taken into clinical trials. Despite the acceptance of an issue in understanding the proliferation mechanisms, this paper does not address the issue of 'failed cell lines' which was encountered within this particular study.

As a result of the differences in proliferation rates, the number of days taken for the cells to reach 30 (and 40) PDs varied significantly between patients. Due to the fact that the number of successful cell lines cultured could not be pre-determined, it was not possible to analyse clonal variation within patients. Evidently there were patients in which only one cell line reached 30 PDs and in a different patient four clonal cell lines reached 30 PDs. It is difficult to state at this point whether the difference was based on the patient and the viability of the cells within patients, or if it was a case of random selection that led to more viable cells being picked by coincidence and vice-versa. The trend that was observed however (which does not take into consideration the 'failed' cell lines) is that clonal cell lines from the same patient appear to proliferate at similar rates. An explanation for this

could be that there are different cohorts of cells within osteoarthritic tissue, and as such the 'high proliferating' cohort behave in a similar way to each other, yet differently to the cohort of cells which are less viable. Understanding the differences between these cohorts of cells is essential as it will highly impact cell selection criteria when using them for reparative purposes.

Indeed, heterogeneity of resident cells in articular cartilage has been documented; Kouri et al., (1996) described three different cell types inhabiting osteoarthritic cartilage specifically. Using ultra-structural studies, the authors identified i) type 1 cells which are single or clustered chondrocyte-like cells, ii) elongated secretory cells termed type 2 cells and iii) type 3 cells which are irregularly shaped cells undergoing degeneration. It is important at this stage to highlight that results from Dowthwaite et al, (1994), Williams et al., (2010) and McCarthy et al., (2011) papers specifically targeted progenitor cells residing in the surface zone of articular cartilage in the respective different species. As such, it is likely that the digested cells used in those studies contained a more uniform, homogeneous population of cells. In the osteoarthritic tissue used for this study, the topographical morphology of the tibial plateaux was so varied; certain regions were eroded to the bone, others were extensively fibrillated and other areas appeared morphologically 'normal'. As such, the typical surface zone seen in healthy articular cartilage was predominantly absent and as a result, any/all of the remaining cartilage was used in the tissue digestion for cell isolation. Undoubtedly, this 'mixed bag' of heterogeneic cells contributed to the inconsistent outcomes encountered throughout this study.

Pellet cultures were established using the clonally derived cell lines isolated and expanded from osteoarthritic tibial plateaux. Morphologically, the pellets were consistent in terms of outer appearance; displaying a smooth, iridescently white surface. The size of pellets from different cell lines was variable. Histologically, the cells within the 3D pellets displayed a more rounded phenotype, characteristic of articular cartilage *in situ*. This is positive following de-differentiation that occurs when culturing cells in monolayer (Schnabel et al., 2002). The pellets consistently formed an outer fibrous layer with fibres running parallel to the pellet periphery. This region bears great resemblance to capsule-like perichondrium which is usually devoid in articular cartilage due to the presence of the protective synovial membrane. Perichondrium is typically a region containing flat and tangentially aligned

chondrocytes, with a higher cell density than deeper regions that is actively involved in developmental stages (Morris, 2002). As such, as these cells have been extracted from their original protected niche, it is understandable that the pellets form this protective outer layer.

The extent to which the cells have the capacity to recapitulate normal articular cartilage was investigated using immunohistochemistry to detect protein expression of specific cartilage ECM components, as well as general stains to demonstrate the level of sulphated GAG production within the matrix. Safranin O and toluidine blue staining demonstrated the presence of sulphated GAGs, particularly around the outer fibrous region of the pellets which, as stated, is congruous to the higher cell densities in this area. Within the central cores of the pellets, there was great variability between the level of GAG deposition of pellets processed at the same PDs, which again highlights inter-population heterogeneity. Both stains were highly detected in the pellets which where chondrogenically induced past 60 PDs. This was an interesting result as it has been suggested in the literature that long term expansion of MSCs in culture results in a decreased ability to differentiate into mesodermal lineages (Digirolamo et al., 1999).

The presence of sulphated GAG alone however, is not enough to state that cells are producing a cartilaginous matrix and as such it is imperative to refer to the immunohistochemistry results. Collagen type II and aggrecan (5C5) labelling was evident in all the chondrogenic pellets regardless of the stage at which the pellet was formed. Having said that, in some pellets the staining was more sparse than in others and as such, variability was present regardless of time in culture or point of pellet formation. This finding again emphasises the heterogeneity which was encountered throughout this study. Combined, these results supply evidence that chondroprogenitor cells excised from osteoarthritic tissue do have the potential to produce a cartilage-like, hyaline matrix rich in GAGs, aggrecan and collagen type II. However, it is also apparent that within the cohort of cells selected using the fibronectin adhesion assay, there are certain cells which respond more positively than others.

Collagen type I was also detected in all of the pellets assessed. In some cases the labelling was restricted to the core, in other instances labelling was heightened around the periphery

and in other pellets, labelling was uniform throughout; demonstrating the inconsistent nature of the labelling observed. Interestingly, there are two approaches which could be seen with regards to collagen type I expression. During growth of the musculoskeletal system, type I collagen expression precedes collagen type II expression at the growth plate during endochondral ossification (Leboy et al., 1988) and so the presence of type I collagen may represent the anlagen phase of the mature tissue. Conversely, type I collagen is present in fibrocartilagenous repair tissues which provide a surface insufficient for weight bearing (Roberts et al., 2009). It is difficult at this point to elucidate which of the two scenarios is occurring as collagen type II was also present deploying a hyaline like resemblance, however, in the 6 week pellet cultures there was no marked reduction in type I collagen synthesis suggesting its continued production, rather than an initiator of type II collagen synthesis.

The ambiguous nature of type X collagen expression found in the pellets further reinforces the heterogeneous nature of the tissue in question. The presence of type X collagen is suggestive of differentiation into terminally differentiated chondrocytes and, in some cases, the formation of a hypertrophic cartilage. This is a renowned phase of endochondral ossification in which the cartilaginous anlagen is transformed into bone (reviewed by Shen, 2005). It is a common phenomenon, as demonstrated by McCarthy et al., (2011) that bone marrow derived stromal cells have the tendency to not only produce a matrix rich in cartilaginous macromolecules following chondrogenic induction; but to also display consistent type X collagen labelling within the matrix; ultimately resulting in the resounding possibility that the tissue may have the tendency to terminally differentiate and calcify. McCarthy et al., (2011) suggested that chondroprogenitors isolated using the fibronectin adhesion assay (as per Dowthwaite et al., (2004)) were superior to conventional bone marrow derived stromal cells due to their lack of type X collagen expression in pellet cultures and therefore their reinstated hyaline cartilage phenotype. It is important to note, however, as previously mentioned that this study used only surface zone cells and therefore, the population of cells initially digested from the tissue was more homogeneous when compared to the range of cells residing in any remaining osteoarthritic cartilage on diseased tibial plateaux. This difference may explain the discrepancy between the solid findings observed in the McCarthy et al., (2011) study compared to the current study. As such, in accordance with McCarthy et al., (2011) it may therefore be suggested

that within the osteoarthritic tibial plateau, there are chondroprogenitor cells with the capacity to regenerate hyaline whilst being devoid of the endochondral fate of terminal differentiation.

Heterogeneity of MSCs is an issue that has been raised many times, and a recent review by Pevsner-Fischer et al., (2011) considers many of the issues surrounding the topic. Questions that are broached in this review include "(1) Does the *in vitro* observed variability reflect the existence of MSC subsets *in vivo*? (2) What is the molecular basis of the *in vitro* observed heterogeneity? and (3) What is the biological significance of this variability?". All of these questions are directly relevant to the results of this chapter in establishing at what point the heterogeneity occurred and what the significance is to this particular population of cells with regards to reparative strategies.

The ability for the chondroprogenitors to produce multi-lineage progeny was examined as the cells were induced into adipogenic and osteogenic lineages. Despite the variation seen in the chondrogenic pellets, results were promising as all cell lines tested produced lipid vacuoles in monolayer cultures, and LPL gene expression was positive following adipogenic induction. Osteogenic progeny was however less affirmative and more variable. Upon von Kossa staining, evidence of mineralisation was heavily detected in some pellets, and absent in other pellets. It was apparent that in certain cases time was a factor as in one particular cell line, no mineralisation was detected after 3 weeks, however, deposits were abundant after 6 weeks. As such, the variable results may be a result of several reasons; a) particular cell lines could (or could not) be osteogenically induced and b) particular cell lines may have the ability to mineralise however the process may be delayed compared to the rate in other cell lines. Again, the fact that some cell lines were able to produce a positive von Kossa stain and others weren't, highlights the heterogeneity within the cells obtained from osteoarthritic tissue; suggesting that there may be some chondroprogenitors which are more 'viable' than others when assessing their MSC characteristics. Indeed, Pittenger et al., (1999) reported heterogeneity within multi-lineage capacities of expanded colonies of cells isolated from bone marrow, which led to the distinction between mesenchymal stem cells and progenitor cells. The former had the capacity for tri-lineage differentiation whereas the latter displayed limited differentiation potentials. As such, it is possible that further classification of cells isolated using the

fibronectin adhesion assay is necessary to allow the most appropriate cohort of cells to be expanded for use within regenerative medicine.

Interestingly, Pevsner-Fischer et al., (2011) discuss in their review that generally calling mesenchymal stem cells 'multipotent stem cells' does not actually reflect their true nature, in that there are not only inter-population heterogeneities, but also intra-population heterogeneities; both of which were observed in this study. A study carried out by Digirolamo et al., (1999) led to the suggestion that "even when derived from a single cell, the progeny of MSCs can be conditioned to behave differently". Differences observed in this study may stem back to the point at which colonies were forming as seeding densities can affect cell morphologies and, to date, it is not known how these differences relate to cell functions and what they may signify. As such, the initial growth rates of the colonies and thus their proximity to other cells may therefore have been an influencing factor leading to heterogeneity within the expanded cell lines.

As briefly mentioned previously, heterogeneity within the chondroprogenitors isolated from osteoarthritic tibial plateaux may be a secondary result of extended *ex vivo* culturing in monolayer, due to *in vivo* heterogeneity of variable phenotypes reflecting the natural repertoire of MSCs, or due to the detachment of the cells from their *in vivo* niche (Pevsner-Fischer et al., 2011), which can result in partial differentiation consequently harvesting a heterogeneous mixture of cells (Wagner et al., 2010). Within diseased tissue particularly, as a result of tissue degradation and inflammation, it is possible that progenitor cells are actively involved in different functions and/or aspects of maintenance and repair and therefore heterogeneity of cells within the tissue may allow for appropriate selection of specific cell 'types' for different functions. "By contrast, homogeneous and rigid populations could be counterproductive under strong demand for tissue repair and immunomodulation" (Pevsner-Fischer et al., 2011). As such, it was proposed that the mixed populations may reflect the varied functions necessary to regulate tissue homeostasis and drive tissue repair, providing a possible explanation to the variation seen in results within this study.

Methods used in this chapter relied heavily on surface markers as a means of identification to distinguish between chondroprogenitor cells and mature chondrocytes. It is important to

mention the stability of these markers following the digestion process. Unpublished work from our laboratory has demonstrated that cells isolated from bovine cartilage display altered characteristics depending on how long after the digestion process they are used. It would therefore also be interesting to investigate whether or not a time dependent difference could be observed following the digestion process in chondroprogenitors isolated from OA cartilage.

Despite the heterogeneity and variation observed, the method of chondroprogenitor cell isolation used in this study in relation to other methods currently used, provides a cohort of cells that are specifically targeted based on their integrin receptor interactions. Therefore, despite a distinctive selection process occurring, varying cohorts of cells remain in which there may be one or more cell types that develop into the progenitor phenotype. Conversely, other methods of progenitor cell isolation used, for example, the Koelling method relies purely on cells migrating from explants cultured *in vitro* (Koelling et al., 2009a). This phenomenon is not only a common occurrence in many different tissues and so should arguably be treated cautiously as a mechanism for isolating 'progenitor' cells, but also inevitably contains a greater selection of various cells with unknown, undisclosed phenotypes.

The method used by Alsalameh et al., to identify progenitor cells relies on the presence of CD105+/166+ cells (Alsalameh et al., 2004a). However, as previously mentioned there has been contradicting data published with regard to these markers in normal and osteoarthritic cartilage, suggesting that further work would need to be carried out before this method became widely accepted (Grogan et al., 2009).

As such, with the rapid advancements and developments in this area of study, the need for a single and accepted method of isolation is essential to allow for further consistency and comparability to results across the board, enabling the issue of heterogeneity to be addressed. Indeed it would be beneficial to decipher the differences between the clonal cell lines and gain a greater understanding in the heterogeneity so that a sound understanding in the mechanisms of cells interactions are known before they are used for reparative techniques.

To further the work described in this chapter, it would be valuable to compare the same tissue used for scoring to the *in vitro* chondroprogenitor cell analysis. This would provide an insight into the reparative potential of OA tissue at specific stages of disease severity. This could provide an indication of whether the cells that adhere to the fibronectin during the adhesion assay all reside in less severely affected tissue, or whether these cells are equally or in fact more abundant in regions of tissue that are more highly affected by the disease. The limiting factor here however is cell numbers, as it may not be possible to digest sufficient cells for *in vitro* culturing from small sections of OA tissue.

Looking forward, it would also be beneficial to seek quantitative molecular approaches to establish any correlations between OA severity and the chondroprogenitor cell profile. These could include quantitative PCR or more simply western blotting, as a means of providing more weight to the qualitative results obtained in this chapter.

As a result of the limitations of the cohort size, differences in age and sex of the patient from which tissue was excised was only briefly touched upon. It would be interesting, given a larger cohort to further investigate the effects of age, sex and anatomical location on the characterisation of chondroprogenitors. Similarly, it would be useful to correlate factors such as pain levels and history of disease progression to see whether these are also contributing factors.

Despite work having previously been carried out in normal human and bovine tissue looking into the differences between chondrocytes and chondroprogenitor cells (Dowthwaite et al., 2004 and Williams et al., 2010), given more time it would have been valuable to conclusively demonstrate that these differences remain in osteoarthritic tissue. Williams et al., 2010 demonstrated that chondrocytes from full depth cartilage had the ability to replicate the characteristics of chondroprogenitor cells up until a certain point, after which they were not able to be further expanded in culture or be differentiated into the chondrogenic pathway. Initial work of a similar tangent was carried out within this study, and preliminary results demonstrated that chondrocytes failed to proliferate beyond 2 passages, however a more extensive and conclusive comparison would reiterate and reinforce the superiority of the chondroprogenitor cells in OA tissue compared to chondrocytes.

Chapter 5:

A preliminary study comparing chondroprogenitor cells from normal and osteoarthritic tissue and an investigation of their integration potentials

5.1. Introduction

One of the persisting problems with regards to cartilage repair is the issue of integration, principally due to the avascular nature of articular cartilage. As quoted by Khan et al. (2008) in a recent review, "one characteristic shared by intrinsic reparative processes and the new surgical therapies is an apparent lack of lateral integration of repair or graft tissue with the host cartilage that can lead to poor prognosis". There are many factors that are known to directly and indirectly affect the process of tissue integration (figure 5.1), however to what extent these variables impede cartilage fusion varies and the mechanisms involved are yet to be fully understood.

The developmental origin of the cell source is believed to be a key factor involved in determining the potential for tissue integration. Indeed, in early development cell sorting occurs as a result of differential cell affinity owing to adhesion molecules present on cell surfaces (Gilbert, 2000). Differences in these molecules and selective affinities allow cells of different embryonic germ layers to repel one another or conversely adhere to 'like' cells (Townes and Holtfreter, 1955). Throughout development, the cell surface adhesion molecules are dynamic and change in type, number and distribution thus allowing for the intricate processes of differentiation and maturation to occur (Fyfe and Hall, 1979).

Experiments directed at the integrative capacities of cartilage from different embryonic regions date back as early as 1957, where Chiakulas et al., looked into the specificity and fusion of cartilage derived from mesodermal origin (using cartilage from the appendicular skeleton) and ectodermal neural-crest origin (using Meckel's cartilage) in larval spotted salamanders. Results of this experiment demonstrated heterogeneity based on embryological origin, whereby two cartilages derived from the same place resulted in fusion, and cartilage from different embryological origins –namely femur cartilage against Meckel's cartilage demonstrated a lack of fusion. Later experiments carried out by Fyfe and Hall reinforced this finding by showing that avian tibial chondrocytes failed to fuse with Meckel's cartilage over a period of ten days, resulting in the authors conclusion that avian embryonic chondrocytes are not all equivalent.

Isogai et al., (2006) used an *in-vitro* culture model to compare differences in chondrocytes excised from bovine articular, nasoseptal, auricular and costal cartilages, looking specifically at neocartilage formation in cell-seeded scaffolds implanted into athymic mice. Results from this experiment again highlighted metabolic differences between the different chondrocytes and concluded that "each chondrocyte type establishes or maintains its particular developmental characteristics, and this observation is critical in the design and elaboration of any tissue-engineered cartilage model".

In support of these data, previous experiments from our lab (unpublished data) have demonstrated a lack of integration using skeletally mature bovine nasal and articular cartilages in an aggregation study. As previously mentioned however, these cartilages are derived from different embryonic origins, thus, using knowledge acquired from previous data, the hypothesis that integration would fail was proven.

As such, the overall purpose of all of these cartilage-to-cartilage integration studies are to potentially find a cell source to be used as a tool for repair and treatment of articular cartilage defects. Many of the current strategies (as summarised in Chapter 1) involve the removal of cells from the joint periphery and culturing these *in-vitro* until sufficient numbers are achieved. These cells are viable candidates as developmentally they are derived from the correct lineage, however there are many problems including donor site morbidity and expansion potentials of these cells *in-vitro*. BMSCs are another pool of cells which have been and continue to be targeted extensively as a source of cells which are easily excised and originate from the same embryonic origin as articular cartilage –the mesoderm; however, as highlighted in the previous chapter this cell source is not optimum due to its tendency to terminally differentiate.

In the previous chapter, progenitor cells from OA cartilage were isolated and expanded presenting with the potential to be targeted as a candidate for repair therapies in diseased articular cartilage. The purpose of this chapter was to preliminarily examine the integration potential of this novel cell source native to osteoarthritic cartilage. Per se, the benefits of these cells are that they are derived from the correct embryonic lineage, they reside within the tissue itself and, therefore, could be targeted for *in situ* regenerative techniques, and

they are not as 'multipotent' as BMSCs and therefore mechanisms of interactions with mature chondrocytes may be more easily channelled.

In this chapter, chondroprogenitor cells from osteoarthritic cartilage are compared to chondroprogenitor cells isolated from normal cartilage using the fibronectin adhesion assay outlined in the previous chapter, in order to provide a direct comparison and elucidate similarities and differences between the two cell types. Integration potentials were examined using the clonally derived populations to see how well the two cell types integrate between and also within 'like' populations. Determining their integration potentials will help to understand whether or not the chondroprogenitor cells present in OA cartilage are similar to the population present in healthy cartilage and whether or not they are able to interact together to produce a tissue targetable for the development of future therapies for cartilage repair.
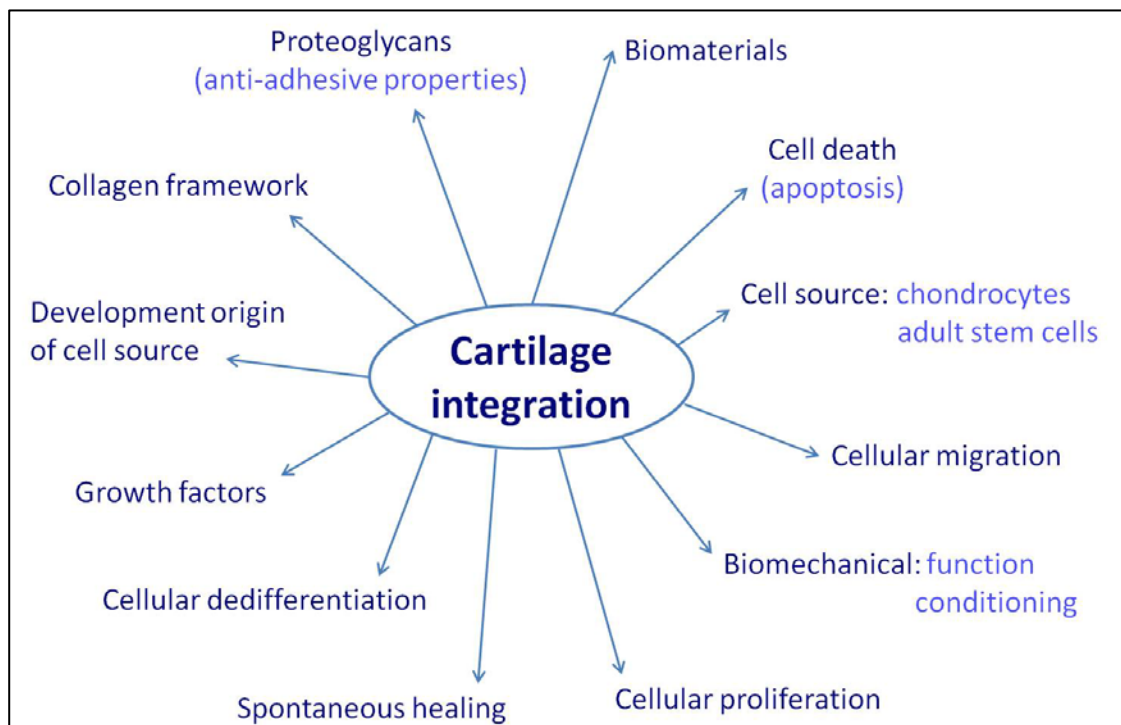
Figure 5.1. Factors that directly or indirectly affect cartilage integration. Figure adapted from Khan et al., (2008).

5.2. Materials

Material	Catalogue number	Supplier
Glutaraldehyde (25%)	R1012	Agar Scientific, UK
G3G4 anti-BrdU antibody	G3G4-(AntiBrdUrd)	Developmental Studies Hybridoma Bank, USA
Penicillin-Streptomycin Sodium pyruvate	15140-122 11360-039	Gibco, UK
CellTracker™ Green CMFDA CellTracker™ Red CMTPX Quant-iT™ PicoGreen® dsDNA Assay Kit	C7025 C34552 P7589	Invitrogen, UK
5-Bromo-4-Chloro-3-Indolyl β-D-Galactopyranoside (X-Gal)	B1690	Molecular Probes, USA
Iodoacetamide 5-Bromo-2′-deoxyuridine (BrdU) Chondroitin sulfate sodium salt from shark cartilage Citric acid monohydrate N,N-Dimethylformamide 1,9-Dimethyl-Methylene Blue DL-Dithiothreitol (DTT) Formaldehyde solution Formic acid Magnesium chloride Papain from papaya latex Potassium ferricyanide Potassium ferrocyanide Sodium phosphate monobasic Trypan Blue solution	A3221 B5002 C4384 C1909 D4551 341088 43817 F8775 F0507 M2393 P3125 P3667 P9387 S3139 T8154	Sigma Aldrich, UK
Hydrochloric acid Sodium chloride	H/1150/PB17 S/3160/53	Thermo Fisher Scientific, UK

Table 5.1. Materials and suppliers.

5.3. Methods

5.3.1. Tissue acquisition & cell culture

Osteoarthritic cartilage was obtained from TKRs as outlined in Chapter 2.3.1. Cartilage was excised, digested and cultured using the methods described in Chapter 4.3.1. Normal cartilage was obtained from patients who underwent knee surgery and institutional safety and ethical guidelines were followed.

For both tissue types, the fibronectin adhesion assay was used to isolate the chondroprogenitors. Normal chondroprogenitors were cultured in optimised media (DMEM containing penicillin 10000 µg ml^{-1}/ streptomycin 10000 U ml^{-1}, 0.1 mM l-ascorbic acid 2-phosphate, 0.5 mg ml^{-1} L-glucose, 100 mM hepes, 1 mM sodium pyruvate, 10% FCS, 1ng ml^{-1} TGF-β2 and 5ng ml^{-1} FGF-2).

As a comparison, whole population of cells (chondroprogenitors and non-binders) were seeded into flasks at a density of 30,000 cells per cm^2. Cells from OA tissue were cultured in OA media and cells from normal tissue were cultured in the media described above. PDs were monitored as outlined in the previous chapter.

5.3.2. Colony forming efficiencies (CFEs)

Twenty-four hours after plating cells by fibronectin adhesion assay, the number of adhered cells was counted in both OA and normal cultures. Between 8 and 14 days after the initial seeding day, clusters of more than 32 cells (defined as a colony) were counted, as this number represents a population of cells derived from more than 5 population doublings of a single cell, thereby discounting a transient amplifying cell cohort. Colony forming efficiencies were then calculated based on a) the initial seeding density and the number of colonies formed and b) the number of cells that initially adhered and the number of colonies formed.

5.3.3. Bromodeoxyuridine (BrdU) labelling of cells

BrdU incorporation into cellular DNA occurs during cell proliferation in place of thymidine. As such, a BrdU assay was carried out in order to elucidate the extent of proliferation within the monoclonal cell lines from normal and osteoarthritic cartilage. Briefly, cells were seeded at 1.0×10^5 in 12 well plates and incubated for 24 hours at 37˚C in 5% CO_2. At this point, 10μM BrdU was added to each well and incubated for a further 24 hours. The cells were then washed several times in PBS prior to being fixed in pre-cooled 70% ethanol for 30 minutes. Subsequent immunodetection of BrdU using a specific G3G4 anti-BrdU mouse monoclonal antibody (at 3μg ml^{-1} for 1 hour at room temperature) allowed for labelling of cells in S-phase of the cell cycle. After several washes in PBS-T, cells were incubated in 3% H_2O_2 diluted in distilled water for 5 minutes. Following this procedure, cells were incubated in 4M HCl for 10 minutes. Reagents from the R.T.U Vectastain kit were used to carry out the remaining steps following the protocol as described in Chapter 3.3.4. DAB substrate was used to visualise the staining. Dishes were washed in distilled water before being imaged using a Nikon E4500 camera attached to an inverted Nikon Eclipse TS100 light microscope.

5.3.4. Senescence associated β-Galactosidase (β-Gal) staining

Cells were initially washed in PBS prior to being fixed in fixation solution (2% formaldehyde and 0.2% glutaraldehyde diluted in PBS) for 5 minutes at room temperature. Following fixation, cells were washed in PBS. Fresh β-Gal stain solution was made immediately before use and consisted of 1mg ml^{-1} 5-Bromo-4-Chloro-3-Indolyl β-D-Galactopyranoside (X-Gal) dissolved in N, N-dimethylformamidine. This was added to 40mM citric acid/ sodium phosphate at pH 6.0, 5mM potassium ferricyanide, 5mM potassium ferrocyanide, 150mM sodium chloride and 2mM magnesium chloride dissolved in distilled water. Cells were incubated with β-Gal solution for 16-24 hours at 37˚C after which they were washed in distilled water and imaged using a Nikon E4500 camera attached to an inverted Nikon Eclipse TS100 light microscope. The assay produces a blue precipitate in cells expressing the senescence marker SA-β-Gal.

5.3.5. Analysis of BrdU and β-Gal staining

Three photographs were taken at random (using x20 objective) in 3 wells per cell line. The numbers of positively stained and unstained cells were counted. The data were used to determine the proportion of proliferating and/ or senescent cells in each cell line. Statistical analysis was carried out using a Students t-test to confirm data significance.

5.3.6. Biochemical analysis of pellets

Three-D pellet cultures were set up using chondroprogenitors from normal cartilage and osteoarthritic cartilage and maintained in culture for three weeks, following the method described in Chapter 4.3.5. After the incubation period, pellets were maintained at -80°C until required.

5.3.6.1. Digestion using papain

Pellets were lysed by adding 0.5ml of papain digestion buffer consisting of 300µg ml^{-1} papain, 20mM sodium phosphate at pH6.8, 1mM EDTA and 2mM DL-Dithiothreitol (DTT) to each pellet-containing Eppendorf tube. These were placed on a hot block at 60°C for one hour or until the pellet had fully lysed, after which 5µl of idoacetamide (at 100µg µl^{-1}) was added to each Eppendorf tube to prevent further action of the digestion buffer. Aliquots of this digest were assayed for DNA and GAG content. Samples were either taken directly for analysis or frozen at -20°C until required.

5.3.6.2. DNA quantification using PICOGREEN

A PICOGREEN kit was used to analyse the quantity of DNA extracted from each sample. Briefly, 1 x TE buffer was made up from the stock supplied within the kit. The reagent was made up by adding 5µl ml^{-1} Quant-IT PICOGREEN to TE buffer. Once prepared, the reagent was kept in the dark as it is light-sensitive. A standard curve was created using DNA component supplied within the kit. Standards were made at 0ng ml^{-1}, 1ng ml^{-1}, 10ng ml^{-1}, 100ng ml^{-1} and 1000ng ml^{-1}. To carry out the sample analysis, a total of 100µl of sample or standard (sample diluted to 1 in 5 in DNA free water) was added to each well of

a 96-well plate. Equal volumes (100µl) of prepared Quant-IT PICOGREEN were then added to each well. Plates were covered in foil and incubated at room temperature for 5 minutes. The plates were read on a FLUOstar OPTIMA (BMG Labtech, USA) plate reader with excitation at 480nm and emission at 520nm using OPTIMA software version 2.00R3.

The value for the concentration of DNA in each sample was divided by two as the total volume used was half the volume of the standard, and then multiplied by the dilution factor of five in order to give the actual concentration of DNA.

5.3.6.3. GAG quantification

A dimethylmethylene blue (DMMB) assay was used for the quantification of GAGs within the digest. Standards were prepared using stock chondroitin-6-sulphate (CS) at $0\mu g\ ml^{-1}$, $10\mu g\ ml^{-1}$, $20\mu g\ ml^{-1}$, $30\mu g\ ml^{-1}$, $40\mu g\ ml^{-1}$ and $50\mu g\ ml^{-1}$ so that a standard curve could be plotted. DMMB reagent contained $16mg\ L^{-1}$ DMMB dissolved in 1 litre dH_2O containing 10ml ethanol, 29ml of 1M sodium hydroxide and 3.5ml formic acid (98%). Forty microlitres of standard or samples were pipetted in duplicate onto a 96-well plate, and 200µl of DMMB was added to each well. The absorbances of the samples were read immediately at 525nm on a FLUOstar OPTIMA plate reader using the OPTIMA software specified previously.

5.3.7. Integration study

Chondroprogenitor cells from normal and osteoarthritic tissue were isolated and cultured using the methods previously described. The separate populations of cells were independently labelled using cell-tracker probes prior to being combined to form aggregates or pellets in order to determine whether patterns of cellular organisation and/or integration could be observed.

5.3.7.1. Fluorescent cell labelling using CellTracker™ probes

Cells were grown in monolayer in supplemented media as described in Chapter 4. Once expanded until the desired number of cells had been achieved, cells were lifted using

trypsin and centrifuged at 2000 rpm x g for 5 minutes. Supernatant was removed and the pellet was resuspended in supplemented serum-free media so that a concentration of 1.0×10^6 cells per ml was achieved. Pre-warmed fluorescent cell trackers CMTPX (red) or CMFDA (green) were added to the suspensions at a working concentration of 5μM and tubes were incubated in the dark at 37˚C on a roller for 45 minutes. After this time, an equal volume of serum containing media was added to the tubes to inactivate the dyes. The tubes were then centrifuged at 2000 rpm x g for 5 minutes and washed with fresh serum containing media. This step was repeated once more to ensure any excess dye was removed. Finally, cells were resuspended into desired volumes to be split into cultures. Labelled cells were always kept out of direct light to protect the cell tracker dyes from decay.

5.3.7.2. Trypan blue exclusion test of cell viability

This test was used to determine whether either of the fluorescent dyes affected cell viability. Following cell labelling using the method described above, cells were re-plated in monolayer and cultured for 5 days at 37˚C in 5% CO_2. The cells were then lifted using trypsin, centrifuged at 2000 rpm x g for 5 minutes and resuspended in serum-free media. Fifty microlitres of cell suspension was mixed with equal volumes of 0.4% trypan blue and the mixture was left to incubate for 3 minutes at room temperature. A haemocytometer was used to count the unstained (viable) and stained (non-viable) cells so that an overall percentage of viable cells could be calculated. One way ANOVAs were used to calculate any statistical significance between groups.

5.3.7.3. Aggregate assembly for integration study

Following fluorescent labelling of chondroprogenitors from OA and normal cartilage, mixed population aggregates were formed by combining 5×10^4 cells from each cell line into 15ml centrifuge tubes containing supplemented DMEM/F12 + 10% FCS containing 1ng ml^{-1} TGF-β2 and 5ng ml^{-1} FGF-2. The tubes were placed on a roller and incubated at 37˚C for 72 hours in the dark. Following the incubation period, aggregates were washed in PBS prior to being fixed in 10% NBFS for 20 minutes. Aggregates were then mounted under raised cover-slips using DAPI to create a concave microscope slide effect.

Aggregate types included i) chondroprogenitors from OA mixed with chondroprogenitors from normal tissue, ii) two different OA chondroprogenitor cell lines pooled together, termed OA polyclonal aggregates, and iii) two different normal chondroprogenitor cell lines combined, termed normal polyclonal aggregates. All ratios were one to one. Aggregates were imaged on a confocal microscope as outlined below.

5.3.7.4. Pellet cultures for integration study

Pellet cultures as described in Chapter 4.3.5 were established following fluorescent labelling of chondroprogenitors from OA and normal cartilage. Briefly, following the tracker labelling, pellets were formed by combining 2.5×10^5 cells from each cell line in a sterile 1.5ml Eppendorf tube containing supplemented DMEM/F12 + 2% FCS as well as 1% ITS, 0.1µM dexamethasone and 5ng ml^{-1} TGF-β2. Eppendorf tubes were centrifuged at 2000 rpm x g for 5 minutes and incubated for 21 days at 37°C with a media change every second day. On completion, pellets were fixed in 70% ethanol for 20 minutes and processed for paraffin wax embedded using the method described in Chapter 4.3.6. The pellets were then sectioned using a microtome as outlined in Chapter 2.3.4, and imaged using a confocal microscope. Pellets were set up as in the aggregate study, with combined OA and normal chondroprogenitor populations, OA polyclonal and normal polyclonal chondroprogenitor populations.

5.3.7.5. Confocal microscopy and imaging

Confocal microscopy was carried out on a Leica TCS SP2 AOBS Confocal Laser Scanning microscope (Leica, Germany) using appropriate excitation and emission settings for simultaneous detection of CMFDA (ex. max: 492nm; em. max: 517nm) and CMTPX (ex. max: 577nm; em. max: 602nm) 'CellTracker' probes. Cell aggregates were scanned through their entire depth using a x20 objective lens employing a z-step of typically between 3 and 5µm to produce a stack of digitised 'optical sections'. Pellet sections were imaged under the confocal microscope using identical settings. 'Maximum intensity'-type projections were then created from the z-stacks using Leica Confocal Software and presented as red-green overlays with a scale bar expressed in microns.

5.4. Results

5.4.1. Colony forming efficiencies

In this preliminary study, comparing chondroprogenitors obtained from osteoarthritic and normal articular cartilage, colony forming efficiencies were calculated based on the initial seeding density (figure 5.2) and on the number of cells which initially adhered (figure 5.3). In the OA samples, CFEs based on the initial seeding densities were consistently below 0.1 (no significant difference within OA group), ranging from 0.04 to 0.09 percent. In the normal samples, CFEs varied significantly ($p<0.05$), ranging between 0.04 to 0.5 percent. Despite the apparent range, T–tests using the averages of samples confirmed that there was no significant difference between CFEs of chondroprogenitors obtained from osteoarthritic and normal specimens, when calculated using the original method based on the initial seeding density.

The number of colonies formed in relation to the number of cells that initially adhered is demonstrated in figure 5.3. The pattern of results is similar to figure 5.2 in that the OA cell lines produced consistently smaller CFEs and the normal cell lines varied significantly ($p<0.05$). T-tests confirmed that there was no significant difference in average CFEs between the two groups. In the OA cell lines, the CFEs ranged from 0.5 to 0.88 percent whereas the normal cell lines ranged from 0.23 to 4.93 percent. These results in both the OA and normal cell lines, are approximately a ten-fold increase, when compared to CFEs obtained using the initial seeding densities.

Initial adhesion to fibronectin was mildly higher in the chondroprogenitors from OA articular cartilage compared to normal counterpart, however this trend was not confirmed statistically ($p>0.05$). In the OA cultures, adhesion ranged between 10.7 and 15.4 percent, and ANOVAs confirmed there was no significant variation within this group ($p>0.05$). In the normal cultures, initial adhesion ranged between 5.3 and 9.9 percent (figure 5.4), and within this group significant variation was confirmed using ANOVAs ($p<0.05$).

Interestingly, in relation to figures 5.3 and 5.4 together it can be seen that there appears to be an inverse trend occurring; a higher percent of cells in the OA cultures initially adhere

compared to the normal cultures; but of these adhered cells, far fewer go on to form colonies in the OA cultures when compared to the normal cultures.

5.4.2. Proliferation and senescence

Cell proliferation in clonally-derived cell lines from OA and normal articular cartilage was assessed using a BrdU assay which incorporates BrdU into cellular DNA in place of thymidine during the replicative process. Three cell lines were examined per donor. Consistency was observed between cell lines of each donor regardless of their origin (OA or normal articular cartilage) (figure 5.6). In the OA category, the percent of BrdU positive cells ranged from 52 to 87. More specifically, the percent of BrdU incorporation in cell lines of the two patients showed a distinct difference; with one demonstrating a higher level of proliferation (mean = 85%) and the other demonstrating a lower level of proliferation (mean=58%). T-tests confirmed that the differences between the two patients were significant ($p<0.05$). A similar trend was observed in the normal category; the percent of positive cells ranged from 64 to 89 however, as mentioned, there was a divide seen between the cell lines of the two donors. The mean of BrdU positive cells in cell lines of one donor was 66 percent, whereas in cell lines from the second patient, figures were significantly higher with a mean of 88 percent BrdU positive cells ($p<0.05$). Using the data between the two cohorts collectively (therefore excluding patient variability), there was no difference between the percentage of BrdU positive cells in the OA and normal cohort ($p<0.05$). Figure 5.5 is a photomicrograph showing the differences of BrdU labelling in the high and low proliferating cell lines obtained from OA and normal articular cartilage.

A senescence associated β-galactosidase assay was used to assess the degree of senescence within chondroprogenitor cell lines from OA and normal donors. A considerable degree of variation was evident between and within cell lineages from patients. Within the OA group, the variation was not significant ($p>0.05$) however within the normal group the variation between patients was significant ($p<0.05$). Senescence was reduced in osteoarthritic cell lines when compared to cell lines from normal articular cartilage, confirmed statistically using a T-test ($p<0.05$). In the OA category, the percent of SA β-gal positive cells ranged between 1.4 and 5.9, whereas in the normal cohort the range was from 5.9 to 15.7 percent. In the normal group, the range was enlarged as a result of cell

lines from one particular patient exhibiting high levels of senescence (mean=15.2). Figure 5.7 is a photomicrograph demonstrating the blue precipitate formed as a result of this assay in each of the cell lines obtained from the OA and normal donors. It can be seen that in image (C) there are noticeably more labelled cells.

Correlating the cell proliferation and senescence results (figures 5.6 and 5.8) it can be noted that in the OA category, the patient whose cell lines elicited a higher percent of BrdU as a result of proliferation (OA-1) presented with relatively low levels of SA β-gal compared to the other patient (OA-2) where higher SA β-gal is accompanied by relatively low levels of BrdU labelling. This pattern was also observed in the normal group –high proliferation was accompanied by relatively low levels of senescence.

5.4.3. Biochemical analysis of pellets

Following 21 days in culture, pellets were lysed using a papain digestion buffer. DNA content in the lysed pellets from OA and normal origins was determined using a PICOGREEN kit (figure 5.9). Each bar represents the mean of 5 pellets. In the OA samples, DNA content of the pellets varied significantly, from 38 to 91 µg per pellet (ANOVAs confirmed $p<0.05$). In the normal samples, DNA content ranged from 22 to 73 µg ($p<0.05$). Due to the similarities in ranges, no trend was observed in relation to DNA content in pellets derived from OA or normal articular cartilage, and this was confirmed statistically using T-tests ($p>0.05$).

Dimethyl methylene blue (DMMB) assays were performed to quantitatively assess GAG content of the pellets. Combining these data with the DNA content is was possible to elucidate the content of GAG relative to DNA (figure 5.10). As a whole, it was apparent that within both OA and normal pellets, there was very little GAG per DNA. In the OA cohort, GAG/DNA ranged between 0.09 to 0.19 µg/µg, and in the normal cohort the range was between 0.16 and 0.5 µg/µg. ANOVAs confirmed that there were significant differences within both the OA and normal groups ($p≤0.05$) and a T-test was used to confirm no significant difference between the OA and normal groups ($p>0.05$). Using this preliminary data it appears that there is no real difference between GAG/DNA in pellets derived from chondroprogenitors from OA and normal origins.

5.4.4. Integration study

Chondroprogenitor cells were successfully labelled with CMTPX and CMFDA cell tracker labels. Concentration and incubation time was optimised in monolayer cultures (figure 5.11). Optimal concentration was 5µM, incubated in a dark room on a roller for 45 minutes. Cell viability was assessed to ascertain whether cell trackers affected cell viability (figure 5.12). In cultures with no tracker, 8.7 % of the cells were trypan blue positive, compared to the 9.9 % and 6.7 % in CMTPX and CMFDA cultures respectively. As such there was no significant difference between viability in cultures labelled with either of the cell trackers when compared to the corresponding control. This was confirmed using a T-test where $p > 0.05$ in both cases (figure 5.13).

Cell aggregates were formed combining clonally-derived chondroprogenitor cell lines. Different OA lines were combined, different normal cell lines were combined and a mixture of OA and normal cell lines were combined (figure 5.14). Figure 5.14.1 demonstrates three different OA: OA cell aggregates. The results amongst the OA aggregates were variable in that cell integration was observed in certain aggregates (represented through figure 5.14.1-i); partial integration was seen in other aggregates (figure 5.14.1-ii) and distinct segregation was observed in others (figure 5.14.1-iii). Where 'partial integration' was observed, it was evident that there were regions in the aggregate where cells failed to integrate, despite other areas of the aggregate showing clear integration. In figure 5.14.1-iii the aggregate has been categorised under 'segregation' as one population of cells can be seen to be heavily weighted on the right side (green CMFDA) whereas the red CMTPX labelling is localised to the left hand side. As such, no definitive pattern was detected when combining chondroprogenitor cell lines from OA articular cartilage.

When two different chondroprogenitor cell lines from normal derivatives were combined, the trend was biased towards segregation rather than integration in the aggregates. In figure 5.14.2-i, there appears to be one dominant cell line (red) that has formed the majority of the aggregate, and cells from the other cell line (green) appear to be largely restricted to a small portion on the bottom left side of the aggregate. In a different aggregate (figure 5.14.2-ii) a similar trend was observed in that there appeared to be a

dominant cell line, with a concentrated area in which the other cell line predominantly resides. In this case however, a small increase in integration was also noted throughout the rest of the structure.

Aggregates formed from OA and normal chondroprogenitor cells can be viewed in figure 5.14.3. In two of the three aggregates presented, widespread integration was observed throughout the structure (i and ii). In the third case, clear segregation was observed between the two different cell lines (iii). Figure 5.14.4 is an aggregate which was formed in the initial optimisation stages, with a seeding density ten times larger than the optimised number (1.0×10^6 cells). As such, for analysis this structure was sectioned before being viewed under the confocal microscope. Despite being distinctly larger in size, clear integration between the two cell lines (OA: normal) was observed.

Alongside the aggregates, pellets were formed which were cultured for 21 days prior to being subject to confocal microscopy (figure 5.15).Variation was again seen within the pellets with no distinct pattern of segregation and/or integration observed. In figure 5.15.1-i, a pellet formed from two OA cell lines, segregation was evident as one cell line adopted the periphery (red), while the other cell line occupied the core (green). Other pellets of mixed OA cell lines however demonstrated greater levels of integration (figures 5.15.1-ii & iii). Integration with pockets of segregation as seen in the aggregates was also observed in the pellets (figure 5.15.1-ii).

Pellets formed by normal cell lines and mixed OA and normal cell lines did not elicit any distinct pattern of organisation (figures 5.15.2 and 5.15.3). Again, in some instances integration was observed and in others clear evidence of segregation was seen. As such, no distinct trend could be defined within the aggregates or pellets formed from normal, OA and/or OA and normal cell lines. Table 5.2 summarises the results of the aggregation study which helps in drawing the conclusion that no defined pattern could be observed.
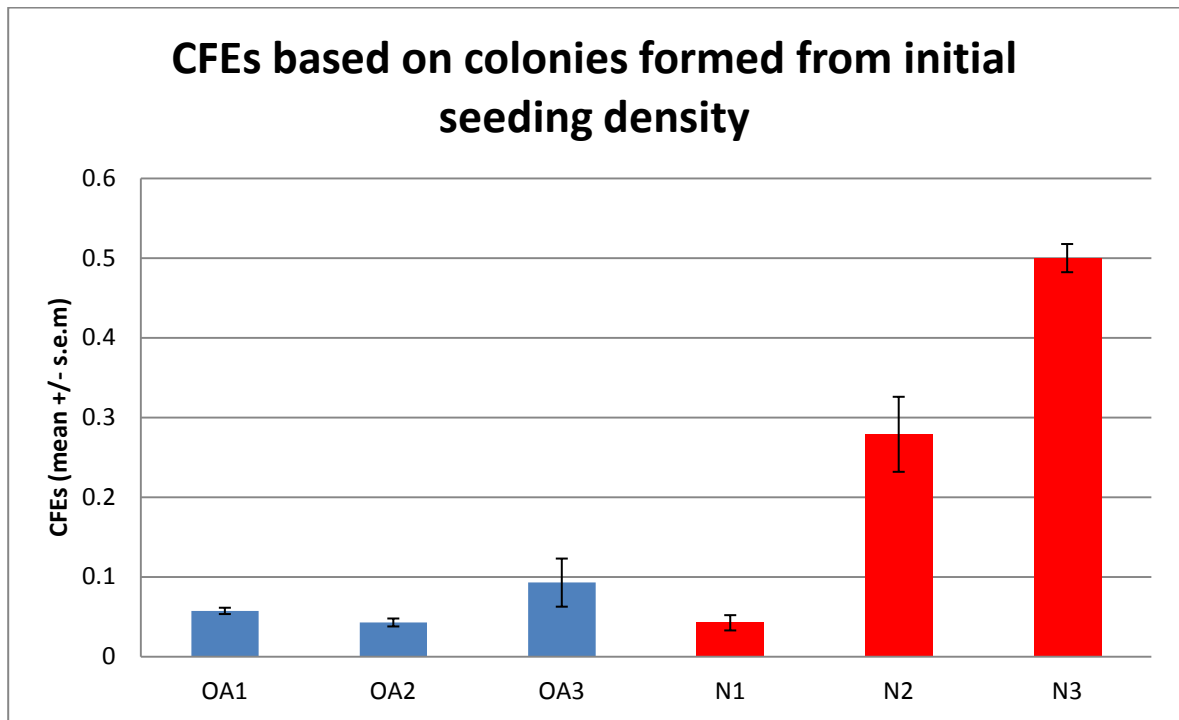
Figure 5.2. CFEs of chondroprogenitor cells isolated from OA (blue) and normal (red) tissue.

CFEs based on the initial seeding density. Combined mean displayed (+/- SEM) (n=3). ANOVAs suggested that there was no significant difference in CFEs within the OA group (p>0.05), yet that there was a significant difference in CFEs within the normal group (p<0.05). Using the averages for each patient, t-tests suggest that there is no significant difference in CFEs between the two (OA and normal) groups (p>0.05).

CFEs based on colonies formed from initially adhered cells
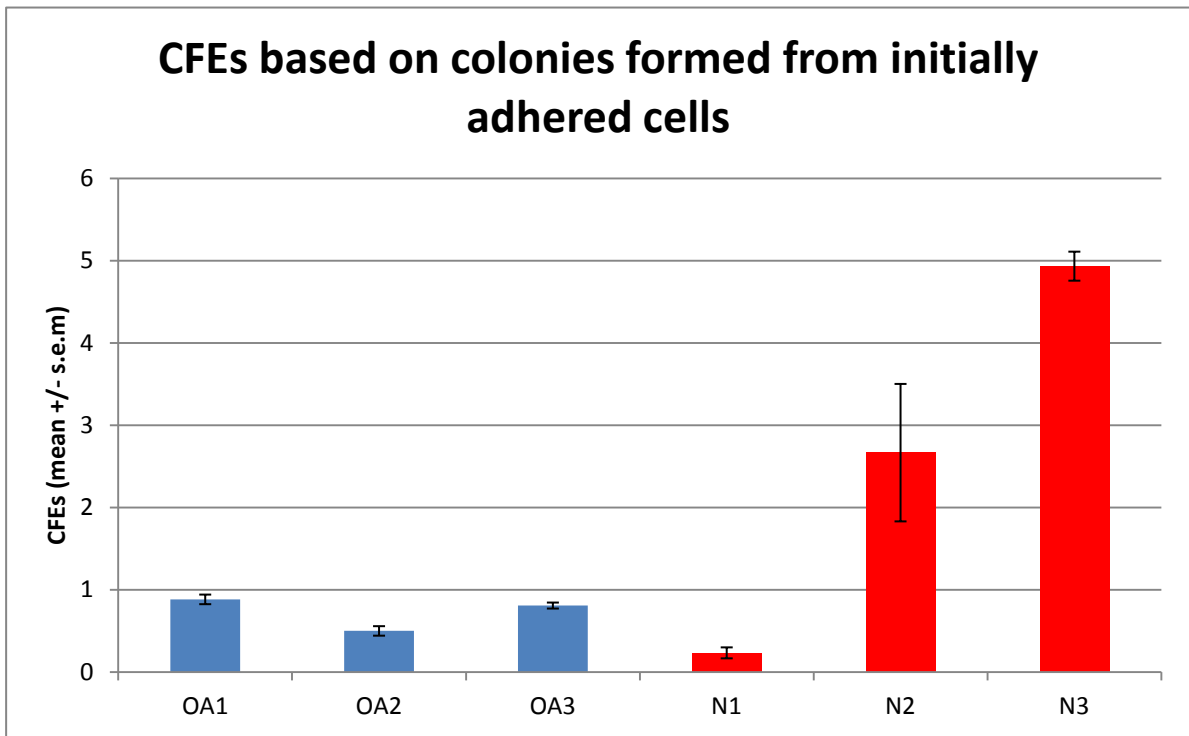
Figure 5.3. CFEs of chondroprogenitor cells isolated from OA (blue) and normal (red) tissue.

CFEs calculated following initial adhesion to fibronectin. Combined mean displayed (+/- SEM) (n=3). ANOVAs suggested that there was no significant difference in CFEs within the OA group (p>0.05), yet that there was a significant difference in CFEs within the normal group (p<0.05). Using the averages for each patient, t-tests suggest that there is no significant difference in CFEs between the two (OA and normal) groups (p>0.05).
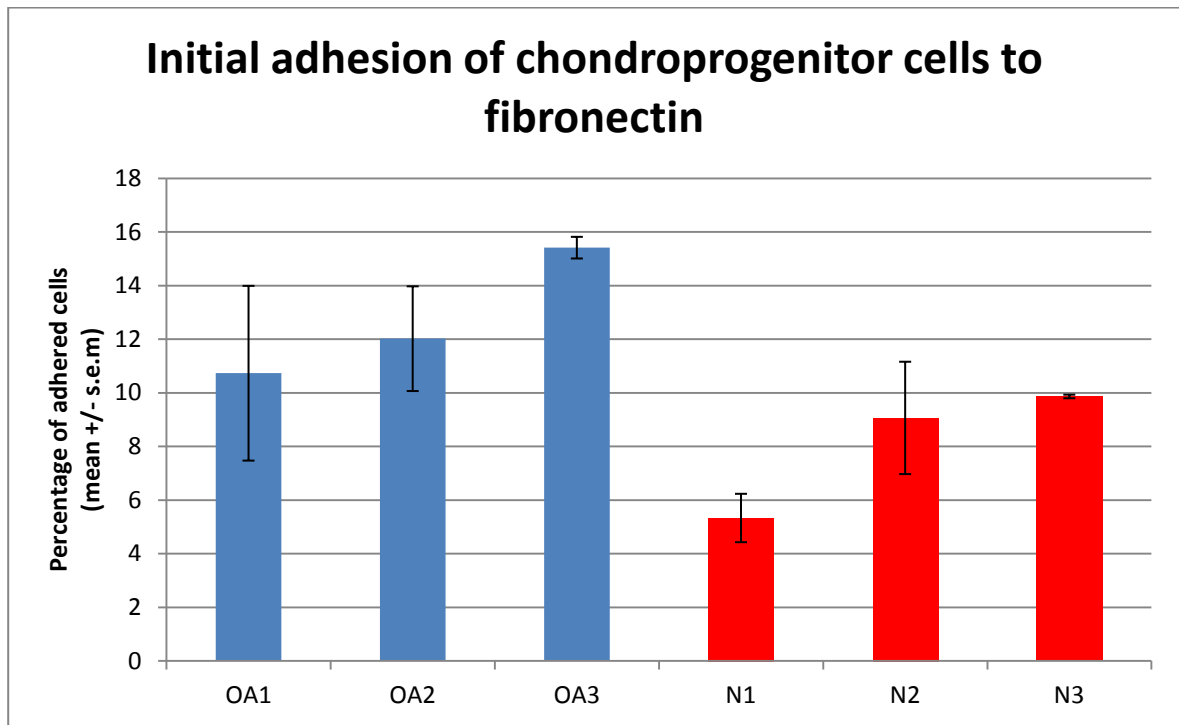
Figure 5.4. Bar chart demonstrating the initial number of cells isolated from OA (blue) and normal (red) articular cartilage adhering to fibronectin within 20 minutes.

Data illustrates the mean, displayed as a percentage of the total (+/- SEM) (n=3). ANOVAs suggested that there was no significant difference in percentage of adhered cells within the OA group (p>0.05), yet that there was a significant variability within the normal group (p<0.05). Using the averages for each patient, t-tests suggest that there is no significant difference in initial adhesion between the two (OA and normal) groups (p>0.05).
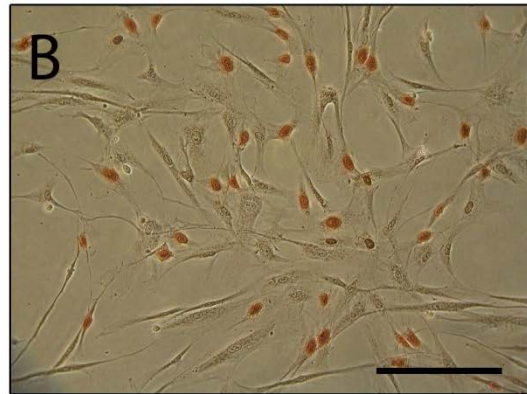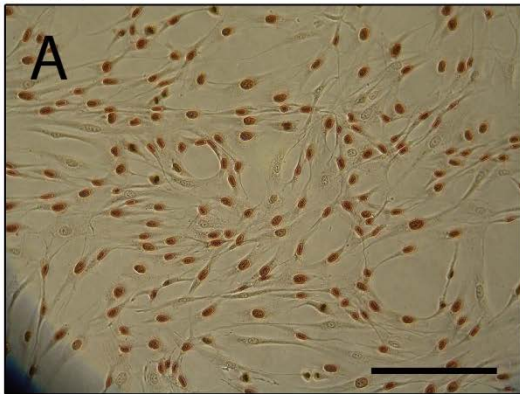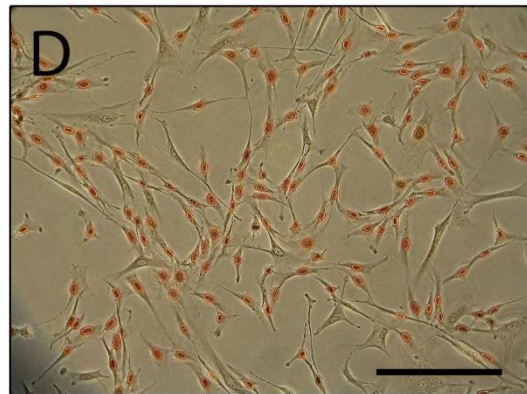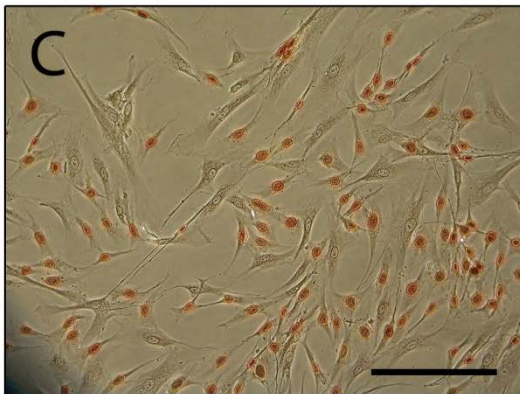
Figure 5.5. Photomicrographs of clonally derived chondroprogenitor cells isolated from OA (A & B) or normal (C & D) articular cartilage treated with BrdU to detect cell proliferation.

Photomicrographs are representative images to demonstrate BrdU incorporation to greater (A & D) and lesser extents (B & C) in both cohorts. Cells were viewed under a Nikon Eclipse TS100 microscope and imaged using a Nikon E4500 camera. Scale bars = 200μm.
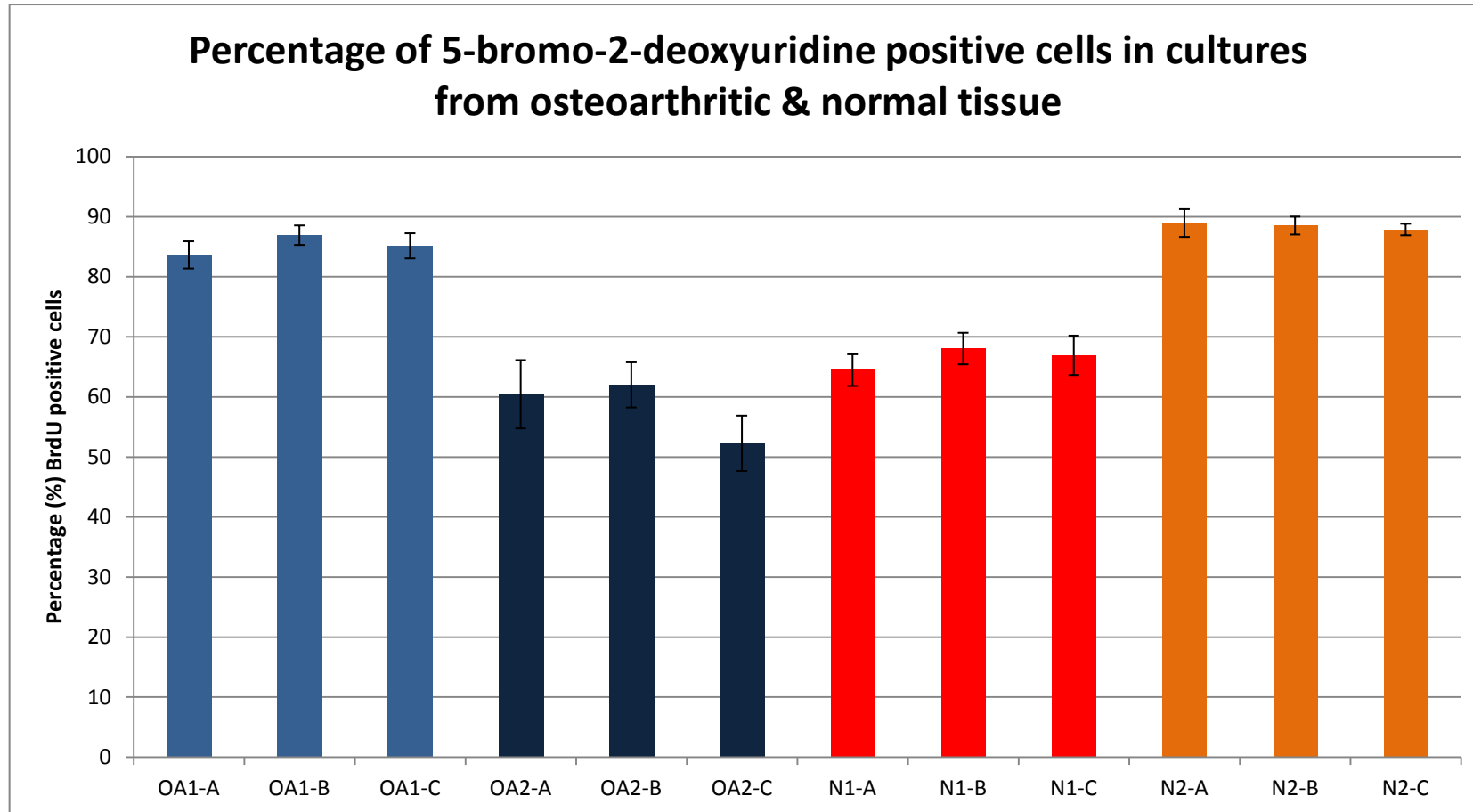
Figure 5.6. Graph representing mean percentage of 5-bromo-2-deoxyuridine (BrdU) positive cells in cells lines (n=3) from different patients (n=2 for OA, n=2 for normal).

Blue bars represent cultures obtained from osteoarthritic patients. Red bars represent cultures obtained from normal un-diseased patients. There was a significant difference in BrdU labelling between patients in both the OA and normal groups, and this was confirmed statistically using t-tests (p<0.05). Comparing the whole OA group against the whole normal group, no difference was found and this was confirmed by a t-test (p>0.05).
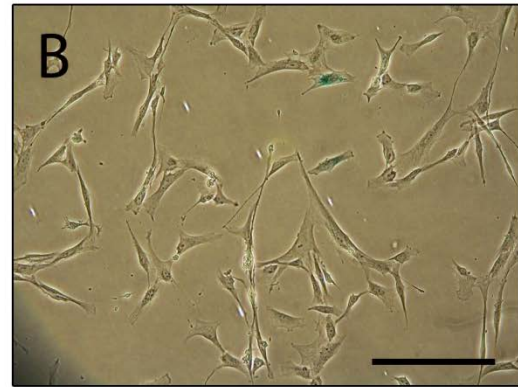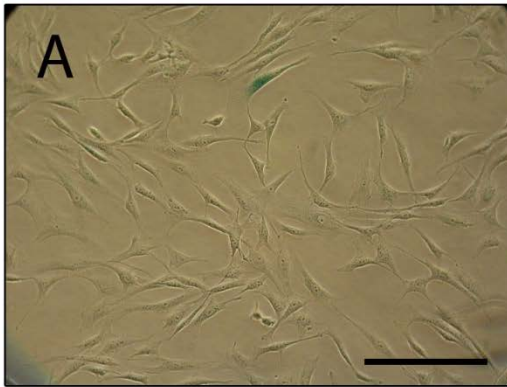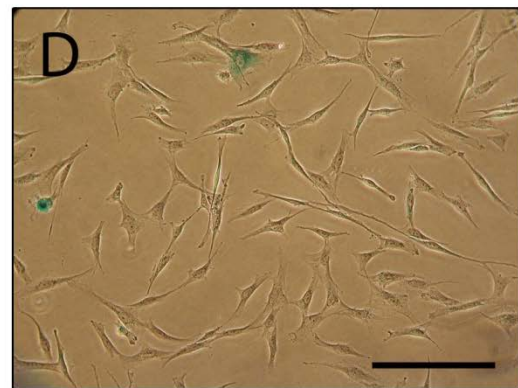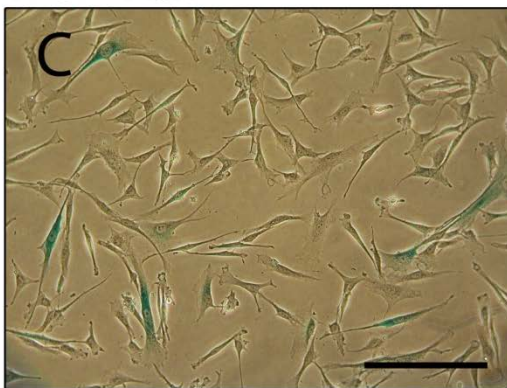
Figure 5.7. Photomicrographs of clonally derived chondroprogenitor cells isolated from OA (A & B) or normal (C & D) articular cartilage stained for senescence associated β-galactosidase (SA-β-Gal) at pH 6.0.

Photomicrographs are representative images to demonstrate senescent cells in which a blue precipitate is formed following the assay. Cells were viewed under a Nikon Eclipse TS100 microscope and imaged using a Nikon E4500 camera. Scale bars = 200µm.
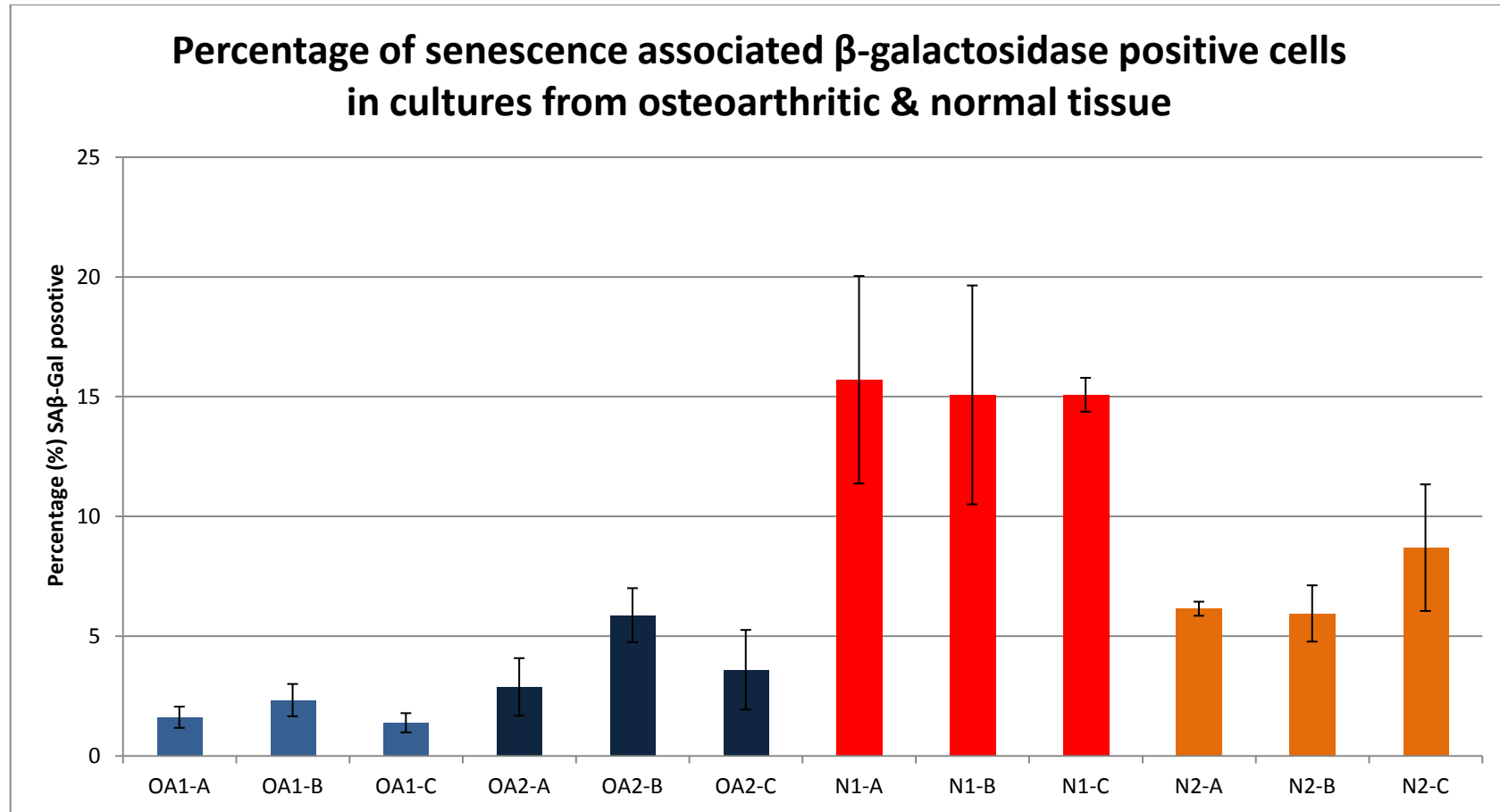
Figure 5.8. Graph representing mean percentage of senescence associated β-galactosidase (SA-β-Gal) positive cells in cells lines (n=3) from different patients (n=2 for OA, n=2 for normal).

Blue bars represent cultures obtained from osteoarthritic patients and red bars represent cultures obtained from normal un-diseased patients. SA-β-Gal labelling did not vary significantly within the OA group as confirmed through a student t-test ($p>0.05$). However, a significant difference in SA-β-Gal labelling within the normal group was confirmed using a t-test ($p<0.05$). A significant difference was observed when comparing SA-β-Gal labelling in the whole OA group against the SA-β-Gal labelling in the normal group, and this was confirmed using a student t-test ($p<0.05$).
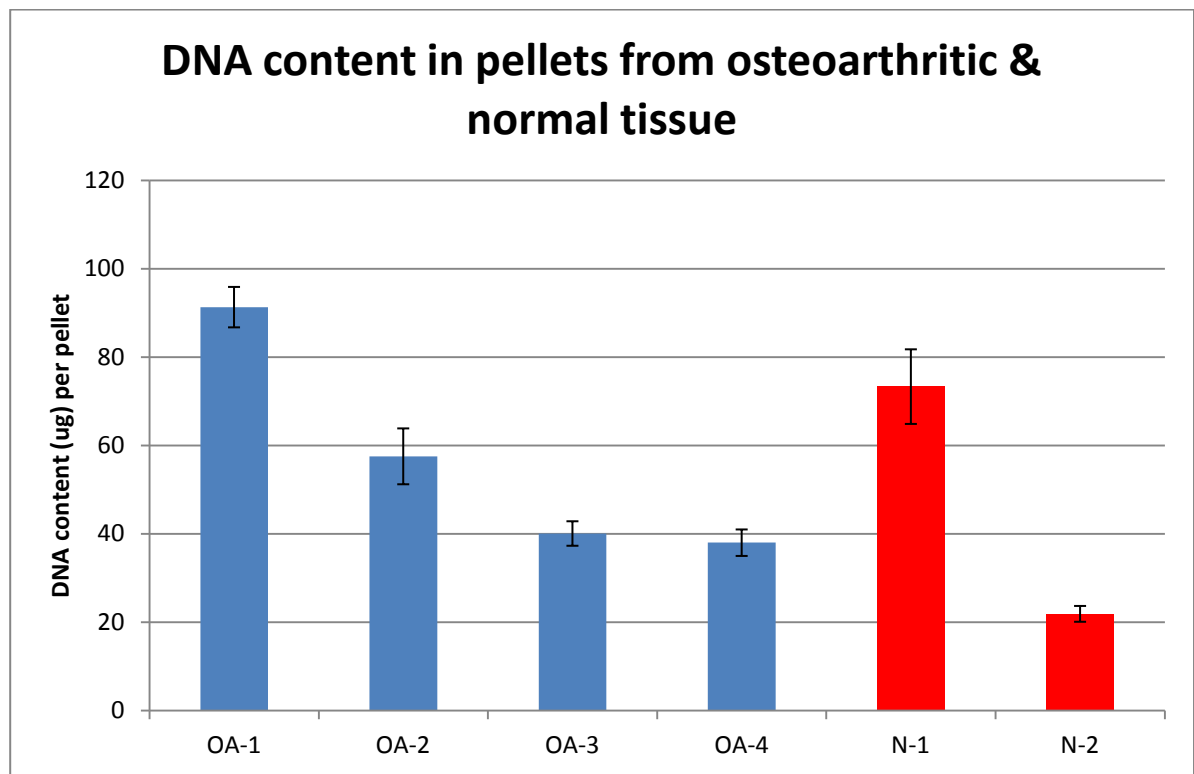
Figure 5.9. Bar chart representing mean DNA content (µg) (n=5) in articular cartilage progenitor cell pellets derived from OA (blue) or normal (red) tissue (+/- SEM) following digestion using papain and DNA quantification using PICOGREEN.

Within both the OA and normal groups, significant variation was observed in DNA content per pellet. This difference was confirmed statistically using ANOVAs where $p < 0.05$. A t-test was used to compare DNA content between the two groups and no significant difference was suggested ($p > 0.05$).
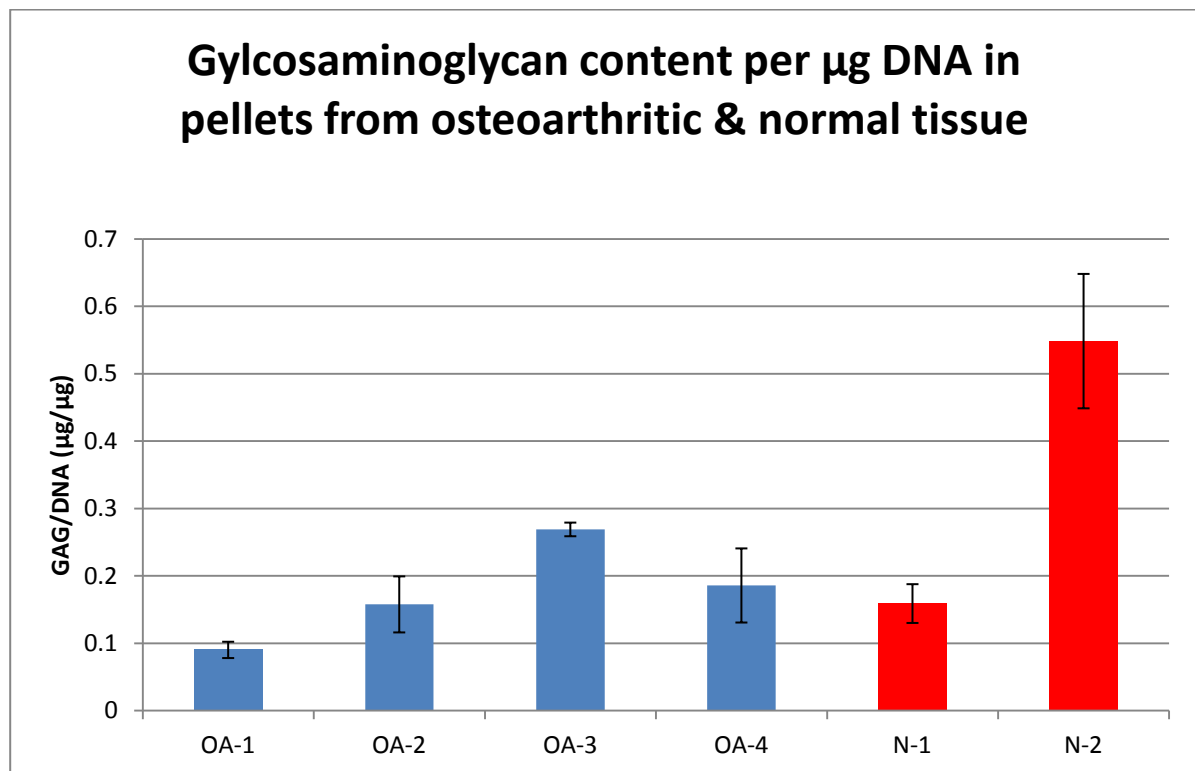
Figure 5.10. Bar chart representing mean glycosaminoglycan (GAG) content per µg DNA of articular cartilage progenitor cell pellets derived from OA (blue) or normal (red) tissue (+/- SEM).

Pellets were digested using papain, DNA quantified using PICOGREEN and GAG quantified using a DMMB assay. Within both the OA and normal groups, significant variation was observed in mean GAG/DNA. This difference was confirmed statistically using ANOVAs where $p<0.05$. A t-test was used to compare GAG/DNA between the two groups and no significant difference was suggested ($p>0.05$).
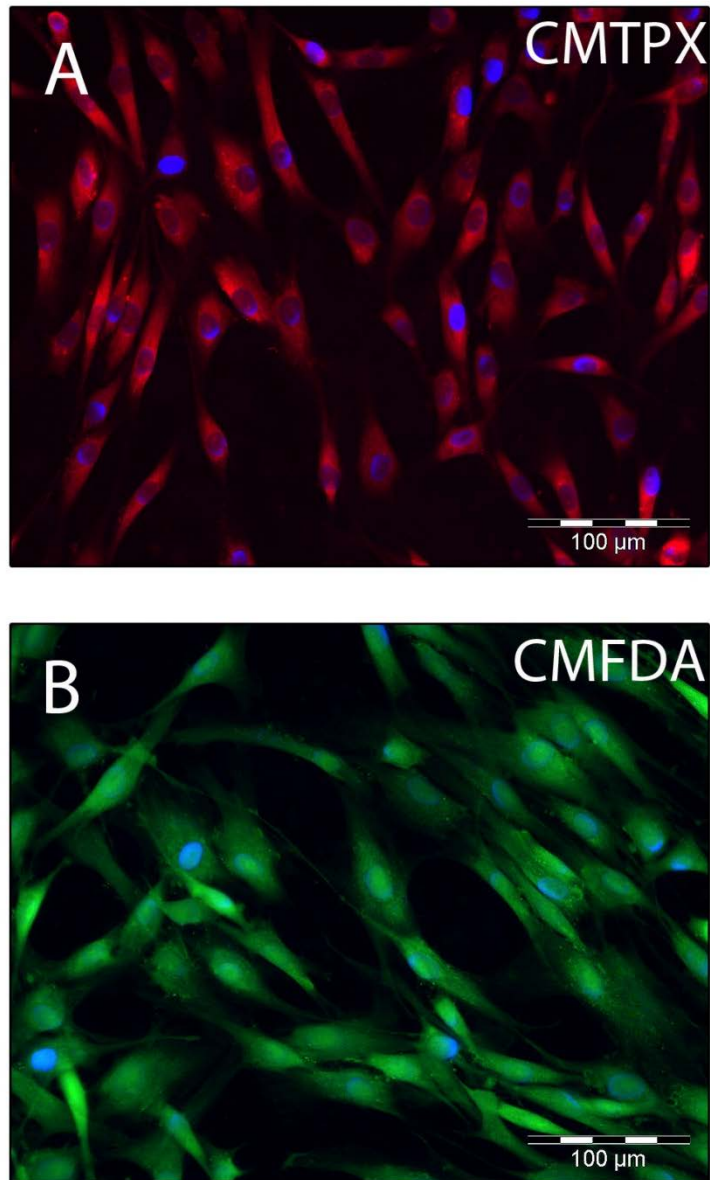
Figure 5.11. Chondroprogenitor cell labelling using 5µM CMTPX red (A) and CMFDA green (B) tracker labels in monolayer cultures.

During labelling, cells were incubated in a dark room at 37°C for 45 minutes. Cultures were viewed and imaged under a BX61 Olympus fluorescent microscope.
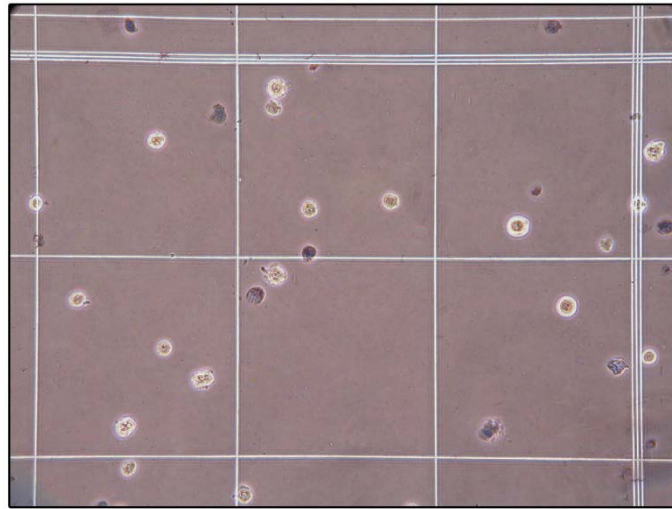
Figure 5.12. Trypan blue exclusion test of cell viability.

Viable (unstained) and non-viable (stained blue) were counted using a haemocytometer. Cells were viewed under a Nikon Eclipse TS100 microscope and imaged using a Nikon E4500 camera.
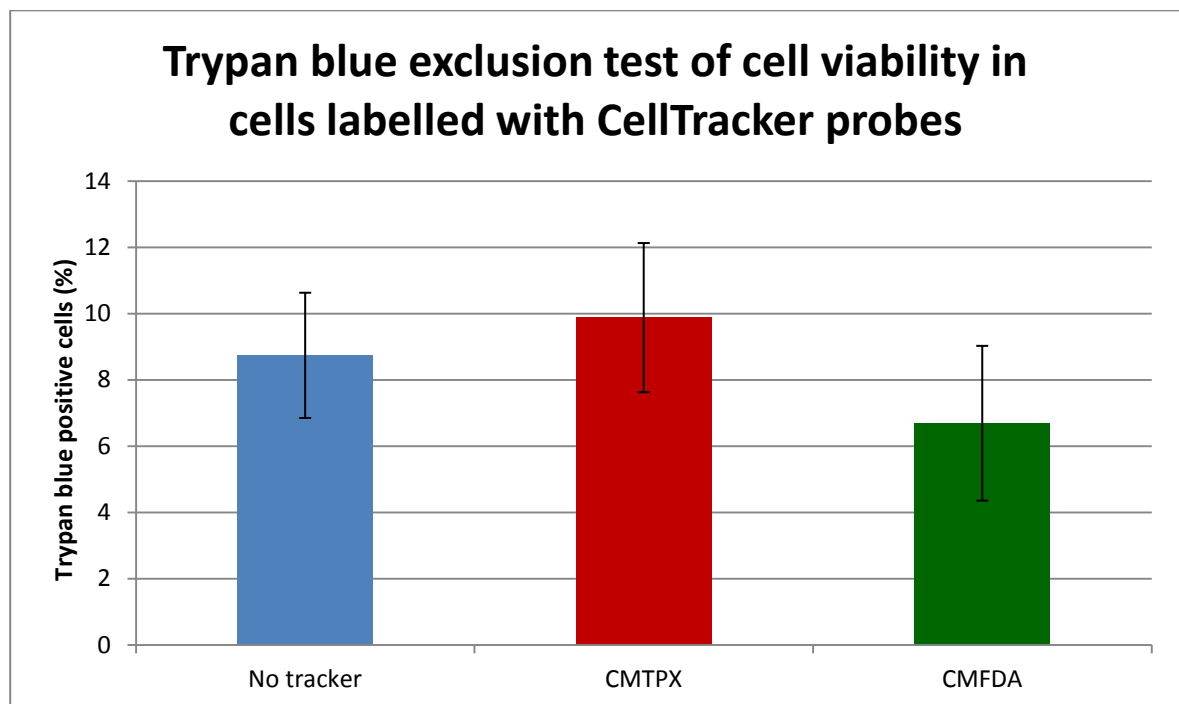
Figure 5.13. Bar chart demonstrating mean cell viability (n=5) after using CMTPX and CMFDA cell trackers in monolayer cultures.

Mean percent of positive cells was 8.7% in control cultures, 9.9% in CMTPX cultures and 6.7% in CMFDA cultures. T-tests confirmed that there was no significant difference in viability between cells labelled with either of the trackers when compared to the control (p>0.05).

Figure 5.14. Fluorescently labelled cell aggregates containing mixed populations of chondroprogenitors (OA:OA, normal:normal and OA:normal) cultured for 4 days in optimised media.

Green CMFDA and red CMTPX cell trackers were used to demonstrate relative positions of labelled cells. Aggregates were viewed and imaged using a confocal laser scanning microscope.

Figure 5.14.1-i: OA:OA

Chondroprogenitor cell aggregates of mixed cells from different OA cell lines (OA:OA) at a ratio of 1:1. CMFDA green and CMTPX red cell trackers distinguish between the two cell populations. (A & C) Position of the individually labelled cells. (B & D) Composite images demonstrating relative positions of cell populations. (A & B) Low power images and higher power images (C & D).
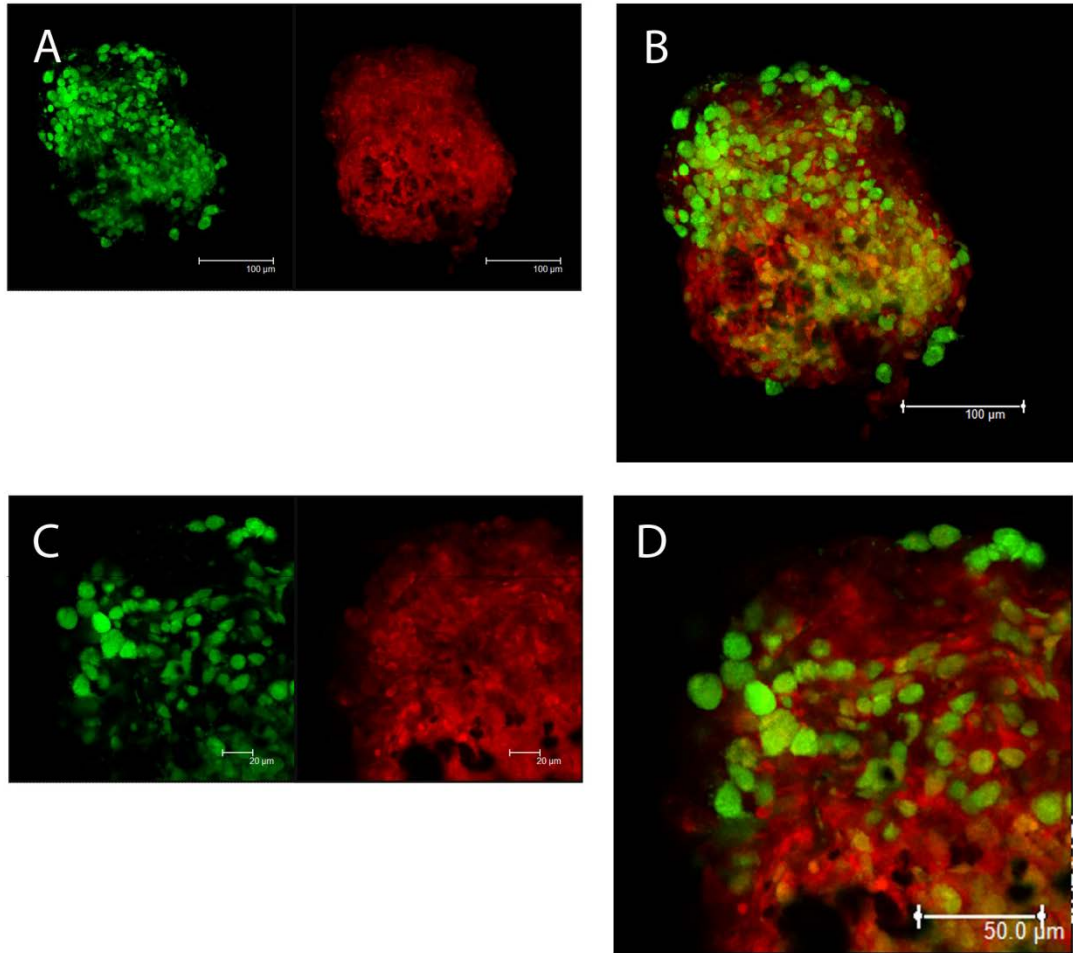
Figure 5.14.1-ii: OA:OA

Chondroprogenitor cell aggregates of mixed cells from different OA cell lines (OA:OA) at a ratio of 1:1. CMFDA green and CMTPX red cell trackers distinguish between the two cell populations. (A & C) Position of the individually labelled cells. (B & D) Composite images demonstrating relative positions of cell populations. (A & B) Low power images and higher power images (C & D).

Figure 5.14.1-iii: OA:OA

Chondroprogenitor cell aggregates of mixed cells from different OA cell lines (OA:OA) at a ratio of 1:1. CMFDA green and CMTPX red cell trackers distinguish between the two cell populations. (A) Position of the individually labelled cells. (B) Composite image demonstrating relative positions of cell populations. (A & B) Low power images.
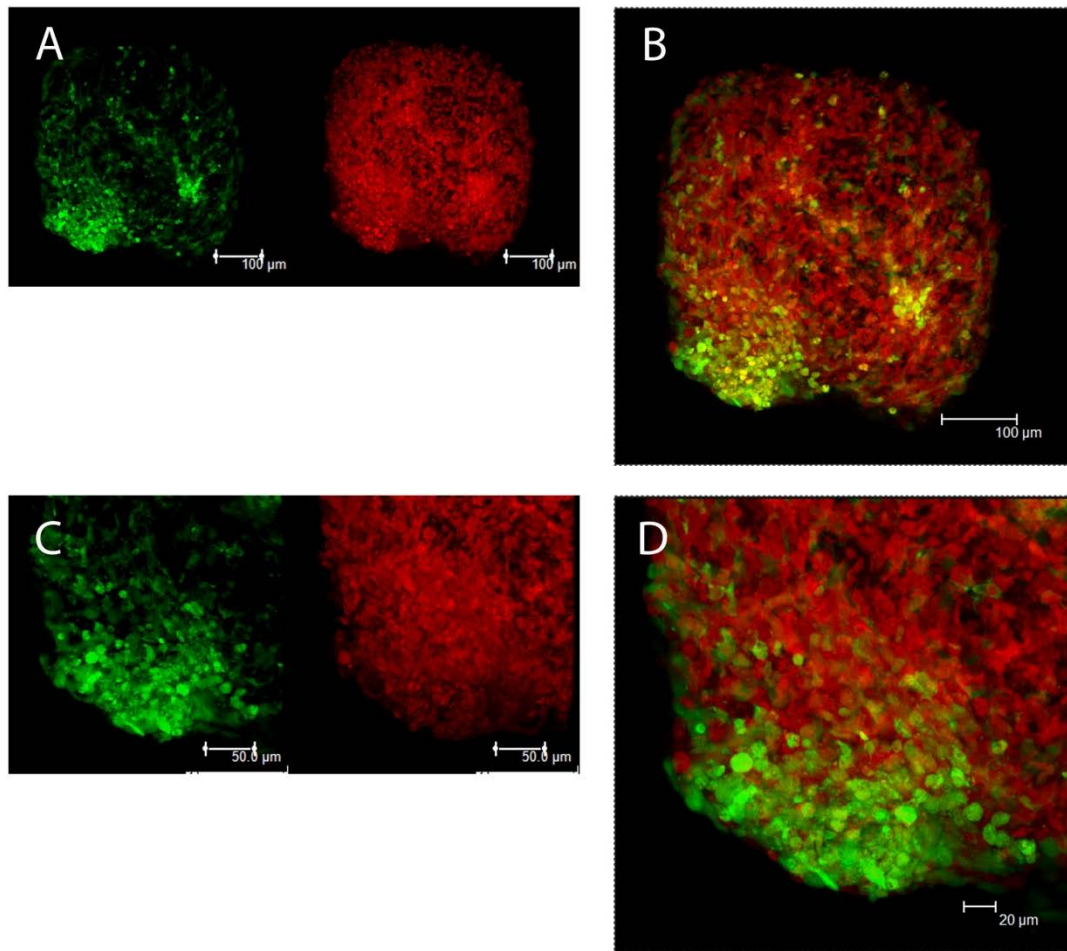
Figure 5.14.2-i: Normal:normal

Chondroprogenitor cell aggregates of mixed cells from normal cell lines (normal : normal) at a ratio of 1:1. CMFDA green and CMTPX red cell trackers distinguish between the two cell populations. (A & C) Position of the individually labelled cells. (B & D) Composite images demonstrating relative positions of cell populations. (A & B) Low power images and higher power images (C & D).
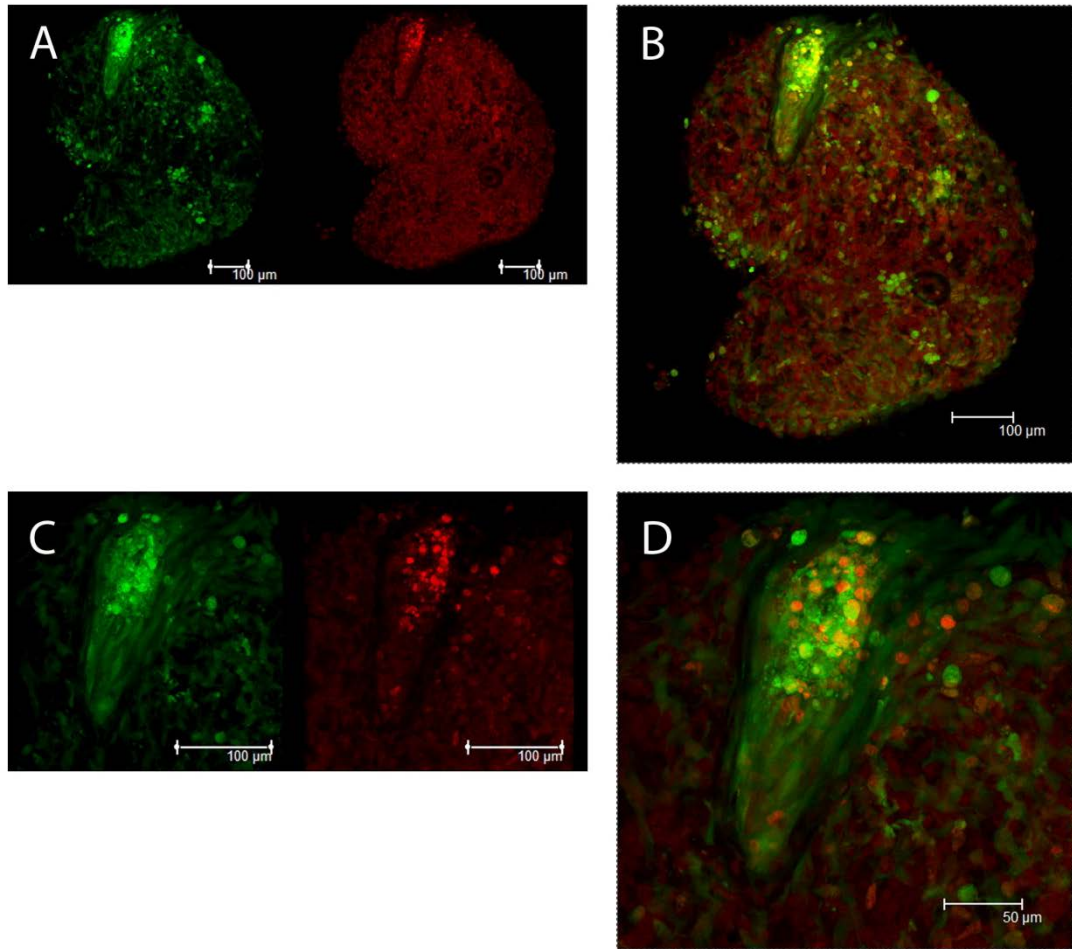
Figure 5.14.2-ii: Normal:normal

Chondroprogenitor cell aggregates of mixed cells from normal cell lines (normal : normal) at a ratio of 1:1. CMFDA green and CMTPX red cell trackers distinguish between the two cell populations. (A & C) Position of the individually labelled cells. (B & D) Composite images demonstrating relative positions of cell populations. (A & B) Low power images and higher power images (C & D).
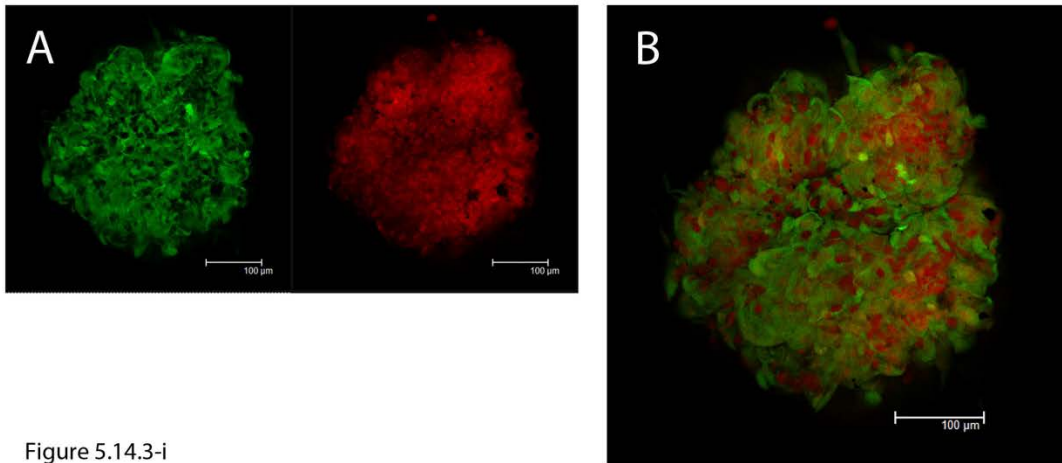
Figure 5.14.3-i
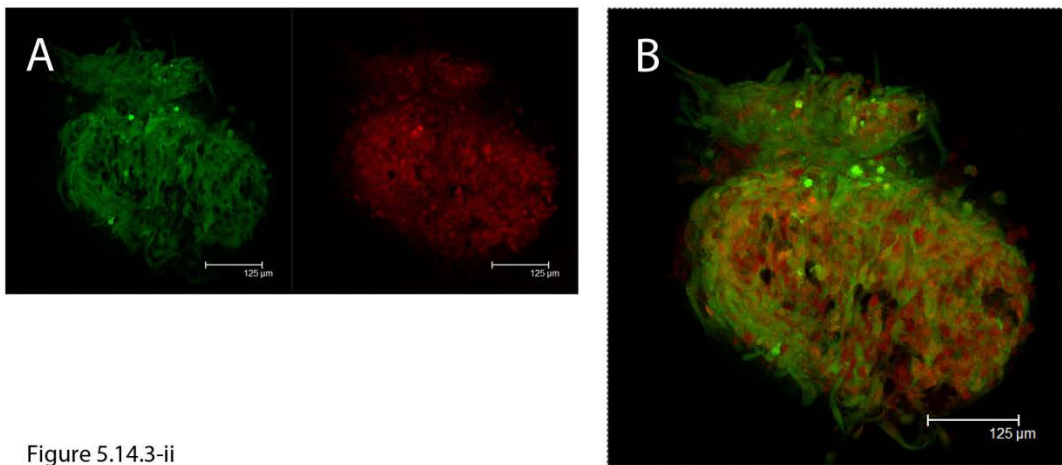
Figure 5.14.3-ii
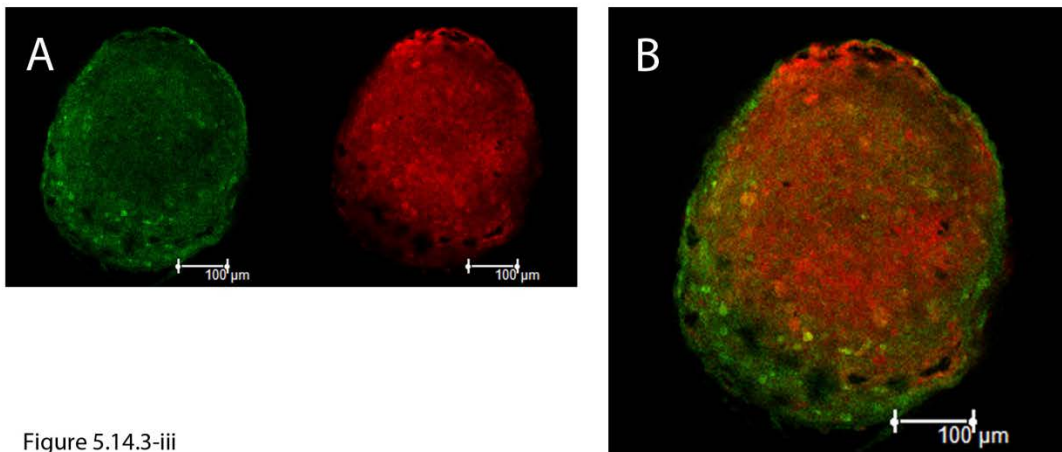
Figure 5.14.3-iii

Figures 5.14.3-i -iii: OA:normal

Chondroprogenitor cell aggregates of mixed cell origins (OA : normal) at a ratio of 1:1. CMFDA green (normal) and CMTPX red (OA) cell trackers distinguish between the two cell populations. (A) Position of the individually labelled cells. (B) Composite image demonstrating relative positions of cell populations. (A & B) Low power images.
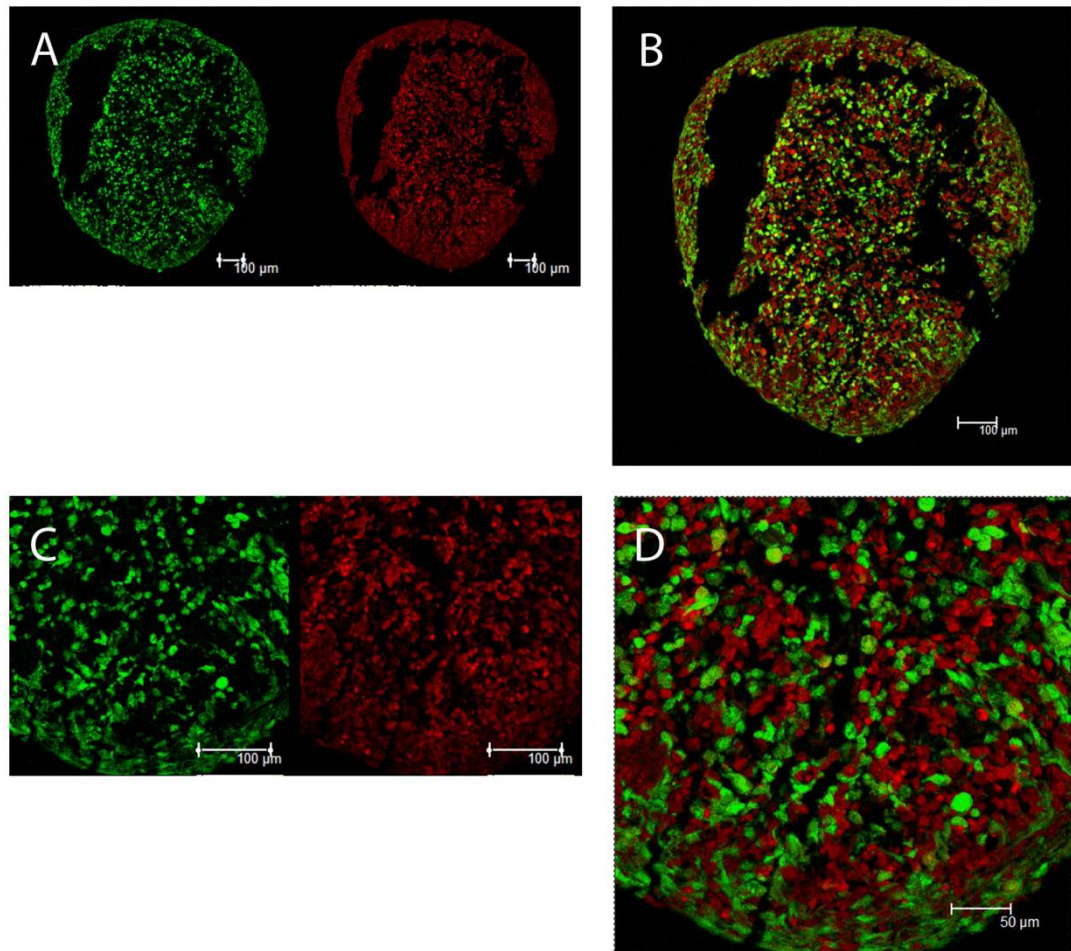
Figure 5.14.4: Sectioned aggregate OA:normal

Sectioned chondroprogenitor cell aggregate of mixed cell origins (OA : normal) at a ratio of 1:1. Initial seeding density of aggregate = 1.0×10^6, formed during optimisation process. CMFDA green (normal) and CMTPX red (OA) cell trackers distinguish between the two cell populations. (A & C) Position of the individually labelled cells. (B & D) Composite images demonstrating relative positions of cell populations. (A & B) Low power images and higher power images (C & D).

Figure 5.15. Fluorescently labelled pellets containing mixed populations of chondroprogenitors (OA:OA, normal:normal and OA:normal) cultured for 21 days in optimised media.

Green CMFDA and red CMTPX cell trackers were used to demonstrate relative positions of labelled cells. Pellets were viewed and imaged using a confocal laser scanning microscope.
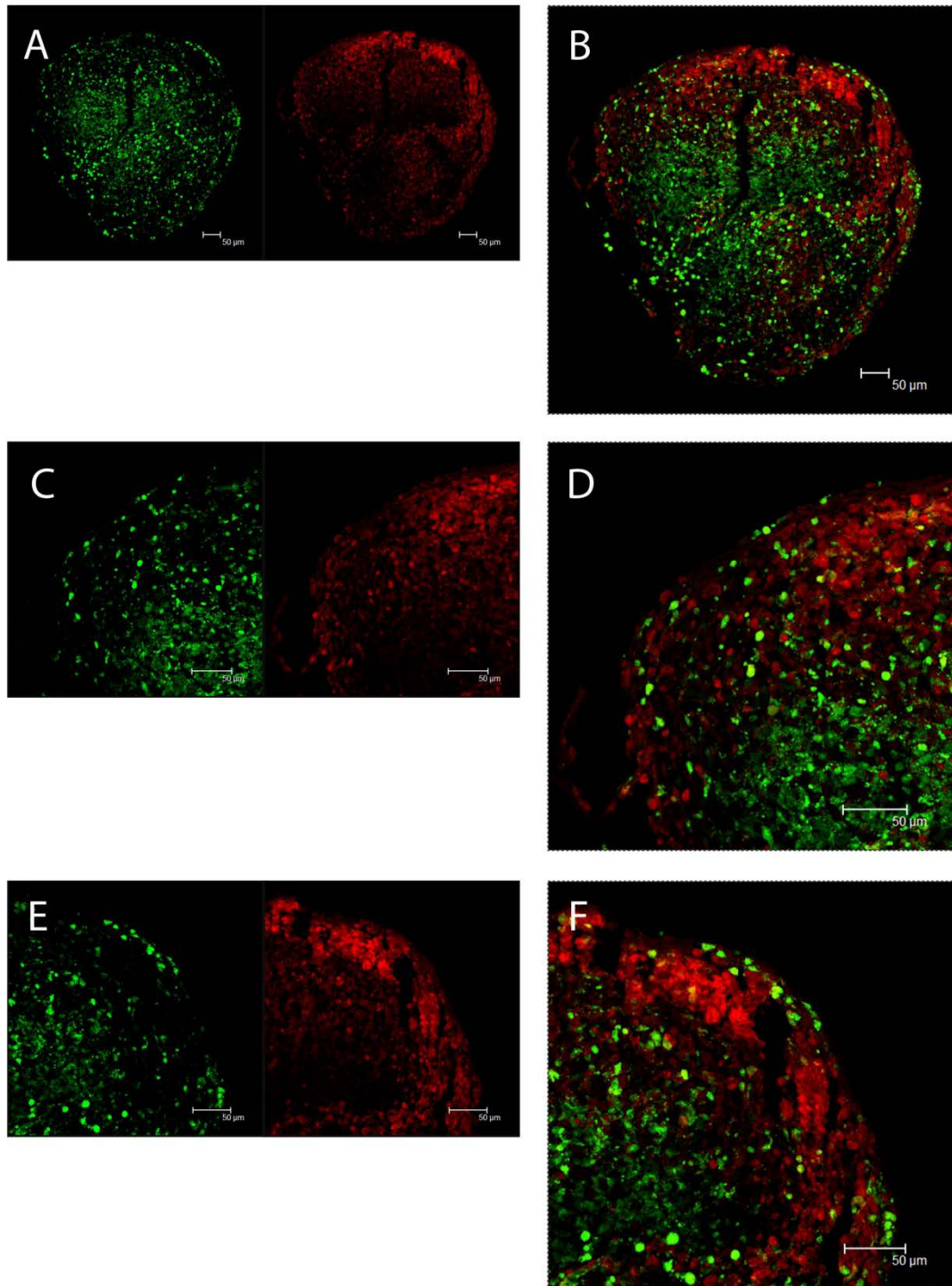
Figure 5.15.1-i: OA:OA

Chondroprogenitor cell pellets of mixed cells from OA cell lines (OA : OA) at a ratio of 1:1. CMFDA green and CMTPX red cell trackers distinguish between the two cell populations. (A, C & E) Position of the individually labelled cells. (B, D & F) Composite images demonstrating relative positions of cell populations. (A & B) Low power images and higher power images (C, D, E, F).
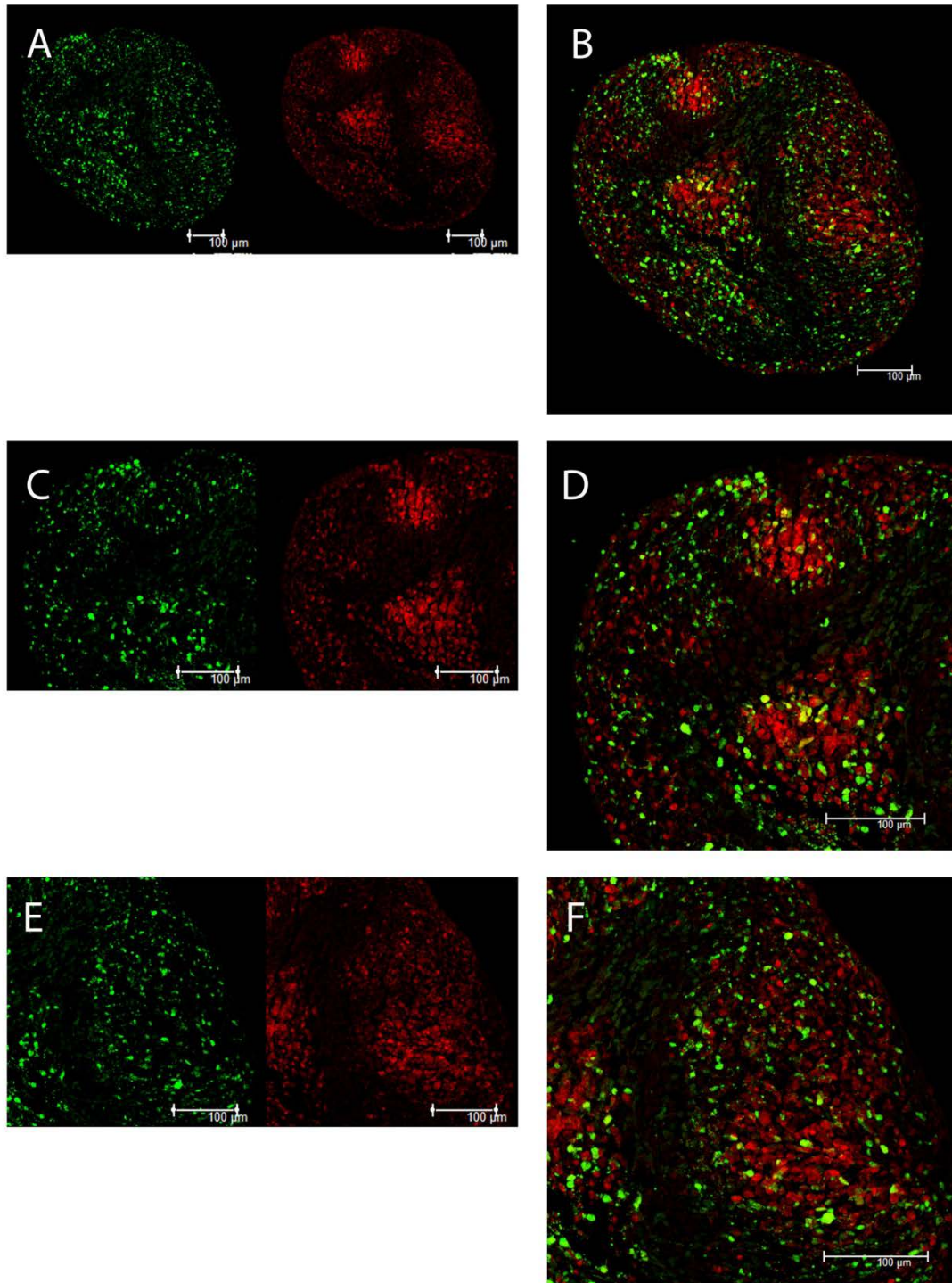
Figure 5.15.1-ii: OA:OA

Chondroprogenitor cell pellets of mixed cells from OA cell lines (OA : OA) at a ratio of 1:1. CMFDA green and CMTPX red cell trackers distinguish between the two cell populations. (A, C & E) Position of the individually labelled cells. (B, D & F) Composite images demonstrating relative positions of cell populations. (A & B) Low power images and higher power images (C, D, E, F).
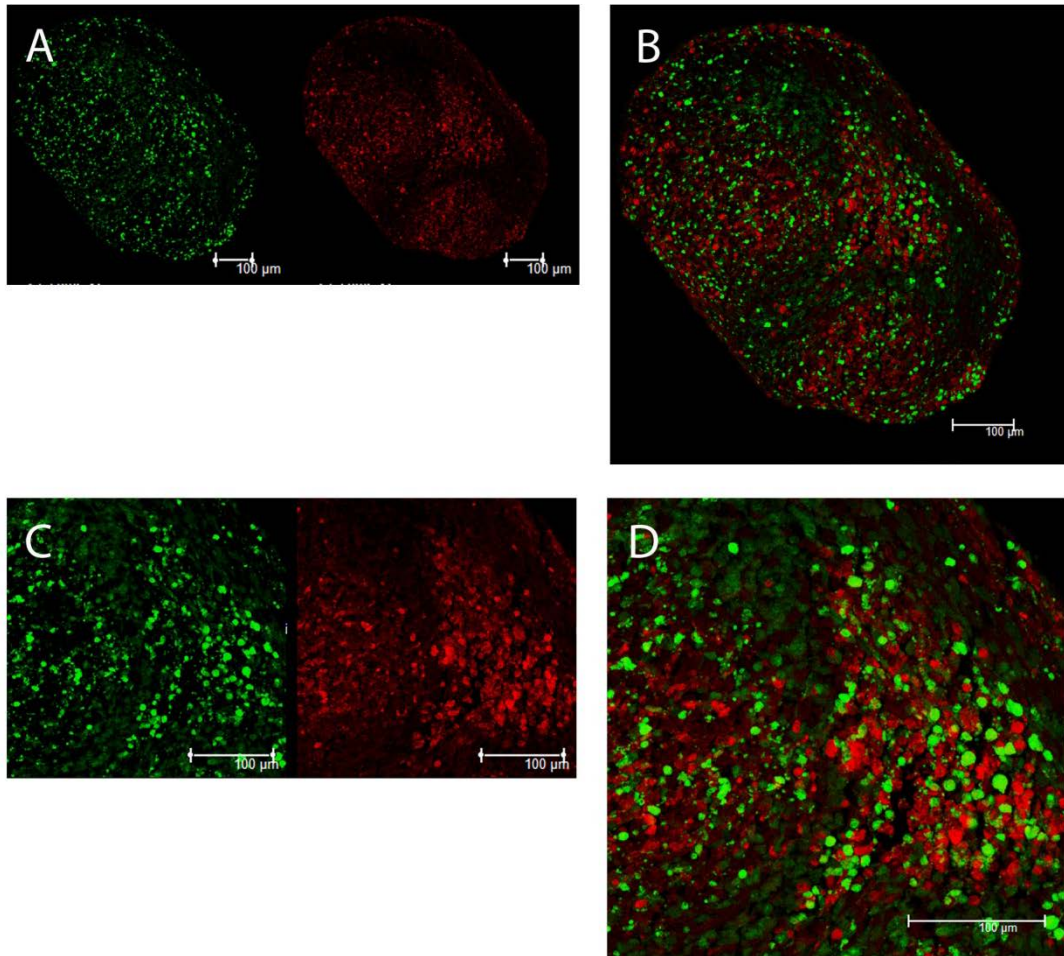
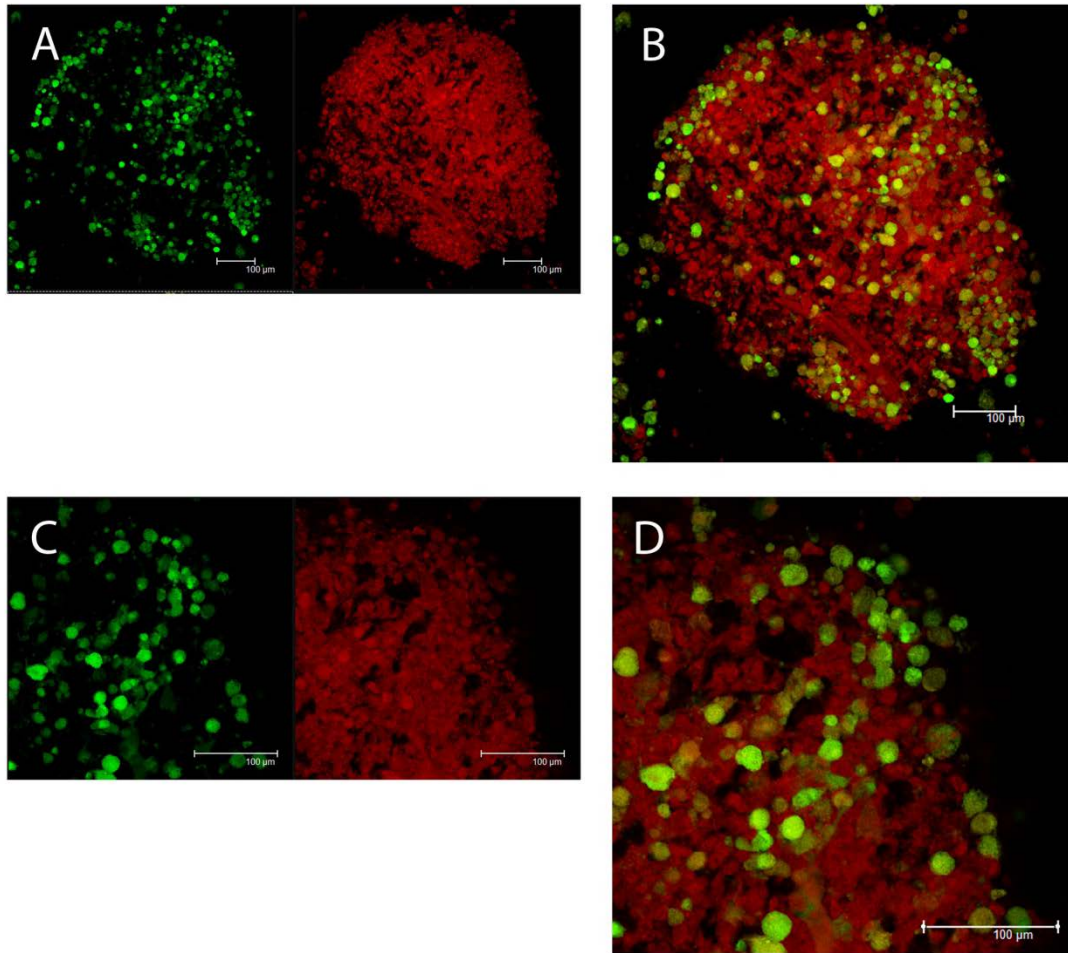**Figure 5.15.1-iii:** OA:OA

Chondroprogenitor cell pellets of mixed cells from OA cell lines (OA : OA) at a ratio of 1:1. CMFDA green and CMTPX red cell trackers distinguish between the two cell populations. (A & C) Position of the individually labelled cells. (B & D) Composite images demonstrating relative positions of cell populations. (A & B) Low power images and higher power images (C & D).
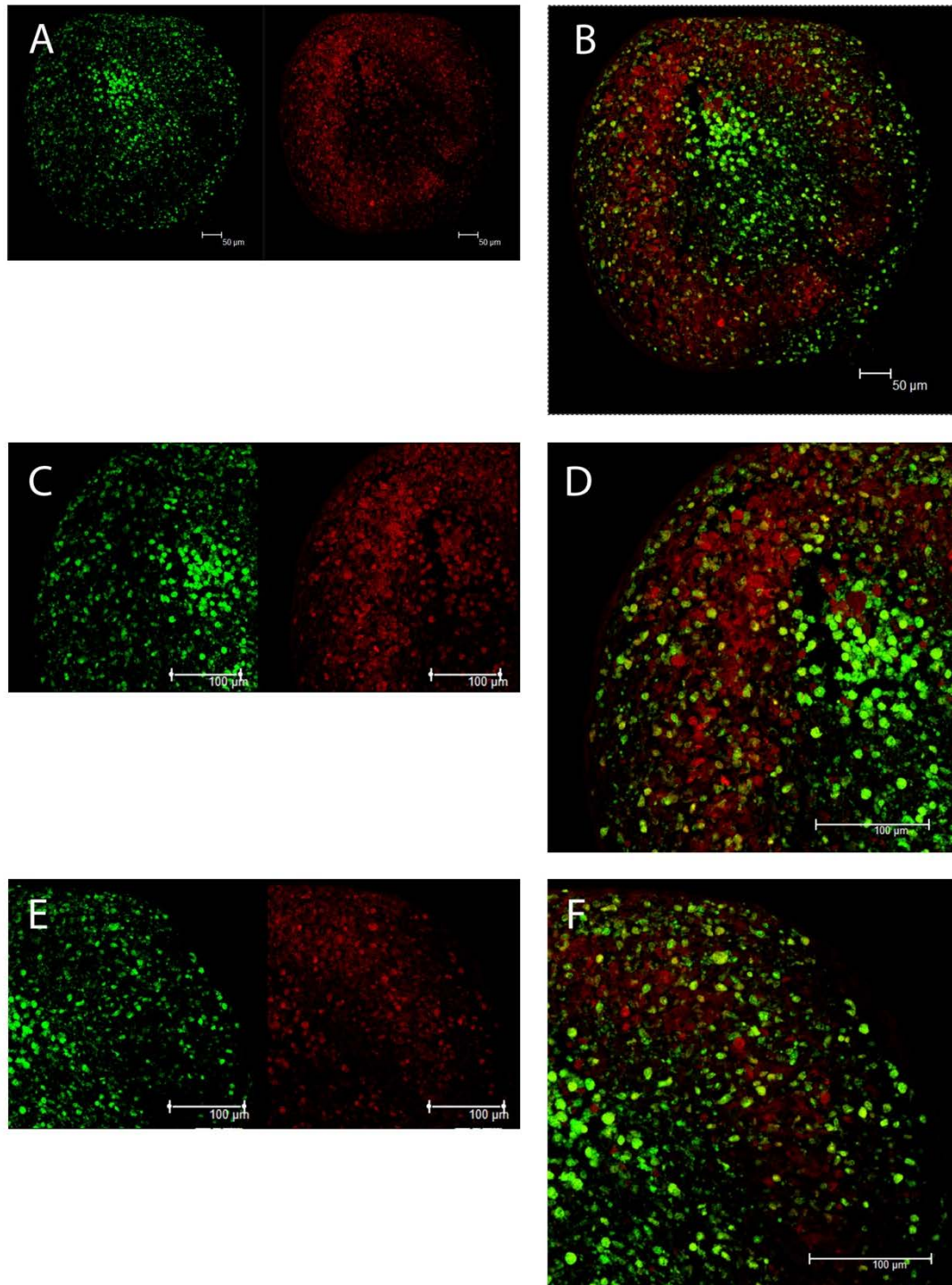
Figure 5.15.2-i: Normal:normal

Chondroprogenitor cell pellets of mixed cells from normal cell lines (normal : normal) at a ratio of 1:1. CMFDA green and CMTPX red cell trackers distinguish between the two cell populations. (A,C & E) Position of the individually labelled cells. (B, D & F) Composite images demonstrating relative positions of cell populations. (A & B) Low power images anf higher power images (C, D, E & F).
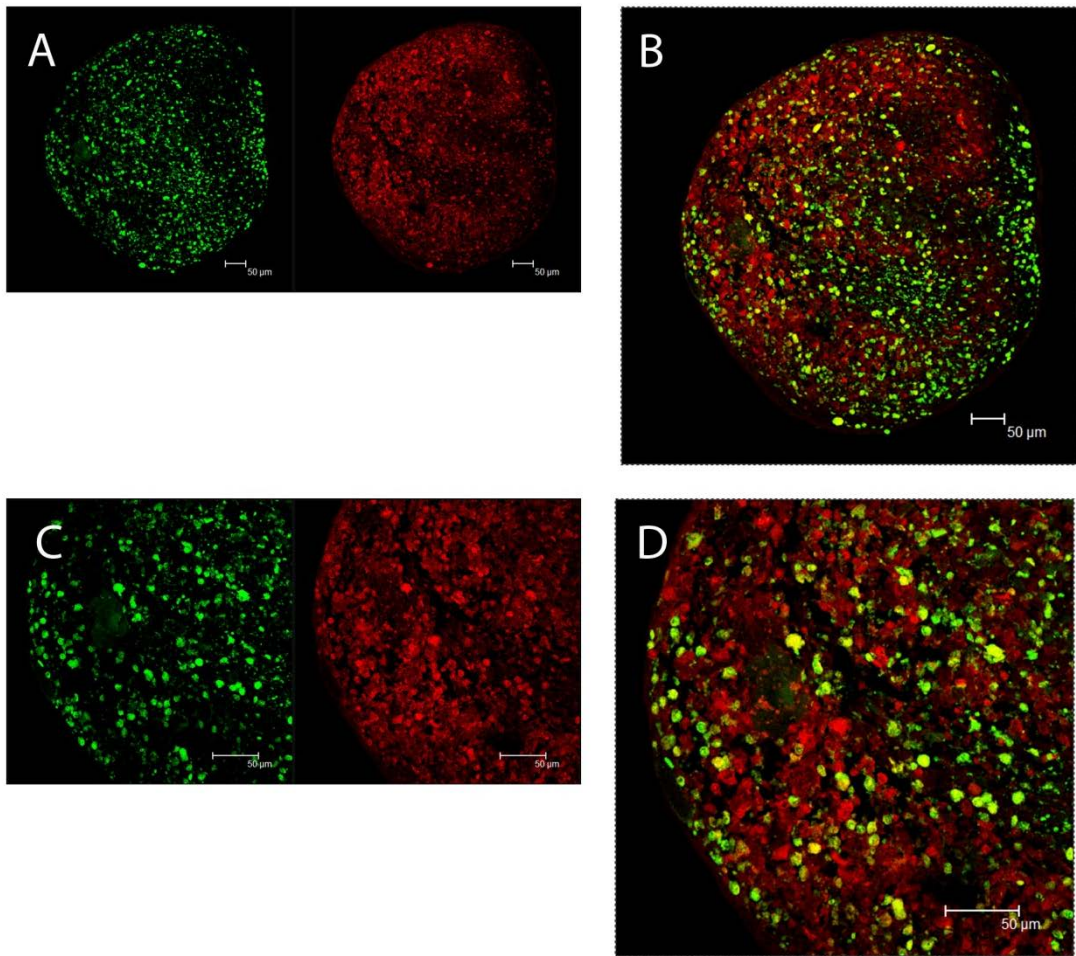
Figure 5.15.2-ii: Normal:normal

Chondroprogenitor cell pellets of mixed cells from normal cell lines (normal : normal) at a ratio of 1:1. CMFDA green and CMTPX red cell trackers distinguish between the two cell populations. (A & C) Position of the individually labelled cells. (B & D) Composite images demonstrating relative positions of cell populations. (A & B) Low power images anf higher power images (C & D).
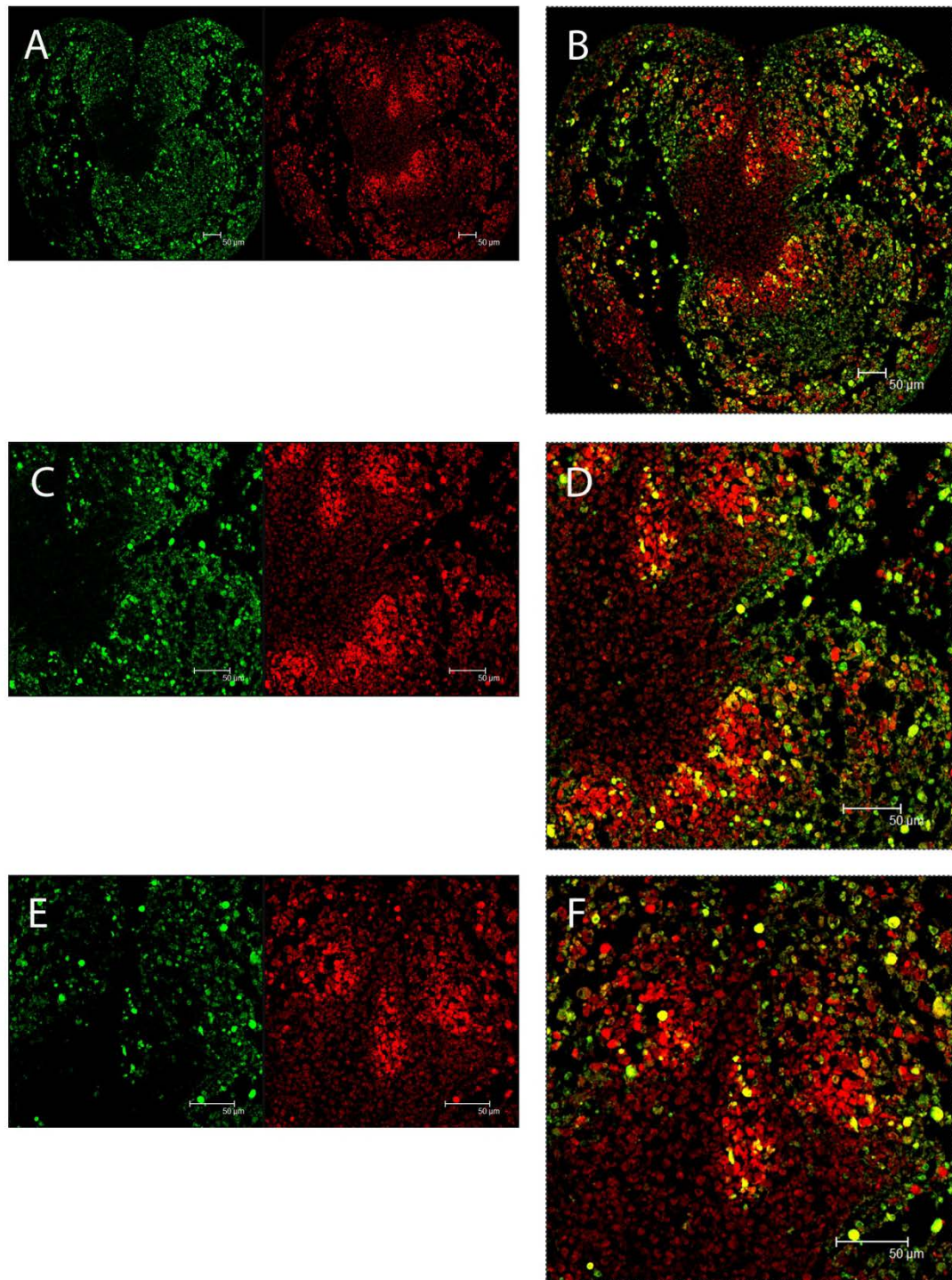
Figure 5.15.3-i: OA:normal

Chondroprogenitor cell pellet of mixed cell origins (OA : normal) at a ratio of 1:1.
CMFDA green (normal) and CMTPX red (OA) cell trackers distinguish between the two
cell populations. (A, C & E) Position of the individually labelled cells. (B, D & F)
Composite images demonstrating relative positions of cell populations. (A & B) Low
power images and higher power images (C, D, E, F).
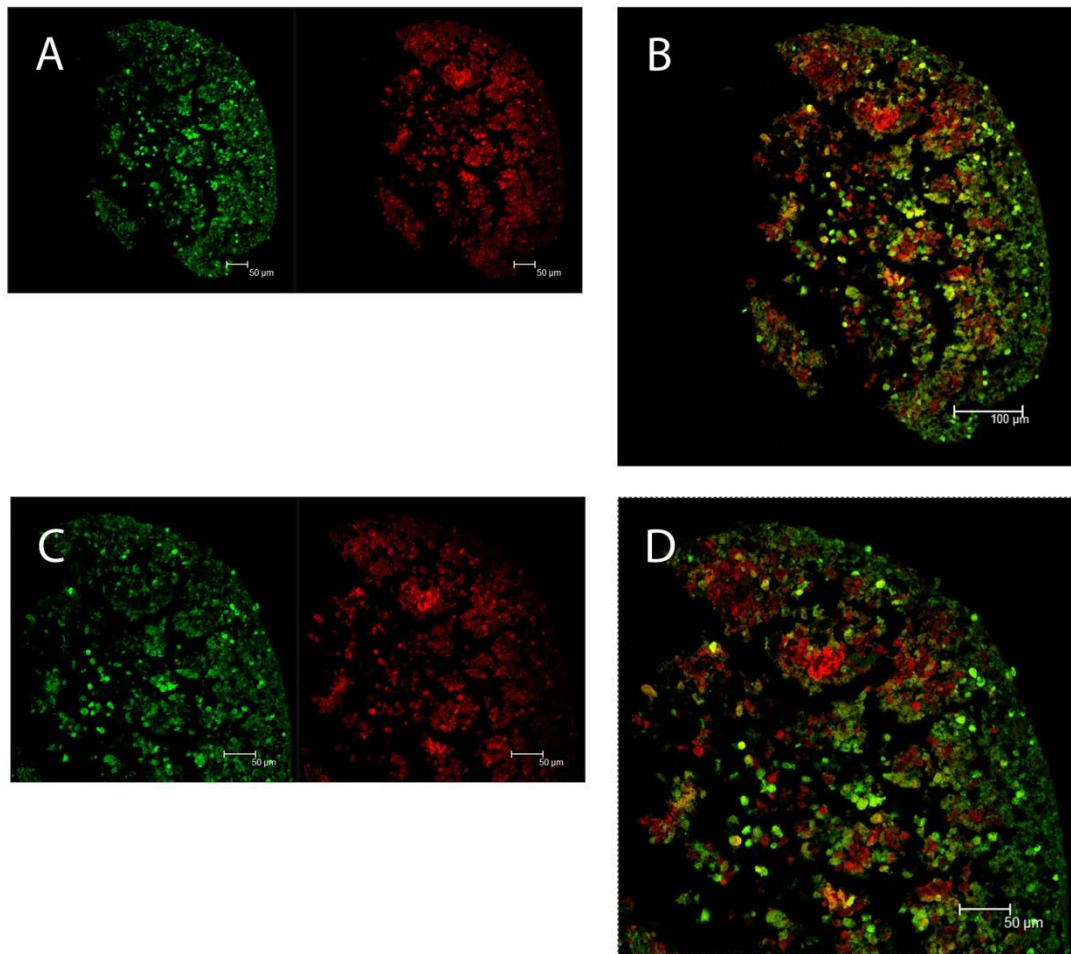
Figure 5.15.3-ii: OA:normal

Chondroprogenitor cell pellet of mixed cell origins (OA : normal) at a ratio of 1:1. CMFDA green (normal) and CMTPX red (OA) cell trackers distinguish between the two cell populations. (A & C) Position of the individually labelled cells. (B & D) Composite images demonstrating relative positions of cell populations. (A & B) Low power images anf higher power images (C & D).
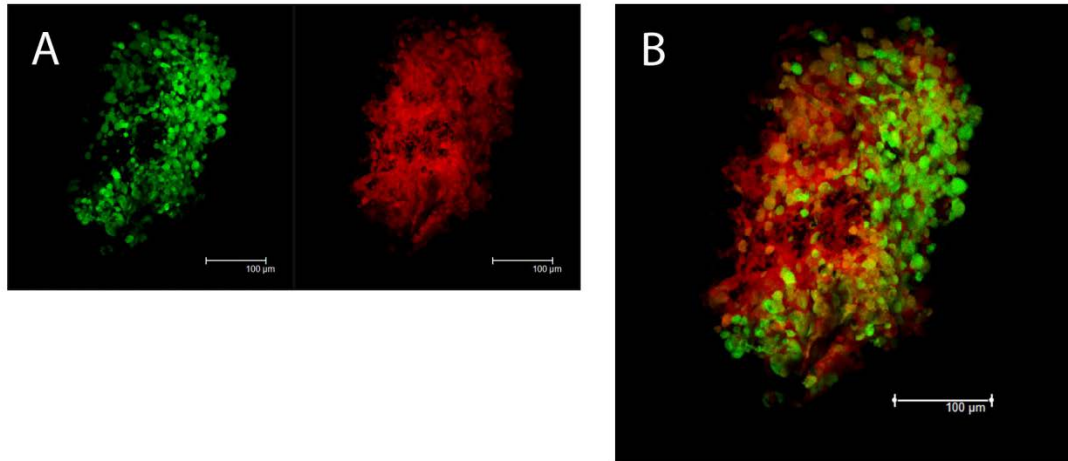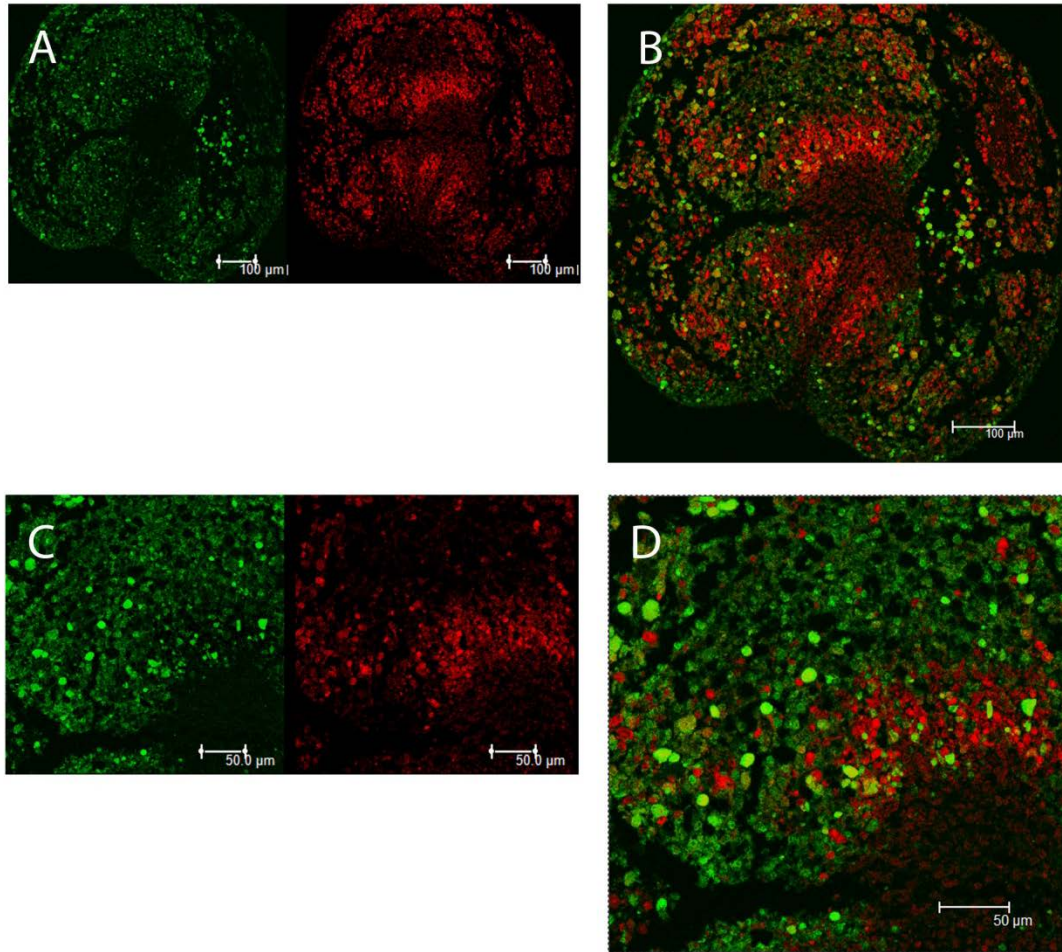
Figure 5.15.3-iii: OA:normal

Chondroprogenitor cell pellet of mixed cell origins (OA : normal) at a ratio of 1:1. CMFDA green (normal) and CMTPX red (OA) cell trackers distinguish between the two cell populations. (A & C) Position of the individually labelled cells. (B & D) Composite images demonstrating relative positions of cell populations. (A & B) Low power images anf higher power images (C & D).

Table 5.2. Summary results table of cell tracker study in aggregates and pellets. Colour code displays results in the form of green (integration), red (segregation) and yellow (largely integrated with distinct areas of segregation).

	OA : OA			Normal : normal		OA : normal		
	i	ii	iii	i	ii	i	ii	iii
Aggregates	I	I (S)	S	S	I (S)	I	I	S
Pellets	S	I (S)	I	S	I (S)	S	I	S

Key

Integration (I)	
Segregation (S)	
Integration with segregation I (S)	

269

5.5. Discussion

The aim of this chapter was to compare chondroprogenitor cells from osteoarthritic cartilage to those isolated from normal cartilage, in order to elucidate whether or not there are distinct differences between the two cell types. Results were also used as a platform to understand integration potentials of the two cell types.

Results from this study should only be used as preliminary data due to the restricted 'n' numbers. Due to time limitations and the difficulties acquiring normal articular cartilage, in certain experiments it was only possible to obtain an n of 2 in the normal category. As such, results may be used only as suggestive data and further data acquisition would be required to give results from this chapter greater weight.

Originally, colony forming efficiencies (CFEs) were calculated using the percentage of colonies formed as a proportion of the initial seeding density (Jones and Watt, 1993). However, depending on seeding densities, cells are known to behave very differently (Melero-Martin et al., 2006). As such, data were represented not only using the traditional method of calculation, but also as a proportion of the number of cells that initially adhered to the tissue culture plastic coated in fibronectin. The difference in results observed may appear to show similar trends, but it is important to highlight the meaning between the two different bar charts. Figure 5.2, demonstrates the percentage of colonies formed based on the initial seeding density. As such, this gives an indication of colony forming cells within the entire collection of cells released during the digestion of the tissue. Within both OA and normal categories, the total percent of colonies formed, according to the colony forming efficiencies was consistently below 0.5 percent. These data are agreeable to that of Dowthwaite et al., (2004) who reported a mean CFE of 0.27 in cells digested from 7-day-old bovine articular cartilage. As such, this population of cells represents a small proportion of the whole contingent in both OA and normal cartilage. Using CFEs as an indicator of the presence of stem cells within the tissue is a justified proposal as these cells are not known to be widely abundant in mature articular cartilage; and as such, a proportion of less than one percent supports these data. It has previously been demonstrated that putative stem cell markers are upregulated in OA tissue (Grogan et al., 2009) and thus, it would be expected that CFEs would be higher in the more diseased state.

270

Ironically, Figure 5.2 demonstrates that this was not the case; however the difference was not statistically significant and so must be regarded cautiously.

The percentage of cells that initially adhered (within 24 hours of plating) to fibronectin gives an indication of the number of active α5β1 integrin receptors on the surface of the digested cells. The trend observed was that there was a higher proportion of cells that initially adhered in the OA cohort when compared to the normal group; however this difference was not statistically significant. This trend however, is agreeable to findings by other authors (Fickert et al., 2004, Grogan et al., 2009) who describe the notable increase in specific stem cell markers in OA tissue. Colonies formed in relation to the number of adherent cells (figure 5.3) therefore, demonstrates the relative proportion of cells that become colony forming in relation to the number cells which were initially selected due to receptor-integrin interactions. As there was a higher proportion of initially adhered cells in the OA group, it may have been hypothesised that this would consequently result in more colonies arising in the OA group. However, this was not the case and, in fact, it was shown that there was a significant decrease in colonies formed in the OA group when compared to colonies formed from the normal group. Consequently, it may be said that within OA, the progenitor cell population is elevated when compared to the normal counterpart (based on the number of initially adhered cells) however, the cells are not fully functioning, and as a result, there is a marked reduction in CFEs in the OA group. Indeed, an editorial by Dealy (2012) states that "the presence of disease may alter endogenous progenitor populations and compromise their ability to accomplish self-repair", which in this case is supported by the reduced CFEs in the diseased tissue.

Within all the categories; CFEs based on initial seeding density, CFEs based on initially adhered cells and numbers of cells that initially adhered to the fibronectin coated plates, significant variation was observed in the normal group. This not only highlights once again heterogeneity between patients, but also the need for larger 'n' numbers in the study. It could also be suggested that within the group of cells that rapidly adhere to fibronectin, there may be sub-groups of cells that can be further classified. As such, it is imperative that a greater understanding is sought not only into the differences between adherent cells, but also into the reasons why cells selected in a like manner form morphologically different colonies. Indeed, work by Barrandon and Green (1987) demonstrated that clones

formed by single human epidermal cells adopted one of three classes. The holoclone which has the greatest reproductive capacity, the paraclone which contains cells with a short replicative lifespan, and the meroclone which encompasses the transitional phase between the two. Upon further study, it may be found that a similar classification phenomenon also occurs in chondroprogenitor cells isolated from articular cartilage.

Primary cultures of normal and OA clonal cell lines were examined for proliferation and senescence using BrdU and SA β-Gal respectively. Relating to the BrdU results specifically, no notable difference was detected between the OA and the normal cultures, however within both individual cohorts there was significant variation. This, therefore suggests, that any differences seen may not necessarily be due to the severity of tissue from which the chondroprogenitor cell is excised, and more so the variation between individual patients.

Proliferation is often assessed using sectioned tissue and immunohistochemistry (as covered in the previous chapter) as a means of detection. It is accepted that chondrocyte proliferation is a characteristic feature typically considered to be part of the OA pathology (Dealy, 2012). However, within this study we are looking specifically into the chondroprogenitors and not the whole chondrocyte population. It could be that this is the reason why the usual discrepancies between proliferation in normal and OA articular cartilage were not observed in this study. As such, one may hypothesise that the chondrocyte clusters as a result of cell proliferation may not be instigated by the residing progenitor cells themselves, but instead, the transient amplifying cells. This hypothesis could explain the failure in self-repair that articular tissue is renowned for –perhaps the chondroprogenitor cells lack the signal necessary for activation. Indeed, a recent study by Pretzel et al., (2011) found that the relative content of superficial and mid-zone progenitors was similar in normal and OA cartilage. As such, it may be suggested that the increased metabolism evident in OA cartilage is not necessarily indicative of increased chondroprogenitor cell activity. Further work would be needed to test this hypothesis.

Clonal cell cultures in both OA and normal categories tested positive for SA β-Gal despite showing continued proliferation. Interestingly it was found that senescence was higher in the normal group when compared to the OA group, although again significant variation

was observed. Clonal cell lines from 'Normal-1' demonstrated particularly high levels of senescence, with a mean of approximately 15 percent labelling positively. If cell lines from this patient were omitted and a comparison was made purely between 'OA-2' and 'Normal-2', no significant difference would have been found. As such, this highlights the issue and need for analysing greater numbers in order to give more statistical validity. As mentioned previously, differences seen may be purely a result of individual patient variation rather than a consequence of disease, however this will not be known until additional numbers are analysed. This issue of low 'n' numbers also applies to the BrdU results obtained through this study and further analysis is imperative in order for solid conclusions to be drawn.

Rate of proliferation may also be a reason for differences observed in senescence results from this study. Unpublished results from our laboratory have shown that some OA cell lines match the proliferation rate of normal cell lines when measured using population doublings, however, other cell lines are far slower. As this experiment was carried out at the same point in time rather than same PD, it may be that the normal cell lines, in this particular instance, proliferated at a faster rate than the OA cell lines and as such were farther along the proliferation timeline when compared to the OA counterpart. This may justify the reason for increased senescence in the normal clonal cell lines. Furthermore, it was also noted in the previous chapter that some cell lines had the tendency to almost suddenly stop proliferating, and so at this stage it is unknown whether or not the cell lines used for this study would have fallen into that category or not.

Potentially affecting both the BrdU and SA β-Gal results in this study, compared to many studies in the literature that rely on histological sections for analysis, are the issues that accompany *in vitro* culturing of cells. Not only are the cells initially stripped from their 3-D environment having adverse effects, the cells are also prone to dedifferentiation (Schnabel et al., 2002). Having said that, this factor does not influence the relative differences observed between chondroprogenitor cells isolated from normal and OA tissue.

Following 21 days in culture, 3-D pellets were digested and analysed for DNA and GAG content as there was no clear morphological difference between the pellets originating from normal or OA articular cartilage. Similar to other findings throughout this chapter,

there was no distinct trend observed between normal and OA pellets it terms of biochemical composition. What was reiterated again however, was the variation between patients within the same cohort. A study conducted by Temple-Wong et al., (2009) demonstrated that GAG levels were also variable in articular cartilage samples which were characteristically normal or showing signs of OA. In this study the variation seen was vast throughout different areas of a specific joint, highlighting the ease of which disparities may arise, when studying human articular cartilage.

Data from this study suggest that GAG content per DNA is very low in both categories, however it is should be noted that in comparison, DNA levels within the pellets of this study appear to be significantly higher than levels reported in other studies. A study by Giovanni et al., (2010) reported less that $10\mu g$ DNA per pellet whereas in this study DNA content per pellet exceeded $90\mu g$. Differences in methods used, therefore, hinders the ability to compare results of this study to previous findings. Perhaps the difference in the way that the pellet cultures were formed and maintained affected the DNA content within the pellet. It may also be that the instruments used in DNA detection in this study was more sensitive or vice versa, raising discrepancies.

It does appear that within this study, levels of GAG are low; particularly in the OA pellets despite there being no statistical significance. Interestingly, it appears that pellets with a higher DNA content do not reciprocate with a higher GAG/DNA content, suggesting that GAG production is hindered in these pellets. This occurred in pellets from both OA and normal origins. The normal pellet which is shown to have the greatest GAG/DNA content is consistent with the pellet with the least DNA content. In this case, it appears that regardless of the low levels of DNA, the pellets were able to produce greater amounts of GAG. As such, the need to further expand this study is emphasized so that definitive trends can be noted. Is this increased GAG production a result of 'normal' chondroprogenitor cells being superior to chondroprogenitor cells isolated from OA tissue? Or is it simply a case of patient variation regardless of OA grade? These are questions that remain to be answered and are essential in the pursuit to understand similarities and differences between chondroprogenitor cells present in normal and OA tissue, so that the true potential of cells in OA tissue can be elucidated.

<u>Aggregation and integration</u>

The integration study of this chapter was carried out in order to determine whether chondroprogenitor cells isolated from OA articular cartilage differ behaviourally from those isolated from normal cartilage; and if so, whether local signals from the normal chondroprogenitor cells would improve cartilage formation in mixed co-cultures. There are many recent studies that look into the effect of combining MSCs to articular cartilage chondrocytes, suggesting that the co-culture system yields a more favourable cartilage phenotype to MSCs alone (Tsuchiya, 2004, Acharya et al., 2011, Bian et al., 2011). Relating back to this study, it was thought that perhaps if the cells showed distinct segregation, indicating two different cohorts of cells, paracrine factors from the normal cells may relay a beneficial effect onto the OA chondroprogenitor cells.

As such, results from the integration study yielded very inconsistent and inconclusive data. It was hypothesised that co-cultures of different OA chondroprogenitors would integrate and show no behavioural differences, however this was not always the case. In both the pellets and aggregates, integration was seen in some cultures and segregation in others. This supports the previous suggestion that within OA articular cartilage, chondroprogenitor cells may be further classified into behaviourally different groups. The pellets, which were cultured for 21 days were given more time to structurally reorganise, however within the OA: OA group, no distinct change in structural conformation could be detected.

The underlying attraction in understanding chondroprogenitor cells in OA tissue is to elucidate whether or not these cells, given the right conditions, have the potential to repair into a hyaline cartilage like tissue. This may be through *in vivo* stimulation or through *in vitro* culture in a laboratory prior to being reinserted into the tissue of interest. Either way it is imperative that the tissue integrates efficiently to produce a decent repair tissue; an issue that is widely discussed in the literature [reviewed by Khan et al., (2008)]. Although further investigations are necessary in order to definitively report this result due to the small 'n' numbers used in this study, these preliminary data suggest that all chondroprogenitor cells isolated from OA tissue using the fibronectin adhesion assay, will not necessarily integrate effortlessly with neighbouring cells. As a result, further work

would need to be carried out in order to determine whether or not, given the right conditions, these cells could be directed into successful integration.

Co-culturing chondroprogenitors from normal origins (normal: normal), and normal with OA (normal: OA) in aggregates and pellets, similarly demonstrated inconsistent data. As such, it appears that the phenomenon of 'good and bad' cell lines that was apparent in the OA group, may also be evident in cells isolated from normal tissue. In the OA: normal group, certain pellets and aggregates were beautifully integrated while others showed pockets of segregation. It may, therefore, be suggested that part of what determines a cell line as a 'good' cell line is its integrative capacity. Circulating paracrine factors from neighbouring cells are involved in improving chondrocyte integration with progenitor cells (Ahmed et al., 2007) and so it would be interesting to investigate these in the cultures used for this study, and identify whether or not paracrine factors are stimulated at differing levels between cell lines. This may reveal information relating to why some cell lines integrate efficiently while others do not.

The protocol used for this co-culture study was adapted from Moscona et al., (1961), however there are currently many intricate scaffolds that have been developed to support 3-D structure formation [recently reviewed by Vinatier et al., (2009)] (Vinatier et al., 2009). As such, it would be beneficial to repeat a similar integration study using a scaffold to support the cells to see if the increased integrity allows scope for better integration between the cells.

In this chapter, mixed cell populations were co-cultured and results demonstrated the compatibility of the different cell types. Testing the integrative capacities of the chondroprogenitor cells to whole cartilage explants would further enhance this work and give a true indication of the integrative capacity of the tissue engineered from chondroprogenitor cells isolated from normal and OA tissue. Additionally, quantitative methods of assessment would then be able to be used to test the adhesive strength of the integration surface using push-out mechanical tests. This work could be coupled with the introduction of scaffolds as mentioned above to achieve greater consistencies and better integrated tissue.

As a whole, this chapter has shown that there is not only great patient variation, but also variation between clonally derived cells lines, which may supersede changes occurring as a result of osteoarthritis. It is also imperative, however, that these results are only regarded as preliminary as 'n' numbers used in this study were restricted. As such a study of a greater magnitude is essential to confirm these results. If, however, these results are shown to be true, it could be positively assumed that chondroprogenitors isolated from OA tissue are not necessarily compromised when compared to normal cells. Instead, it highlights the importance to understand why cells isolated using a single technique are so variable. Understanding this will undoubtedly help with achieving the goal of obtaining a reliable cell type to be used in cartilage repair and regeneration.

Chapter 6:

General Discussion

6. General discussion

A Scottish anatomist and physician, William Hunter, wrote his first paper to the Royal Society in 1743 on articular cartilage and its diseases. In this paper he wrote "If we consult the standard Chirurgical Writers from Hippocrates down to the present age, we shall find, that an ulcerated cartilage is universally allowed to be a very troublesome disease; that it admits of a Cure with more Difficulty than carious Bone; and that, when destroyed, it is never recovered" (Hunter, 1743). Despite the age of this quote, the poor intrinsic capacity for articular cartilage to repair itself continues to be a challenge to scientists and clinicians alike.

The inherently poor repair capacity of articular cartilage is due to the avascular, alymphatic and aneural nature of the tissue, combined with low cellularity and the absence of a germinal layer. The structural and biochemical composition of articular cartilage, however, gives the tissue its characteristic features including resilience, ability to bear high tensile forces and ability to withstand and restore itself after compression (Benjamin, 1999). In health, metabolism and mitotic activity are low resulting in a stable tissue that can be regarded as 'low maintenance' however, this asset in a healthy state exacerbates the problem when diseased.

Osteoarthritis is one of many diseases that affects articular cartilage. Despite the involvement of many surrounding tissues including the subchondral bone, synovium and meniscus; the hyaline cartilage has traditionally been the prime target when investigating the morbid disease (Martel-Pelletier and Pelletier, 2010).

Congruent to the work of others, within this study, the main focus was directed towards evaluating the potential for hyaline cartilage repair using progenitor cells resident in the diseased tissue. However a subset of the work was also directed towards exposing the relationship of neighbouring bone and the clinical implications that this could lead towards.

Figure 6.1 is a summary flow chart which outlines the development of work carried out within this study.
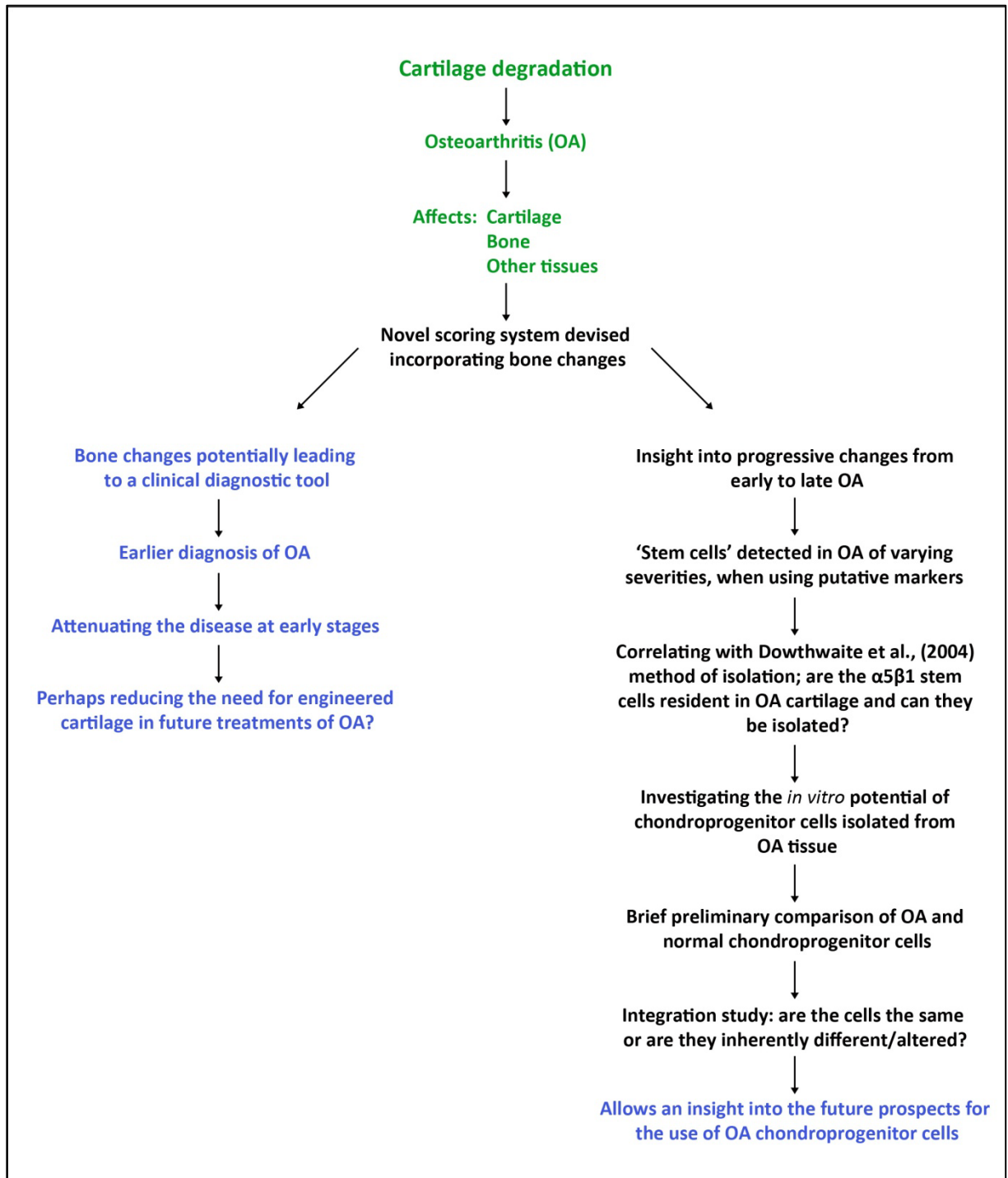
Figure 6.1. Summary flow chart outlining briefly the topic of work (green), the development of work carried out within the study (black) and indications of future benefits which may arise from the work (blue).

As a means of histologically assessing the severity of OA, many scoring systems have been devised; however, the focus of these established scoring systems, as previously mentioned, is the hyaline cartilage (Mainil-Varlet et al., 2003, Mankin et al., 1971, O'Driscoll et al., 1988, Roberts et al., 2003). With the increase in literature highlighting the involvement of bone in the osteoarthritic process, a novel scoring system was devised within the study which incorporates this neighbouring tissue.

An observation that was evident and consistent throughout the study was the degree of variation. It is accepted that cartilage changes occur alongside bony changes (Lajeunesse and Reboul, 2003). However, as disease progression varies so significantly from patient to patient, the involvement of the bone in the development of the disease may also differ. Therefore, bone changes should not be eliminated from the histological assessment process. As such, the new scoring method is more encompassing and consequently provides a more accurate representation of the severity of disease in the histological specimens.

Upon analysis of the scoring system by comparing individual parameters, it was seen that bone changes may precede the degenerative change that occurs in the cartilage. This is a significant finding which needs to be further addressed as it could lead to major repercussions. Is it that metabolic changes occur more quickly in bone and, as such, the bone starts to be symptomatic earlier than the cartilage? Or is it, in fact, a signal that initiates in the bone? Not only does this finding draw upon the "chicken or egg" analogy of which comes first, which in turn could affect targeted treatments, but this also has major clinical implications with regards to diagnostic tools. Indeed, understanding the correlation of bone changes in relation to other changes in OA, if developed properly, could provide a means for diagnosis at early stages of disease, using a minimally invasive bone-based method. Hypothetically, this early diagnosis could translate into early attenuation of the disease, perhaps reducing the need for cartilage repair and regeneration which is currently so critical.

In order for this to be achievable, however, a study of a significantly larger scale would be essential, so that the entire range of scores are covered. This information is vital, ensuring that each stage of progression can be accounted for. A study of a larger scale would also

allow for a better indication of patient variability, as well as inter- and intra-observer variability which will ultimately affect the validity of the new scoring system.

Within this study, the newly devised scoring system was used to correlate disease severity with the expression of matrix markers, chondrocyte proliferation & putative stem cell markers so that progressive changes could be mapped out. The scoring system yielded scores ranging from a possible 0 to 17, where lower scores were representative of a more normal state and high scores were suggestive of thick, eburnated bone. As scores greater than 10 contained little exposed cartilage, it is important to put into context what is meant by a 'high' score, when referring to immunolabelling in the articular cartilage. For instance, immunolabelling in the articular cartilage of OCPs scored between 11 and 17 would not have demonstrated vast amounts of labelling, if any, due to the mere absence of cartilage. As such, the discussion of immunolabelling in the cartilage is only inclusive of OCPs that actually contained a layer of articular cartilage over the subchondral bone.

The presence of type I collagen and procollagen type IIA was confirmed in the early stages of tissue degeneration, suggesting that early remodelling was occurring in an attempt to repair the tissue whilst it was still recoverable. Dissimilar to many articles in the literature, type X collagen expression remained in the deep and calcified cartilage regions, without spreading into other regions of the tissue, upon disease progression. Results of this study demonstrated the difficulty in extrapolating likely trends, and again, highlights the need for a clear understanding in the changes that occur throughout OA to be sought.

Within the small scale of this study, an anomalous OCP was clearly distinct from others. It would be of use to elucidate whether or not OA, as a disease, does in fact rear these different histological specimens or, if perhaps, patients' symptoms are being misdiagnosed. As OA is a multifactoral disease that affects patients to different extents, it seems plausible that this may happen; however, moving on it is essential that patients receive the right diagnosis so that they can receive optimum treatment.

Together with the matrix markers, the scoring system was used to quantify the presence of putative stem cell markers Stro-1 and Notch-1 in tissue of varying severities. Although some data in the literature suggest that these markers can be used as stem cell markers

(Dennis et al., 2002, Dowthwaite et al., 2004), others have reported a surprisingly high number of these cells in OA tissue, questioning their validity as a stem cell marker whilst confirming their involvement in the abnormal cell activation and differentiation process that occurs in OA (Grogan et al., 2009). Results from this study confirmed the suggestion of Grogan et al., (2009) in that over 40 percent of cells in the surface zone labelled positively for both Stro-1 and Notch-1.

The difficulty in identifying stem cells of mesenchymal origin is that, unlike hematopoietic stem cells, there is no single marker that can be used, and the identified markers are not exclusively restricted to the cohort of specialised stem cells. Despite this difficulty, they may however be indicative of stem cell interaction. Previous work from our laboratory has identified a method that relies on $\alpha5\beta1$ interactions to isolate a progenitor cell population from normal articular cartilage of several different species (Dowthwaite et al., 2004, Williams et al., 2010, McCarthy et al., 2011).

Within this study, the question was asked 'Are the chondroprogenitor cells that are present in normal articular cartilage also present in diseased osteoarthritic cartilage, and can they be isolated and expanded?' The answer to this question was 'yes' and it was shown for the first time that these cells could be isolated, and did have capacity to proliferate beyond the potential of chondrocytes, whilst maintaining the chondrogenic phenotype. That said, this result requires further investigation as not all of the cells behaved in the same manner and, as such, the heterogeneity observed between the cells has left many unanswered questions.

Heterogeneity was observed throughout all stages of experimentation; colony morphology, proliferation potential, rate of proliferation and chondrogenic capabilities were all factors which, in some cases, yielded very positive results and, in other cases, raised concern over the potential of these cells. Plasticity into osteogenic and adipogenic lineages was also achieved however, the time required for osteogenic induction varied between cells. This leads to the proposition that perhaps the chondroprogenitors isolated using this method can still be further refined so that the deranged cells are excluded. Indeed, the long-term outlook of these cells is that they would be used for repair and, thus, it is imperative that the cells behave accordingly and homogeneously so that the desired output can be achieved.

Interestingly, unpublished work from our laboratory has investigated telomere length in chondroprogenitors isolated from normal and OA tissue. Telomeres are terminal regions of linear chromosomes that function to allow chromosomal replication and prevent chromosomal fusion and rearrangements (Blackburn, 1991). Telomeres shorten with each cycle of genomic replication, resulting in the cell eventually reaching replicative senescence (Hastie et al., 1990). There is strong evidence to suggest that telomere length is maintained in stem cell populations to facilitate and maintain the cell division required for tissue homeostasis (Allen and Baird, 2009). Results from co-workers have shown that within the normal group of chondroprogenitors, there is a high average telomere length, whereas in the group of chondroprogenitors isolated from OA tissue, there is a distinct division whereby 60 percent of the cells display lower telomere lengths. Telomere length of the remaining 40 percent is slightly lower, yet comparable, to that of the normal group. As such, these findings support the results of this study in that the heterogeneity observed may in fact be due to different groups of cells exhibiting behavioural discrepancies.

In a continued attempt to decipher whether or not chondroprogenitor cells isolated from OA tissue was similar or dissimilar to chondroprogenitors of normal origin, a preliminary study was carried out to initially compare the two populations of cells. Contradictory to previous work from our laboratory, heterogeneity was also observed within the normal cohort. As such, no significant difference between the OA and normal groups was observed when comparing colony forming efficiencies of cell lines, BrdU incorporation of cells, and biochemical composition of pellets. Senescence associated β- galactosidase was surprisingly higher in the normal group, however, this may be due to the cells being at a later population doubling as a result of faster proliferation rates. This would need to be further investigated in order to make a solid conclusion.

An integration study was carried out to see whether any structural reorganisation would occur upon mixing different populations of cells, as local circulating paracrine factors are known to influence cell interactions (Ahmed et al., 2007). Integration between normal and OA cells could be indicative of a positive effect of the normal chondroprogenitor cells on the OA cells, and/or, suggestive of the fact that perhaps the cells are indeed similar with comparable behavioural responses therefore resulting in no segregation between the cells.

Unfortunately, within this study it was not possible to extrapolate any conclusions, and these results must be used merely as a springboard for more experimentation. It is necessary to undertake this study on a much larger scale in order to elucidate conclusively the similarities or differences between chondroprogenitor cells isolated from normal and OA articular cartilage.

As a whole, it can be said that osteoarthritic tissue does contain a group of chondroprogenitor cells, and it has been shown that some of these cells do have the potential to repair articular cartilage. This is a pivotal finding as many characteristics seen within this study reflect those of other stem cells, highlighting their capability potentials which can be further exploited to aid the field of regenerative medicine.

That said, this study has also highlighted the importance of carrying out further work in order to establish sufficient groundwork to be able to consider these cells as suitable candidates for translational use in the future.

6.1. Further work

Referring back to the early work on the scoring system and the correlation between bone and cartilage, it would be interesting to determine conclusively whether the trend of the bone changes preceding the cartilage changes in humans, is in fact true, as this could offer clinical implications. On a similar note, it would be of interest to further this study by assessing the correlation between the degree of pain experienced by the patient, and scores obtained using this new scoring system. If pain was directly related to the score, and the score tied-in with degree of bone change, then this could further enhance the case for developing a method for a bone-based diagnostic tool.

One of the major challenges faced in part of this study was the issue of auto-fluorescence in the osteochondral plugs. Many failed attempts were carried out to reduce this hindrance during this study and, as such, the less sensitive method of peroxidise labelling as used rather than fluorescent labelling. Background labelling is a well known issue particularly in aged, human tissue; however, it may also be exacerbated by tissue preparation and fixation techniques. As such, although seemingly basic, it would be of use to methodically

try different fixation, decalcification, and auto-fluorescence reducing techniques in order to establish a method that can be used successfully using immunofluorescence. Similarly, epitope unmasking and antigen retrieval techniques can also contribute to the problem, so it would be of use to include these in the study.

With regards to the *in vitro* work, heterogeneity was a distinguishable recurring factor throughout this study. As such, it would be of use to know whether additional factors affected the results of this study or if the cells are inherently enigmatic. As such, it would be interesting to determine whether expansion time affected the composition of the engineered pellets. In other words, do the growth kinetics of particular cell lines affect the chondrogenicity and integrity of a pellet? Similarly, it would be of use to further investigate the underlying reason behind the different colonies which initially form, so that the colony selection process need not be at random. Equally, this may result in reduced heterogeneity and more consistent data.

Additionally, it would be interesting to investigate whether maturity, or age of patient affects the structural integrity and composition of the chondrogenic pellets. This is difficult, however, due to the lack of availability of osteoarthritic tissue in patients of a young age.

The *in vitro* section of this study relied heavily on the Dowthwaite et al., (2004) method of isolating chondroprogenitors cells from articular cartilage. In his study, he identifies the progenitor cells in the surface zone of the tissue. Due to the lack of uniform tissue acquired from total knee replacements in patients with OA, it is difficult to definitively separate cells from the surface from the remaining regions. As such, cells from regions other than the surface were included in this study and this may have been another cause for the heterogeneity in this study. Indeed, a study by Siczkowski and Watt (1990) have demonstrated that cells from the upper zone of articular cartilage adhere and proliferate more slowly than cells from the lower zones when cultured *in vitro*. As such, as it was not only the surface zone that was being digested for cell isolation, could it be that during the 20 minute adhesion period, chondroprogenitors were adhering together with deep zone chondrocytes purely because they have a tendency to adhere quickly? It would be interesting to investigate this further, as it may again, be a contributing factor to the

heterogeneity observed within this study. Perhaps the isolation procedure in osteoarthritic cartilage needs to be further refined in order to obtain a more specific cohort of cells.

Linking the work on histological sections with the *in vitro* findings, it would also be interesting to determine whether there is a correlation between the cells which labelled positively for Stro-1 and Notch-1, and the cells that adhere during the fibronectin adhesion assay. As such, a fluorescently activated cell sorter could be used to sort and replate positively immunolabelled cells, and subsequently, colony forming efficiencies and percentage of initial adhesion to fibronectin following the 'Dowthwaite method' could be investigated. This would give us an indication as to whether or not it is in fact the same cells which label positively for Stro-1 and/or Notch-1 that are involved in the $\alpha5\beta1$ interactions. Not only would this enable us to decipher a more specific means of chondroprogenitor cell selection, but it will also unveil more crucial information regarding stem cells in osteoarthritic tissue.

Lastly, with regards to the final chapter which addressed similarities and differences between chondroprogenitors from OA and normal tissue, as well as their integrative capacities; it would be necessary to repeat this study on a larger scale. A solid conclusion to that study would reveal information that could be critical, when considering taking this work forward into translational science.

7: References

7. References

Acharya C, Adesida A, Zajac P, et al. (2011) Enhanced chondrocyte proliferation and mesenchymal stromal cells chondrogenesis in coculture pellets mediate improved cartilage formation. *J Cell Physiol,* **227,** 88-97.

Ahmed N, Dreier R, Gopferich A, Grifka J, Grassel S (2007) Soluble signalling factors derived from differentiated cartilage tissue affect chondrogenic differentiation of rat adult marrow stromal cells. *Cell Physiol Biochem,* **20,** 665-78.

Aigner T, Haag J, Martin J, Buckwalter J (2007) Osteoarthritis: aging of matrix and cells--going for a remedy. *Curr Drug Targets,* **8,** 325-31.

Aigner T, Zhu Y, Chansky HH, Matsen FA, 3rd, Maloney WJ, Sandell LJ (1999) Reexpression of type IIA procollagen by adult articular chondrocytes in osteoarthritic cartilage. *Arthritis Rheum,* **42,** 1443-50.

Aigner T, Zien A, Hanisch D, Zimmer R (2003) Gene expression in chondrocytes assessed with use of microarrays. *J Bone Joint Surg Am,* **85-A Suppl 2,** 117-23.

Akiyama H, Chaboissier MC, Martin JF, Schedl A, de Crombrugghe B (2002) The transcription factor Sox9 has essential roles in successive steps of the chondrocyte differentiation pathway and is required for expression of Sox5 and Sox6. *Genes Dev,* **16,** 2813-28.

Alberts B, Johnson A, Lewis J (2002) *Molecular biology of the cell,* Garland Science, New York.

Allard SA, Maini RN, Muirden KD (1988) Cells and matrix expressing cartilage components in fibroblastic tissue in rheumatoid pannus. *Scand J Rheumatol Suppl,* **76,** 125-9.

Allen ND, Baird DM (2009) Telomere length maintenance in stem cell populations. *Biochim Biophys Acta,* **1792,** 324-8.

Alsalameh S, Amin R, Gemba T, Lotz M (2004) Identification of mesenchymal progenitor cells in normal and osteoarthritic human articular cartilage. *Arthritis Rheum,* **50,** 1522-32.

Altindag O, Erel O, Aksoy N, Selek S, Celik H, Karaoglanoglu M (2007) Increased oxidative stress and its relation with collagen metabolism in knee osteoarthritis. *Rheumatol Int,* **27,** 339-44.

Amin AK, Huntley JS, Simpson AH, Hall AC (2009) Chondrocyte survival in articular cartilage: the influence of subchondral bone in a bovine model. *J Bone Joint Surg Br,* **91,** 691-9.

Andriamanalijaona R (2010) Cell therapies for articular cartilage repair: chondrocytes and mesenchymal stem cells. In *Regenerative medicine and biomaterials for the repair of connective tissues* (ed Archer CW, Ralphs, J.). Woodhead Publishing Limited.

Appleyard RC, Burkhardt D, Ghosh P, et al. (2003) Topographical analysis of the structural, biochemical and dynamic biomechanical properties of cartilage in an ovine model of osteoarthritis. *Osteoarthritis Cartilage,* **11,** 65-77.

Archer CW (1994) Skeletal development and osteoarthritis. *Ann Rheum Dis,* **53,** 624-30.

Archer CW, Dowthwaite GP, Francis-West P (2003) Development of synovial joints. *Birth Defects Res C Embryo Today,* **69,** 144-55.

Archer CW, Francis-West P (1999) The development of joints and articular cartilage. In *Biology of the synovial joint* (eds Archer CW, Caterson B, Benjamin M, Ralphs JR). Amsterdam: Harwood academic publishers.

Archer CW, Francis-West P (2003) The chondrocyte. *Int J Biochem Cell Biol,* **35,** 401-4.

Archer CW, McDowell J, Bayliss MT, Stephens MD, Bentley G (1990) Phenotypic modulation in sub-populations of human articular chondrocytes in vitro. *J Cell Sci,* **97 (Pt 2),** 361-71.

Archer CW, Morrison EH, Bayliss MT, Ferguson MW (1996) The development of articular cartilage: II. The spatial and temporal patterns of glycosaminoglycans and small leucine-rich proteoglycans. *J Anat,* **189 (Pt 1),** 23-35.

Archer CW, Morrison H, Pitsillides AA (1994) Cellular aspects of the development of diarthrodial joints and articular cartilage. *J Anat,* **184 (Pt 3),** 447-56.

Arican M, Carter SD, Bennett D, Ross G, Ayad S (1996) Increased metabolism of collagen VI in canine osteoarthritis. *J Comp Pathol,* **114,** 249-56.

Arnoldi CC, Lemperg R, Linderholm H (1971) Immediate effect of osteotomy on the intramedullary pressure in the femoral head and neck in patients with degenerative osteoarthritis. *Acta Orthop Scand,* **42,** 454-5.

Artavanis-Tsakonas S, Rand MD, Lake RJ (1999) Notch signaling: cell fate control and signal integration in development. *Science,* **284,** 770-6.

Austin CP, Feldman DE, Ida JA, Jr., Cepko CL (1995) Vertebrate retinal ganglion cells are selected from competent progenitors by the action of Notch. *Development,* **121,** 3637-50.

Awad HA, Halvorsen YD, Gimble JM, Guilak F (2003) Effects of transforming growth factor beta1 and dexamethasone on the growth and chondrogenic differentiation of adipose-derived stromal cells. *Tissue Eng,* **9,** 1301-12.

Ayad S, Boot-Handford RP, Humphries MJ, Kadler KE, Shuttleworth CA (1998) *The extracellular matrix: Facts book.,* Academic Press, Harcourt Brace & Company, Publishers.

Bailey AJ, Mansell JP (1997) Do subchondral bone changes exacerbate or precede articular cartilage destruction in osteoarthritis of the elderly? *Gerontology,* **43,** 296-304.

Bailey AJ, Sims TJ, Knott L (2002) Phenotypic expression of osteoblast collagen in osteoarthritic bone: production of type I homotrimer. *Int J Biochem Cell Biol,* **34,** 176-82.

Baron M (2003) An overview of the Notch signalling pathway. *Semin Cell Dev Biol,* **14,** 113-9.

Barrandon Y, Green H (1987) Three clonal types of keratinocyte with different capacities for multiplication. *Proc Natl Acad Sci U S A,* **84,** 2302-6.

Barry F, Boynton RE, Liu B, Murphy JM (2001) Chondrogenic differentiation of mesenchymal stem cells from bone marrow: differentiation-dependent gene expression of matrix components. *Exp Cell Res,* **268,** 189-200.

Barry FP (2003) Mesenchymal stem cell therapy in joint disease. *Novartis Found Symp,* **249,** 86-96; discussion 96-102, 170-4, 239-41.

Bayliss MT, Howat S, Davidson C, Dudhia J (2000) The organization of aggrecan in human articular cartilage. Evidence for age-related changes in the rate of aggregation of newly synthesized molecules. *J Biol Chem,* **275,** 6321-7.

Bayliss MT, Osborne D, Woodhouse S, Davidson C (1999) Sulfation of chondroitin sulfate in human articular cartilage. The effect of age, topographical position, and zone of cartilage on tissue composition. *J Biol Chem,* **274,** 15892-900.

Bayliss MT, Roughley PJ (1985) The properties of proteoglycan prepared from human articular cartilage by using associative caesium chloride gradients of high and low starting densities. *Biochem J,* **232,** 111-7.

Benjamin M (1999) An introduction to synovial joints. In *Biology of the synovial joint* (eds Archer CW, Caterson B, Benjamin M, Ralphs JR), pp. 1- 9. Amsterdam: Harwood Academic Publishers.

Benninghof A (1925) Spaltlinen am Knochen, eine Mrthode zur Ermittlung der Architektur platter Knochen. *Verh Anat Ges,* **34,** 189.

Bentley G, Greer RB, 3rd (1971) Homotransplantation of isolated epiphyseal and articular cartilage chondrocytes into joint surfaces of rabbits. *Nature,* **230,** 385-8.

Benya PD, Padilla SR, Nimni ME (1978) Independent regulation of collagen types by chondrocytes during the loss of differentiated function in culture. *Cell,* **15,** 1313-21.

Benya PD, Shaffer JD (1982) Dedifferentiated chondrocytes reexpress the differentiated collagen phenotype when cultured in agarose gels. *Cell,* **30,** 215-24.

Beris AE, Lykissas MG, Papageorgiou CD, Georgoulis AD (2005) Advances in articular cartilage repair. *Injury,* **36 Suppl 4,** S14-23.

Berthiaume MJ, Raynauld JP, Martel-Pelletier J, et al. (2005) Meniscal tear and extrusion are strongly associated with progression of symptomatic knee osteoarthritis as assessed by quantitative magnetic resonance imaging. *Ann Rheum Dis,* **64,** 556-63.

Bertrand J, Cromme C, Umlauf D, Frank S, Pap T (2010) Molecular mechanisms of cartilage remodelling in osteoarthritis. *Int J Biochem Cell Biol,* **42,** 1594-601.

Bian L, Zhai DY, Mauck RL, Burdick JA (2011) Coculture of human mesenchymal stem cells and articular chondrocytes reduces hypertrophy and enhances functional properties of engineered cartilage. *Tissue Eng Part A,* **17,** 1137-45.

Bieback K, Kern S, Kluter H, Eichler H (2004) Critical parameters for the isolation of mesenchymal stem cells from umbilical cord blood. *Stem Cells,* **22,** 625-34.

Birk DE, Fitch JM, Babiarz JP, Linsenmayer TF (1988) Collagen type I and type V are present in the same fibril in the avian corneal stroma. *J Cell Biol,* **106,** 999-1008.

Blackburn EH (1991) Structure and function of telomeres. *Nature,* **350,** 569-73.

Blaney Davidson EN, Remst DF, Vitters EL, et al. (2009) Increase in ALK1/ALK5 ratio as a cause for elevated MMP-13 expression in osteoarthritis in humans and mice. *J Immunol,* **182,** 7937-45.

Boos N, Nerlich AG, Wiest I, von der Mark K, Ganz R, Aebi M (1999) Immunohistochemical analysis of type-X-collagen expression in osteoarthritis of the hip joint. *J Orthop Res,* **17,** 495-502.

Bora FW, Jr., Miller G (1987) Joint physiology, cartilage metabolism, and the etiology of osteoarthritis. *Hand Clin,* **3,** 325-36.

Breinan HA, Minas T, Hsu HP, Nehrer S, Sledge CB, Spector M (1997) Effect of cultured autologous chondrocytes on repair of chondral defects in a canine model. *J Bone Joint Surg Am,* **79,** 1439-51.

Brew CJ, Clegg PD, Boot-Handford RP, Andrew JG, Hardingham T (2010) Gene expression in human chondrocytes in late osteoarthritis is changed in both fibrillated and intact cartilage without evidence of generalised chondrocyte hypertrophy. *Ann Rheum Dis,* **69,** 234-40.

Brittberg M (1999) Autologous chondrocyte transplantation. *Clin Orthop Relat Res*, S147-55.

Brittberg M, Lindahl A, Nilsson A, Ohlsson C, Isaksson O, Peterson L (1994) Treatment of deep cartilage defects in the knee with autologous chondrocyte transplantation. *N Engl J Med,* **331,** 889-95.

Brown RA, Jones KL (1990) The synthesis and accumulation of fibronectin by human articular cartilage. *J Rheumatol,* **17,** 65-72.

Brunet LJ, McMahon JA, McMahon AP, Harland RM (1998) Noggin, cartilage morphogenesis, and joint formation in the mammalian skeleton. *Science,* **280,** 1455-7.

Buckland-Wright C (2004) Subchondral bone changes in hand and knee osteoarthritis detected by radiography. *Osteoarthritis Cartilage,* **12 Suppl A,** S10-9.

Buckley CT, Vinardell T, Kelly DJ (2010) Oxygen tension differentially regulates the functional properties of cartilaginous tissues engineered from infrapatellar fat pad derived MSCs and articular chondrocytes. *Osteoarthritis Cartilage,* **18,** 1345-54.

Buckwalter JA (1995a) Activity vs. rest in the treatment of bone, soft tissue and joint injuries. *Iowa Orthop J,* **15,** 29-42.

Buckwalter JA (1995b) Osteoarthritis and articular cartilage use, disuse, and abuse: experimental studies. *J Rheumatol Suppl,* **43,** 13-5.

Buckwalter JA (1999) New approaches to articular cartilage repair and regeneration. In *Biology of the Synovial Joint* (eds Archer CW, Caterson B, Benjamin M, Ralphs JR), pp. 201-221. Amsterdam: Harwood academic publishers.

Buckwalter JA, Hunziker EB (1999) Articular cartilage morphology and biology. In *Biology of the synovial joint* (eds Archer CW, Caterson B, Benjamin M, Ralphs JR). Amsterdam: Harwood academic publishers.

Buckwalter JA, Lohmander S (1994) Operative treatment of osteoarthrosis. Current practice and future development. *J Bone Joint Surg Am,* **76,** 1405-18.

Buckwalter JA, Mankin HJ (1997) Articular cartilage II. Degeneration and osteoarthritis, repair, regeneration and transplantation. *J Bone Joint Surg* **79A,** 612- 632.

Buckwalter JA, Mankin HJ (1998) Articular cartilage: tissue design and chondrocyte-matrix interactions. *Instr Course Lect,* **47,** 477-86.

Buckwalter JA, Martin JA (2006) Osteoarthritis. *Adv Drug Deliv Rev,* **58,** 150-67.

Buckwalter JA, Mow VC (1992) Cartilage repair in osteoarthritis. In *Osteoarthritis diagnosis and management* (eds Moskowitz RW, Howell DS, Goldberg VM, Mankin HJ). Philadelphia: Saunders.

Buckwalter JA, Rosenberg LA, Hunziker EB (1990) Articular cartilage: composition, structure, response to injury, and methods of facilitation repair. In *Articular cartilage and knee joint function basic science and arthroscopy* (ed Ewing JW). New York: Raven Press.

Burton-Wurster N, Lust G, Macleod JN (1997) Cartilage fibronectin isoforms: in search of functions for a special population of matrix glycoproteins. *Matrix Biol,* **15,** 441-54.

Caplan AI (1991) Mesenchymal stem cells. *J Orthop Res,* **9,** 641-50.

Caplan AI, Goldberg VM (1999) Principles of tissue engineered regeneration of skeletal tissues. *Clin Orthop Relat Res***,** S12-6.

Chang J, Poole CA (1996) Sequestration of type VI collagen in the pericellular microenvironment of adult chrondrocytes cultured in agarose. *Osteoarthritis Cartilage,* **4,** 275-85.

Chang RW, Falconer J, Stulberg SD, Arnold WJ, Manheim LM, Dyer AR (1993) A randomized, controlled trial of arthroscopic surgery versus closed-needle joint lavage for patients with osteoarthritis of the knee. *Arthritis Rheum,* **36,** 289-96.

Chevalier X, Groult N, Larget-Piet B, Zardi L, Hornebeck W (1994) Tenascin distribution in articular cartilage from normal subjects and from patients with osteoarthritis and rheumatoid arthritis. *Arthritis Rheum,* **37,** 1013-22.

Chia SL, Sawaji Y, Burleigh A, et al. (2009) Fibroblast growth factor 2 is an intrinsic chondroprotective agent that suppresses ADAMTS-5 and delays cartilage degradation in murine osteoarthritis. *Arthritis Rheum,* **60,** 2019-27.

Chiakulas JJ (1957) The specificity and differential fusion of cartilage derived from mesendoderm and mesectoderm. *J Exp Zool,* **136,** 287-300.

Chiquet-Ehrismann R, Kalla P, Pearson CA, Beck K, Chiquet M (1988) Tenascin interferes with fibronectin action. *Cell,* **53,** 383-90.

Chiquet M, Fambrough DM (1984) Chick myotendinous antigen. I. A monoclonal antibody as a marker for tendon and muscle morphogenesis. *J Cell Biol,* **98,** 1926-36.

Cohen J, Lacroix P (1955) Bone and cartilage formation by periosteum; assay of experimental autogenous grafts. *J Bone Joint Surg Am,* **37-A,** 717-30.

Collins DH, Mc ET (1960) Sulphate (35SO4) uptake by chondrocytes in relation to histological changes in osteoarthritic human articular cartilage. *Ann Rheum Dis,* **19,** 318-30.

Conget PA, Minguell JJ (1999) Phenotypical and functional properties of human bone marrow mesenchymal progenitor cells. *J Cell Physiol,* **181,** 67-73.

Conlon RA, Reaume AG, Rossant J (1995) Notch1 is required for the coordinate segmentation of somites. *Development,* **121,** 1533-45.

Couchourel D, Aubry I, Delalandre A, et al. (2009) Altered mineralization of human osteoarthritic osteoblasts is attributable to abnormal type I collagen production. *Arthritis Rheum,* **60,** 1438-50.

Craig FM, Bentley G, Archer CW (1987) The spatial and temporal pattern of collagens I and II and keratan sulphate in the developing chick metatarsophalangeal joint. *Development,* **99,** 383-91.

Csaki C, Matis U, Mobasheri A, Ye H, Shakibaei M (2007) Chondrogenesis, osteogenesis and adipogenesis of canine mesenchymal stem cells: a biochemical, morphological and ultrastructural study. *Histochem Cell Biol,* **128,** 507-20.

Csaki C, Schneider PR, Shakibaei M (2008) Mesenchymal stem cells as a potential pool for cartilage tissue engineering. *Ann Anat,* **190,** 395-412.

Dahlberg L, Billinghurst RC, Manner P, et al. (2000) Selective enhancement of collagenase-mediated cleavage of resident type II collagen in cultured osteoarthritic cartilage and arrest with a synthetic inhibitor that spares collagenase 1 (matrix metalloproteinase 1). *Arthritis Rheum,* **43,** 673-82.

Davis MA, Ettinger WH, Neuhaus JM, Hauck WW (1988) Sex differences in osteoarthritis of the knee. The role of obesity. *Am J Epidemiol,* **127,** 1019-30.

Dealy C (2012) Chondrogenic Progenitors for Cartilage Repair and Osteoarthritis Treatment. *Rheumatol Curr Res,* **S3-e001**.

Dell'Accio F, De Bari C, El Tawil NM, et al. (2006) Activation of WNT and BMP signaling in adult human articular cartilage following mechanical injury. *Arthritis Res Ther,* **8,** R139.

Dennis JE, Carbillet JP, Caplan AI, Charbord P (2002) The STRO-1+ marrow cell population is multipotential. *Cells Tissues Organs,* **170,** 73-82.

Derfoul A, Perkins GL, Hall DJ, Tuan RS (2006) Glucocorticoids promote chondrogenic differentiation of adult human mesenchymal stem cells by enhancing expression of cartilage extracellular matrix genes. *Stem Cells,* **24,** 1487-95.

Diaz-Romero J, Gaillard JP, Grogan SP, Nesic D, Trub T, Mainil-Varlet P (2005) Immunophenotypic analysis of human articular chondrocytes: changes in surface markers associated with cell expansion in monolayer culture. *J Cell Physiol,* **202,** 731-42.

Digirolamo CM, Stokes D, Colter D, Phinney DG, Class R, Prockop DJ (1999) Propagation and senescence of human marrow stromal cells in culture: a simple colony-forming assay identifies samples with the greatest potential to propagate and differentiate. *Br J Haematol,* **107,** 275-81.

Dominici M, Le Blanc K, Mueller I, et al. (2006) Minimal criteria for defining multipotent mesenchymal stromal cells. The International Society for Cellular Therapy position statement. *Cytotherapy,* **8,** 315-7.

Dowthwaite GP, Bishop JC, Redman SN, et al. (2004) The surface of articular cartilage contains a progenitor cell population. *J Cell Sci,* **117,** 889-97.

Duance VC, Vaughan-Thomas A, Wardale RJ, Wotton SF (1999) The collagens of articular and meniscal cartilages. In *Biology of the synovial joint* (eds Archer CW, Caterson B, Benjamin M, Ralphs JR). Amsterdam: Harwood academic publishers.

Durr J, Goodman S, Potocnik A, von der Mark H, von der Mark K (1993) Localization of beta 1-integrins in human cartilage and their role in chondrocyte adhesion to collagen and fibronectin. *Exp Cell Res,* **207,** 235-44.

Echtermeyer F, Bertrand J, Dreier R, et al. (2009) Syndecan-4 regulates ADAMTS-5 activation and cartilage breakdown in osteoarthritis. *Nat Med,* **15,** 1072-6.

Echtermeyer F, Streit M, Wilcox-Adelman S, et al. (2001) Delayed wound repair and impaired angiogenesis in mice lacking syndecan-4. *J Clin Invest,* **107,** R9-R14.

Edwards JC, Wilkinson LS, Jones HM, et al. (1994) The formation of human synovial joint cavities: a possible role for hyaluronan and CD44 in altered interzone cohesion. *J Anat,* **185 (Pt 2),** 355-67.

Englund M (2010) The role of biomechanics in the initiation and progression of OA of the knee. *Best Pract Res Clin Rheumatol,* **24,** 39-46.

Enomoto-Iwamoto M, Iwamoto M, Nakashima K, et al. (1997) Involvement of alpha5beta1 integrin in matrix interactions and proliferation of chondrocytes. *J Bone Miner Res,* **12,** 1124-32.

Erickson HP, Bourdon MA (1989) Tenascin: an extracellular matrix protein prominent in specialized embryonic tissues and tumors. *Annu Rev Cell Biol,* **5,** 71-92.

Eyre D (2002) Collagen of articular cartilage. *Arthritis Res,* **4,** 30-5.

Eyre DR (1991) The collagens of articular cartilage. *Semin Arthritis Rheum,* **21,** 2-11.

Eyre DR, Apon S, Wu JJ, Ericsson LH, Walsh KA (1987) Collagen type IX: evidence for covalent linkages to type II collagen in cartilage. *FEBS Lett,* **220,** 337-41.

Eyre DR, Pietka T, Weis MA, Wu JJ (2004) Covalent cross-linking of the NC1 domain of collagen type IX to collagen type II in cartilage. *J Biol Chem,* **279,** 2568-74.

Eyre DR, Weis MA, Wu JJ (2006) Articular cartilage collagen: an irreplaceable framework? *Eur Cell Mater,* **12,** 57-63.

Fernandes JC, Martel-Pelletier J, Lascau-Coman V, et al. (1998) Collagenase-1 and collagenase-3 synthesis in normal and early experimental osteoarthritic canine cartilage: an immunohistochemical study. *J Rheumatol,* **25,** 1585-94.

Fickert S, Fiedler J, Brenner RE (2004) Identification of subpopulations with characteristics of mesenchymal progenitor cells from human osteoarthritic cartilage using triple staining for cell surface markers. *Arthritis Res Ther,* **6,** R422-32.

Flannery CR, Hughes CE, Schumacher BL, et al. (1999a) Articular cartilage superficial zone protein (SZP) is homologous to megakaryocyte stimulating factor precursor and Is a multifunctional proteoglycan with potential growth-promoting, cytoprotective, and lubricating properties in cartilage metabolism. *Biochem Biophys Res Commun,* **254,** 535-41.

Flannery CR, Little CB, Hughes CE, Caterson B (1999b) Expression of ADAMTS homologues in articular cartilage. *Biochem Biophys Res Commun,* **260,** 318-22.

Flemming A (2010) Target identification: HIF2alpha central player in osteoarthritis. *Nat Rev Drug Discov,* **9,** 517.

Francis-West PH, Abdelfattah A, Chen P, et al. (1999) Mechanisms of GDF-5 action during skeletal development. *Development,* **126,** 1305-15.

Fuchs E, Tumbar T, Guasch G (2004) Socializing with the neighbors: stem cells and their niche. *Cell,* **116,** 769-78.

Furuzawa-Carballeda J, Macip-Rodriguez PM, Cabral AR (2008) Osteoarthritis and rheumatoid arthritis pannus have similar qualitative metabolic characteristics and pro-inflammatory cytokine response. *Clin Exp Rheumatol,* **26,** 554-60.

Fyfe DM, Hall BK (1979) Lack of association between avian cartilages of different embryological origins when maintained in vitro. *Am J Anat,* **154,** 485-96.

Gering M, Patient R (2010) Notch signalling and haematopoietic stem cell formation during embryogenesis. *J Cell Physiol,* **222,** 11-6.

Ghosh P, Holbert C, Read R, Armstrong S (1995) Hyaluronic acid (hyaluronan) in experimental osteoarthritis. *J Rheumatol Suppl,* **43,** 155-7.

Gilbert JE (1998) Current treatment options for the restoration of articular cartilage. *Am J Knee Surg,* **11,** 42-6.

Gilbert SF (2000) Principles in Experimental Biology. In *Developmental biology).* Sunderland, Mass: Sinauer Associates.

Giovannini S, Diaz-Romero J, Aigner T, Heini P, Mainil-Varlet P, Nesic D (2010) Micromass co-culture of human articular chondrocytes and human bone marrow mesenchymal stem cells to investigate stable neocartilage tissue formation in vitro. *Eur Cell Mater,* **20,** 245-59.

Girkontaite I, Frischholz S, Lammi P, et al. (1996) Immunolocalization of type X collagen in normal fetal and adult osteoarthritic cartilage with monoclonal antibodies. *Matrix Biol,* **15,** 231-8.

Giurea A, Ruger BM, Hollemann D, Yanagida G, Kotz R, Fischer MB (2006) STRO-1+ mesenchymal precursor cells located in synovial surface projections of patients with osteoarthritis. *Osteoarthritis Cartilage,* **14,** 938-43.

Goldring MB, Birkhead J, Sandell LJ, Kimura T, Krane SM (1988) Interleukin 1 suppresses expression of cartilage-specific types II and IX collagens and increases types I and III collagens in human chondrocytes. *J Clin Invest,* **82,** 2026-37.

Goldring MB, Marcu KB (2009) Cartilage homeostasis in health and rheumatic diseases. *Arthritis Res Ther,* **11,** 224.

Goldring MB, Otero M, Tsuchimochi K, Ijiri K, Li Y (2008) Defining the roles of inflammatory and anabolic cytokines in cartilage metabolism. *Ann Rheum Dis,* **67 Suppl 3,** iii75-82.

Goldwasser M, Astley T, van der Rest M, Glorieux FH (1982) Analysis of the type of collagen present in osteoarthritic human cartilage. *Clin Orthop Relat Res***,** 296-302.

Goodman SB, Lee J, Smith RL, Csongradi JC, Fornasier VL (1991) Mechanical overload of a single compartment induces early degenerative changes in the rabbit knee: a preliminary study. *J Invest Surg,* **4,** 161-70.

Gould SE, Upholt WB, Kosher RA (1992) Syndecan 3: a member of the syndecan family of membrane-intercalated proteoglycans that is expressed in high amounts at the onset of chicken limb cartilage differentiation. *Proc Natl Acad Sci U S A,* **89,** 3271-5.

Grigoriadis AE, Heersche JN, Aubin JE (1988) Differentiation of muscle, fat, cartilage, and bone from progenitor cells present in a bone-derived clonal cell population: effect of dexamethasone. *J Cell Biol,* **106,** 2139-51.

Grogan SP, Miyaki S, Asahara H, D'Lima DD, Lotz MK (2009) Mesenchymal progenitor cell markers in human articular cartilage: normal distribution and changes in osteoarthritis. *Arthritis Res Ther,* **11,** R85.

Grynpas MD, Alpert B, Katz I, Lieberman I, Pritzker KP (1991) Subchondral bone in osteoarthritis. *Calcif Tissue Int,* **49,** 20-6.

Guilak F, Ratcliffe A, Lane N, Rosenwasser MP, Mow VC (1994) Mechanical and biochemical changes in the superficial zone of articular cartilage in canine experimental osteoarthritis. *J Orthop Res,* **12,** 474-84.

Hagiwara H, Schroter-Kermani C, Merker HJ (1993) Localization of collagen type VI in articular cartilage of young and adult mice. *Cell Tissue Res,* **272,** 155-60.

Hall BK, Miyake T (1995) Divide, accumulate, differentiate: cell condensation in skeletal development revisited. *Int J Dev Biol,* **39,** 881-93.

Hambach L, Neureiter D, Zeiler G, Kirchner T, Aigner T (1998) Severe disturbance of the distribution and expression of type VI collagen chains in osteoarthritic articular cartilage. *Arthritis Rheum,* **41,** 986-96.

Han SH, Kim YH, Park MS, et al. (2008) Histological and biomechanical properties of regenerated articular cartilage using chondrogenic bone marrow stromal cells with a PLGA scaffold in vivo. *J Biomed Mater Res A,* **87,** 850-61.

Hangody L, Kish G, Karpati Z, Szerb I, Udvarhelyi I (1997) Arthroscopic autogenous osteochondral mosaicplasty for the treatment of femoral condylar articular defects. A preliminary report. *Knee Surg Sports Traumatol Arthrosc,* **5,** 262-7.

Hartmann C, Tabin CJ (2001) Wnt-14 plays a pivotal role in inducing synovial joint formation in the developing appendicular skeleton. *Cell,* **104,** 341-51.

Hascall VC, Sandy JD, Handley CJ (1999) Regulation of proteoglycan metabolism in articular cartilage. In *Biology of the synovial joint* (eds Archer CW, Caterson B, Benjamin M, Ralphs JR). Amsterdam: Harwood academic publishers.

Hashimoto G, Aoki T, Nakamura H, Tanzawa K, Okada Y (2001) Inhibition of ADAMTS4 (aggrecanase-1) by tissue inhibitors of metalloproteinases (TIMP-1, 2, 3 and 4). *FEBS Lett,* **494,** 192-5.

Hastie ND, Dempster M, Dunlop MG, Thompson AM, Green DK, Allshire RC (1990) Telomere reduction in human colorectal carcinoma and with ageing. *Nature,* **346,** 866-8.

Havelka S, Horn V (1999) Observations on the tidemark and calcified layer of articular cartilage In *Biology of the synovial joint* (eds Archer CW, Caterson B, Benjamin M, Ralphs JR). Amsterdam: Harwood academic publishers.

Hayes AJ, MacPherson S, Morrison H, Dowthwaite G, Archer CW (2001) The development of articular cartilage: evidence for an appositional growth mechanism. *Anat Embryol (Berl),* **203,** 469-79.

Hedbom E, Antonsson P, Hjerpe A, et al. (1992) Cartilage matrix proteins. An acidic oligomeric protein (COMP) detected only in cartilage. *J Biol Chem,* **267,** 6132-6.

Heinegard D, Lorenzo P, Sommarin Y (1995) Articular cartilage matrix proteins. In *Osteoarthritic disorders* (eds Kuettner KE, Goldberg VM). Rosemont, IL: American Academy of Orthopaedic Surgeons.

Heinegard D, Oldberg A (1989) Structure and biology of cartilage and bone matrix noncollagenous macromolecules. *FASEB J,* **3,** 2042-51.

Heinegard D, Oldberg A (2002) Glycosylated matrix proteins. In *Connective tissue and its heritable disorders : molecular, genetic, and medical aspects* (eds Royce PM, Steinmann BU), pp. xvii, 1201 p. New York, NY: Wiley-Liss.

Hellio Le Graverand MP, Sciore P, Eggerer J, et al. (2001) Formation and phenotype of cell clusters in osteoarthritic meniscus. *Arthritis Rheum,* **44,** 1808-18.

Hendren L, Beeson P (2009) A review of the differences between normal and osteoarthritis articular cartilage in human knee and ankle joints. *Foot.*

Hollander AP, Heathfield TF, Webber C, et al. (1994) Increased damage to type II collagen in osteoarthritic articular cartilage detected by a new immunoassay. *J Clin Invest,* **93,** 1722-32.

Holmes MW, Bayliss MT, Muir H (1988) Hyaluronic acid in human articular cartilage. Age-related changes in content and size. *Biochem J,* **250,** 435-41.

Holmvall K, Camper L, Johansson S, Kimura JH, Lundgren-Akerlund E (1995) Chondrocyte and chondrosarcoma cell integrins with affinity for collagen type II and their response to mechanical stress. *Exp Cell Res,* **221,** 496-503.

Homandberg GA, Costa V, Wen C (2002) Fibronectin fragments active in chondrocytic chondrolysis can be chemically cross-linked to the alpha5 integrin receptor subunit. *Osteoarthritis Cartilage,* **10,** 938-49.

Homandberg GA, Davis G, Maniglia C, Shrikhande A (1997) Cartilage chondrolysis by fibronectin fragments causes cleavage of aggrecan at the same site as found in osteoarthritic cartilage. *Osteoarthritis Cartilage,* **5,** 450-3.

Howlett CR (1979) The fine structure of the proximal growth plate of the avian tibia. *J Anat,* **128,** 377-99.

Hulejova H, Baresova V, Klezl Z, Polanska M, Adam M, Senolt L (2007) Increased level of cytokines and matrix metalloproteinases in osteoarthritic subchondral bone. *Cytokine,* **38,** 151-6.

Hunter W (1743) On the structure and diseases of the articular cartilages. *Philos Trans Roy Soc,* **42B,** 514- 521.

Hunziker EB (2001) Articular cartilage repair: basic science and clinical progress. A review of the current status and prospects. *Osteo Cart,* **10,** 432-63.

Hunziker EB, Kapfinger E (1998) Removal of proteoglycans from the surface of defects in articular cartilage transiently enhances coverage by repair cells. *J Bone Joint Surg Br,* **80,** 144-50.

Huss R, Lange C, Weissinger EM, Kolb HJ, Thalmeier K (2000) Evidence of peripheral blood-derived, plastic-adherent CD34(-/low) hematopoietic stem cell clones with mesenchymal stem cell characteristics. *Stem Cells,* **18,** 252-60.

Hynes RO (1992) Integrins: versatility, modulation, and signaling in cell adhesion. *Cell,* **69,** 11-25.

Im GI, Kim DY, Shin JH, Hyun CW, Cho WH (2001) Repair of cartilage defect in the rabbit with cultured mesenchymal stem cells from bone marrow. *J Bone Joint Surg Br,* **83,** 289-94.

Isacke CM (1994) The role of the cytoplasmic domain in regulating CD44 function. *J Cell Sci,* **107 (Pt 9),** 2353-9.

Ishida O, Tanaka Y, Morimoto I, Takigawa M, Eto S (1997) Chondrocytes are regulated by cellular adhesion through CD44 and hyaluronic acid pathway. *J Bone Miner Res,* **12,** 1657-63.

Iso T, Kedes L, Hamamori Y (2003) HES and HERP families: multiple effectors of the Notch signaling pathway. *J Cell Physiol,* **194,** 237-55.

Jackson RW, Dieterichs C (2003) The results of arthroscopic lavage and debridement of osteoarthritic knees based on the severity of degeneration: a 4- to 6-year symptomatic follow-up. *Arthroscopy,* **19,** 13-20.

Jakob M, Demarteau O, Schafer D, et al. (2001) Specific growth factors during the expansion and redifferentiation of adult human articular chondrocytes enhance chondrogenesis and cartilaginous tissue formation in vitro. *J Cell Biochem,* **81,** 368-77.

Jakob RP, Franz T, Gautier E, Mainil-Varlet P (2002) Autologous osteochondral grafting in the knee: indication, results, and reflections. *Clin Orthop Relat Res***,** 170-84.

Jay GD, Tantravahi U, Britt DE, Barrach HJ, Cha CJ (2001) Homology of lubricin and superficial zone protein (SZP): products of megakaryocyte stimulating factor (MSF) gene expression by human synovial fibroblasts and articular chondrocytes localized to chromosome 1q25. *J Orthop Res,* **19,** 677-87.

Jiang R, Lan Y, Chapman HD, et al. (1998) Defects in limb, craniofacial, and thymic development in Jagged2 mutant mice. *Genes Dev,* **12,** 1046-57.

Jiang X, Cui PC, Chen WX, Zhang ZP (2003) [In vivo chondrogenesis of induced human marrow mesenchymal stem cells in nude mice]. *Di Yi Jun Yi Da Xue Xue Bao,* **23,** 766-9, 773.

Johnson LC (1962) Joint remodelling as a basis for osteoarthritis. *J Am Vet Med Assoc***,** 1237- 41.

Johnstone B, Hering TM, Caplan AI, Goldberg VM, Yoo JU (1998) In vitro chondrogenesis of bone marrow-derived mesenchymal progenitor cells. *Exp Cell Res,* **238,** 265-72.

Jones PH, Watt FM (1993) Separation of human epidermal stem cells from transit amplifying cells on the basis of differences in integrin function and expression. *Cell,* **73,** 713-24.

Karlsson C, Brantsing C, Egell S, Lindahl A (2008) Notch1, Jagged1, and HES5 are abundantly expressed in osteoarthritis. *Cells Tissues Organs,* **188,** 287-98.

Karlsson C, Lindahl A (2009) Articular cartilage stem cell signalling. *Arthritis Res Ther,* **11,** 121.

Karsdal MA, Leeming DJ, Dam EB, et al. (2008) Should subchondral bone turnover be targeted when treating osteoarthritis? *Osteoarthritis Cartilage,* **16,** 638-46.

Kashiwagi M, Tortorella M, Nagase H, Brew K (2001) TIMP-3 is a potent inhibitor of aggrecanase 1 (ADAM-TS4) and aggrecanase 2 (ADAM-TS5). *J Biol Chem,* **276,** 12501-4.

Khan IM, Gilbert SJ, Caterson B, Sandell LJ, Archer CW (2008) Oxidative stress induces expression of osteoarthritis markers procollagen IIA and 3B3(-) in adult bovine articular cartilage. *Osteoarthritis Cartilage,* **16,** 698-707.

Khan IM, Gilbert SJ, Singhrao SK, Duance VC, Archer CW (2008) Cartilage integration: evaluation of the reasons for failure of integration during cartilage repair. A review. *Eur Cell Mater,* **16,** 26-39.

Khan IM, Redman SN, Williams R, Dowthwaite GP, Oldfield SF, Archer CW (2007) The development of synovial joints. In *Current topics in developmental biology* (ed Schatten GP). San Diego: Elsevier.

Khan IM, Williams R, Archer CW (2009) One flew over the progenitor's nest: migratory cells find a home in osteoarthritic cartilage. *Cell Stem Cell,* **4,** 282-4.

Kielty CM, Whittaker SP, Grant ME, Shuttleworth CA (1992) Type VI collagen microfibrils: evidence for a structural association with hyaluronan. *J Cell Biol,* **118,** 979-90.

Kim HK, Moran ME, Salter RB (1991) The potential for regeneration of articular cartilage in defects created by chondral shaving and subchondral abrasion. An experimental investigation in rabbits. *J Bone Joint Surg Am,* **73,** 1301-15.

Knudson CB (1993) Hyaluronan receptor-directed assembly of chondrocyte pericellular matrix. *J Cell Biol,* **120,** 825-34.

Koelling S, Kruegel J, Irmer M, et al. (2009) Migratory chondrogenic progenitor cells from repair tissue during the later stages of human osteoarthritis. *Cell Stem Cell,* **4,** 324-35.

Kouri JB, Jimenez SA, Quintero M, Chico A (1996) Ultrastructural study of chondrocytes from fibrillated and non-fibrillated human osteoarthritic cartilage. *Osteoarthritis Cartilage,* **4,** 111-25.

Koyama E, Leatherman JL, Shimazu A, Nah HD, Pacifici M (1995) Syndecan-3, tenascin-C, and the development of cartilaginous skeletal elements and joints in chick limbs. *Dev Dyn,* **203,** 152-62.

Krane SM, Byrne MH, Lemaitre V, et al. (1996) Different collagenase gene products have different roles in degradation of type I collagen. *J Biol Chem,* **271,** 28509-15.

Kreis T, Vale R (1999) *Guidebook to the extracellular matrix, anchor, and adhesion proteins,* Oxford University Press, Oxford [England] ; New York.

Kronenberg HM (2003) Developmental regulation of the growth plate. *Nature,* **423,** 332-6.

Kuo CK, Li WJ, Mauck RL, Tuan RS (2006) Cartilage tissue engineering: its potential and uses. *Curr Opin Rheumatol,* **18,** 64-73.

Kwan AP, Cummings CE, Chapman JA, Grant ME (1991) Macromolecular organization of chicken type X collagen in vitro. *J Cell Biol,* **114,** 597-604.

Lajeunesse D, Massicotte F, Pelletier JP, Martel-Pelletier J (2003) Subchondral bone sclerosis in osteoarthritis: not just an innocent bystander. *Mod Rheumatol,* **13,** 7-14.

Lajeunesse D, Reboul P (2003) Subchondral bone in osteoarthritis: a biologic link with articular cartilage leading to abnormal remodeling. *Curr Opin Rheumatol,* **15,** 628-33.

Leboy PS, Shapiro IM, Uschmann BD, Oshima O, Lin D (1988) Gene expression in mineralizing chick epiphyseal cartilage. *J Biol Chem,* **263,** 8515-20.

Ledingham J, Regan M, Jones A, Doherty M (1993) Radiographic patterns and associations of osteoarthritis of the knee in patients referred to hospital. *Ann Rheum Dis,* **52,** 520-6.

Lee ER, Smith CE, Poole R (1996) Ultrastructural localization of the C-propeptide released from type II procollagen in fetal bovine growth plate cartilage. *J Histochem Cytochem,* **44,** 433-43.

Lee KB, Hui JH, Song IC, Ardany L, Lee EH (2007) Injectable mesenchymal stem cell therapy for large cartilage defects--a porcine model. *Stem Cells,* **25,** 2964-71.

Li Q, Zhang L (2009) [Research progress on relationship between subchondral bone and cartilage degeneration in osteoarthritis]. *Zhongguo Xiu Fu Chong Jian Wai Ke Za Zhi,* **23,** 245-8.

Li Y, Tew SR, Russell AM, Gonzalez KR, Hardingham TE, Hawkins RE (2004) Transduction of passaged human articular chondrocytes with adenoviral, retroviral, and lentiviral vectors and the effects of enhanced expression of SOX9. *Tissue Eng,* **10,** 575-84.

Lim ST, Longley RL, Couchman JR, Woods A (2003) Direct binding of syndecan-4 cytoplasmic domain to the catalytic domain of protein kinase C alpha (PKC alpha) increases focal adhesion localization of PKC alpha. *J Biol Chem,* **278,** 13795-802.

Lin AC, Seeto BL, Bartoszko JM, et al. (2009) Modulating hedgehog signaling can attenuate the severity of osteoarthritis. *Nat Med,* **15,** 1421-5.

Ling W, Regatte RR, Navon G, Jerschow A (2008) Assessment of glycosaminoglycan concentration in vivo by chemical exchange-dependent saturation transfer (gagCEST). *Proc Natl Acad Sci U S A,* **105,** 2266-70.

Livesley PJ, Doherty M, Needoff M, Moulton A (1991) Arthroscopic lavage of osteoarthritic knees. *J Bone Joint Surg Br,* **73,** 922-6.

Loeser RF (2000) Chondrocyte integrin expression and function. *Biorheology,* **37,** 109-16.

Lohmander LS, Saxne T, Heinegard DK (1994) Release of cartilage oligomeric matrix protein (COMP) into joint fluid after knee injury and in osteoarthritis. *Ann Rheum Dis,* **53,** 8-13.

Lorenz H, Richter W (2006) Osteoarthritis: cellular and molecular changes in degenerating cartilage. *Prog Histochem Cytochem,* **40,** 135-63.

Lorenzo P, Bayliss MT, Heinegard D (2004) Altered patterns and synthesis of extracellular matrix macromolecules in early osteoarthritis. *Matrix Biol,* **23,** 381-91.

Lories RJ, Luyten FP (2005) Bone morphogenetic protein signaling in joint homeostasis and disease. *Cytokine Growth Factor Rev,* **16,** 287-98.

Lotz M, Blanco FJ, von Kempis J, et al. (1995) Cytokine regulation of chondrocyte functions. *J Rheumatol Suppl,* **43,** 104-8.

Lotz MK, Otsuki S, Grogan SP, Sah R, Terkeltaub R, D'Lima D (2010) Cartilage cell clusters. *Arthritis Rheum,* **62,** 2206-18.

Lutfi AM (1974) The ultrastructure of cartilage cells in the epiphyses of long bones in the domestic fowl. *Acta Anat (Basel),* **87,** 12-21.

Mackie EJ, Thesleff I, Chiquet-Ehrismann R (1987) Tenascin is associated with chondrogenic and osteogenic differentiation in vivo and promotes chondrogenesis in vitro. *J Cell Biol,* **105,** 2569-79.

Magnuson PB (1946) Technique of debridement of the knee joint for arthritis. *Surg Clin North Am,* **26,** 149-66.

Mainil-Varlet P, Aigner T, Brittberg M, et al. (2003) Histological assessment of cartilage repair: a report by the Histology Endpoint Committee of the International Cartilage Repair Society (ICRS). *J Bone Joint Surg Am,* **85-A Suppl 2,** 45-57.

Mankin HJ (1962) Localisation of tritiated thymidine in articular cartilage of rabbits. I Growth in immature cartilage. *J Bone Joint Surg,* **44A,** 682- 88.

Mankin HJ, Dorfman H, Lippiello L, Zarins A (1971) Biochemical and metabolic abnormalities in articular cartilage from osteo-arthritic human hips. II. Correlation of morphology with biochemical and metabolic data. *J Bone Joint Surg Am,* **53,** 523-37.

Mansell JP, Tarlton JF, Bailey AJ (1997) Biochemical evidence for altered subchondral bone collagen metabolism in osteoarthritis of the hip. *Br J Rheumatol,* **36,** 16-9.

Mansell JP, Bailey AJ (1998) Abnormal cancellous bone collagen metabolism in osteoarthritis. *J Clin Invest,* **101,** 1596-603.

Marcelino J, McDevitt CA (1995) Attachment of articular cartilage chondrocytes to the tissue form of type VI collagen. *Biochim Biophys Acta,* **1249,** 180-8.

Maroudas A (1979) Physicochemical properties of articular cartilage. In *Adult articular cartilage* (ed Freeman MAR), pp. 215-290. London: Pitman Medical.

Maroudas A (1980) Metabolism of cartilaginous tissues: a quantitative approach. In *Studies in Joint Disease* (ed Maroudas A, Holborow, E. J.), pp. 59-86. Bath: Pitman Press.

Martel-Pelletier J, Pelletier JP (2010) Is osteoarthritis a disease involving only cartilage or other articular tissues? *Eklem Hastalik Cerrahisi,* **21,** 2-14.

Martin I, Jakob M, Schafer D, Dick W, Spagnoli G, Heberer M (2001) Quantitative analysis of gene expression in human articular cartilage from normal and osteoarthritic joints. *Osteoarthritis Cartilage,* **9,** 112-8.

Martin JA, Buckwalter JA (2002) Aging, articular cartilage chondrocyte senescence and osteoarthritis. *Biogerontology,* **3,** 257-64.

Martin JM, Smith M, Al-Rubeai M (2005) Cryopreservation and in vitro expansion of chondroprogenitor cells isolated from the superficial zone of articular cartilage. *Biotechnol Prog,* **21,** 168-77.

Martinez Arias A, Zecchini V, Brennan K (2002) CSL-independent Notch signalling: a checkpoint in cell fate decisions during development? *Curr Opin Genet Dev,* **12,** 524-33.

Matyas JR, Ehlers PF, Huang D, Adams ME (1999) The early molecular natural history of experimental osteoarthritis. I. Progressive discoordinate expression of aggrecan and type II procollagen messenger RNA in the articular cartilage of adult animals. *Arthritis Rheum,* **42,** 993-1002.

McCarthy HE, Bara JJ, Brakspear K, Singhrao SK, Archer CW (2011) The comparison of equine articular cartilage progenitor cells and bone marrow-derived stromal cells as potential cell sources for cartilage repair in the horse. *Vet J.*

McDevitt C, Gilbertson E, Muir H (1977) An experimental model of osteoarthritis; early morphological and biochemical changes. *J Bone Joint Surg Br,* **59,** 24-35.

Meachim G, Roy S (1967) Intracytoplasmic filaments in the cells of adult human articular cartilage. *Ann Rheum Dis,* **26,** 50-8.

Meachim G, Stockwell R (1973) The matrix. In *Adult articular cartilage* (ed Freeman MAR), pp. 1-50. London: Pitman Medical.

Melero-Martin JM, Dowling MA, Smith M, Al-Rubeai M (2006) Optimal in-vitro expansion of chondroprogenitor cells in monolayer culture. *Biotechnol Bioeng,* **93,** 519-33.

Mendler M, Eich-Bender SG, Vaughan L, Winterhalter KH, Bruckner P (1989) Cartilage contains mixed fibrils of collagen types II, IX, and XI. *J Cell Biol,* **108,** 191-7.

Minas T, Gomoll AH, Rosenberger R, Royce RO, Bryant T (2009) Increased failure rate of autologous chondrocyte implantation after previous treatment with marrow stimulation techniques. *Am J Sports Med,* **37,** 902-8.

Minguell JJ, Erices A, Conget P (2001) Mesenchymal stem cells. *Exp Biol Med (Maywood),* **226,** 507-20.

Miosge N, Hartmann M, Maelicke C, Herken R (2004) Expression of collagen type I and type II in consecutive stages of human osteoarthritis. *Histochem Cell Biol,* **122,** 229-36.

Miosge N, Waletzko K, Bode C, Quondamatteo F, Schultz W, Herken R (1998) Light and electron microscopic in-situ hybridization of collagen type I and type II mRNA in the fibrocartilaginous tissue of late-stage osteoarthritis. *Osteoarthritis Cartilage,* **6,** 278-85.

Mitrovic DR (1977) Development of the metatarsophalangeal joint of the chick embryo: morphological, ultrastructural and histochemical studies. *Am J Anat,* **150,** 333-47.

Mobasheri A, Csaki C, Clutterbuck AL, Rahmanzadeh M, Shakibaei M (2009) Mesenchymal stem cells in connective tissue engineering and regenerative medicine: applications in cartilage repair and osteoarthritis therapy. *Histol Histopathol,* **24,** 347-66.

Mohtai M, Smith RL, Schurman DJ, et al. (1993) Expression of 92-kD type IV collagenase/gelatinase (gelatinase B) in osteoarthritic cartilage and its induction in normal human articular cartilage by interleukin 1. *J Clin Invest,* **92,** 179-85.

Mollenhauer J, Mok MT, King KB, et al. (1999) Expression of anchorin CII (cartilage annexin V) in human young, normal adult, and osteoarthritic cartilage. *J Histochem Cytochem,* **47,** 209-20.

Molteni A, Modrowski D, Hott M, Marie PJ (1999) Differential expression of fibroblast growth factor receptor-1, -2, and -3 and syndecan-1, -2, and -4 in neonatal rat mandibular condyle and calvaria during osteogenic differentiation in vitro. *Bone,* **24,** 337-47.

Moore KL, Persaud TVN (2003) *The developing human : clinically oriented embryology,* Saunders, Philadelphia, Pa.

Morales TI (2007) Chondrocyte moves: clever strategies? *Osteoarthritis Cartilage,* **15,** 861-71.

Morris N, Keene D, Horton W (2002) Morphology and chemical composition of connective tissue: cartilage. In *Connective tissue and its heritable disorders : molecular, genetic, and medical aspects* (eds Royce PM, Steinmann BU). New York, NY: Wiley-Liss.

Morris NP, Keene, D.R, Horton, W.A (2002) Cartilage. In *Connective tissue and its heritable disorders* (ed Royce PM, Steinmann, B.), pp. 41-67. New York: Wiley-Liss.

Morrison EH, Ferguson MW, Bayliss MT, Archer CW (1996) The development of articular cartilage: I. The spatial and temporal patterns of collagen types. *J Anat,* **189 (Pt 1),** 9-22.

Moscona A (1961) Rotation-mediated histogenetic aggregation of dissociated cells. A quantifiable approach to cell interactions in vitro. *Exp Cell Res,* **22,** 455-75.

Mouw JK, Case ND, Guldberg RE, Plaas AH, Levenston ME (2005) Variations in matrix composition and GAG fine structure among scaffolds for cartilage tissue engineering. *Osteoarthritis Cartilage,* **13,** 828-36.

Muir H (1986) Current and future trends in articular cartilage research and osteoarthritis. In *Articular cartilage biochemistry* (eds Kuettner KE, Schleyerbach R, Hascall VC). New York: Raven Press.

Murphy G, Nagase H (2008) Reappraising metalloproteinases in rheumatoid arthritis and osteoarthritis: destruction or repair? *Nat Clin Pract Rheumatol,* **4,** 128-35.

Murphy JM, Fink DJ, Hunziker EB, Barry FP (2003) Stem cell therapy in a caprine model of osteoarthritis. *Arthritis Rheum,* **48,** 3464-74.

Nah HD, Swoboda B, Birk DE, Kirsch T (2001) Type IIA procollagen: expression in developing chicken limb cartilage and human osteoarthritic articular cartilage. *Dev Dyn,* **220,** 307-22.

Nah HD, Upholt WB (1991) Type II collagen mRNA containing an alternatively spliced exon predominates in the chick limb prior to chondrogenesis. *J Biol Chem,* **266,** 23446-52.

Naot D, Sionov RV, Ish-Shalom D (1997) CD44: Structure, function, and association with the malignant process. *Adv Cancer Res,* **71,** 241- 319.

Neame PJ, Tapp H, Azizan A (1999) Noncollagenous, nonproteoglycan macromolecules of cartilage. *Cell Mol Life Sci,* **55,** 1327-40.

Nerlich AG, Wiest I, von der Mark K (1993) Immunohistochemical analysis of interstitial collagens in cartilage of different stages of osteoarthrosis. *Virchows Arch B Cell Pathol Incl Mol Pathol,* **63,** 249-55.

Nishida K, Inoue H, Murakami T (1995) Immunohistochemical demonstration of fibronectin in the most superficial layer of normal rabbit articular cartilage. *Ann Rheum Dis,* **54,** 995-8.

Niswander L (2002) Interplay between the molecular signals that control vertebrate limb development. *Int J Dev Biol,* **46,** 877-81.

Nixon AJ, Brower-Toland BD, Bent SJ, et al. (2000) Insulinlike growth factor-I gene therapy applications for cartilage repair. *Clin Orthop Relat Res***,** S201-13.

Noth U, Steinert AF, Tuan RS (2008) Technology insight: adult mesenchymal stem cells for osteoarthritis therapy. *Nat Clin Pract Rheumatol,* **4,** 371-80.

Nowicki JL, Burke AC (2000) Hox genes and morphological identity: axial versus lateral patterning in the vertebrate mesoderm. *Development,* **127,** 4265-75.

O'Driscoll SW (1999) Articular cartilage regeneration using periosteum. *Clin Orthop Relat Res***,** S186-203.

O'Driscoll SW, Keeley FW, Salter RB (1988) Durability of regenerated articular cartilage produced by free autogenous periosteal grafts in major full-thickness defects in joint surfaces under the influence of continuous passive motion. A follow-up report at one year. *J Bone Joint Surg Am,* **70,** 595-606.

Oganesian A, Zhu Y, Sandell LJ (1997) Type IIA procollagen amino propeptide is localized in human embryonic tissues. *J Histochem Cytochem,* **45,** 1469-80.

Okimura A, Okada Y, Makihira S, et al. (1997) Enhancement of cartilage matrix protein synthesis in arthritic cartilage. *Arthritis Rheum,* **40,** 1029-36.

Ostergaard K, Andersen CB, Petersen J, Bendtzen K, Salter DM (1999) Validity of histopathological grading of articular cartilage from osteoarthritic knee joints. *Ann Rheum Dis,* **58,** 208-13.

Ostergaard K, Petersen J, Andersen CB, Bendtzen K, Salter DM (1997) Histologic/histochemical grading system for osteoarthritic articular cartilage: reproducibility and validity. *Arthritis Rheum,* **40,** 1766-71.

Ostergaard K, Salter DM, Petersen J, Bendtzen K, Hvolris J, Andersen CB (1998) Expression of alpha and beta subunits of the integrin superfamily in articular cartilage from macroscopically normal and osteoarthritic human femoral heads. *Ann Rheum Dis,* **57,** 303-8.

Pacifici M (1995) Tenascin-C and the development of articular cartilage. *Matrix Biol,* **14,** 689-98.

Pacifici M, Iwamoto M, Golden EB, Leatherman JL, Lee YS, Chuong CM (1993) Tenascin is associated with articular cartilage development. *Dev Dyn,* **198,** 123-34.

Pacifici M, Koyama E, Iwamoto M (2005) Mechanisms of synovial joint and articular cartilage formation: recent advances, but many lingering mysteries. *Birth Defects Res C Embryo Today,* **75,** 237-48.

Pacifici M, Koyama E, Kirsch T, Leatherman JL, Golden EB (1999) Involvement of tenascin-C and syndecan-3 in the development of chick limb diarthrodial joints. In *Biology of the synovial joint* (eds Archer CW, Caterson B, Benjamin M, Ralphs JR). Amsterdam: Harwood academic publishers.

Paunesku T, Mittal S, Protic M, et al. (2001) Proliferating cell nuclear antigen (PCNA): ringmaster of the genome. *Int J Radiat Biol,* **77,** 1007-21.

Pavesio A, Abatangelo G, Borrione A, et al. (2003) Hyaluronan-based scaffolds (Hyalograft C) in the treatment of knee cartilage defects: preliminary clinical findings. *Novartis Found Symp,* **249,** 203-17; discussion 229-33, 234-8, 239-41.

Pelletier JP, Jovanovic DV, Lascau-Coman V, et al. (2000) Selective inhibition of inducible nitric oxide synthase reduces progression of experimental osteoarthritis in vivo: possible link with the reduction in chondrocyte apoptosis and caspase 3 level. *Arthritis Rheum,* **43,** 1290-9.

Pelletier JP, Martel-Pelletier J, Abramson SB (2001) Osteoarthritis, an inflammatory disease: potential implication for the selection of new therapeutic targets. *Arthritis Rheum,* **44,** 1237-47.

Pelttari K, Winter A, Steck E, et al. (2006) Premature induction of hypertrophy during in vitro chondrogenesis of human mesenchymal stem cells correlates with calcification and vascular invasion after ectopic transplantation in SCID mice. *Arthritis Rheum,* **54,** 3254-66.

Petersson IF, Boegard T, Svensson B, Heinegard D, Saxne T (1998) Changes in cartilage and bone metabolism identified by serum markers in early osteoarthritis of the knee joint. *Br J Rheumatol,* **37,** 46-50.

Pevsner-Fischer M, Levin S, Zipori D (2011) The origins of mesenchymal stromal cell heterogeneity. *Stem Cell Rev,* **7,** 560-8.

Pfander D, Rahmanzadeh R, Scheller EE (1999) Presence and distribution of collagen II, collagen I, fibronectin, and tenascin in rabbit normal and osteoarthritic cartilage. *J Rheumatol,* **26,** 386-94.

Pfander D, Swoboda B, Kirsch T (2001) Expression of early and late differentiation markers (proliferating cell nuclear antigen, syndecan-3, annexin VI, and alkaline phosphatase) by human osteoarthritic chondrocytes. *Am J Pathol,* **159,** 1777-83.

Pierschbacher MD, Ruoslahti E (1984) Cell attachment activity of fibronectin can be duplicated by small synthetic fragments of the molecule. *Nature,* **309,** 30-3.

Pitsillides AA (1999) The role of hyaluronan in joint cavitation. In *Biology of the synovial joint* (eds Archer CW, Caterson B, Benjamin M, Ralphs JR), pp. 41-62. Amsterdam: Harwood academic publishers.

Pittenger MF, Mackay AM, Beck SC, et al. (1999) Multilineage potential of adult human mesenchymal stem cells. *Science,* **284,** 143-7.

Poole CA, Ayad S, Gilbert RT (1992) Chondrons from articular cartilage. V. Immunohistochemical evaluation of type VI collagen organisation in isolated chondrons by light, confocal and electron microscopy. *J Cell Sci,* **103 (Pt 4),** 1101-10.

Poole CA, Flint MH, Beaumont BW (1987) Chondrons in cartilage: ultrastructural analysis of the pericellular microenvironment in adult human articular cartilages. *J Orthop Res,* **5,** 509-22.

Pousty I, Bari-Khan MA, Butler WF (1975) Leaching of glycosaminoglycans from tissues by the fixatives formalin-saline and formalin-cetrimide *Histochem J,* **7,** 361-65.

Pretzel D, Linss S, Rochler S, et al. (2011) Relative percentage and zonal distribution of mesenchymal progenitor cells in human osteoarthritic and normal cartilage. *Arthritis Res Ther,* **13,** R64.

Pritzker KP, Gay S, Jimenez SA, et al. (2006) Osteoarthritis cartilage histopathology: grading and staging. *Osteoarthritis Cartilage,* **14,** 13-29.

Quinn TM, Grodzinsky AJ, Hunziker EB, Sandy JD (1998) Effects of injurious compression on matrix turnover around individual cells in calf articular cartilage explants. *J Orthop Res,* **16,** 490-9.

Radin EL (1976) Mechanical aspects of osteoarthritis. *Bulletin on Rheumatic Diseases,* **26,** 862-865.

Radin EL, Rose RM (1986) Role of subchondral bone in the initiation and progression of cartilage damage. *Clin Orthop Relat Res***,** 34-40.

Ramage L, Nuki G, Salter DM (2009) Signalling cascades in mechanotransduction: cell-matrix interactions and mechanical loading. *Scand J Med Sci Sports,* **19,** 457-69.

Rapport MM, Weissmann B, Linker A, Meyer K (1951) Isolation of a crystalline disaccharide, hyalobiuronic acid, from hyaluronic acid. *Nature,* **168,** 996-7.

Ratcliffe A, Doherty M, Maini RN, Hardingham TE (1988) Increased concentrations of proteoglycan components in the synovial fluids of patients with acute but not chronic joint disease. *Ann Rheum Dis,* **47,** 826-32.

Ratcliffe A, Mow VC (1996) Articular cartilage. In *Extracellular matrix: Tissue function* (ed Comper WD), pp. 234- 302. Harwood Academic Publishers.

Redman SN, Oldfield SF, Archer CW (2005) Current strategies for articular cartilage repair. *Eur Cell Mater,* **9,** 23-32; discussion 23-32.

Reid DL, Aydelotte MB, Mollenhauer J (2000) Cell attachment, collagen binding, and receptor analysis on bovine articular chondrocytes. *J Orthop Res,* **18,** 364-73.

Rhee DK, Marcelino J, Baker M, et al. (2005) The secreted glycoprotein lubricin protects cartilage surfaces and inhibits synovial cell overgrowth. *J Clin Invest,* **115,** 622-31.

Roberts S, Hollander AP, Caterson B, Menage J, Richardson JB (2001) Matrix turnover in human cartilage repair tissue in autologous chondrocyte implantation. *Arthritis Rheum,* **44,** 2586-98.

Roberts S, McCall IW, Darby AJ, et al. (2003) Autologous chondrocyte implantation for cartilage repair: monitoring its success by magnetic resonance imaging and histology. *Arthritis Res Ther,* **5,** R60-73.

Roberts S, Menage J, Sandell LJ, Evans EH, Richardson JB (2009) Immunohistochemical study of collagen types I and II and procollagen IIA in human cartilage repair tissue following autologous chondrocyte implantation. *Knee,* **16,** 398-404.

Rodan GA (1992) Introduction to bone biology. *Bone,* **13 Suppl 1,** S3-6.

Roughley PJ (2001) Articular cartilage and changes in arthritis: noncollagenous proteins and proteoglycans in the extracellular matrix of cartilage. *Arthritis Res,* **3,** 342-7.

Roughley PJ (2006) The structure and function of cartilage proteoglycans. *Eur Cell Mater,* **12,** 92-101.

Rucklidge GJ, Milne G, Robins SP (1996) Collagen type X: a component of the surface of normal human, pig, and rat articular cartilage. *Biochem Biophys Res Commun,* **224,** 297-302.

Ruoslahti E (1991) Integrins. *J Clin Invest,* **87,** 1-5.

Ryan MC, Sandell LJ (1990) Differential expression of a cysteine-rich domain in the amino-terminal propeptide of type II (cartilage) procollagen by alternative splicing of mRNA. *J Biol Chem,* **265,** 10334-9.

Saito T, Fukai A, Mabuchi A, et al. (2010) Transcriptional regulation of endochondral ossification by HIF-2alpha during skeletal growth and osteoarthritis development. *Nat Med,* **16,** 678-86.

Salmivirta M, Elenius K, Vainio S, et al. (1991) Syndecan from embryonic tooth mesenchyme binds tenascin. *J Biol Chem,* **266,** 7733-9.

Salter DM (1993) Tenascin is increased in cartilage and synovium from arthritic knees. *Br J Rheumatol,* **32,** 780-6.

Salter DM, Godolphin JL, Gourlay MS (1995) Chondrocyte heterogeneity: immunohistologically defined variation of integrin expression at different sites in human fetal knees. *J Histochem Cytochem,* **43,** 447-57.

Salter DM, Hughes DE, Simpson R, Gardner DL (1992) Integrin expression by human articular chondrocytes. *Br J Rheumatol,* **31,** 231-4.

Sandell LJ, Morris N, Robbins JR, Goldring MB (1991) Alternatively spliced type II procollagen mRNAs define distinct populations of cells during vertebral development: differential expression of the amino-propeptide. *J Cell Biol,* **114,** 1307-19.

Sassi N, Laadhar L, Driss M, Kallel-Sellami M, Sellami S, Makni S (2011) The role of the Notch pathway in healthy and osteoarthritic articular cartilage: from experimental models to ex vivo studies. *Arthritis Res Ther,* **13,** 208.

Savarese JJ, Erickson H, Scully SP (1996) Articular chondrocyte tenascin-C production and assembly into de novo extracellular matrix. *J Orthop Res,* **14,** 273-81.

Saxne T, Heinegard D (1992) Cartilage oligomeric matrix protein: a novel marker of cartilage turnover detectable in synovial fluid and blood. *Br J Rheumatol,* **31,** 583-91.

Scadden DT (2006) The stem-cell niche as an entity of action. *Nature,* **441,** 1075-9.

Scanzello CR, Umoh E, Pessler F, et al. (2009) Local cytokine profiles in knee osteoarthritis: elevated synovial fluid interleukin-15 differentiates early from end-stage disease. *Osteoarthritis Cartilage,* **17,** 1040-8.

Scharstuhl A, Glansbeek HL, van Beuningen HM, Vitters EL, van der Kraan PM, van den Berg WB (2002) Inhibition of endogenous TGF-beta during experimental osteoarthritis prevents osteophyte formation and impairs cartilage repair. *J Immunol,* **169,** 507-14.

Schmid TM, Linsenmayer TF (1985) Developmental acquisition of type X collagen in the embryonic chick tibiotarsus. *Dev Biol,* **107,** 373-81.

Schnabel M, Marlovits S, Eckhoff G, et al. (2002) Dedifferentiation-associated changes in morphology and gene expression in primary human articular chondrocytes in cell culture. *Osteoarthritis Cartilage,* **10,** 62-70.

Schumacher BL, Block JA, Schmid TM, Aydelotte MB, Kuettner KE (1994) A novel proteoglycan synthesized and secreted by chondrocytes of the superficial zone of articular cartilage. *Arch Biochem Biophys,* **311,** 144-52.

Schweisguth F (2004) Regulation of notch signaling activity. *Curr Biol,* **14,** R129-38.

Setton LA, Zhu W, Mow VC (1993) The biphasic poroviscoelastic behavior of articular cartilage: role of the surface zone in governing the compressive behavior. *J Biomech,* **26,** 581-92.

Shapiro F, Koide S, Glimcher MJ (1993) Cell origin and differentiation in the repair of full-thickness defects of articular cartilage. *J Bone Joint Surg Am,* **75,** 532-53.

Sharif M, George E, Dieppe PA (1995a) Correlation between synovial fluid markers of cartilage and bone turnover and scintigraphic scan abnormalities in osteoarthritis of the knee. *Arthritis Rheum,* **38,** 78-81.

Sharif M, Saxne T, Shepstone L, et al. (1995b) Relationship between serum cartilage oligomeric matrix protein levels and disease progression in osteoarthritis of the knee joint. *Br J Rheumatol,* **34,** 306-10.

Shea CM, Edgar CM, Einhorn TA, Gerstenfeld LC (2003) BMP treatment of C3H10T1/2 mesenchymal stem cells induces both chondrogenesis and osteogenesis. *J Cell Biochem,* **90,** 1112-27.

Shen G (2005) The role of type X collagen in facilitating and regulating endochondral ossification of articular cartilage. *Orthod Craniofac Res,* **8,** 11-7.

Shibakawa A, Aoki H, Masuko-Hongo K, et al. (2003) Presence of pannus-like tissue on osteoarthritic cartilage and its histological character. *Osteoarthritis Cartilage,* **11,** 133-40.

Short B, Brouard N, Occhiodoro-Scott T, Ramakrishnan A, Simmons PJ (2003) Mesenchymal stem cells. *Arch Med Res,* **34,** 565-71.

Siczkowski M, Watt FM (1990) Subpopulations of chondrocytes from different zones of pig articular cartilage. Isolation, growth and proteoglycan synthesis in culture. *J Cell Sci,* **97 (Pt 2),** 349-60.

Simmons PJ, Torok-Storb B (1991) Identification of stromal cell precursors in human bone marrow by a novel monoclonal antibody, STRO-1. *Blood,* **78,** 55-62.

Smith MD, Triantafillou S, Parker A, Youssef PP, Coleman M (1997) Synovial membrane inflammation and cytokine production in patients with early osteoarthritis. *J Rheumatol,* **24,** 365-71.

Solchaga LA, Penick K, Porter JD, Goldberg VM, Caplan AI, Welter JF (2005) FGF-2 enhances the mitotic and chondrogenic potentials of human adult bone marrow-derived mesenchymal stem cells. *J Cell Physiol,* **203,** 398-409.

Spring J, Beck K, Chiquet-Ehrismann R (1989) Two contrary functions of tenascin: dissection of the active sites by recombinant tenascin fragments. *Cell,* **59,** 325-34.

Steadman JR, Briggs KK, Rodrigo JJ, Kocher MS, Gill TJ, Rodkey WG (2003) Outcomes of microfracture for traumatic chondral defects of the knee: average 11-year follow-up. *Arthroscopy,* **19,** 477-84.

Stevens A, Lowe JS, Wheater PR, Burkitt HG (1992) *Histology,* Gower Medical, London.

Stockwell R (1979) Biology of cartilage cells. *Cambridge: Cambridge university press.*

Storm EE, Huynh TV, Copeland NG, Jenkins NA, Kingsley DM, Lee SJ (1994) Limb alterations in brachypodism mice due to mutations in a new member of the TGF beta-superfamily. *Nature,* **368,** 639-43.

Storm EE, Kingsley DM (1999) GDF5 coordinates bone and joint formation during digit development. *Dev Biol,* **209,** 11-27.

Tang BL (2001) ADAMTS: a novel family of extracellular matrix proteases. *Int J Biochem Cell Biol,* **33,** 33-44.

Temple-Wong MM, Bae WC, Chen MQ, et al. (2009) Biomechanical, structural, and biochemical indices of degenerative and osteoarthritic deterioration of adult human articular cartilage of the femoral condyle. *Osteoarthritis Cartilage,* **17,** 1469-76.

Teshima R, Ono M, Yamashita Y, Hirakawa H, Nawata K, Morio Y (2004) Immunohistochemical collagen analysis of the most superficial layer in adult articular cartilage. *J Orthop Sci,* **9,** 270-3.

Tetlow LC, Adlam DJ, Woolley DE (2001) Matrix metalloproteinase and proinflammatory cytokine production by chondrocytes of human osteoarthritic cartilage: associations with degenerative changes. *Arthritis Rheum,* **44,** 585-94.

Thompson WO, Thaete FL, Fu FH, Dye SF (1991) Tibial meniscal dynamics using three-dimensional reconstruction of magnetic resonance images. *Am J Sports Med,* **19,** 210-5; discussion 215-6.

Timpl R, Engel J (1987) Type VI collagen. In *Structure and function of the collagen types* (eds Mayne RE, Burgeson R), pp. 105- 43. Orlando: Academic Press.

Tkachenko E, Rhodes JM, Simons M (2005) Syndecans: new kids on the signaling block. *Circ Res,* **96,** 488-500.

Tortora GJ, Anagnostakos NP (1990) *Principles of anatomy and physiology,* Harper & Row, New York ; London.

Townes PL, Holtfreter J (1955) Directed movements and selective adhesion of embryonic amphibian cells. *J Exp Zool A Comp Exp Biol,* **128**.

Tsai CL, Liu TK (1992) Osteoarthritis in women: its relationship to estrogen and current trends. *Life Sci,* **50,** 1737-44.

Tsuchiya K, Chen, G., Ushida, T., Matsuno, T., Tateishi, T. (2004) The effect of coculture of chondrocytes with mesenchymal stem cells on their cartilaginous phenotype in vitro. *Materials Science and Engineering C,* **24,** 391–396.

Tsutsumi S, Shimazu A, Miyazaki K, et al. (2001) Retention of multilineage differentiation potential of mesenchymal cells during proliferation in response to FGF. *Biochem Biophys Res Commun,* **288,** 413-9.

Tuli R, Li WJ, Tuan RS (2003) Current state of cartilage tissue engineering. *Arthritis Res Ther,* **5,** 235-8.

Ustunel I, Ozenci AM, Sahin Z, et al. (2008) The immunohistochemical localization of notch receptors and ligands in human articular cartilage, chondroprogenitor culture and ultrastructural characteristics of these progenitor cells. *Acta Histochem,* **110,** 397-407.

van den Berg WB (1995) Growth factors in experimental osteoarthritis: transforming growth factor beta pathogenic? *J Rheumatol Suppl,* **43,** 143-5.

van der Rest M, Mayne R (1988) Type IX collagen proteoglycan from cartilage is covalently cross-linked to type II collagen. *J Biol Chem,* **263,** 1615-8.

Vaughan-Thomas A, Young RD, Phillips AC, Duance VC (2001) Characterization of type XI collagen-glycosaminoglycan interactions. *J Biol Chem,* **276,** 5303-9.

Vinatier C, Bouffi C, Merceron C, et al. (2009) Cartilage tissue engineering: towards a biomaterial-assisted mesenchymal stem cell therapy. *Curr Stem Cell Res Ther,* **4,** 318-29.

von der Mark K (1980) Immunological studies on collagen type transition in chondrogenesis. In *Current topics in developmental biology: Immunological approaches to embryonic development and differentiation part II* (ed Friedlander M), pp. 199 - 222. New York: Academic Press, Inc.

von der Mark K, Kirsch T, Nerlich A, et al. (1992) Type X collagen synthesis in human osteoarthritic cartilage. Indication of chondrocyte hypertrophy. *Arthritis Rheum,* **35,** 806-11.

von der Mark K, Mollenhauer J (1997) Annexin V interactions with collagen. *Cell Mol Life Sci,* **53,** 539-45.

von der Mark K, von der Mark H, Gay S (1976) Study of differential collagen synthesis during development of the chick embryo by immunofluroescence. II. Localization of type I and type II collagen during long bone development. *Dev Biol,* **53,** 153-70.

Wagner W, Ho AD, Zenke M (2010) Different facets of aging in human mesenchymal stem cells. *Tissue Eng Part B Rev,* **16,** 445-53.

Walker GD, Fischer M, Gannon J, Thompson RC, Jr., Oegema TR, Jr. (1995) Expression of type-X collagen in osteoarthritis. *J Orthop Res,* **13,** 4-12.

Ward AC, Dowthwaite GP, Pitsillides AA (1999) Hyaluronan in joint cavitation. *Biochem Soc Trans,* **27,** 128-35.

Westacott CI, Webb GR, Warnock MG, Sims JV, Elson CJ (1997) Alteration of cartilage metabolism by cells from osteoarthritic bone. *Arthritis Rheum,* **40,** 1282-91.

Wieland HA, Michaelis M, Kirschbaum BJ, Rudolphi KA (2005) Osteoarthritis - an untreatable disease? *Nat Rev Drug Discov,* **4,** 331-44.

Williams R, Khan IM, Richardson K, et al. (2010) Identification and clonal characterisation of a progenitor cell sub-population in normal human articular cartilage. *PLoS One,* **5,** e13246.

Williams R, Nelson L, Dowthwaite GP, Evans DJ, Archer CW (2009) Notch receptor and Notch ligand expression in developing avian cartilage. *J Anat,* **215,** 159-69.

Wolf F, Candrian C, Wendt D, et al. (2008) Cartilage tissue engineering using pre-aggregated human articular chondrocytes. *Eur Cell Mater,* **16,** 92-9.

Wotton SF, Duance VC, Fryer PR (1988) Type IX collagen: a possible function in articular cartilage. *FEBS Lett,* **234,** 79-82.

Wotton SF, Jeacocke RE, Maciewicz RA, Wardale RJ, Duance VC (1991) The application of scanning confocal microscopy in cartilage research. *Histochem J,* **23,** 328-35.

Yang S, Kim J, Ryu JH, et al. (2010) Hypoxia-inducible factor-2alpha is a catabolic regulator of osteoarthritic cartilage destruction. *Nat Med,* **16,** 687-93.

Young AA, Smith MM, Smith SM, et al. (2005) Regional assessment of articular cartilage gene expression and small proteoglycan metabolism in an animal model of osteoarthritis. *Arthritis Res Ther,* **7,** R852-61.

Yuan GH, Tanaka M, Masuko-Hongo K, et al. (2004) Characterization of cells from pannus-like tissue over articular cartilage of advanced osteoarthritis. *Osteoarthritis Cartilage,* **12,** 38-45.

Yudoh K, Nguyen T, Nakamura H, Hongo-Masuko K, Kato T, Nishioka K (2005) Potential involvement of oxidative stress in cartilage senescence and development of osteoarthritis: oxidative stress induces chondrocyte telomere instability and downregulation of chondrocyte function. *Arthritis Res Ther,* **7,** R380-91.

Zhou S, Eid K, Glowacki J (2004) Cooperation between TGF-beta and Wnt pathways during chondrocyte and adipocyte differentiation of human marrow stromal cells. *J Bone Miner Res,* **19,** 463-70.

Ziskoven C, Jager M, Zilkens C, Bloch W, Brixius K, Krauspe R (2010) Oxidative stress in secondary osteoarthritis: from cartilage destruction to clinical presentation? *Orthop Rev (Pavia),* **2,** e23.

Zuk PA, Zhu M, Ashjian P, et al. (2002) Human adipose tissue is a source of multipotent stem cells. *Mol Biol Cell,* **13,** 4279-95.

8: Appendix

8: Appendix

Massons trichrome stain:

Stain in Celestine blue B (10 minutes)

Wash in running tap water until clear

Stain in Mayer's Haematoxylin (10 minutes)

Wash in running tap water (10 minutes)

Stain in Ponceau/acid fuchin (5 minutes)

Wash in running tap water (1 minute)

Differentiate in 1% phosphomolydic acid (5 minutes)

Transfer to light green stain (3 minutes)

Wash in running tap water (1 minute)

Wash in 1% acetic acid (1 minute)

Rinse in running tap water (30 seconds)

Dehydrate in alcohols

Clear in xylene

Mount in DPX

9: Publications

8. Publications arising from this work

Abstracts

1. **L Nelson**, HE McCarthy, J Fairclough, CW Archer (2011). Human derived osteoarthritic cartilage progenitor cells elicit in vitro regenerative capacity. UKNSCN meeting, York.

2. **L Nelson**, HE McCarthy, J Fairclough, CW Archer (2011). A new scoring system for osteoarthritis of the knee. BORS, Cambridge.

Full length publications

1. **L Nelson**, HE McCarthy, J Fairclough, CW Archer (2012). A new scoring system for osteoarthritis of the knee. Osteoarthritis and Cartilage. *Manuscript in preparation*.

2. CW Archer, R Williams, **L Nelson**, IM Khan (2012). Articular Cartilage-Derived Stem Cells: Identification, Characterisation and their Role in Spontaneous Repair. Rheumatology: Current Research, S3.

3. R Williams, I Khan, K Richardson, **L Nelson**, H McCarthy, T Analbelsi, SK Singhrao, GP Dowthwaite, RE Jones, DM Baird, H Lewis, S Roberts, HM Shaw, J Dudhia, J Fairclough, T Briggs, CW Archer (2010). Identification and clonal characterisation of a progenitor cell sub-population in normal human articular cartilage. PLoS ONE, 5:e13246.

4. **L Nelson**, J Fairclough, CW Archer (2010). Use of stem cells in the biological repair of articular cartilage. Expert Opinion on Biological Therapy Vol 10 (1) pp43-55(13).